Connecting Coastal Domains in Morphodynamic Modelling

van Westen, B.

DOI
10.4233/uuid:688bb951-0cfa-44c1-82d6-22f9b80ac32c

Publication date
2025

Document Version
Final published version

Citation (APA)
van Westen, B. (2025). *Connecting Coastal Domains in Morphodynamic Modelling*. [Dissertation (TU Delft), Delft University of Technology]. https://doi.org/10.4233/uuid:688bb951-0cfa-44c1-82d6-22f9b80ac32c

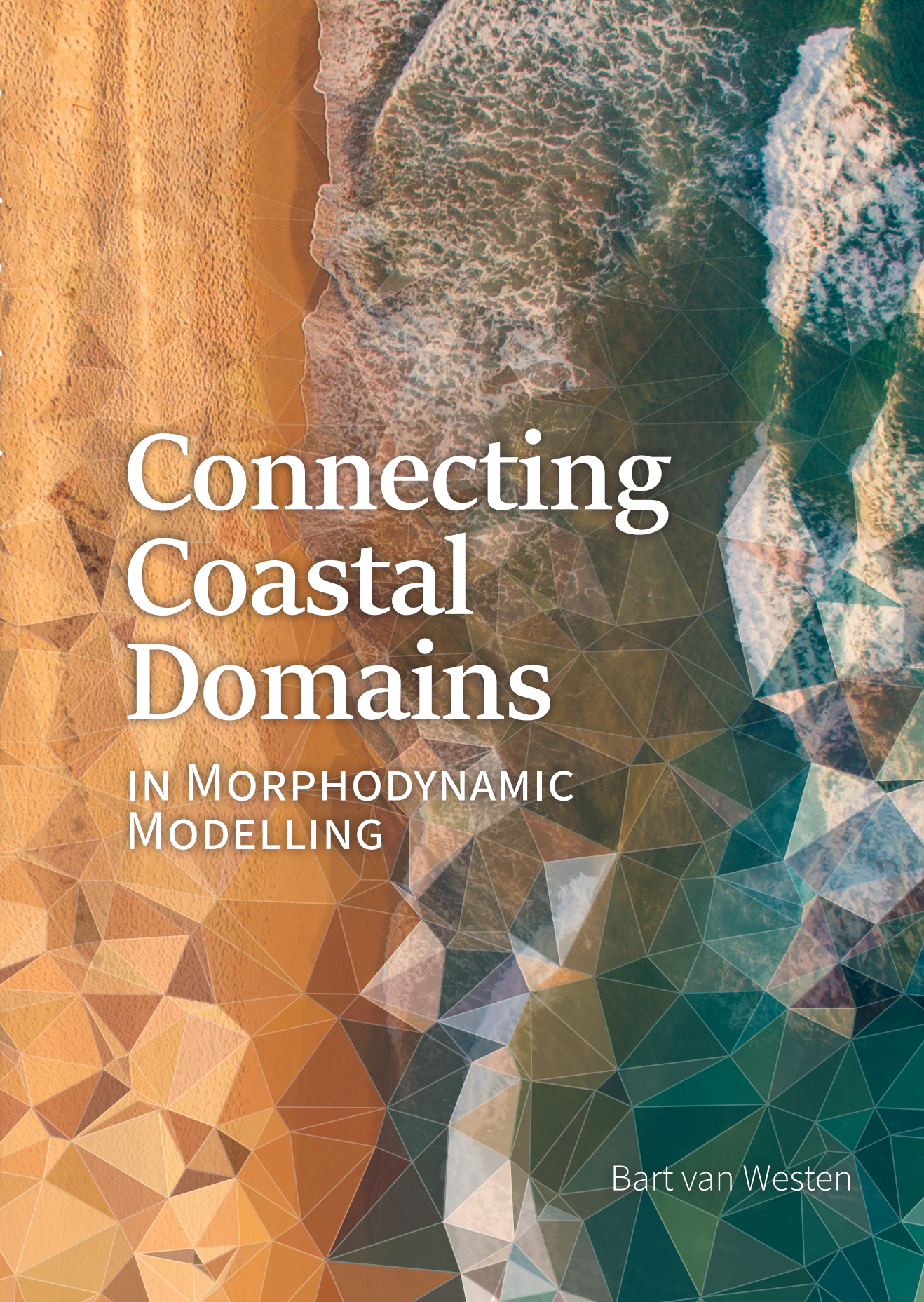

Connecting Coastal Domains

in Morphodynamic Modelling

Bart van Westen

Connecting Coastal Domains in Morphodynamic Modelling

Connecting Coastal Domains in Morphodynamic Modelling

Proefschrift

ter verkrijging van de graad van doctor
aan de Technische Universiteit Delft,
op gezag van de Rector Magnificus, Prof. dr. ir. T.H.J.J. van der Hagen,
voorzitter van het College voor Promoties,
in het openbaar te verdedigen op donderdag 2 oktober 2025 om 17:30 uur

door

Bart VAN WESTEN

Ingenieur in de Civiele Techniek,
Technische Universiteit Delft, Nederland,
geboren te 's-Gravendeel, Nederland.

Dit proefschrift is goedgekeurd door de promotoren en copromotor.

Samenstelling promotiecommissie:

Rector Magnificus,	voorzitter
Dr. ir. M.A. de Schipper,	Technische Universiteit Delft, *promotor*
Dr. ir. S. de Vries,	Technische Universiteit Delft, *promotor*
Dr. ir. A.P. Luijendijk,	Technische Universiteit Delft / Deltares, *copromotor*
Onafhankelijke leden:	
Prof. dr. ir. J.A. Roelvink,	Technische Universiteit Delft / IHE Delft
Prof. dr. K.M. Wijnberg,	Universiteit Twente
Prof. dr. I. Overeem,	University of Colorado Boulder, USA
Prof. dr. J.W. Long,	University of North Carolina Wilmington, USA
Prof. dr. ir. A.J.H.M. Reniers,	Technische Universiteit Delft, reservelid

This research has been financed by the Dutch Coastline Challenge project (DCC) of TKI Deltatechnology (with partners Rijksdienst voor Ondernemend Nederland (RVO), Dutch Ministry of Infrastructure and Water, Rijkswaterstaat, Vereniging van Waterbouwers, EcoShape, Delft University of Technology, and Deltares), the Deltares Strategic Research Programme 'Seas and Coastal Zones', the Deltares Moonshot 2 - 'Making the world safer from flooding', and the research programme DuneForce with project number 17064 which was (partly) financed by the Dutch Research Council (NWO).

Keywords: coast; morphodynamics; numerical modelling; dunes; model coupling; sediment pathways.

Printed by: www.ridderprint.nl

ISBN 978-94-6522-643-9

An electronic copy of this dissertation is available at
https://repository.tudelft.nl/.

When we try to pick out anything by itself,
we find it hitched to everything else in the Universe.

John Muir

Contents

Summary

Coastal systems provide numerous services to communities worldwide, including flood protection, recreational spaces, and biodiversity support. However, these valuable environments face increasing pressure from climate change, sea-level rise, and growing coastal populations. Coastal management aiming to preserve these services is evolving from traditional "grey" towards sandy Nature-based Solutions (NBS). The success of NBS inherently relies on natural processes driving their evolution. NBS typically aim to fulfil multiple objectives, while having lasting impact crossing multiple domains (such as the nearshore, beach and dunes). This increases the need quantitative tools that describe sediment transport and morphodynamic development across the nearshore-dune system.

This dissertation addresses the challenge of modelling coastal evolution across multiple domains through four complementary aims: (A) enabling process-based description of dune development, (B) demonstrating the technical feasibility of coupling numerical models, (C) mapping sediment pathways across the nearshore-dune system, and (D) demonstrating the practical utilisation of these tools for informing NBS design.

To enable the process-based description of coastal dune development in engineering contexts, the existing aeolian transport model AEOLIS is enhanced with landform-shaping processes, including vegetation growth, topographic steering of wind flow, and avalanching. The goal was enabling the simulation of realistic coastal dune evolution at scales relevant to engineering applications. The enhanced model successfully reproduces four distinct dune landforms under real-world conditions. The simulation of barchan dunes closely matched dimensions and migration rates observed in Morocco. Simulated parabolic dunes reproduced migration rates and seasonal dynamics observed in Brazil. The simulation of an embryo dune field captured the seasonality and spatial sheltering effect as observed at De Hors, Netherlands. Finally, the spatial patterns and volumetric changes of excavated foredune notches along the Dutch coast were successfully replicated. Simulating this blowout development on an engineering scale demonstrated the model's practical applicability.

The nearshore and dune domains function as an integrated system, yet they are typically studied separately using different models. To address this limitation, a coupling framework was developed that enables continuous exchange of bed levels, wave heights, and water levels between three process-based models: DELFT3D Flexible Mesh, SWAN, and the enhanced AEOLIS model. The framework was applied to the Sand Engine mega-nourishment in the Netherlands, accurately reproducing observed marine-driven longshore erosion (4.1 Mm^3) and aeolian deposition patterns. The simulation results en-

able the quantification of interactions between domains. Aeolian extraction of sediment from the shared sediment budget reduces marine-driven longshore dispersion by 2%. Meanwhile, marine-driven morphodynamics cause variations in foredune growth; up to 24% lower dune growth in sheltered areas and 7% higher growth along accretive beaches in the fifth year. As these morphological deviations accumulate over time, the effect of these cross-domain interactions intensifies over time. This study demonstrates the feasibility of coupling models at scales relevant to coastal management—spanning multiple kilometres over five years.

Understanding coastal evolution requires more than quantifying morphological changes; it demands insight into how sediment moves through the system. To address this need, a Lagrangian particle-tracking approach was developed that accounts for morphodynamic-driven burial. This extends Lagrangian analysis beyond traditional timescales to multi-year periods. Applied to the Sand Engine simulation, the simulated pathways reveal movement patterns impossible to detect through conventional Eulerian approaches. We analysed both the dispersion of nourished sediment and the origin of accumulated sediment at the Sand Engine's flanks. During initial stages, nourished sediment dispersal is severely restricted by rapid burial. The displacement of particles is reduced by an order of magnitude compared to displacement expected along undisturbed coastlines. Sediment accumulation south of the perturbation includes both direct supply from the nourishment (41%) and indirect contributions from updrift sources (59%). As the coastline perturbation diffuses over time, transport patterns gradually transition toward those of an undisturbed coast. These result enable improved understanding of sediment movement between sources to sinks and thereby the causal relationships that drive coastal change. Rather than indirectly inferring connectivity from Eulerian morphological comparisons, sediment pathways explicitly visualize sediment movement between domains.

The practical utility of the developed tools was demonstrated by examining how specific design choices might influence dune evolution in both large-scale mega-nourishments and smaller beach nourishments. For the Sand Engine, the impact of multiple alternative design considerations on dune growth was explored. The simulations indicated that removing the artificial dune lake would increase dune growth by 42,000 m^3 over 10 years, with effects extending 1,200 m alongshore. Reducing coarse sediment content enhanced dune growth by 65%, and lowering the crest elevation increased sediment availability through more frequent mixing. In a smaller-scale application, we explored using certain decisions in nourishment design to steer sediment supply as an abiotic condition for vegetation growth. Incorporating a lagoon in beach nourishment design restricted sediment supply toward the foredune, reducing total dune growth by 62%. Under the assumption that vegetation depends on sediment burial, vegetation growth was limited, maintaining wider blowout entrances. As a result, the simulated amount of backdune deposition was 23% higher for the scenario with lagoon. Particle tracking analysis revealed that the lagoon design more than doubled the contribution from nearshore sediment sources to backdune accumulation. These applications demonstrate how the developed tools can support the design of NBS aiming to achieve objectives across multiple domains.

This dissertation advances our ability to model coastal processes across domain boundaries, connecting the marine and aeolian environments that have traditionally been studied separately. The development from enhanced dune modelling to coupled nearshore-dune frameworks, advanced sediment pathway analysis, and practical design applications creates new possibilities for coastal management. While challenges remain in computational efficiency and process representation, these tools enable coastal engineers and managers to examine how interventions impact evolution across the nearshore-dune system. As coastal regions continue to face increasing pressures, the ability to connect domains in morphodynamic modelling provides a valuable tool for integrated coastal management.

Samenvatting

Wereldwijd leveren kustsystemen essentiële diensten aan lokale gemeenschappen, waaronder bescherming tegen overstromingen, recreatiemogelijkheden en de ondersteuning van biodiversiteit. Deze waardevolle gebieden staan echter onder toenemende druk door klimaatverandering, zeespiegelstijging en de groeiende kustbevolking. Kustbeheer is erop gericht deze diensten te behouden. De afgelopen decennia heeft het beheer zich ontwikkeld van traditionele 'grijze' oplossingen naar natuurlijke oplossingen (Nature-based Solutions, NBS). Het succes van NBS is afhankelijk van natuurlijke processen die hun ontwikkeling sturen. NBS streven doorgaans meerdere doelen na, met een blijvende impact die vaak verschillende domeinen beïnvloedt (zoals de vooroever, het strand en de duinen). Dit vergroot de behoefte aan kwantitatieve instrumenten die het sedimenttransport en de morfologische ontwikkeling van vooroever tot duin nauwkeurig beschrijven.

Dit proefschrift richt zich op de uitdaging van het modelleren van kustontwikkeling over meerdere domeinen door middel van vier complementaire doelstellingen: (A) het mogelijk maken van een procesgebaseerde beschrijving van duinvorming, (B) het aantonen van de technische haalbaarheid van het koppelen van numerieke modellen, (C) het in kaart brengen van sedimenttransportroutes over het vooroever-duinsysteem, en (D) het demonstreren van de praktische toepassing van deze instrumenten voor het ontwerpen van NBS.

Om de procesgebaseerde beschrijving van kustduinvorming in praktische toepassingen te integreren, is het bestaande eolische transportmodel AEOLIS uitgebreid met de processen die verantwoordelijk zijn voor het ontstaan van duinen, waaronder vegetatiegroei, topografische sturing van de wind en het afschuiven van zand. Het doel was om de simulatie van realistische kustduinevolutie mogelijk te maken op schalen die relevant zijn voor praktisch beheer. Het verbeterde model reproduceert met succes vier verschillende duinvormen onder realistische omstandigheden. De simulatie van barchaanduinen kwam nauw overeen met afmetingen en migratiesnelheden zoals waargenomen in Marokko. Gesimuleerde paraboolduinen reproduceerden migratiesnelheden en seizoensgebonden dynamiek zoals waargenomen in Brazilië. De simulatie van een embryonaal duinveld toonde de seizoensgebondenheid zoals waargenomen bij De Hors, Nederland. Ten slotte werden de ruimtelijke patronen en volumeveranderingen van uitgegraven kerven in de zeereep langs de Nederlandse kust succesvol gerepliceerd. Het simuleren van deze stuifkuilontwikkeling op praktische schaal demonstreerde de toepasbaarheid van het model.

De vooroever en de duinen functioneren als een geïntegreerd systeem, maar worden doorgaans afzonderlijk bestudeerd met verschillende modellen. Om deze beperking te overkomen, werd een koppelingsraamwerk ontwikkeld dat continue uitwisseling mogelijk maakt van bodemhoogtes, golfhoogtes en waterstanden tussen drie procesgebaseerde modellen: DELFT3D Flexible Mesh, SWAN en het verbeterde AEOLIS-model. Het raamwerk werd toegepast op de Zandmotor mega-suppletie in Nederland, waarbij de waargenomen mariene kustlangse erosie (4,1 Mm^3) en eolische depositie nauwkeurig werden gereproduceerd. De simulatieresultaten maken de kwantificering van interacties tussen domeinen mogelijk. Eolische onttrekking van sediment uit het gedeelde sedimentbudget vermindert de mariene kustlangse verspreiding met 2%. Ondertussen veroorzaken mariene morfologische processen variaties in de groei van de zeereep; tot 24% lagere duingroei in beschutte gebieden en 7% hogere groei langs aangroeiende stranden in het vijfde jaar. Naarmate deze morfologische afwijkingen zich in de loop van de tijd opstapelen, intensiveert het effect van deze domeinoverschrijdende interacties. Deze studie toont de haalbaarheid aan van het koppelen van modellen op schalen die relevant zijn voor kustbeheer—over meerdere kilometers gedurende vijf jaar.

Het begrijpen van kustevolutie vereist meer dan het kwantificeren van morfologische veranderingen; het vraagt inzicht in de manier waarop sediment zich door het systeem verplaatst. Om aan deze behoefte te voldoen, werd een Lagrangiaanse aanpak ontwikkeld om zandkorrels te volgen, waarbij rekening wordt gehouden met morfologisch gedreven begraving. Dit breidt Lagrangiaanse analyse uit naar meerjarige perioden, voorbij traditionele tijdschalen. Toegepast op de Zandmotor-simulatie onthullen de gesimuleerde trajecten bewegingspatronen die onmogelijk te detecteren zijn met conventionele Euleriaanse methoden. We analyseerden zowel de verspreiding van gesuppleerd sediment als de oorsprong van aangezande sediment aan de flanken van de Zandmotor. Tijdens de beginfase wordt de verspreiding van gesuppleerd sediment sterk beperkt door snelle begraving. De verplaatsing van zanddeeltjes wordt met een orde van grootte verminderd in vergelijking met de verwachte verplaatsing langs ongestoorde kustlijnen. Aangroei ten zuiden van de verstoring omvat zowel directe aanvoer vanuit de suppletie (41%) als indirecte bijdragen van bovenstroomse bronnen (59%). Naarmate de kustlijnverstoring in de loop van de tijd afneemt, gaan transportpatronen geleidelijk over in die van een ongestoorde kust. Deze resultaten maken een beter begrip mogelijk van sedimentbeweging tussen bron en bestemming en daarmee van de causale relaties die kustverandering sturen. In plaats van verbindingen indirect af te leiden uit Euleriaanse morfologische vergelijkingen, visualiseren sedimentroutes expliciet de trajecten die het zand aflegt tussen domeinen.

De praktische bruikbaarheid van de ontwikkelde instrumenten werd aangetoond door te onderzoeken hoe specifieke ontwerpkeuzes de duinevolutie zouden kunnen beïnvloeden in zowel grootschalige megasuppleties als kleinere strandsuppleties. Voor de Zandmotor werd de impact van verschillende alternatieve ontwerpoverwegingen op duingroei onderzocht. De simulaties gaven aan dat het verwijderen van het kunstmatige duinmeer de duingroei met 42.000 m^3 over 10 jaar zou vergroten, met effecten die zich 1.200 m langs de kust uitstrekken. Het verminderen van het aandeel grof sediment verhoogde de duingroei met 65%, en het verlagen van de kruinhoogte verhoogde de sedi-

mentbeschikbaarheid door frequentere menging. In een kleinschaliger toepassing onderzochten we het gebruik van bepaalde beslissingen in het suppletieontwerp om sedimenttoevoer te sturen als een abiotische conditie voor vegetatiegroei. Het opnemen van een lagune in het strandsuppletieontwerp beperkte de sedimenttoevoer naar de zeereep, waardoor de totale duingroei met 62% afnam. Onder de aanname dat vegetatie afhankelijk is van zandbedekking, werd vegetatiegroei beperkt, waardoor bredere stuifkuilingangen behouden bleven. Als gevolg hiervan was de gesimuleerde hoeveelheid achterduindepositie 23% hoger voor het scenario met lagune. Langriaanse analyse onthulde dat het laguneontwerp de bijdrage van vooroeversedimentbronnen aan achterduinophoping meer dan verdubbelde. Deze toepassingen tonen aan hoe de ontwikkelde instrumenten het ontwerp van NBS kunnen ondersteunen die gericht zijn op het bereiken van doelstellingen over meerdere domeinen.

Dit proefschrift verbetert ons vermogen om kustprocessen over domeingrenzen heen te modelleren, waardoor de mariene en eolische omgevingen, die traditioneel afzonderlijk werden bestudeerd, met elkaar worden verbonden. De ontwikkeling van verbeterde duinmodellering naar gekoppelde vooroever-duin modellen, geavanceerde sedimentroute-analyse en praktische ontwerptoepassingen creëert nieuwe mogelijkheden voor kustbeheer. Hoewel er uitdagingen blijven op het gebied van rekenefficiëntie en procesbeschrijving, stellen deze instrumenten kustingenieurs en -beheerders in staat om te onderzoeken hoe interventies de evolutie over het vooroever-duinsysteem beïnvloeden. Nu kustgebieden onder toenemende druk blijven staan, biedt het vermogen om domeinen te verbinden in morfologische modellering een waardevol instrument voor geïntegreerd kustbeheer.

1

Introduction

1.1. Motivation

Coastal systems provide numerous services to communities worldwide (Figure 1.1). The coast offers recreational opportunities, supports unique habitats and biodiversity, protects against coastal flooding, and contributes to the provision of drinking water (Arkema et al., 2013; Barbier et al., 2011; Sutton-Grier et al., 2015). However, coastal regions are facing increasing pressure due to the combined effects of sea-level rise and increasing population, critical infrastructure and economic value in coastal areas (Ranasinghe, 2016; Vousdoukas et al., 2020). This phenomenon, known as "coastal squeeze," threatens both the sustainability of these systems and their ability to deliver services (Pontee, 2013).

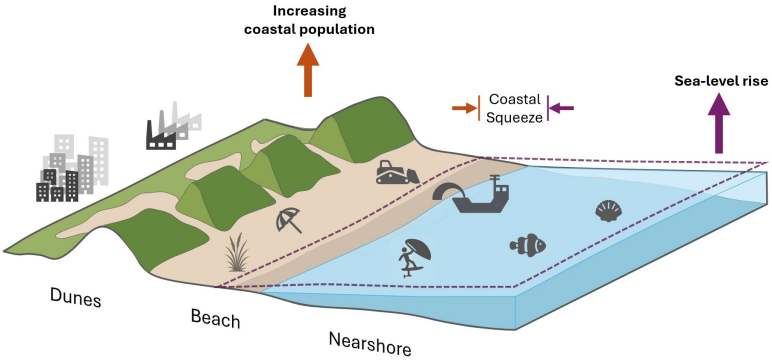

Figure 1.1.: The provision of coastal services is threatened by sea level rise and growing coastal populations, a phenomenon called "coastal squeeze".

From "Grey" to Nature-based Solutions

Coastal management strategies aim to safeguard the variety of benefits provided by coastal systems. Assessing the impact of management decisions has become increasingly challenging due to the growing complexity of coastal strategies implemented in recent decades. The Dutch coast illustrates this evolution particularly well. Historically, coastal protection relied on "grey" engineering solutions such as groynes, breakwaters, and seawalls—interventions with localized impact and singular objectives like preventing erosion. By the mid-20th century, "soft" solutions emerged with nourishments placed directly on beaches and dunes to compensate for local erosion (Brand et al., 2022). The 1990s marked a shift to a national strategy, with the Dutch "Dynamic Preservation" policy (Ministerie van Verkeer en Waterstaat, 1990). This policy aims to maintain the coastline at its 1990 position by an annual nourishment strategy. Shoreface nourishments were more often used, relying on natural processes to increase sediment volume on the landward beach (Brand et al., 2022), ultimately improving cost-effectiveness.

More recently, Nature-based Solutions (NBS) have emerged as a promising approach to coastal management. NBS harness natural processes to enhance coastal resilience while providing multiple environmental and societal benefits (Barciela Rial, 2019; van der Meulen et al., 2014; van der Meulen et al., 2023; Sutton-Grier et al., 2015; de Vriend et al., 2015). The Sand Engine mega-nourishment (Figure 1.2), constructed along the Delfland coast in 2011, exemplifies this approach (Stive et al., 2013). This 21.5 Mm^3 peninsula was designed to gradually disperse along the coastline through natural processes. The Sand Engine aims to enhance coastal protection, while simultaneously creating recreational opportunities and habitat development.

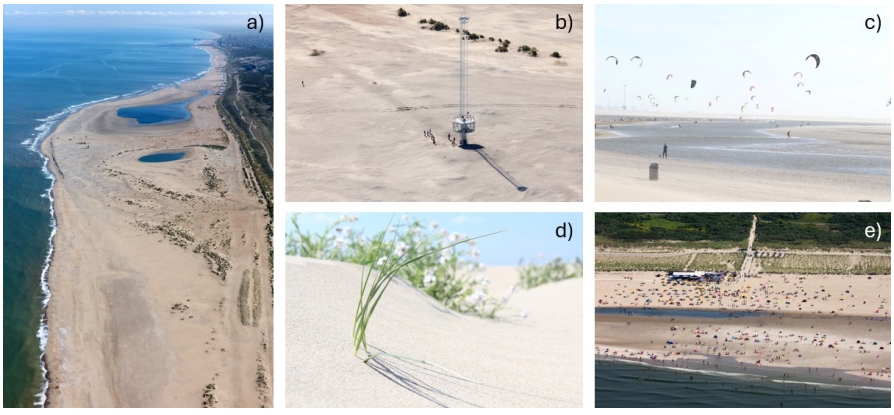

Figure 1.2.: The Sand Engine mega-nourishment, an example of sandy Nature-based Solutions (NBS), feeds the adjacent beaches through longshore dispersion (a), while providing research opportunities such as the Argus station (Wengrove et al., 2013) (b), surface area for recreation (c & e) and ecological value (d). Photo credits: Rijkswaterstaat (a), Jurriaan Brobbel (b,e) & Leo Linnartz (c,d).

Different sandy NBS may aim for diverse objectives and be based on varying design principles, but they all share a fundamental dependency on sediment movement. Some NBS consist of sandy buffers placed in front of existing infrastructure to protect against flooding, like the Hondsbossche dunes (Kroon et al., 2022) and Prins Hendrikzanddijk (Perk et al., 2019). Along the Belgian coast, a similar buffer is established through growing artificial dunes by planting marram grass (Strypsteen et al., 2024a). This approach to sandy protection is also used to shelter the Marker Wadden artificial islands from wave impact (Ton et al., 2021). Habitat-oriented projects like Spanjaardsduin (van der Meulen et al., 2014; Vrielink et al., 2021) rely on natural succession processes to create desired ecological habitats. Smaller interventions such as excavated foredune notches (Figure 1.3) are implemented to reintroduce dune dynamics (Arens et al., 2013a; van Boxel et al., 1997; Castelle et al., 2019; Riksen et al., 2016; Ruessink et al., 2018; Terlouw & Slings, 2005; Walker et al., 2013). Despite their differences in concept, objective, scale, and implementation approach, in all cases understanding sediment movement is crucial to the intervention's evolution and ultimately its success.

Figure 1.3.: Excavated notches evolved into foredune blowouts along the Dutch coast. Photo credits: Patrick Hesp.

Process Interactions Across Domain Boundaries

The nearshore, beach, and dune domains function as an integrated system, with morphological changes in one zone influencing the others (Aagaard et al., 2004; Houser, 2009; Pellón et al., 2020; Sherman & Bauer, 1993; Short & Hesp, 1982). The nearshore spans from the shoreline to deeper waters, encompassing the morphodynamically active underwater domain. The beach serves as the interface between the subaqueous and subaerial environments, while dunes form the landward barrier shaped by wind-driven transport and vegetation stabilization.

Sediment moves continuously across these domains through interacting processes. Wave- and tide-driven currents redistribute sediment in the nearshore, sediment availability and subsequent beach width. Under accretive conditions, beaches grow, creating favourable conditions for dune development (Cohn et al., 2017; Houser, 2009). Conversely, storm events can erode both beaches and dunes, adversely affecting the system's sediment budget (Costas et al., 2020; González-Villanueva et al., 2023; Quartel et al., 2008).

The effectiveness of aeolian transport is governed by more than just wind strength—it depends on supply limitations often controlled by marine processes (Costas et al., 2020; de Vries et al., 2014a). Soil moisture in the intertidal zone restricts sand mobilization (Bauer et al., 2009; Hallin et al., 2023b; Ruessink et al., 2022), while wave-driven mixing of surface sediments prevents or resets desert pavement formation (Carter, 1976; Hoonhout & de Vries, 2017; van IJzendoorn et al., 2023a). These interactions mean that dune development ultimately reflects sediment availability throughout the nearshore-dune system (Short & Hesp, 1982).

Unlike traditional engineering approaches designed to resist natural forces, NBS fundamentally depend on these cross-domain processes to shape their development. The success of sandy interventions—whether for coastal protection, habitat creation, or recreation—hinges on understanding this sediment exchange. This philosophy aligns with similar approaches worldwide, including Engineering with Nature (Bridges et al., 2021a) and Living Shorelines (Powell et al., 2019), which likewise leverage natural dynamics to achieve sustainable coastal management objectives.

Limitations of Current Modelling Approaches

Numerical models have become important tools for studying coastal morphodynamics and assessing the impacts of management interventions. They allow researchers and engineers to explore physical processes, evaluate design alternatives, and support informed decision-making (Barbour & Krahn, 2004). Historically, numerical model development has concentrated predominantly on processes within the nearshore domain (Lesser et al., 2004; Roelvink et al., 2009). This focus has proven adequate for conventional engineering solutions and smaller nourishments where simple assumptions about sediment redistribution suffice. The capability of these models is demonstrated by their predictions of the longshore evolution of large-scale interventions such as the Sand Engine (Huisman et al., 2018; Luijendijk et al., 2017; Tonnon et al., 2018), confirming their utility for predicting marine-driven morphodynamics.

In contrast, the integration of aeolian transport and dune evolution into numerical models remains less developed, despite the importance of dunes for coastal protection and ecosystem services (Barbier et al., 2011; Biel et al., 2017; van der Meulen & de Haes, 1996). While several aeolian and dune models exist (Baas & Nield, 2007; Durán et al., 2010; Hoonhout & de Vries, 2016; Roelvink & Costas, 2019; Ruessink et al., 2022), their practical application in detailed coastal design typically remains limited. Most practical design efforts rely on simplified empirical formulations that, in more complex environments, cannot adequately capture the spatiotemporal variability inherent in coastal settings.

The limitations of current modelling approaches were particularly evident during the design and evaluation of the Sand Engine. Initial predictions for dune growth were based on simplified empirical relationships derived from observations in more natural coastal settings (Mulder & Tonnon, 2011). These simplified methods substantially overestimated the actual dune growth and failed to reproduce the observed spatial variability (Hoonhout & de Vries, 2017; Huisman et al., 2021). This discrepancy arose because factors such as supply-limiting conditions and sediment trapping by waterbodies were not included in the simplified description. Addressing these factors requires incorporating process-based descriptions that account for spatially and temporally varying influences.

Additionally, the lack of integration between nearshore and subaerial domains within numerical models limits the description of integrated coastal evolution. Current modelling approaches typically treat these domains independently, neglecting how morphodynamic changes in one domain impact processes in the other. This separation reduces the practical effectiveness of numerical models for informing coastal management across domains. Assessing mutual influences between nearshore and dune evolution requires coupling of these physical domains. This limitation is particularly relevant when considering the multi-functional nature of NBS. Various coastal state indicators beyond general sediment distribution become important for different objectives: dune volume for protection, beach width for recreation, and natural dynamics for habitat development. Predicting these different indicators often requires consideration of processes in multiple domains.

Beyond Morphological Change: The Need for Sediment Pathways

Understanding coastal evolution requires more than just quantifying morphological changes; it demands insight into how sediment actually moves through the system (Pearson et al., 2020; Ruggiero et al., 2016). Similar patterns of erosion and deposition can result from entirely different sediment pathways—a property known as equifinality. Conventional coastal modelling approaches can reveal net volumetric changes but cannot track the movement of specific sediment parcels between sources and sinks. Mapping sediment pathways can provide useful information for coastal management. For large scale coastal engineering projects, it can reveal how nourished sand disperses along the coast. In dune management, it can identify whether sand accumulating in backdunes originates from the nourished beach or from the blowout deflation basin itself. Without tracing these connections, our understanding on the inner workings of intervention remains incomplete.

Problem Statement

State-of-the-art coastal models lack process-based descriptions of morphodynamic development and sediment transport across the nearshore-dune system. This gap is particularly problematic for NBS, which evolution relies on sediment movement across multiple physical domains. Consequently, existing models cannot sufficiently inform engineers and decision-makers about how specific NBS design choices affect integrated evolution of the coast.

1.2. Research Objectives

The main objective of this research is to provide a toolkit for the numerical description of morphological development and sediment movement across the nearshore-dune system.

This requires more detailed process-based descriptions of dune development (**A**), enabling the interactions between the nearshore and dune domains (**B**), unravelling sediment pathways across the system (**C**) and demonstrating the utility of the presented tools to inform design decisions (**D**). The current work has consequently four research aims that contribute to the main objective:

- **A.** Enable process-based simulations of coastal dune development on engineering scales, by implementing landform-shaping processes in an aeolian transport model.
- **B.** Demonstrate the technical feasibility and added value of coupling numerical models in morphodynamic modelling of the nearshore-dune system.
- **C.** Map sediment pathways across a dynamically evolving coast by tracing particles from source to sink using Lagrangian analysis.
- **D.** Demonstrate the utility of the presented multi-domain tools for better informed decision-making in NBS design.

1.3. Thesis Outline

Objective A

Chapter 2 describes the inclusion of landform shaping processes in an existing aeolian transport model (AeoLiS). The goal is to enable the quantitative description of coastal dune development for coastal engineering applications. The models ability to describe a variety of landforms (barchan, parabolic and embryo dunes) is shown by applying it in various environments, under real-world conditions. The final application on five real-world excavated notches demonstrates its applicability in coastal engineering projects.

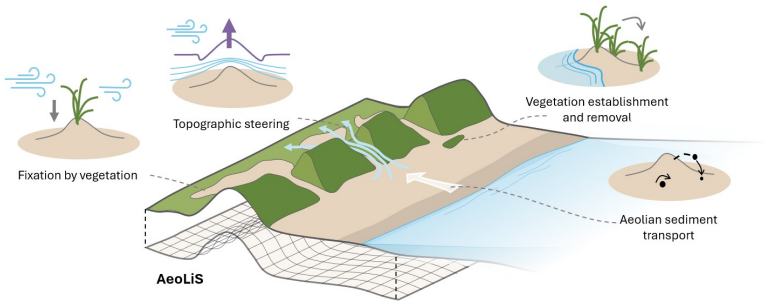

Figure 1.4.: Modelling coastal dune development with AeoLiS using process-based descriptions of aeolian transport, topographic steering and vegetation.

Objective B

Chapter 3 describes the development of a coupling framework, connecting the aeolian dune model from Chapter 2 with an nearshore morphodynamic model. The technical feasibility of continuously coupling large-scale, two-dimensional nearshore and aeolian domains for a multi-year period is demonstrated. By applying this coupled model on the Sand Engine mega-nourishment, the interactions and sediment exchanges between the nearshore and dune domains are quantified.

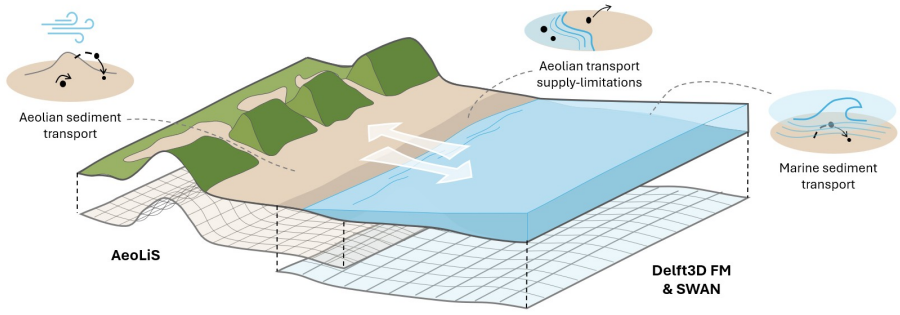

Figure 1.5.: Modelling interactions between wind- and wave-driven transport across the nearshore-dune system by coupling AeoLiS and Delft3D FM.

Objective C

Chapter 4 maps the sediment pathways across the nearshore-dune system based on sediment transport fields provided by the coupled numerical model from Chapter 3. This chapter demonstrates how a Lagrangian approach can be used in a morphodynamic nearshore-dune system. By applying it to the Sand Engine, it offers new insights into where nourished sand is deposited and where accumulating sand originates from.

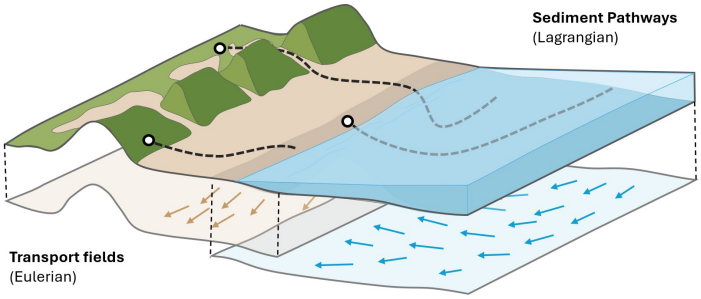

Figure 1.6.: Mapping sediment pathways across nearshore-dune system, utilizing the underlying (Eulerian) flow fields in both marine and aeolian domains.

Objective D

Chapter 5 combines the previously presented tools to demonstrate their utility in improving informed practical decisions in nourishment design, with dune development as primary objective. The impact of certain decisions in design of the Sand Engine and a smaller beach nourishment on dune development are assessed by comparing various coupled simulation alternatives.

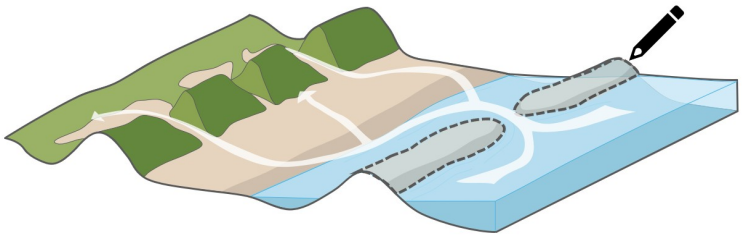

Figure 1.7.: Assessing the impact of certain decisions in nourishment design for dune development and the transport of sediment from nearshore into the dunes.

MODELLING COASTAL DUNES

Coastal dunes have received relatively little attention compared to their marine counterpart in numerical modelling. Current state-of-the-art models lack the ability to simulate dune development, especially on an engineering scale. Enabling the quantitative description of landform-shaping processes in coastal environments is our first step towards modelling the morphodynamic evolution of the nearshore-dune system.


2

Photo: Eric van der Eijk – https://duinlandschap.nl/

2

Modelling Coastal Dunes

AEOLIS: NUMERICAL MODELLING OF COASTAL DUNES AND AEOLIAN LANDFORM DEVELOPMENT FOR REAL-WORLD APPLICATIONS

Abstract The formation and evolution of coastal dunes result from a complex interplay of eco-morphodynamic processes. State-of-the-art models can simulate aeolian transports and morphological dune evolution under certain conditions. However, a model combining these processes for coastal engineering applications was not yet available. This study aims to develop a predictive tool for dune development to inform coastal management decisions and interventions. The aeolian sediment transport model AeoLiS is extended with functionalities that allow for simulations of coastal landforms. The added functionalities include the effect of topographic steering on wind shear, avalanching of steep slopes and vegetation processes in the form of growth and wind shear reduction. The model is validated by simulating four distinct coastal landforms; barchan-, parabolic-, embryo dunes and blowouts. Simulations, based on real-world conditions, replicate the landform formation, migration rates and seasonal variability.

This chapter is based on: van Westen, B., de Vries, S., Cohn, N., van IJzendoorn, C., Strypsteen, G., & Hallin, C. (2024). AeoLiS: Numerical modelling of coastal dunes and aeolian landform development for real-world applications. *Environmental Modelling & Software, 179*, 106093.

2.1. Introduction

Coastal dunes display a variety of shapes, sizes and behaviours that support numerous ecosystem services. Such ecosystem services include enhancing flood protection, increasing natural and recreational value, and reducing sand nuisance on adjoining infrastructure (Barbier et al., 2011; Biel et al., 2017; van der Biest et al., 2017; Borsje et al., 2011; Everard et al., 2010; van der Meulen & de Haes, 1996; Strypsteen et al., 2024a). At some locations, primarily in the Netherlands, coastal dunes also assist in the provision of drinking water (Bakker & Stuyfzand, 1993; Geelen et al., 2017). The dynamic eco-morphological development of coastal dunes results in different characteristic landforms, such as linear foredune ridges, hummocky dunes, parabolic dunes, and blowouts (Hesp, 2002). Dunes in the coastal zone naturally evolve in response to a combination of aeolian processes (e.g., wind energy and sediment supply), biotic processes (e.g., growth of plant communities), and marine processes (e.g., wave energy, tide and littoral drift direction) (Brodie et al., 2019; Cohn et al., 2018; Hesp, 2002; Hesp & Smyth, 2016; Martínez & Psuty, 2004; Pye, 1983; Short & Hesp, 1982), as well as, active and passive anthropogenic influences (Delgado-Fernandez et al., 2019; Jackson & Nordstrom, 2011; Martínez et al., 2013; Nordstrom et al., 2000; Provoost et al., 2011; Wijnberg et al., 2021).

Management of coastal dunes is increasingly applied to optimize different ecosystem services. The flood protection service is typically enhanced through nourishments and the planting of *Ammophila arenaria* (marram grass) to stabilize, restore or promote the generation of (new) coastal dunes (Bakker et al., 2012; Brand et al., 2022; Derijckere et al., 2022; 2023; Hoonhout & de Vries, 2017; Kroon et al., 2022; Matias et al., 2005; Ranwell & Rosalind, 1986; de Schipper et al., 2021; Sigren et al., 2014; Stive et al., 2013; Strypsteen et al., 2024a; van der Wal, 2004; Walker et al., 2023; van Westen et al., 2024a; Wittebrood et al., 2018). In contrast, biodiversity may be promoted by the removal of vegetation and sediment by excavating notches in the foredune. Removing vegetation and sediment may promote sediment transport beyond the foredune towards the hinterland, and facilitate landward dune migration in response to sea level rise (Arens et al., 2013a; van Boxel et al., 1997; Castelle et al., 2019; Ruessink et al., 2018; Walker et al., 2013). The photos in Figure 2.1 show three specific examples of active dune interventions; i) excavated foredune notches at Dutch National Park Zuid-Kennemerland promoting dune dynamics (Ruessink et al., 2018); ii) the Sand Engine mega nourishment designed to feed the adjacent coast and stimulate dune development (Stive et al., 2013); iii) an artificially constructed dune along the Belgium coast to mitigate sand nuisance (Derijckere et al., 2022; 2023; Strypsteen et al., 2024a). Although some coastal communities share positive experiences as a result of dune management, debates exist about the general usefulness of measures to optimize ecosystem services (Arens et al., 2020; Delgado-Fernandez et al., 2019). Dune management has even been critically labelled as *dune gardening* by some (Cooper & Jackson, 2021). At the same time, uncertainties with respect to the foreseen benefits of dune management measures remain.

Figure 2.1.: Three dune intervention projects with varying objectives: Five foredune notches at National Park Zuid-Kennemerland excavated to reintroduce dune dynamics (a), the 21 Mm^3 Sand Engine mega nourishment, constructed to stimulate dune development (b) and artificial dune constructed in front of an existing seawall to limit sand nuisance (c).

To reduce uncertainties about the impact of dune management measures, numerical modelling tools may assist in describing and predicting the future development of coastal dunes. To be able to inform the design of dune management interventions, a numerical tool should involve accurate, quantitative and reliable descriptions of the *processes governing dune development* (Section 2.2.1) and thus, be capable of simulating typical *coastal dune landforms* (Section 2.2.2). In recent years some notable *state-of-the-art dune models* (Section 2.2.3) have been proposed that may inspire a new comprehensive approach and provide a starting point.

Recognizing some of the deficiencies in current open-source tools for simulating the range of relevant eco-morphodynamic processes that drive coastal dune evolution for engineering timescales (days to decades), the objective of this study is to present an improved model to simulate the development of dunes in coastal areas that is applicable in practical situations. In the paper, the model's capabilities are demonstrated by simulating four distinct aeolian dune landforms (see Figure 2.2) and validating the outcomes with available data. Background information regarding processes governing dune development, typical coastal dune landforms and state-of-the-art dune models is given in Section 2.2. Section 2.3 presents new formulations added to the AeoLiS model (Hoonhout & de Vries, 2016) to achieve these applied objectives. Section 2.4 presents the model setup and validation approach for these four demonstration cases and Section 2.5 presents results for these select cases. A discussion and conclusions are provided in Sections 2.6 and 2.7, respectively.

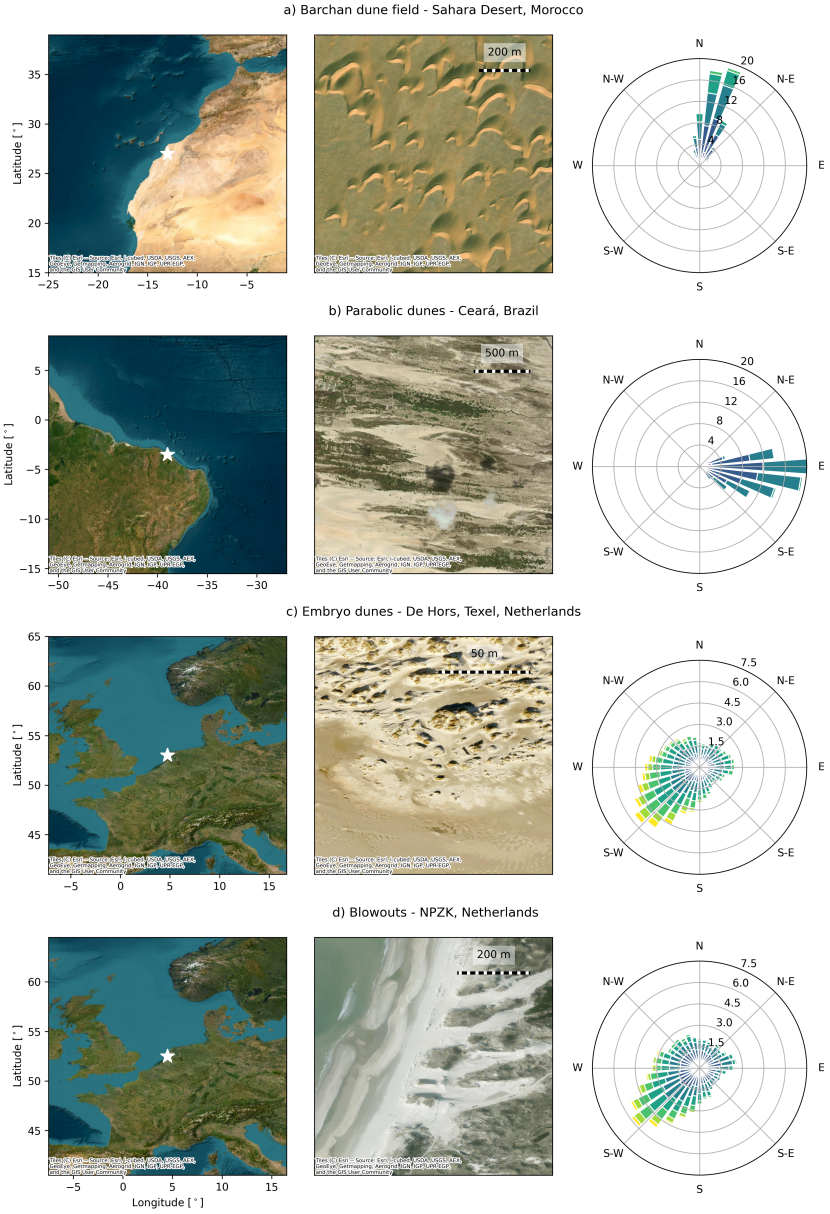

Figure 2.2.: An overview of real-world cases of four aeolian landforms central in this study: a) barchan dunes, b) parabolic dunes, c) embryo dunes, and d) artificial blowouts. The centre panels show a satellite view of each landform. The selected locations are shown in the left panels, and the wind forcing in the right panels, which are based on the ERA5 hindcast.

2.2. Coastal dune processes, landforms, and models

2.2.1. Processes governing landform development

Wind-driven sediment transport is the main driver of dune growth. The majority of available methods to predict aeolian sediment transport rates are based on the pioneering work by Bagnold (1937), describing the magnitude of aeolian sediment transport being dependent on a 3rd power of the wind velocity. However, in coastal environments, supply-limitations are believed to reduce aeolian transport to below the potential wind-driven transport capacity (Davidson-Arnott & Law, 1996; de Vries et al., 2014a). Many factors that can limit sediment supply have been described in literature. Examples of supply-limiting conditions are soil moisture (Bauer et al., 2009; Hallin et al., 2023a; Ruessink et al., 2022), and sediment sorting leading to the formation of desert pavements and armouring of the sediment surface (Carter, 1976; Hoonhout & de Vries, 2017; van IJzendoorn et al., 2023a; Strypsteen & Rauwoens, 2023; Uphues et al., 2022).

Wind shear varies spatially due to the interaction between coastal topography and wind flow. Horizontal wind flows may converge and diverge vertically when travelling up and downhill respectively. Converging and diverging wind flows lead to respective acceleration and deceleration of flow. Topographic features (steep gradients and/or structures) can also disrupt the flow, causing separation and even reversal of flow (Bauer et al., 2012; Hesp et al., 2015; Strypsteen et al., 2020; Walker & Nickling, 2002). The topographic steering of wind in coastal environments can shape coastal dune and beach morphology by influencing the location of sediment erosion and deposition (Arens, 1996). As a result, the topographic steering of wind can play a significant role in maximizing the heights of foredunes (Durán & Moore, 2013), stimulating blowout formation (Hesp, 2002; van Kuik et al., 2022; Ruessink et al., 2018), and modulating wind shear stresses across the beachface (Bauer, 1991).

Vegetation plays a key role in the development of dunes (Bonte et al., 2021). The presence of vegetation reduces the wind shear near the bed which may cause a spatial gradient in sediment transport and local depositions of sediments (Durán & Herrmann, 2006; Keijsers et al., 2015; Raupach et al., 1993). Dune vegetation species, such as marram grass, are characterized by their sand-trapping ability and capacity to grow with significant burial. The growth of some vegetation species may even be enhanced for certain sediment burial rates (Baas & Nield, 2007; Keijsers et al., 2016; Maun, 2009; Nolet et al., 2018). In addition to sediment burial rates, the establishment, growth, and resilience of dune vegetation are governed by numerous biotic and abiotic conditions, such as salinity, acting wind stress, groundwater levels, competition and removal by storm erosion (Homberger et al., 2024; Maun, 2009; van Puijenbroek et al., 2017a).

In addition to aeolian processes, the development of coastal dunes is influenced by marine dynamics (Cohn et al., 2018; van Westen et al., 2024a). The waterline provides a boundary condition to the aeolian domain and the exchange of sediment across the intertidal zone is governed by both marine and aeolian activities (Houser, 2009; Short & Hesp, 1982). Wave actions may influence the sediment availability for aeolian transport (Bauer et al., 2009; Hallin et al., 2023a; de Vries et al., 2014a). Also, extreme weather events can kill or remove vegetation causing erosion of the dunes. The combination of marine and aeolian processes contribute to the formation of coastal dunes.

2.2.2. Aeolian landforms and coastal dunes

Aeolian landforms are shaped by a complex interplay of the governing processes. In this study, four distinct types of aeolian landforms, having unique characteristics in terms of dimensions and dynamics, are used as demonstration cases. Real-world examples, as shown in Figure 2.2 are used for the setup and validation of the model (Section 2.3).

Barchan dunes (Figure 2.2-a) are crescent-shaped and migrate windward under relatively uniform wind conditions, which are characteristic of desert environments with limited sediment supply (Hersen, 2004; Hersen et al., 2002; Hesp & Hastings, 1998; Sauermann et al., 2000). Several measurements have been carried out to measure the morphological shape, size, and migration velocity (Hamdan et al., 2016; Hesp & Hastings, 1998; Sauermann et al., 2000). Barchan dunes have previously been used in modelling studies due to their typical and measurable shape and the simple conditions under which barchan dunes develop (Durán et al., 2010; Hersen, 2004; Parteli et al., 2007; 2014; Zhang et al., 2010).

Parabolic dunes (Figure 2.2-b) are vegetated dunes that migrate along the prevailing wind direction (Durán et al., 2008). The growth of vegetation can cause crescent dunes to be fixated and transformed into parabolic dunes, as addressed by several observations and modelling applications (Anthonsen et al., 1996; Baas & Nield, 2007; Barchyn & Hugenholtz, 2012; Durán & Herrmann, 2006; Reitz et al., 2010). Regions with relatively large sediment transports stay morphologically active and are often covered by vegetation, as erosion is strong enough to prevent growth. At the trailing horns, the stabilizing effect of vegetation is dominant, resulting in a U-shaped landform with its nose pointing downwind as opposed to the barchan dunes. In models that describe the formation of a parabolic dune, the magnitude of the active sediment transport must be in balance with the stabilizing effects of vegetation. Parabolic dunes make an ideal demonstration case for the impact of vegetation on sedimentation and erosion patterns and, thus, the long-term morphodynamic landform development.

Embryo dunes (Figure 2.2-c), alternatively referred to as incipient or Nebhka dunes, are the first stage of development of coastal dunes (Bonte et al., 2021; Hesp, 1989; 2002; Hesp & Smyth, 2017; Nield & Baas, 2008; van Puijenbroek et al., 2017b). After establishment, initial vegetation grows vertically and laterally, causing an embryo dune to grow. The formation of several embryo dunes may occur in parallel over a large space, and embryo dunes of similar shape and size can often be found in fields. Embryo dunes and accompanying vegetation may be washed away when they are submerged during high-water events. Embryo dunes may, therefore, often be a temporary or intermittent feature. However, embryo dunes can also grow to become established coastal foredunes (Montreuil et al., 2013).

Blowouts (Figure 2.2-d) are erosional features that form depressions within coastal dune systems (Hesp, 2002). Blowout initiation primarily occurs through the action of wind erosion, often at locations where the vegetation cover is weakened due to natural or anthropogenic impact, such as trampling (Schwarz et al., 2018). The wind erosion enlarges and deepens these initial depressions, creating the distinct bowl-shaped or elongated structures characteristic of blowouts. Vegetation growth on the trailing arms can transform the blowout into a parabolic-shaped landform (Arens et al., 2013a; Hesp, 2002; van Kuik et al., 2022; Laporte-Fauret et al., 2022). The closure of blowouts is driven by the re-establishment of vegetation at the blowout entrance, partially stabilizing the surface and preventing further erosion (Schwarz et al., 2018). In recent years, artificial blowouts created through vegetation removal or sand excavation have been implemented for nature conservation purposes (Figure 2.1).

2.2.3. Aeolian transport and dune models

In recent decades, development has shifted from qualitative descriptions of coastal dune development (Hesp, 2002; Short & Hesp, 1982) to more quantitatively predictive tools (Durán & Moore, 2013; Keijsers et al., 2016; Roelvink & Costas, 2019; de Vries et al., 2014a). We give an overview of several numerical models for coastal dune development that have been presented in recent years.

DUBEVEG, DUne BEach VEGetation, (Keijsers et al., 2016; Wijnberg et al., 2021) is a cellular automaton simulating long-term growth of extensive dune systems using probabilistic rules for erosion, deposition, and vegetation dynamics. DUBEVEG includes vegetation growth as a function of sedimentation, destruction due to seawater, lateral propagation, and establishment.

CDM, the Coastal Dune Model, (Durán & Moore, 2013) depicts the morphodynamic evolution of vegetated coastal foredunes. CDM can simulate rates of aeolian sediment transport and the eco-morphological feedback with topography and vegetation. It can produce complex shapes that rely on morphological feedbacks like parabolic and barchan dunes. However, it does not account for supply limitations affecting sediment availability for transport, and the wind conditions are implemented only for winds directly perpendicular to the shoreline.

DUNA (Roelvink & Costas, 2019) is a 1D dune profile model, particularly developed as an aeolian extension to the XBEACH model (Roelvink et al., 2009). This coupling to the XBEACH model allows for marine-aeolian interactions. Similarly to CDM, DUNA is based on a process-based description of aeolian sediment transport, in combination with topographic feedback and the shear-reducing effect of vegetation. Supply limitations are included through a parameterized approach, which may improve quantitative predictions. The current one-dimensional setup limits its applicability to coastal profiles only.

PSAMATHE (Ruessink et al., 2022) is a model that focuses on predicting aeolian sediment transport and the associated growth of foredunes on narrow beaches over periods ranging from months to years. The model uses a fetch based approach to account for sediment supply limitations, integrating processes related to spatiotemporally varying groundwater table, surface moisture content and aeolian sand transport rates.

AEOLIS is a process-based model simulating aeolian sediment transport under supply-limited conditions. It is based on one-dimensional process descriptions by Hoonhout and de Vries; de Vries et al. (2016, 2014a). Hoonhout and de Vries (2019) extended the model to be applicable to two-dimensional spatial domains that are relevant to specific management situations. Up until the current work it mainly describes multi-fractional sediment transport and various controls on sediment availability in both one and two spatial dimensions (Hallin et al., 2023a; van IJzendoorn et al., 2023a). At the start of this study, it did not encompass morphological feedback and dune-building processes like topographic steering and vegetation dynamics.

State-of-the-art numerical tools that describe sediment transport and dune development have provided valuable insights. However, the usability of these individual models remains limited for management applications because the processes, spatiotemporal resolutions and timescales between models and applications do not match. Either not all relevant processes are sufficiently included, or the applicability of the model is restricted by practical limitations (e.g., one-dimensional profile model or only perpendicular winds).

For this study, we use the AEOLIS sediment transport model as a starting point, given its open-source availability and modular setup. We extend the AEOLIS sediment transport model using new process implementations of essential processes that describe dune development. Concepts of existing models like CDM and DUBEVEG serve as inspiration for part of this work and we provide references to the original work where appropriate.

2.3. Model Implementations of Processes

AEOLIS is extended here with functionalities relative to the original open-source model as presented by Hoonhout and de Vries (2016) that allow for the simulation of landforms by implementing the effect of topographic steering on wind shear, vegetation processes in the form of vertical growth, lateral spreading, and reduced wind shear, as well as avalanching of steep slopes and swash impact on vegetation and dune formation.

For comprehensive details on the pre-existing core functionalities of the AEOLIS model readers are directed to de Vries et al. (2014a), Hoonhout and de Vries (2016) and van IJzendoorn et al. (2023a). For the landform development described in this paper, the moisture module (Hallin et al., 2023a) and grain size sorting module (van IJzendoorn et al., 2023a) are not used. The model structure and the relation between all implemented processes are illustrated in Figure 2.3.

The forcing conditions of AEOLIS consist of wind speed, wind direction, water levels and wave conditions. All forcing conditions can be assumed constant but may also vary in time. Although not applied in this study, it is technically also feasible to input spatially variable forcings into the model.

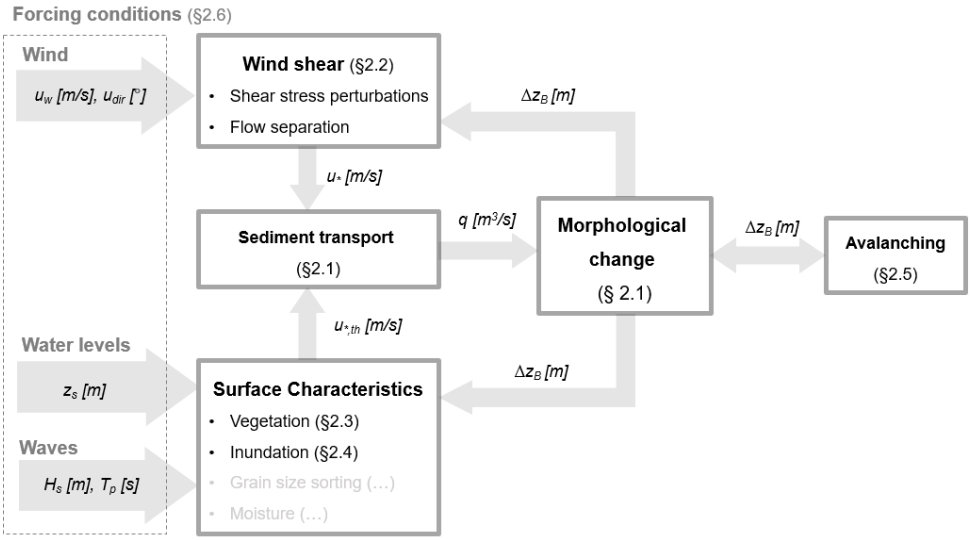

Figure 2.3.: Flowchart showing the implemented processes in AEOLIS.

2.3.1. Sediment transport and morphological change

AEOLIS involves a two-dimensional continuum approach to sediment transport including sedimentation and erosion in Eulerian space. This is described after Hoonhout and de Vries (2019) as:

$$\frac{\partial c}{\partial t} + u_{\text{sed,x}} \frac{\partial c}{\partial x} + u_{\text{sed,y}} \frac{\partial c}{\partial y} = E - D \tag{2.1}$$

where c [kg/m^3] is the sediment concentration in the air. $u_{\text{sed,x}}$ [m/s] and $u_{\text{sed,y}}$ [m/s] are horizontal sediment velocities in x- and y-direction respectively. The right-hand side of equation (2.1) describes the exchange of sediment with the bed where D [kg/m^2/s] represents potential deposition and E [kg/m^2/s] the potential erosion. Erosion and deposition is governed by the concentration at transport saturation c_{sat} [kg/m^3] and available sediment at the bed m_{a} [kg/m^2] through:

$$E - D = \min\left(\frac{\partial m_{\text{a}}}{\partial t} \quad ; \quad \frac{c_{\text{sat}} - c}{T} \right) \tag{2.2}$$

where T [s] is a timescale for sediment exchange between the sediment bed and the transport layer in the air. For the details on calculating saturated sediment transports and the potential erosion and deposition, we refer to the work in de Vries et al. (2014a) and Hoonhout and de Vries (2016). For simplicity, the horizontal sediment velocity u_{sed} may be assumed to be equal to the wind velocity u_w [m/s]. But, predictions of the actual saltation velocity could provide a more realistic description of the horizontal sediment velocity (Sauermann et al., 2001). The horizontal sediment velocity can be determined from the momentum balance that is described in Durán (2007) by three terms. Term I: the drag force acting on the grains. Term II: the loss of momentum when they splash on the ground. Term III: the downhill gravity force:

$$\frac{(\vec{v_{eff}} - \vec{u_{sed}})|\vec{v_{eff}} - \vec{u_{sed}}|}{u_f^2} - \frac{\vec{u_{sed}}}{2\alpha|\vec{u_{sed}}|} - \nabla\vec{z}_B = 0 \tag{2.3}$$

where v_{eff} [m/s] is the effective wind velocity driving the grains, resulting from the feedback effect of sand transport within the saltation layer, being a function of the shear velocity u_* [m/s] and shear velocity threshold $u_{*,th}$ [m/s]. Furthermore, u_f [m/s] is the grain settling velocity and ∇z_B [-] is the downhill gravity force. The parameter α (=0.42 [-] for d=250 μm), acts as an effective restitution coefficient for the grainbed interaction. Note that the computed u_{sed} represents the collective horizontal sediment movement and not the velocity of individual grains. AEOLIS solves equation (2.3) iteratively for each timestep.

The update of bed levels z [m] is introduced as a function of erosion and deposition, varying over time:

$$\frac{\partial z}{\partial t} = \rho_{\text{sed}} \frac{1}{1-p} (E - D) \tag{2.4}$$

where ρ_{sed} [kg/m^3] is the sediment density and p [-] is the sediment porosity. (Note that equations (2.1) and (2.4) are equivalent to the general Exner equation (Paola & Voller, 2005) when $\frac{\partial c}{\partial t} = 0$).

2.3.2. Wind shear and topographic steering

To simulate the topographic steering effects on desert and coastal landforms, numerous studies have utilized computational fluid dynamics (Bauer & Wakes, 2022; Hesp et al., 2015; Pourteimouri et al., 2023; Smyth et al., 2011; Wakes et al., 2010). However, the computational costs of these methods currently limit their use when long-term morphodynamic simulations tailored for engineering applications are pursued. To reduce computational costs, we adopt the techniques proposed by Durán and Moore (2013) that consist of an analytical approach tailored for calculating topographic wind steering for smooth topographies combined with a modelled separation bubble mechanism. In addition to the adopted techniques by Durán and Moore (2013) we implemented the ability to use varying wind directions that occur in realistic situations.

The starting point for calculating near-bed shear velocity u_* [m/s] and topographic steering is the Prandtl-Von Karman's Law of the Wall. The Law of the wall is used to convert the wind velocity u_w [m/s] at height z [m] above the bed to the near-bed shear velocity:

$$u_* = \frac{u_w}{\ln \frac{z}{z_0}} \kappa \tag{2.5}$$

where z_0 [m] is the roughness height above the bed and κ [-] is the von Kármán constant for turbulent flow. z_0 can also be determined based on a roughness height predictor as described by van Rijn and Strypsteen (2020) and Strypsteen (2023).

The topographic steering of the wind due to smooth gradients is implemented following an analytical perturbation theory for turbulent boundary layer flow (Kroy et al., 2002; Weng et al., 1991), as shown in Figure 2.4. This method describes the topographic impact through perturbations in the shear stress τ [N/m^2] ($\tau = \rho_a {u_*}^2$):

$$\vec{\tau}(x,y) = \vec{\tau}_0 + |\vec{\tau}_0| \delta\vec{\tau}(x,y) \tag{2.6}$$

where $\delta\vec{\tau}(x,y)$ is the shear stress perturbation and τ_0 is the computed shear stress on a flat topography. For two-dimensional situations, the shear stress perturbation in x- and y-direction ($\delta\tau_x$ and $\delta\tau_y$) is computed in Fourier space. A more detailed description of the shear stress perturbation theory is given in Appendix A.

The implementation of the shear perturbation theory by Weng et al. (1991) is only valid in situations with relatively smooth surfaces. In coastal environments, the existence of slipfaces and vegetation often results in rougher terrain, featuring sharp edges and steep slopes which lead to separation of wind flow (Davidson et al., 2022; Jackson et al., 2011). The occurrence of such steep slopes limits the validity of the Weng et al. (1991) approach.

To address this, a heuristic description of flow separation is used following CDM (Durán & Moore, 2013; Kroy et al., 2002; Sauermann et al., 2001). A smooth envelope is created, which separates the main flow when a sharp edge is detected in windward direction. This smooth envelope is called a separation bubble z_{sep} [m].

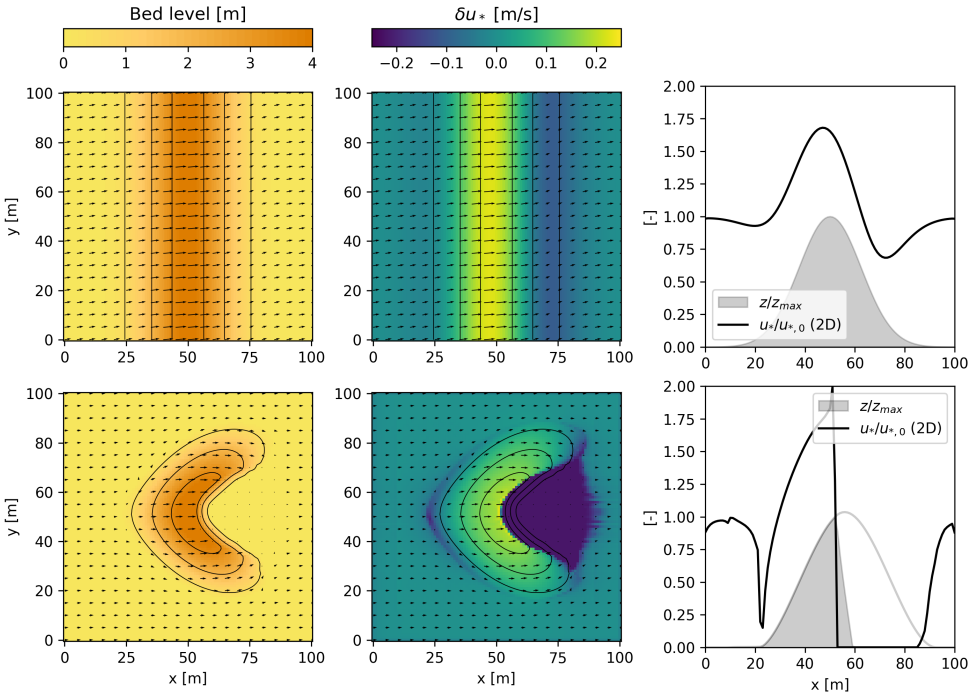

Figure 2.4.: Spatial variation in shear stress due to topographic steering of the wind field. The upper panels show the bed level z_B [m] and shear stress velocity perturbation δu_* [m/s] over a uniform Gaussian hill. The lower panels show topographic steering over a barchan dune, including the influence of flow separation. The right panels compare outcomes of the one- and two-dimensional approaches.

This separation bubble represents the surface that divides the region of flow reversal from the main flow stream along the smooth hill. Subsequently, in all cells for which the bed level is lower than the separation bubble ($z_B < z_{sep}$), the shear velocity u_* is set to 0 m/s. This assumes that eventual flow reversal velocities are not significant enough to initiate aeolian transport. The formulations describing the shape of the separation bubble are given in A.

Figure 2.4 shows the decrease on the windward- and lee-side of both Gaussian- and barchan-shaped landforms and an increase over the crest. Additionally, a shear velocity of zero is shown below the separation bubble. Studies have demonstrated the accuracy of the general analytical shear stress prediction approach applied to coastal dunes by comparing it with real-world measurements and detailed numerical simulation results acquired with CFD, Computational Fluid Dynamics, models (Cecil et al., 2024; Kombiadou et al., 2023).

The implementation of the perturbation theory and separation bubble allows only for wind conditions that are perpendicular to the grid. To enable model applicability independent of wind direction, we developed a method that creates a secondary rotational grid that is aligned with the wind direction at each timestep, as shown in Video S1[1].

2.3.3. Vegetation at the sediment surface

Vegetation acts as a natural obstacle to aeolian sediment transport by reducing the near-bed shear stresses. The impact of vegetation on dune development is included in AEOLIS by describing the intrinsic development of vegetation, considering growth and decay due to burial (Durán & Moore, 2013), lateral growth and establishment (Keijsers et al., 2016), and the destruction of vegetation due to hydrodynamic processes is simulated by reducing vegetation density after cell inundation.

Durán and Moore (2013) describe the reduction of shear stress as a function of vegetation density (ρ_{veg}) and a dimensionless roughness factor (Γ).

$$\tau_s = \frac{\tau}{1 + \Gamma \rho_{veg}} \tag{2.7}$$

where τ_s is the remaining shear stress at the sediment surface. The default value of Γ=16 is derived from vegetation geometry (Durán & Herrmann, 2006).

The vegetation density ρ_{veg} varies in time and space as a function of vegetation growth and burial, and is assumed to be dependent on the maximum vegetation height $h_{veg,max}$ [m] and the vegetation height h_{veg} [m]:

$$\rho_{veg} = \left(\frac{h_{veg}}{h_{veg,max}} \right)^2 . \tag{2.8}$$

where vegetation growth and decay are computed according to Durán and Herrmann (2006), reads:

$$\frac{\delta h_{veg}}{\delta t} = V_{ver} \left(1 - \frac{h_{veg}}{h_{veg,max}} \right) - \gamma_{veg} \left| \frac{\delta z_{b,veg}}{\delta t} \right| \tag{2.9}$$

with V_{ver} [m/s] representing the vertical growth rate of vegetation. The γ_{veg} [-] parameter is a sediment burial factor that accommodates the influence of sediment burial on vegetation growth.

[1]Video S1: Rotational grid method for wind direction alignment.
Available at: https://ars.els-cdn.com/content/image/1-s2.0-S1364815224001543-mmc1.mp4

The onset of vegetation may occur due to lateral propagation of vegetation or random establishment through germination. Once vegetation is established it is assumed to be able to grow and propagate laterally. The inherent uncertainties related to the random establishment of vegetation are implemented on a cell-by-cell basis by using a probabilistic approach, comparable to the cellular automata method discussed by Keijsers et al. (2016). AEOLIS accommodates assuming a germination probability ρ_{ger} [-] in every grid cell. This probability is assumed equal over the domain except for eroding grid cells (negative bed elevation change) where ρ_{ger} is assumed 0.

The onset of vegetation through lateral propagation per grid cell is derived by identifying the interfaces between vegetated and non-vegetated cells. The parameter ρ_{lat} alters the probability of lateral propagation at each interface.

2.3.4. Avalanching

Steep slopes may result from bed level changes that occur due to simulated sedimentation and erosion. The angle of repose θ_{ava} (default: 33 °) determines the maximum slope that may exist due to the sediments' angle of internal friction. AEOLIS derives the spatial distribution of slopes based on each timestep's spatial gradients in morphology. If a critical slope is exceeded, a mass-conserving gravity-driven (downward) transport of sediment is simulated until all cells in the domain satisfy the critical slope. This technique is adopted from Durán and Moore (2013).

2.3.5. Marine influence

The sediment surface is submerged when the bed level is lower than the total water level (TWL). TWL is computed by adding the still water level and the computed run-up Stockdon et al. (2006). The model effects are threefold:

(i) Vegetation parameters are reset to zero, indicating the death of vegetation. This results in the intertidal zone or areas frequently inundated, typically lacking vegetation. Post-high water events, vegetation must re-establish in these areas;

(ii) The bed level slowly resets towards its initial position once submerged. Small dune features, such as embryo dunes, are levelled, and eroded sediment transport from the intertidal is re-supplied. This is based on the assumption that marine-driven morphodynamics dominate the intertidal.

(iii) The inundation of cells causes sand to be wet, reducing the aeolian sediment transport to 0 according to Hallin et al. (2023b).

2.4. Landform Simulations

Simulations of four distinct landforms are used to illustrate the model's application range. The simulations are either subjected to academic conditions, to showcase key fundamental landform development, or real-world conditions to demonstrate the model's practical applicability at engineering scales. Wind data employed in the real-world simulations are derived from the ERA5 dataset (Hersbach et al., 2020), as illustrated in Figure 2.2, except where specified otherwise. For consistency, all simulations are performed with one sand fraction, assuming a diameter of 250 μm.

Both academic and real-world simulations are validated against existing literature and measurement data. Depending on the landform type and the availability of data, different characteristics are used for validation. Each landform-type simulation is connected to one of the landform-shaping processes. Barchan dunes are simulated to demonstrate the description of topographic steering. The influence of vegetation on sediment transport and vegetation establishment is demonstrated by simulating parabolic and embryo dunes, respectively. The development of real-world blowouts is simulated to demonstrate all the processes above under real-world conditions, at an engineering scale. A key aspect of the model setup is ensuring complete reproducibility of all simulations. Table B.1 (B) provides a summary of these landform simulations, including the simulation names for reproduction.

2.4.1. Barchan dunes

A set of academic simulations is performed to verify the model's technical capacity to describe the characteristic crescentic shape of barchan dunes under varying wind conditions. Three mean wind directions are chosen (μ: 270, 45, 170 [°]). For each direction, different degrees of wind spreading are introduced (σ: 0, 22.5, 45 [°]), resulting in nine unique synthetic wind time series. The resulting crescentic shape should be independent of the wind direction, while the introduction of wind spreading is anticipated to yield a more rounded dune shape. Each series is generated by selecting 500 random wind events from a normal distribution based on each μ and σ pairing. The wind speed u_w is set at 12 m/s at a height of 10 m above the surface. The initial topography of each simulation is a cone-shaped feature in the centre of the computational domain with a volume of 13404 m^3, placed on top of a non-erodible layer (z_{ne} = 0 m).

For quantitative model validation, barchan dunes are simulated under real-world conditions in the Sahara desert, southern Morocco (see Figure 2.2-a). In 1999, Sauermann et al. (2000) measured various characteristic dimensions of eight barchan dunes. The wind conditions for the simulation are derived for the 1995-1999 period, preceding measurements by Sauermann et al. (2000). The initial topography replicates a cone-shaped feature, with the initial volume set to match the volumes by Sauermann et al. (2000). Circular boundary conditions are imposed to ensure mass conservation and a constant barchan dune volume over the simulation duration. The simulated period totals 24 years.

To validate the simulated barchan shape, the reported linear scalings between barchan dune volume, V [m^3], height, h [m], length, L [m] and width, W [m] are used (Hesp & Hastings, 1998; Sauermann et al., 2000). While the migration velocity was not directly measured by Sauermann et al. (2000), various literature reported the migration velocity to scale with saturated transport on a flat bed, and the inverse of the dune size (Durán et al., 2010):

$$v \approx \alpha q_{sat,0}/W \tag{2.10}$$

Where $q_{sat,0}$ $[m^3/m]$ is the saturated sediment flux over a flat bed (= $C_{sat,0} \cdot u_{sed,0}$), and constant α being approximately equal to 50 [-].

2.4.2. Parabolic dunes

Dynamic parabolic dunes are in a transitional state, starting with active barchan dunes with no vegetation towards static vegetated parabolic dunes (Durán et al., 2008). Durán and Herrmann (2006) introduced a fixation index as a measure of dune activity to quantify the balance between the stabilizing influence of vegetation and active sediment transport:

$$\Theta \equiv \frac{q_{sat,0}}{V^{1/3} V_{\text{ver}}} \tag{2.11}$$

where $V^{1/3}$ is a length scale related to the dune volume V. Durán and Herrmann (2006) found that when $\Theta \gtrapprox 0.5$ [-], the impact of the active sediment transport is larger than the fixation by vegetation leading to a non-stabilized dune. To evaluate the model's ability to simulate the vegetation fixation-mobilization balance, three parabolic dunes are simulated, each with differing rates of vegetation growth (V_{ver}) at 3.5, 6.0, and 8.5 m/year. A constant wind speed of 10 m/s in a positive x-direction is used. In this case, both wind conditions and vegetation growth rates solely serve an academic objective. These wind speeds and growth rates correspond to fixation indices θ of approximately 0.85, 0.50, and 0.35, respectively.

For a quantitative model validation, the 'real-world' conditions along the coast of Ceará in Brazil are simulated (see Figure 2.2-b). This coastline is characterized by many sections covered with coastal dunes experiencing varying levels of stabilization (Durán et al., 2008). The wind conditions for the simulation are derived for the 1995-1999 period, preceding the measurements by Sauermann et al. (2000). The period from July to December is characterized by dry, windy conditions favourable for dune mobilization, while January to June marks the rainy season, typically featuring winds below the threshold velocity for aeolian transport. In two different simulations, vegetation growth is modelled at a constant 0.18 and 0.25 m/year. Therefore, the influence of seasonal abiotic factors like rainfall and temperature on vegetation growth is ignored. The initial topography replicates a cone-shaped feature, with the initial volume set to match the volumes by Sauermann et al. (2000). The landform's centre of gravity is tracked to determine the migration velocity over a simulation period of 40 years. To our knowledge, no measurement data is available over such extensive periods. Therefore, validation is primarily based on typical migration rates mentioned in literature (Goudie, 2011).

2.4.3. Embryo dunes

In coastal environments, marine influences on aeolian sediment transport and vegetation significantly impact the ecomorphological development of landforms. The presence of a waterline is lacking in both barchan and parabolic dune simulations. To assess the model's ability to describe dune development in a coastal setting, the formation of an embryo dune field under marine influences is simulated. Our simulation is based on observations of an embryo dune field along the coast of the island Texel, Netherlands (van Puijenbroek et al., 2017c). Drone photography was used to construct digital elevation models, encompassing both summer and winter.

We attempt to reproduce the observations by van Puijenbroek et al. (2017c) by simulating a flat, sloping beach with randomized vegetation establishment and the presence of a waterline. The simulation period is 5 years. Water levels and wave conditions are obtained from Rijkswaterstaat's Waterinfo database at Eurogeul (Rijkswaterstaat, 2024), located ≈ 100 km south of the location of interest. A non-erodible layer is implemented just below the initial bed level ($z_{ne} = z_{B,0} - 0.1$), stabilizing the coastal profile. The bed levels in submerged cells are gradually reset to their original elevation, compensating for aeolian erosion and replicating marine-driven supply into the intertidal zone. The model's implementation of storm erosion lacks an accurate description of sediment transport due to surf- and swash-related processes. Therefore, it's unrealistic to expect accurate reproduction of the removal of embryo dune features.

The model assumes a vegetation establishment probability of 0.05 m^2/year and lateral vegetation spread at 0.2 m^2/year, aligning with the model settings of DUBEVEG in Keijsers et al. (2016). Once cells are submerged, vegetation is removed. To restrict our focus to the establishment and removal of vegetation, the vertical vegetation growth V_{ver} is set at 10 m/year, meaning that vegetation can outgrow any burial rate. A benchmark simulation, without vegetation establishment, is conducted to validate the onshore aeolian transport flux, yielding an average influx of ≈16 m^3/m/year, lower than van Puijenbroek et al. (2017c) found at ≈30 m^3/m/year.

The validation is aimed at qualitatively reproducing the seasonal variability in dune establishment, removal and growth. Additionally, we want to assess whether the model is capable of reproducing the sheltering effect of other dunes on growth as found by van Puijenbroek et al. (2017c).

2.4.4. Blowouts

The blowout simulation is based on the evolution of five foredune notches located in National Park Zuid-Kennemerland (NPZK), the Netherlands (see Figure 2.2-d). We attempt to simulate the geomorphic response of this coastal area after the excavation of the notches as examined by Ruessink et al. (2018). The simulation is set up for 10 years (2013-2023), extending upon the evaluation period by Ruessink et al. (2018). The initial topography obtained from DEMs is built upon LiDAR measurements of the Dutch dunes (Bochev-van der Burgh et al., 2011). The water level and wave conditions are obtained from observations at Eurogeul (Rijkswaterstaat, 2024).

For the sake of applicability and reproducibility, the model complexity is reduced by making some heuristic assumptions. The groundwater table is located 0.1 meters below the initial bed level across the domain, similar to the embryo dune simulations. This prevents erosion from the upper beachface, while sediment availability is ensured in the intertidal area by resetting the bed level elevation of submerged cells. Additionally, the groundwater has a maximum level of 5.5 m+NAP, setting a maximum erosion depth within the blowout features. The vegetation density ρ_{veg} is set to 1.0 [-] landward of the dunefoot (2 m+NAP), while the notches are non-vegetated. The vertical growth rate of vegetation V_{ver} is set to be 3 m/year. This growth rate is slightly higher compared to marram grass typically found along the Dutch coast, to ensure the foredune vegetation survives high deposition rates. The ability of the vegetation to re-establish is excluded by turning off lateral growth and germination, disabling blowout closure. To replicate the stabilizing effect of roots on the sediment, the angle of repose is increased to 44° The separation bubble is disabled, as the implementation is deemed not suitable for such a complex and dynamic coastal environment. The computational domain, vegetation coverage and initial topography are shown in Figure 2.5.

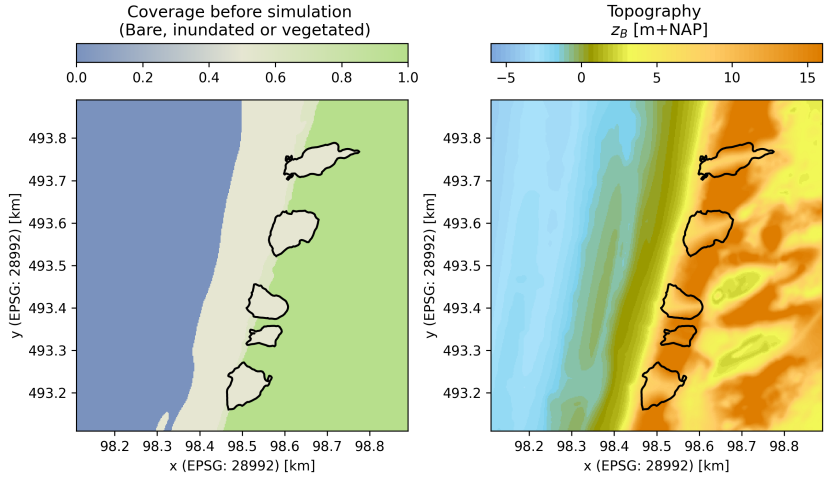

Figure 2.5.: Setup of a simulation of five excavated notches at the National Park Zuid-Kennemerland (NPZK). The left panel shows the sand coverage, being inundated (blue), vegetated (green) or bare (yellow) at the start of the simulation. The right panel shows initial bed levels based on LiDAR.

For validation, the simulated bed level change is compared with the measured annual topography (Bochev-van der Burgh et al., 2011). All data points that could potentially be inundated (<2 m+NAP) are filtered out of the measurement data to prevent inconsistencies due to ocean surface reflections. The simulation and measurement results are visually compared and analysis of the erosional and depositional sediment volumes from the blowouts into the backdune is carried out for a quantitative validation.

2.5. Results

2.5.1. Barchan dunes

The results of the barchan dune simulations using academic wind conditions coming from varying directions are presented in Figure 2.6. The left panels reveal that the dunes' migration direction and orientation consistently align with the wind direction. The imposed wind direction does not significantly alter the crescentic shape of the dunes. The simulated features are mass conserving. Also, when increasing the directional spread ($\sigma = 0°$ in the left panels to $\sigma = 45°$ in the right panels) a different (less pronounced) crescentic shape was simulated.

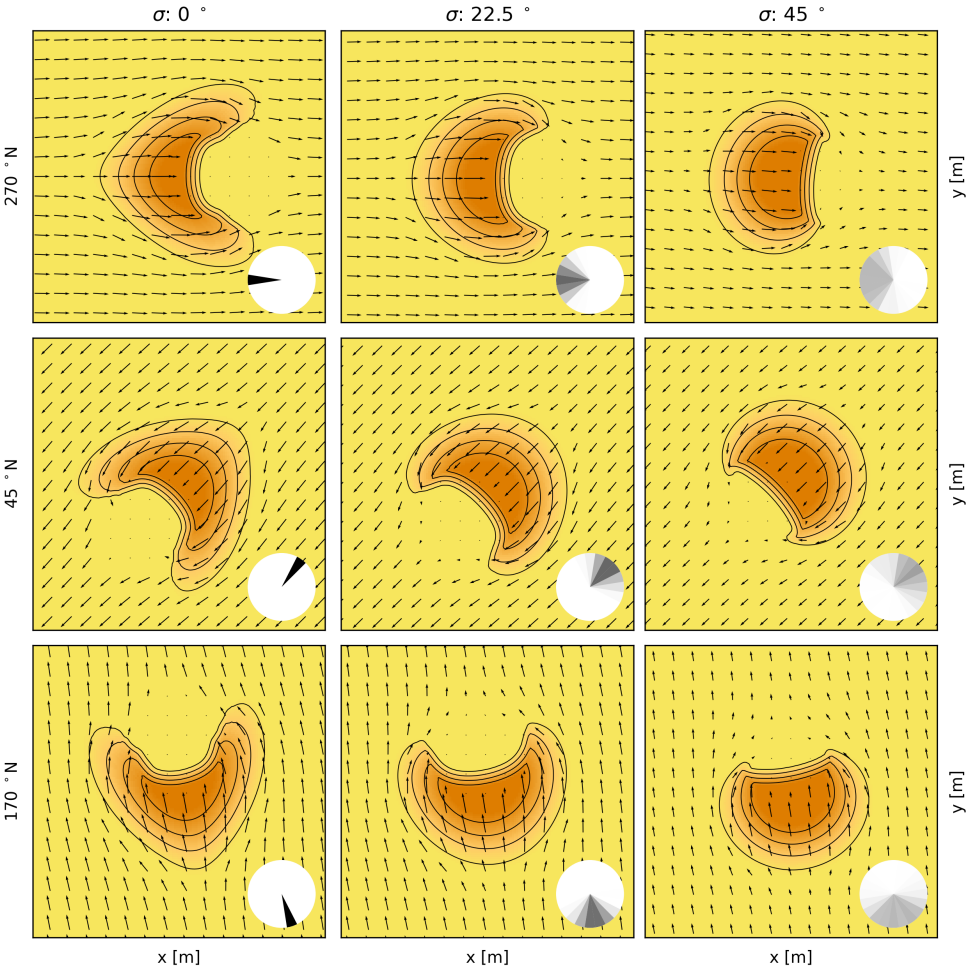

Figure 2.6.: Demonstration of the model's ability to simulate landforms for wind coming from different directions (top to bottom) and for different spreading rates (left to right).

The shape and migration velocity of the eight simulated Moroccan barchan dunes, compared with real-world measurements by Sauermann et al. (2000), are depicted in Figure 2.7. After 5-10 years of simulation the equilibrium shape of these dunes is achieved (top-left panel of Figure 2.7). Dune dimensions are calculated using a rotated coordinate system with the dune's crest as the origin, as shown in the bottom-left panel of Figure 2.7. Dune heights vary between 3-9 meters and align with the height-to-volume ratio (h and V) observed by Sauermann et al. (2000). However, the dune length (L) relative to height is slightly underpredicted, as shown in the top-right panel of Figure 2.7. The height-to-width (h and W) ratio matches closely with observations by Sauermann et al. (2000), Finkel (1959) and Hastenrath (1967) as shown in the bottom-right panel of Figure 2.7.

The migration velocity of the simulated barchan dunes is determined by tracking the location of the dune crest, with the results displayed in the bottom-centre panel of Figure 2.7. The findings reveal that the dunes' migration velocity decreases as their size increases, aligning well with Eq. 2.10 proposed by Durán et al. (2010).

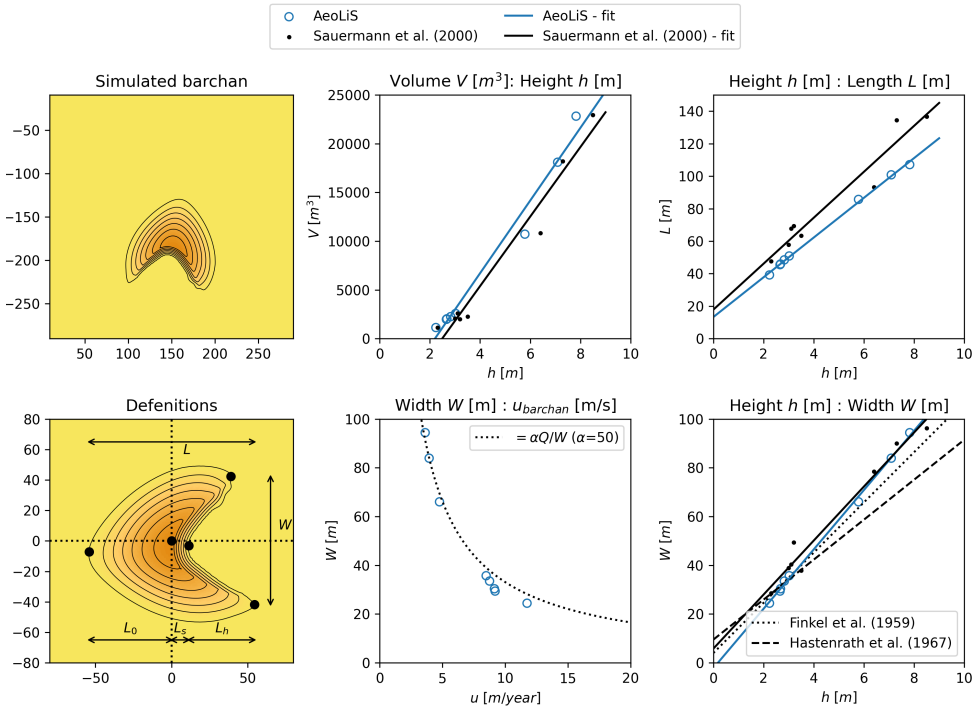

Figure 2.7.: Quantitative comparison between the simulated and observed volume V, height h, length L and width W for eight barchan dunes located in Morocco (Finkel, 1959; Hastenrath, 1967; Sauermann et al., 2000). The migration velocity is compared with the proposed relation in Eq. 2.10 (Durán et al., 2010).

2.5.2. Parabolic dunes

The results of the parabolic dune simulations with varying fixation indices are displayed in Figure 2.8. For animated simulation results, see Video S2[2].

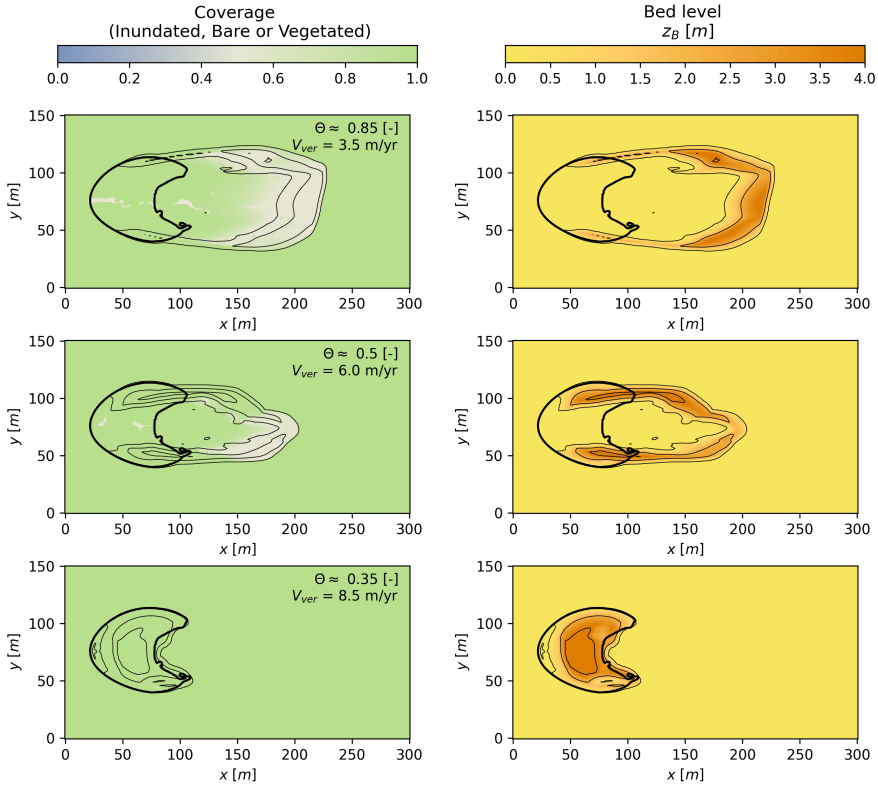

Figure 2.8.: Simulation overview of three simulated parabolic dunes for varying settings of fixation index ($\Theta \approx$ 0.85, 0.50, and 0.35 [-]) by varying vegetation growth speed (V_{ver}: 3.5, 6.0, and 8.5 m/year, resp.).

The left panels show the simulated sand cover – bare (yellow) or vegetated (green) – based on the vegetation density ρ_{veg} at corresponding times. The right panels illustrate the topographic result after 4 years. The upper panels illustrate a dune with a vegetation growth V_{ver} of 3.5 m/year, resulting in a fixation index Θ of 0.85 (-), where the dune is mostly unvegetated and migrates windward. This aligns with the observations by Durán and Herrmann (2006) that landforms with a Θ larger than approximately 0.5 are too dynamic to stabilize. Increasing V_{ver} to 6.0 m/year, Θ = 0.50 (-), leads to a more significant fixation of the dune, as shown by the thicker trailing arms and greater vegetated areas in the centre panels.

[2]Video S2: Development of parabolic dunes under varying growth conditions.
Available at: https://ars.els-cdn.com/content/image/1-s2.0-S1364815224001543-mmc2.mp4

The highest vegetation growth rate simulation (V_{ver} = 8.5 m/year), corresponding to the lowest fixation index Θ = 0.35, results in almost immediate dune stabilization. Although this trend of decreasing dynamics with higher vegetation growth aligns with earlier work, the extent of stabilization in these simulations is more severe than reported by Durán and Herrmann (2006) for comparable fixation indices.

The results of the simulated parabolic dune development under real-world Brazilian wind conditions are illustrated in Figure 2.9. For animated simulation results, see Video S3[3]. Generally, parabolic dunes worldwide migrate at velocities ranging from 2 to 7 m/year, as detailed in Goudie (2011). In these simulations, despite neglecting vegetation's dependency on abiotic conditions, the incorporation of real-world wind data introduces seasonal variability. With a vertical vegetation growth, V_{ver}, of 0.18 m/year, the average annual migration rate is between 2-3 m/year, as shown by the blue dotted line in Figure 2.9. For a slightly higher V_{ver} of 0.25 m/year, the migration rate decreases over time, leading to near-complete fixation after 40 years, indicated by the orange dotted line. Also, the simulations include some significant seasonal variability in migration speed. Monthly averages of migration rates reach up to 9 m/year during windy periods. Complete stabilization is simulated in calmer months. This suggests substantial differences in fixation index across seasons.

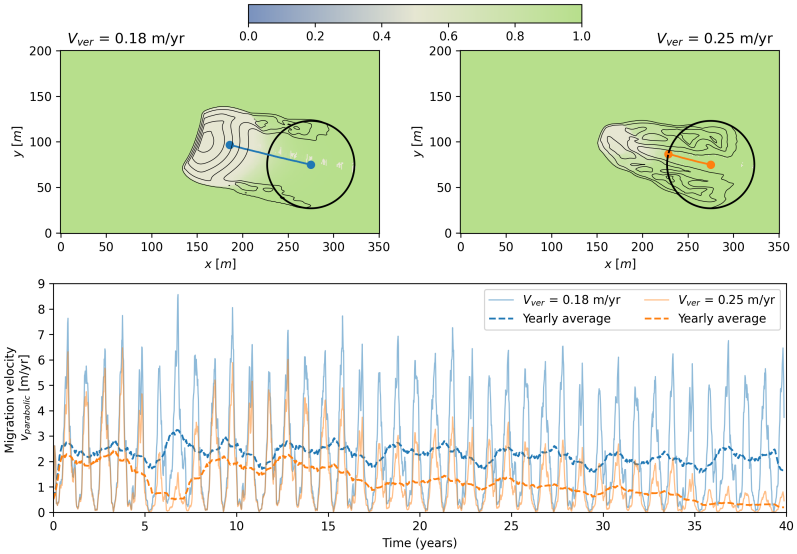

Figure 2.9.: Migration of parabolic dunes under real-world, Brazilian, wind conditions. The centre of both dunes is traced, indicated by the blue and orange lines. The lower panel displays the monthly (continuous) and yearly (dotted) averaged migration rates for both simulations.

[3]Video S3: Development of excavated notches.
Available at: https://ars.els-cdn.com/content/image/1-s2.0-S1364815224001543-mmc3.mp4

2.5.3. Embryo dunes

Figure 2.10 showcases the simulated initialization, growth, and destruction of embryo dunes. The top-left panels illustrate the early establishment of vegetation. Subsequently, vegetation patches begin to grow both vertically and laterally due to sediment deposition and lateral vegetation spread. This leads to an increase in the footprint and volume of the embryo dunes, which gradually coalesce into larger dune formations. The progression of this growth and merging of dunes over time is depicted in the centre and right panels of Figure 2.10, corresponding to 2.5 and 4.5 years into the simulation, respectively.

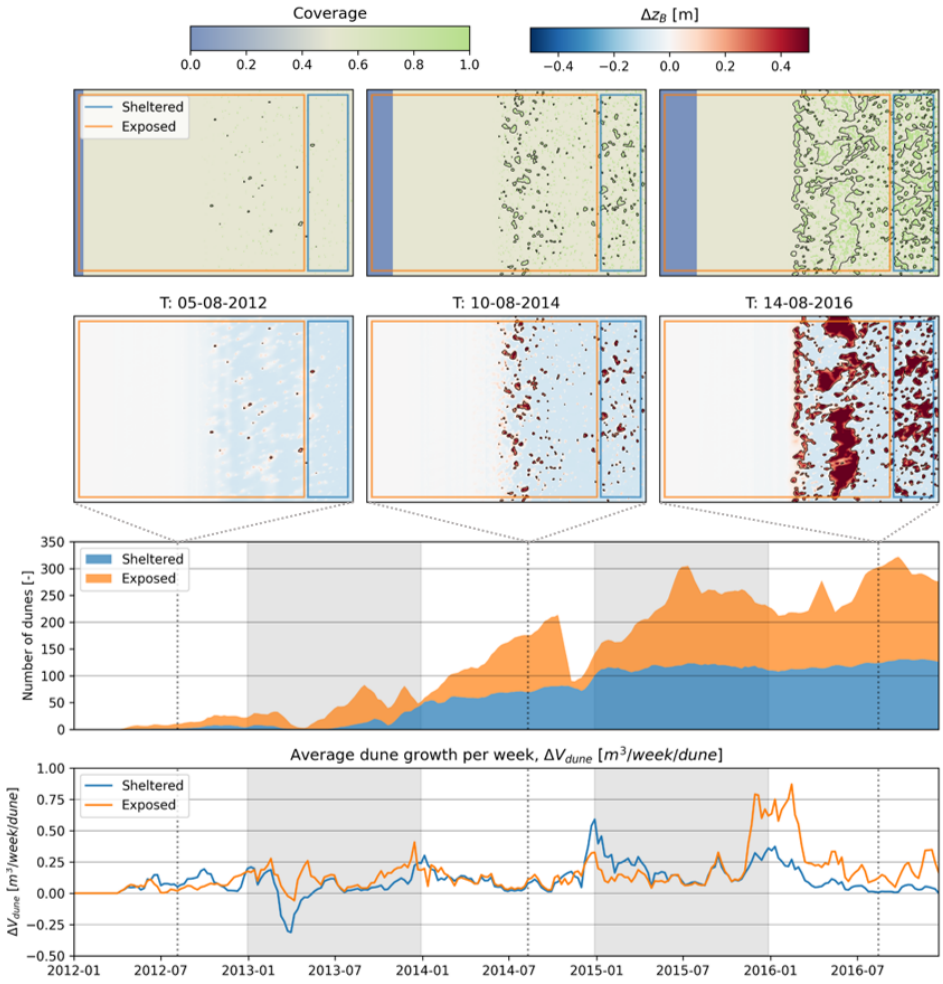

Figure 2.10.: Simulation overview of the development of an embryonic dune field, including vegetation establishment, growth, and destruction.

The third panel of Figure 2.10 illustrates the evolution in the number of embryo dunes, highlighting marked developmental differences between dunes in the zone exposed to marine influences and the zone sheltered from marine influences. Exposed dunes see their numbers sharply decrease at the onset of several stormy seasons, particularly during the winter of 2014/2015. Conversely, the count of sheltered dunes steadily rises and stabilizes around 120 after three years. Initially, when the exposed embryo dunes are relatively small, both sheltered and exposed dunes exhibit similar growth rates, as illustrated by their respective weekly volumetric growth ΔV_{dune} shown in the fourth panel. This may suggests that sediment capture by seaward dunes did not significantly affect the sheltered dunes. However, this dynamic changes after the exposed dunes undergo significantly more growth than the sheltered ones in the winter of 2015/2016, likely because they capture the majority of the sediment, limiting the remaining flux towards the sheltered zone. This simulated behaviour is consistent with the findings by van Puijenbroek et al. (2017c), whose measurements occurred in a dune field estimated to be in a similar stage of development—about five years after its initial formation — as the final year of our simulation.

2.5.4. Blowouts

For the model-data comparison, the volumetric analysis carried out by Ruessink et al. (2018) is partly reproduced and extended, as displayed in Figure 2.11e. Volumetric analysis is carried out based on three geomorphic units: 1) notches; 2) foredune; 3) backdune; after (Ruessink et al., 2018). The domain is and these respective units are shown in Figure 2.11c.

The initiation and early development of the notches in the coastal foredunes along the NPZK region are simulated over a 10-year period. The erosion from the notches, driven by airflow acceleration throughout the blowouts (see arrows in Figure 2.11d), is visually similar to observations (Figure 2.11a & b). The centre of the blowout erodes up to the assumed non-erodible layer due to soil moisture and most wind-erosion happens at the erosional walls. The simulated volume eroded from the notches corresponds well with the observations (purple line in Figure 2.11e). Measurements show much of the eroded sediment to be deposited in the backdune, resulting in an onshore migration of the overall dune volume, as shown by the red patches in Figure 2.11a. Although this behaviour is reproduced by the model, the backdune deposition is underpredicted by the model with 62.5% when compared to measurements. As the erosional volume from the notches is slightly overestimated at 25.5%, sediment which is expected to be deposited in the backdune, a limited amount of pick-up from the beachface likely explains the majority of this underprediction in deposition.

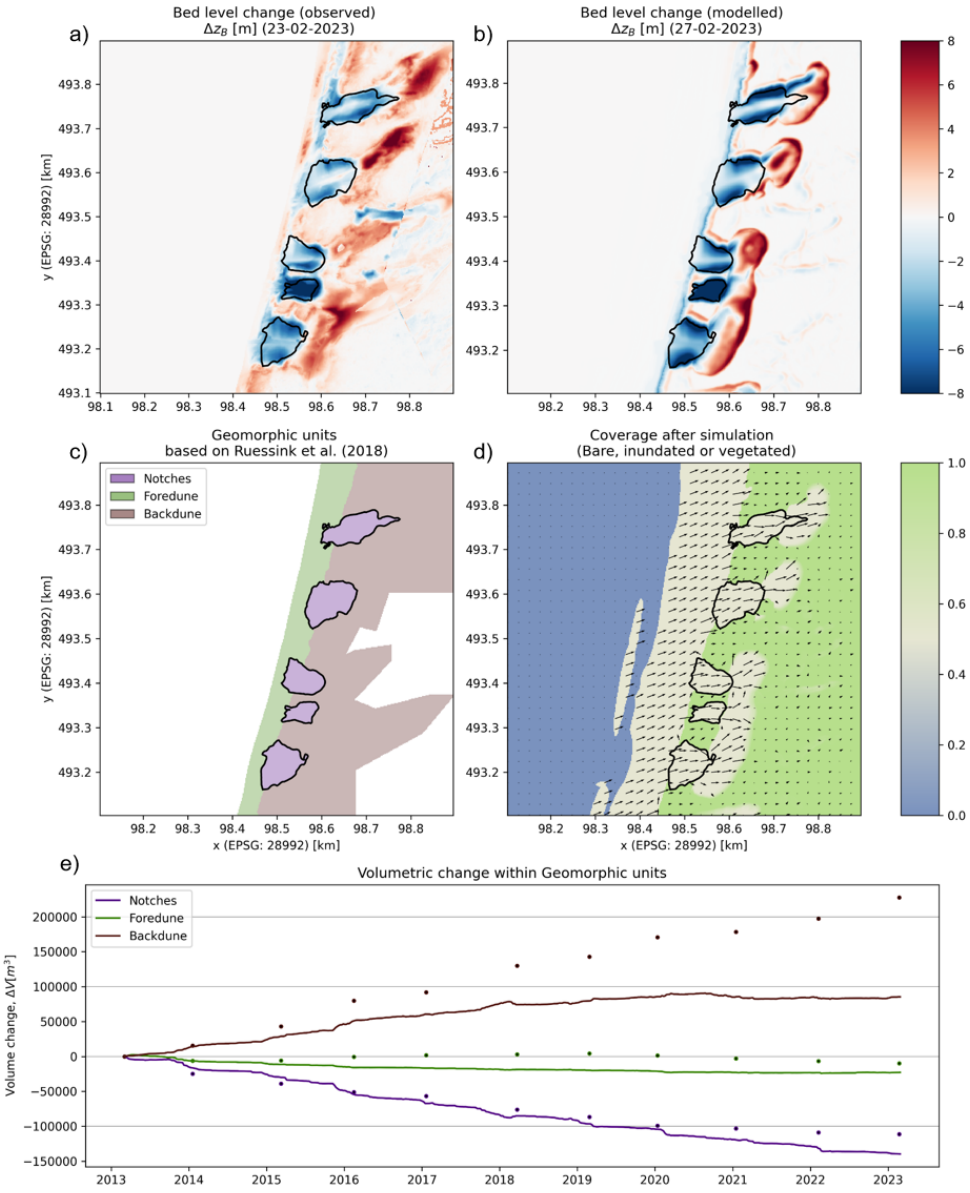

Figure 2.11.: Comparison between model outcomes and measurements. The observed (a) and modelled (b) erosion (blue) and sedimentation (red) patterns are compared. Panel c) shows the three defined units for which the volumetric change is computed. The outcomes of the volumetric comparison are shown over time in panel e).

2.6. Discussion

So far, this paper has given a detailed display of the assumptions in the AeoLiS model and the corresponding results for the four particular cases. Barchan dunes, parabolic dunes, embryo dunes and blowouts are simulated using open-source AeoLiS code and, consistent with other applications in the literature, implementing the relevant physics for each case (e.g., vegetation dynamics, multidirectional winds, shear, non-erodible layers) to generate morphological forms as observed in nature. The model reproduced the crescentic shape of barchan dunes, with the spatial dimensions' ratios matching those recorded in earlier studies (Finkel, 1959; Hastenrath, 1967; Hersen, 2004; Hesp & Hastings, 1998; Sauermann et al., 2000). This outcome gives confidence in the model's new topographic steering process, as adopted from Durán and Moore (2013) with the exception that a custom grid rotation scheme implemented in AeoLiS allows for multidirectional winds. This capability is particularly necessary for accurate simulation of real world dune modeling applications, where wind directions are highly variable and for which wind direction has critical implications both of sediment input into dune complexes (Delgado-Fernandez, 2010) and on wind flow patterns over the dune form (Hesp & Smyth, 2021; Kombiadou et al., 2023).

Whereas the original AeoLiS model presented by Hoonhout and de Vries (2016) included multifraction sediment transport processes and various supply limiters, the model at the time did not include capabilities to simulate the full suite of processes that result in aeolian sediment transport gradients that contribute to net landform change. In coastal environments, vegetation is one of the most effective agents for dune formation. In this study, the transition of dynamic crescentic dunes into u-shaped parabolic dunes was successfully simulated through a simple representation of vegetation growth and the interaction with shear stress (Anthonsen et al., 1996; Barchyn & Hugenholtz, 2012; Durán et al., 2008; Reitz et al., 2010).

In the blowout simulation illustrated in Figure 2.11, the model effectively replicated observed erosion and deposition patterns in both spatial and volumetric terms (Ruessink et al., 2018). Historically, artificial blowout projects have had mixed success, often due to limited impacts on dune systems or natural infilling post-excavation (Arens et al., 2013a; Castelle et al., 2019; Riksen et al., 2016). The prediction of dune responses to such interventions could inform decision-making in terms of excavation volume, location, timing, and combining with other measures.

The presented model may open new possibilities in the field of coastal engineering, landscape management and -planning. However some limitations in its current implementations remain. Especially when accurately reproducing real-world landforms in specific situations. The blowout simulation, despite illustrating the model's collective advancements, also exhibits most of the assumptions that involve limitations. Future updates of the model may include enhanced descriptions of relevant processes, with several key areas identified for further improvement:

Complex wind fields - The model cannot describe complex wind fields that go beyond the scope of Weng et al. (1991)'s theory. Flow structures around steep topographic gradients and flow reversal on the lee side of dunes are observed in field studies (Lynch et al., 2009) but cannot be described by the current code. Additionally, while the existing analytical shear stress theory allows for rapid computation, low slope assumptions of this formulation may require more complex numerical approaches to effectively simulate wind flow dynamics over steep or complex terrain (Cecil et al., 2024). However, vegetation roughness is likely to be dominant over the effect of topographic steering. Therefore, the implications of this particular limitation are expected to be limited for typical vegetated foredunes.

Avalanching - The model's constant angle of repose is an important assumption for the avalanching process. However, it does not account for potential variations in the angle of repose due to sediment characteristics, moisture, or vegetation root systems. These parameters may influence slope stability and avalanching processes (Davis et al., 2024; Rahn, 1969). This limitation is illustrated by our need to adjust the angle of repose across the entire domain, as a means to at least partially incorporate the impact of vegetation and root systems on stability.

Vegetation growth - The model's representation of vegetation growth and its interaction with morphodynamics is simplified to a limited set of parameters and processes. The response of vegetation to burial (Nolet et al., 2018), as well as the influence of other abiotic factors like salinity, drought, and temperature on vegetation growth (Homberger et al., 2024; van Puijenbroek et al., 2017b) could be elaborated in future modelling efforts. This knowledge gap in vegetation modelling was highlighted during the blowout simulation which required significant calibration to achieve realistic outcomes. And yet, erosion and deposition patterns still deviated from actual observations (Dickey et al., 2023).

Multiple species - The current model supports only one type of vegetation characteristic, whereas multiple species with distinct growth functions may be needed for alternative landform simulations (Baas & Nield, 2007). This factor may be especially important in coastal settings where mixed species plots are common on natural coastal foredunes and differing plant species have widely differing morphological characteristics (Goldstein et al., 2018; Walker & Zinnert, 2022).

Removal and establishment - The binary approach for vegetation establishment and removal in the model does not reflect the gradual erosion and persistence of vegetation in natural settings. The model could incorporate the influence of seed dispersal and various abiotic conditions on vegetation establishment. Additionally, it seems improbable that transient inundation would be immediately fatal to vegetation. Enhancing the implementation of vegetation response to hydrodynamic stresses could improve the inclusion of vegetation zoning.

Supply-limitations - The underestimation of onshore aeolian flux in the embryo dune and blowout simulations, though not directly related to landform shaping processes, highlights the critical need for precise modelling of sediment supply on the beach face. Accurately capturing this aspect is essential, as inaccuracies can significantly impact the outcome of landform simulations.

Despite these limitations, the AEOLIS model has made contributions to several engineering projects. The Sand Engine mega-nourishment in the Netherlands was designed to develop in a dynamic coastal dune landscape over several decades (Stive et al., 2013). Simulations by Hoonhout and de Vries (2019) have explained the spatiotemporal distributions of sediment at the site. These simulations have been used to evaluate its design and make management decisions related to beach nourishment and dune management along the Dutch coast. Leveraging a subset of the model advancements presented in this manuscript, van Westen et al. (2024a) further extended the model domain alongshore, increased spatial resolution, and coupled the model with a hydrodynamic model component to introduce the interplay between aeolian- and marine-driven morphological change. This enabled the inclusion of marine-driven impact on beach width, sediment availability and dune growth. A growing set of use applied engineering use cases is now possible given new capabilities included within AEOLIS that allow for aeolian transport and related morphological changes to be simulated across broad spatial scales (meters to kilometres; e.g., Figure 2.11), temporal scales (e.g., days to decades), and including a range of physical and ecological processes. Continued demonstration and assessment of capabilities for simulating real-world 1D and 2D profile change will further enable the use of AEOLIS as a practical tool for engineering planning and design work related to managing sediment transport pathways and/or optimizing landform evolution in coastal systems to add flood or ecosystem service benefits.

2.7. Conclusion

The AEOLIS model provides an implementation of a quantitative set of process-based descriptions regarding wind-flow, aeolian sediment transport, vegetation growth, submersion and the feedback with coastal morphology. The model is built on the principle of supply-limited aeolian sediment transport where wind shear and surface characteristics determine sediment transports that cause morphological changes. The model is forced with wind speed, water levels and wave heights as boundary conditions and solves for intrinsic process interactions related to morphology, vegetation growth and topographic steering of wind flow. Assumptions can be varied depending on the specific goal of the simulation.

Several characteristic aeolian (coastal) landform shapes can be simulated using the novel implementations in the AEOLIS model. Barchan dunes can be simulated by combining assumptions that describe aeolian sediment transport, topographic steering and avalanching. Comparison with real-world measurements of barchan dunes located in Morocco gives confidence in the model to simulate landform development under realistic wind conditions.

Parabolic dunes can be simulated when taking into account the description of vegetation development and extending the temporal scale of the barchan dune simulation. The establishment of vegetation on the relatively stable sides of the dune causes further stabilization and the subsequent development into a parabolic-shaped dune corresponds well with the literature, as do simulated migration rates.

Embryo dunes are simulated by adding a probabilistic approach to vegetation establishment and lateral propagation and the influence of swash processes in the domain. The simulated behaviour in seasonal variation and the sheltering impact of seaward-located dunes are similar to earlier measurements carried out at the Hors, Texel, The Netherlands.

The model's applicability in practical engineering cases is demonstrated by simulating the development of five foredune notches along the Dutch coast. The simulated spatial pattern and volumetric landward movement of sediment show that the combined implementation of the presented processes is capable of describing real-world coastal dune development on engineering spatiotemporal scales.

Although the AEOLIS model can describe several theoretical and practical behaviours of coastal aeolian dune landscapes, the implementation of some additional assumptions may improve the model's predictive capability. Examples are (amongst others) the implementation of different vegetation species or secondary flow patterns.

The AEOLIS model is openly accessible and all results in this publication are reproducible in the open source domain. This way we aim to underscore AEOLIS' potential as a basis for collaborative development towards a more comprehensive description of coastal dunes.

COUPLING NEARSHORE TO DUNE

The nearshore, beach and dune form an integrated system where sediment crosses the waterline and marine processes influence aeolian transport. This chapter presents a coupling between the aeolian transport model from Chapter 2 and a hydromorphodynamic model, exploring the benefits and technical feasibility of connecting these domains in coastal applications.


3

Photo: Eric van der Eijk – https://duinlandschap.nl/

3

Coupling Nearshore to Dune

PREDICTING MARINE AND AEOLIAN CONTRIBUTIONS TO THE SAND ENGINE'S EVOLUTION USING COUPLED MODELLING

Abstract Predictions of marine and aeolian sediment transport in nearshore-beach-dune systems are essential for designing Nature-Based Solutions (NBS). To quantify marine-aeolian interactions, we present a framework coupling DELFT3D Flexible Mesh, SWAN, and AEOLIS, enabling continuous exchange of bed levels, water levels, and wave properties. The coupled model simulates the morphodynamic evolution of the Sand Engine mega-nourishment, showing good agreement with observed volumetric developments, including marine-driven erosion of the peninsula and aeolian-driven dune lake infilling.To assess aeolian–marine interactions, we compare coupled and stand-alone models. Aeolian transport to the foredune (214,000 m³ over 5 years) removes sediment from the marine domain, reducing alongshore sediment redistribution by 70,000 m³ (1.7% of total marine-driven dispersion). Marine-driven deposition and erosion reshape the cross-shore profile, regulating aeolian transport and foredune deposition. On the accreting southern flank, foredune growth increased by up to 6.7% in year 5, whereas on the northern flank, sheltered by a lagoon and tidal channel, foredune deposition decreased by 11.5%. Our findings highlight how aeolian and marine processes reshape nourished sand, with each domain influencing the other. This interplay is crucial for accurately predicting sandy NBS and optimizing coastal interventions.

This chapter is based on: van Westen, B., Luijendijk, A. P., de Vries, S., Cohn, N., Leijnse, T. W., & de Schipper, M. A. (2024). Predicting marine and aeolian contributions to the Sand Engine's evolution using coupled modelling. *Coastal Engineering, 188,* 104444.

3.1. Introduction

In recent years, Nature-Based Solutions (NBS) have become increasingly popular soft engineering features which provide ecosystem services and add coastal resilience to coastal areas (Barciela Rial, 2019; van der Meulen et al., 2014; Stive et al., 2013; Sutton-Grier et al., 2015; de Vriend et al., 2015). NBS, which may include constructed beach and dune features, are designed to be dynamic and their subsequent morphologic evolution is governed by the interplay of hydrodynamic, morphodynamic and ecological processes on timescales of hours to decades (van der Meulen et al., 2023). Therefore, to successfully design and predict the long-term benefits of coastal NBS, it is necessary to have a (a) comprehensive understanding of and (b) quantitative predictive tools that can resolve the drivers of sediment transport gradients across the foreshore, surfzone, beach and dunes (Bridges et al., 2021b; Cohn et al., 2019; Luijendijk & van Oudenhoven, 2019).

Shoreface and beach nourishments are widely used in erosive coastal systems to buffer storm impacts and add recreational and ecological value (de Schipper et al., 2021). While the placement of sand has been globally adopted to enhance coastal resilience, recently, mega-nourishments have been trialled to add immediate local and long-term benefits through leveraging the longshore redistribution of placed sediments. An example of this type of NBS is the Sand Engine, a 21.5 Mm^3 mega-nourishment (Stive et al., 2013), constructed in 2011 along the Delfland coast in the Netherlands (Figure 3.1). Since its construction, many studies have monitored, analysed, and modelled the Sand Engine's evolution (Luijendijk et al., 2017; Roest et al., 2021; de Schipper et al., 2016; Tonnon et al., 2018). The Sand Engine was constructed with various goals, from nourishing the adjacent coast, to promoting dune growth, and enhancing the region's natural and recreational values. However, successfully predicting volumetric changes in the different parts of the NBS, and thus effectively accomplishing these diverse objectives, has proven challenging. During the design phase, it was estimated that the foredune growth in the Sand Engine's direct vicinity would approximately double the dune growth compared to the original situation (Mulder & Tonnon, 2011). This estimation was based on an empirically developed relationship between dunefoot migration and beach width (de Vriend et al., 1989). In practice, foredune deposition was measurably lower than along the adjacent coast in the years following the mega nourishment construction (Hoonhout & de Vries, 2017; Huisman et al., 2021).

Hoonhout and de Vries (2017) linked the observed reduction in foredune growth along the Sand Engine to supply limitations. While the theoretical rate of saturated, wind-driven transport is a function of local grain size and wind speed (Bagnold, 1937; Sherman & Li, 2012; Sørensen, 2004), numerous factors may limit supply in coastal environments and reduce local aeolian transport rates below the theoretical maximum rate of saturation (de Vries et al., 2014a). This finding is consistent with multiple studies from other field sites that have found that the observed volumetric growth of coastal dunes is typically lower than that predicted from the wind-driven potential transport capacity (Costas et al., 2020; de Vries et al., 2014b).

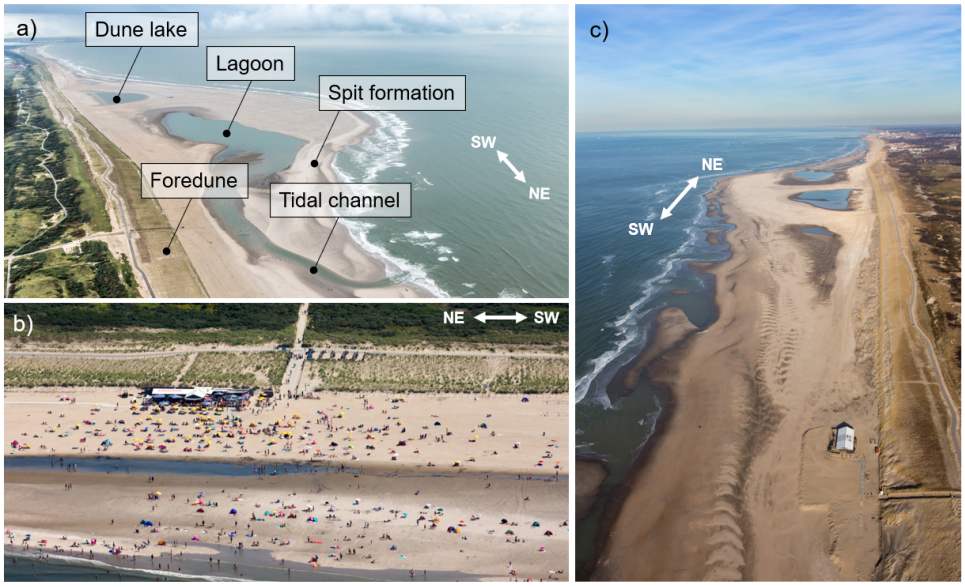

Figure 3.1.: Photos of the Sand Engine mega nourishment. (a) The Sand Engine one year post-construction, with the key geomorphological features. (b) Beachgoers at the Sand Engine's northern flank with the foredune in the back. (c) The southern flank of the Sand Engine 5 years after construction. The white arrows illustrate the Sand Engine's orientation, pointing towards the Northeast (NE) and Southwest (SW). (Photo credits: Rijkswaterstaat/Joop van Houdt and Jurriaan Brobbel)

.

Supply limiting conditions in coastal environments can especially be attributed to surface moisture (Hallin et al., 2023b) and sediment sorting (van IJzendoorn et al., 2023a). The wetting of the surface in the intertidal zone due to wave runup and groundwater effects results in an increased wind velocity threshold for initiating aeolian transport (Bauer et al., 2009; Hallin et al., 2023b; Ruessink et al., 2022). Despite this constraint on aeolian transport near the land-water interface, the intertidal zone is often considered the primary source of sediment contributing to dune growth (Hoonhout & de Vries, 2017; Houser, 2009). Both within the intertidal zone and higher up on the dry beach, aeolian sediment transport can result in armouring of the bed as fine grain sediment is winnowed from the bed surface, preferentially leaving behind a layer of course material at the surface (i.e. lag deposits) that similarly contributes to supply limitations (Carter, 1976; Hoonhout & de Vries, 2017). At elevations lower than the total water level elevation, however, wave-induced forces can mix different sediment fractions, removing potential armouring and thus enabling more sediment supply (van IJzendoorn et al., 2023a; van IJzendoorn et al., 2023b).

Since the intertidal zone is a primary zone of sediment pickup for wind-driven sediment transport, marine-driven sediment supply towards the intertidal zone can positively enhance aeolian transport rates (Aagaard et al., 2004). Cohn et al. (2017) showed that the landward migration and welding of breaker bars can contribute to rapid beach growth, which some studies have related to enhanced dune growth (Houser, 2009) perhaps due to the introduction of finer grained sediments and widening of the beach which reduced fetch limitations. These factors may similarly explain why aeolian transport and net dune growth rates are often higher immediately following beach nourishments (Arens et al., 2013b; van Rijn, 1997; van der Wal, 2004). High energy events (i.e. storms) can induce beach and dune erosion, potentially adversely impacting the intertidal sediment budget (Costas et al., 2020; González-Villanueva et al., 2023; Quartel et al., 2008), potentially stimulating aeolian transport as a consequence of increased intertidal width and subsequent sediment availability. Aeolian pickup from the intertidal zone also modifies the intertidal sediment budget. To date, it is unclear to what extent removing this sediment by aeolian transport affects marine-driven transport through changes in grain size and morphodynamic feedback.

The multitude of interactive processes and scales hampers quantifying the impact of aeolian and marine interactions on long-term morphological development (Aagaard et al., 2004; Bauer et al., 2009; Moulton et al., 2021). As a result, the current understanding of the nearshore-beach-dune system primarily relies on observations, and conceptual and rule-based models, describing relations between the marine and aeolian domains (Aagaard et al., 2004; Bauer & Davidson-Arnott, 2003; Costas et al., 2020; González-Villanueva et al., 2023; Hallin et al., 2019a; Houser, 2009; Pellón et al., 2020; Sherman & Bauer, 1993; Short & Hesp, 1982; Silva et al., 2019). Despite the conceptual understanding of the impact that interactions between marine and aeolian processes have on coastal evolution, quantitative tools are still lacking.

To quantify marine-driven influences on aeolian developments, a fetch-based approach can be used (Bauer & Davidson-Arnott, 2003; Delgado-Fernandez, 2010; Ruessink et al., 2022). This approach is based on the concept that some critical fetch distance in downwind direction is needed to reach the wind-driven transport capacity. Sediment transport is limited in relation to the transport capacity by the limited distance (smaller than the critical fetch distance) in the direction of the wind relative to the waterline. This approach (over)simplifies the dynamic, time-varying conditions such as tidal excursion and storm events and does not take the impact of the system's evolving morphology on supply-limiters into account (Houser, 2009).

Semi-empirical models describing beach-dune dynamics, like the CS-model developed by Larson et al. (2016), use a combination of physics and empirical observations to simulate the cross-shore exchange of sand and the consequent profile development. Building upon this, Zhang and Larson (2022) incorporated dune erosion into the model using the wave impact theory described by Larson et al. (2004). This model has proven fast and effective in predicting the evolution of beach-dune systems on yearly to decadal timescales (Hallin et al., 2019b; Palalane et al., 2016). However, its semi-empirical nature introduces a degree of site-specificity to some coefficients, necessitating data for calibration to ensure confidence in its application to specific locations. This aspect compromises the predictive ability in environments where data is scarce or when designing complex and novel NBS.

Process-based models have proven their use in quantitatively predicting the effects of natural events and human interventions on coastal evolution, e.g. at the Sand Engine (Hoonhout & de Vries, 2019; Luijendijk et al., 2017). Yet, most of these coastal process-based models mainly focus on distinct sub-domains, analyzing either the marine (Booij et al., 1999; Hervouet & Bates, 2000; Lesser et al., 2004; Roelvink et al., 2009; Warren & Bach, 1992) or the aeolian (Durán et al., 2010; Hoonhout & de Vries, 2017; Keijsers et al., 2016) domains separately. Consequently, these models often neglect the interactions between aeolian and marine subdomains.

Integrating morphodynamic evolution across subdomains requires a tool that allows for the simultaneous prediction of multiple subdomains and a continuous exchange of morphological and hydrodynamic information between these domains. Several studies have made progress towards such integration. Roelvink and Costas (2019) included integrated dune development mechanics into the hydrodynamic XBeach model (Roelvink et al., 2009). The WindSurf framework (Cohn et al., 2019) employed a coupling between XBeach and the aeolian transport model AeoLiS (Hoonhout & de Vries, 2016). These frameworks proved valuable in advancing the understanding of interactions within the nearshore-dune system and showed the added value in adding them (Hovenga et al., 2023; van Westen et al., 2023). However, a common limitation of these coupling frameworks is the prerequisite that the submodels have to operate on the same, one-dimensional cross-shore grid. Depending on spatiotemporal scale, longshore variations could significantly contribute to the overall development coastal environments. Also, different parts of the coastal domain could require descriptions of different levels of detail. Therefore, to simulate real-world coastal environments, a numerical coupling tool is required that supports two-dimensional subdomains, regardless of their respective grid resolution or type. Luijendijk et al. (2019a) solved this by proposing a coupling between Delft3D (Lesser et al., 2004) and AeoLiS (Hoonhout & de Vries, 2016) models, both covering two-dimensional domains. Luijendijk et al. (2019a) demonstrated the ability to include the interactions between the marine and aeolian morphodynamics by coupling these numerical models. However, a detailed analysis of the impact of these interactions on the system's integrated morphodynamics was lacking. Besides, limited spatial resolution restricted the model from including detailed aeolian landforms, e.g. foredunes, in this initial study.

The current study extends the current numerical frameworks and focuses on quantifying volumetric changes in the aeolian and marine parts of the Sand Engine to explore interactions between marine- and aeolian-driven portions of the study site. The impact of these interactions on the system's integrated morphodynamics is studied using a 2D coupled model encompassing both aeolian and marine domains. We define two Research Objectives:

1. The development of a coupling framework that enables simultaneous modelling of the aeolian and marine domains in 2D, thereby introducing the interactions between marine and aeolian morphodynamics;
2. Estimating the magnitude of the interactions between marine and aeolian morphodynamics and their impacts on the Sand Engine's evolution.

The development of this DELFT3D-SWAN-AEOLIS coupling framework facilitates simultaneous computation of multiple subdomains, including potential interactions that cross the land-sea boundary. Individual model components can successfully provide predictions of net landscape change of the subaerial (AEOLIS) and subaqueous (DELFT3D-SWAN) portions of the coastal zone, but independent models inherently ignore part of the sediment budget. For example, large amounts of sediment that are being deposited in the Sand Motor dune system would not be included in a budget analysis obtained from any stand-alone subaqueous model application or, vice versa, the subaqueous morphological development would lack in a model framework that only accounts for subaerial processes.

Due to interactions between the subdomains, we expect small deviations in morphological development to occur if the coupled model outcomes are compared to the sum of stand-alone outcomes. Since the individual model components have been specifically calibrated for standalone operation, we do not anticipate significant improvement of model skill in the central part of the domain the submodels were designed for. However, it might be expected that there are noteable differences in the zones where both marine and aeolian processes operate, such as within the intertidal zone. This work aims to demonstrate new capabilities enabled by connecting multiple coastal domains within a single model framework that, through expanding both quantitative and qualitative understanding of system behavior (Barbour & Krahn, 2004), allows for improved understanding of cross-domain interactions and integrated nearshore-beach-dune systems.

3.2. Coupled modelling of Sand Engine morphodynamics

3.2.1. Case study: the Sand Engine

The Sand Engine is a 21.5 Mm^3 hook-shaped mega-nourishment constructed in 2011 along the Delfland coast (Stive et al., 2013), shown in Figure 3.1. The average yearly northward alongshore sediment transport along the Delfland coast is estimated to be 0.38 Mm^3, resulting from gross transports of 0.76 Mm^3 northward and 0.38 Mm^3 southward (van Rijn, 1995; de Schipper et al., 2016).

The Delfland has historically been retreating approximately 1 km inland from 1600 to 1990, as it faced structural erosion (de Schipper et al., 2016). After the Dynamic Preservation Act was implemented in 1990, mandating the maintenance of the 1990 coastline position (van Koningsveld & Mulder, 2004), nourishment construction started to increase. Before the Sand Engine's construction, nourishment volumes in this area rose to approximately 1.7 Mm^3/year. The advantages thought of during its design, involving a high concentration of sediment nourishment at a single longshore location, are the reduced frequency of nourishments needed, the longshore spreading causing neighbouring shorelines to advance more naturally, the large initial land reclamation providing increased space for recreation activities and ecological development and the ecological stress remaining confined to a relatively small area, limiting its overall environmental impact (Stive et al., 2013).

For further information on the background, coastal setting, and governing conditions of the Sand Engine see Stive et al. (2013), de Schipper et al. (2016), Hoonhout and de Vries (2017), and Huisman et al. (2021).

3.2.2. Coupling approach

The framework presented in this study enables the coupling of three existing process-based models. This is achieved through the simultaneous execution of these models, hereafter model components, and the exchange of information between them. To achieve this, the Basic Model Interface (BMI) protocol is utilized (Hutton et al., 2020), as it serves as an efficient way of coupling numerical models through the provision of dedicated functions.

Our work builds upon earlier studies that developed coupling tools for coastal applications. The initial BMI-enabled coupling framework is WindSurf as coded by Hoonhout (2016). WindSurf supports the coupling between one-dimensional AeoLiS (Hoonhout & de Vries, 2016) and XBeach (Roelvink et al., 2009) models, with an application of these couplings presented in Cohn et al. (2019). Additionally, Luijendijk et al. (2019a) utilized a similar BMI protocol to facilitate the exchange of parameters between two-dimensional model components.

In this study, we have combined the generic structure of the BMI-version of the Windsurf framework (Hoonhout, 2016), with some of the model schematization and exchange methods from Luijendijk et al. (2019a) to enable comprehensive 2D model coupling capabilities. A central grid is utilized as a communication layer between models, ensuring the model components are not required to have the same central model grid coordinates or resolution (Figure 3.2). This method eliminates the need for setting up numerous individual exchanges between the multiple model components. Additionally, having one shared morphological state minimizes the discrepancy across model components. For our case study, the central grid is based upon the DELFT3D-FM grid (§3.2.3, Figure 3.3b).

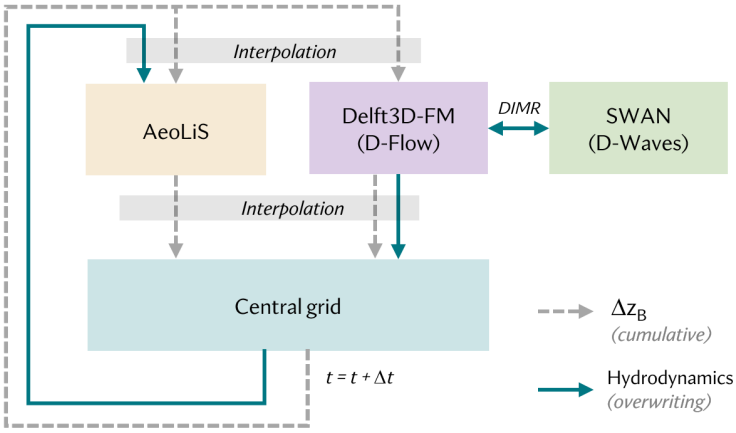

Figure 3.2.: Schematic representation of the parameter exchange settings between AeoLiS (Hoonhout & de Vries, 2016) and DELFT3D-FM (Kernkamp et al., 2011; Lesser et al., 2004) model components. The arrows indicate the exchange of ΔZ_B (adding bed level change to existing bed elevation) and hydrodynamics (water levels, wave heights and wave period). The information is exchanged for every timestep Δt (=1200s) in morphological time.

To increase the flexibility and application range, the coupling framework is made compatible with different grid types (e.g., rectangular, curvilinear, unstructured). To enable the exchange of information between these grids, we implemented a re-gridding functionality, which is based on a simple linear interpolation method. The influence of the coupling and interpolation approach on mass-conservation will be reflected upon in §3.2.5.

3.2.3. Model components

The coupled model consists of three model components. Throughout the setup of our coupled model, we aimed to maintain the setups of each component as closely as possible to earlier Sand Engine research (Hoonhout & de Vries, 2019; Luijendijk et al., 2017) to minimize the effort required for setting up and calibrating the model components. Our main focus is on quantifying the added value of enabling interaction between models, instead of demonstrating the performance within the individual subdomains.

The primary hydrodynamic component, DELFT3D Flexible Mesh (Kernkamp et al., 2011), hereafter DELFT3D-FM, simulates sediment transport and morphological change in the marine domain (Figure 3.3b) under the influence of tidal, wind, and wave-driven water levels and currents, following the methods of Lesser et al. (2004). The setup of DELFT3D-FM is described in §3.2.3. The SWAN model (Figure 3.3a) simulates the propagation and transformation of wind-generated waves (Booij et al., 1999) that is linked with DELFT3D-FM through a wrapper called D-Waves, see §3.2.3.. The morphological evolution in the aeolian domain (Figure 3.3c), influenced by aeolian-driven, supply-limited transport, is simulated by the AeoLiS model (Hoonhout & de Vries, 2016), see §3.2.3.

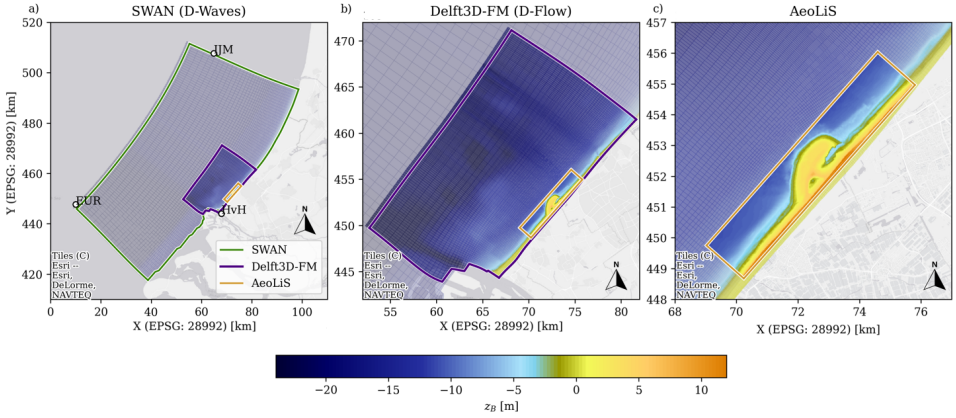

Figure 3.3.: Computational domains of SWAN (a, green), DELFT3D-FM and refined SWAN (b, purple), and AeoLiS (c, orange). HvH, EUR and IJM indicate the wind and offshore wave stations used for the wave boundary conditions. Colours indicate bed level with respect to NAP (Dutch datum at approximately mean sea level).

DELFT3D-FM configuration

The configuration of the DELFT3D-FM model component builds upon the Sand Engine simulations by Luijendijk et al. (2017). The computational domain covers an alongshore stretch of coast of nearly 20 km from Hoek van Holland to just north of Scheveningen (Figure 3.3b). It extends approximately 15 km offshore. The cross-shore grid resolution is 1000 m at the offshore boundary and 35 m at the surfzone (Figure 3.3b). Considering the width of the surfzone varying between approx. 150m at the tip of the peninsula to 300m along the more natural coast, the chosen cross-shore resolution results in at least 5 grid cells in the surfzone. To more accurately resolve detailed surf zone processes a finer resolution in the surfzone could be beneficial, but here we compromise between sufficiently detailed resolution to resolve dominant behavior at the study site and non-exorbitant computational times. Among the processes that this resolution was optimized for was the ability to successfully capture longshore transport rates and the capacity of the model to reproduce the Sand Engine's historical dispersion. As shown in §3.2.6, the model effectively reproduces these longshore processes, hence justifying the chosen resolution. At the lateral boundaries, zero-gradient alongshore water level, or Neumann, conditions are enforced (Roelvink & Walstra, 2004).

The model has been upgraded from DELFT3D version v4 (Lesser et al., 2004) to DELFT3D Flexible Mesh solver (Kernkamp et al., 2011), allowing for more efficient grid refinement opportunities. This upgrade required a re-calibration of the sediment transport-related factors for suspended and bedload transport (*sus* and *bed*). To match the volume change within the main Sand Engine peninsula as modelled by Luijendijk et al. (2017), the values for *sus* and *bed* were set to 1.4 [-]. Additionally, the sediment transport factors for wave-driven transport (*susw* and *bedw*) were set to 0.5 [-].

SWAN configuration

Like the DELFT3D-FM configuration, the SWAN setup is based on Luijendijk et al. (2017). Two domains are used in a nesting approach. The larger wave domain extends ~10 km in both longshore directions (north and south) and ~15 km in offshore direction to adequately describe wave transformation. A finer grid that matches the DELFT3D-FM grid is nested inside the larger grid (Figure 3.3 a, b), with an increased cross-shore resolution of roughly 35 m around the shoreline.

AeoLiS configuration

The AeoLiS setup primarily relies on the previous work by Hoonhout and de Vries (2019). The area of interest has been extended to cover a more extensive alongshore coastal stretch. Moreover, a finer grid, increasing the resolution from 50×50 m to 12.5×12.5 m (equidistant), is applied to acquire sufficient resolution for the simulation of foredune development. The offshore boundary of the AeoLiS domain is defined by the edge of the aeolian zone, as indicated by the orange box in Figure 3.3.

The influence of vegetation cover is included by locally reducing the shear stress following the methods of Durán and Moore (2013). In the absence of comprehensive spatial measurements of vegetation cover, vegetation presence and growth are currently implemented following simple rules based on general field observations. The vegetation coverage is determined based on the evolving bed level elevation [m] and slope [°]. No vegetation is present below 4m+NAP, while all cells above 6m+NAP are fully covered. Between 4 and 6m+NAP, only cells with a bed slope of at least 24° are covered with vegetation. Including avalanching ensures that the bed slope does not exceed the imposed angle of repose (33°). These chosen values are iteratively determined to reproduce key aspects of the cross-shore profile evolution. This implementation resulted in a gradual and realistic seaward migration of the dunefoot, while maintaining a realistic foredune slope.

Due to the absence of run-up processes within the hydrodynamic model components, AeoLiS uses the regridded wave characteristics to calculate wave run-up, based on the empirical formula by Stockdon et al. (2006). While the Stockdon et al. (2006) formula fundamentally relies on offshore wave heights, in the present setup, local wave conditions are employed. Since the local wave height is lower than the offshore conditions due to wave breaking, this approach is expected to lead to an underestimation of wave run-up and subsequently in a smaller area of inundation.

3.2.4. Setup of the 5-year model hindcast

The coupled model is tailored to simulate the morphological development of the Sand Engine for the first 5 years after construction, from August 1^{st}, 2011, to August 1^{st}, 2016. All three model components use the same initial topographic and bathymetric data. The description of obtaining and processing this bed elevation data for input to the models is added to Appendix C.

Parameter exchange

The coupling interval of the parameter exchange between the model components is 1200 s in morphological time. Bed levels are continuously exchanged between DELFT3D-FM and AEOLIS to include the morphodynamic interactions between the aeolian and marine domains. To reduce the impact of continuously overwriting bed levels on mass conservation and preservation of details involving grids of different dimensions and resolutions, the bed level change is computed using a cumulative approach. This means that rather than repeatedly replacing existing bed levels with new values calculated by the DELFT3D-FM and AEOLIS model components after ($z_{B,central}$[t] = $z_{B,model}$[t]), we update the bed level of the central grid incrementally, adding only the calculated change in bed level, Δz_B [m] ($z_{B,central}$[t] = $z_{B,central}$[t-1] + $\Delta z_{B,model}$[t]). This process is facilitated by tracking the changes in bed level calculated by different model components during each step.

To incorporate the marine-driven sediment supply-limiters on aeolian transport dynamics, including the aforementioned hydrodynamic reworking of grain size distributions in the swash zone and soil moisture content of the bed surface from wave runup, the water levels z_s [m+NAP], wave height H_s [m], and wave period T_p [m] are exchanged from DELFT3D-FM to AEOLIS through the central grid. The exchange of wave-related information between DELFT3D-FM and SWAN occurs through the DIMR-coupler (Deltares, 1982, Deltares Integrated Model Runner) with a coupling interval 3600 s in morphological time.

During simulations, we stored the marine- and aeolian-driven bed level change separately, allowing us to determine their relative contributions to the overall development. To exclude the aeolian- or marine-driven morphodynamics from the simulation results entirely, two additional simulations were conducted by disabling the bed level updates from (1) the AEOLIS model (see Figure 3.3d-e) and (2) the DELFT3D-FM model (see Figure 3.3f-e). Despite not being fully uncoupled, these simulations are referred to as AEOLIS-only or DELFT3D-FM-only, respectively. By keeping the model components integrated within the coupling framework, we maintain the exchange of water levels and wave properties between the domains while eliminating morphodynamic interactions. This method ensures that deviations arising from information exchange and re-gridding do not influence the outcomes of later comparative analysis.

Forcing Conditions

The boundary conditions for the model set-up are generated following the methodology of Luijendijk et al. (2017). Alongshore variable astronomical tidal components are imposed on the offshore boundary of the hydrodynamic model and observed surge levels at Hoek van Holland are added to these tidal levels (Figure 3.3a).

Wind speed and direction data are obtained from 10-minute averaged observations at Hoek van Holland. Wave characteristics are sourced from two offshore platforms: Europlatform and IJmuiden Munitiestortplaats (Figure 3.3a). Data gaps in the wave timeseries from both offshore platforms are filled using information from the other platform. The remaining data gaps in wave (2%) and wind (7%) timeseries are filled with zero values. This conservative approach may result in a slight underestimation of wave- and wind-driven transport.

Upscaling techniques

The boundary conditions generated in this study undergo a series of processing procedures to reduce computational expenses by implementing filtering and acceleration techniques (Luijendijk et al., 2019a).

The boundary conditions are filtered based on wave and wind criteria. First, periods with offshore-directed waves ($40°N < H_{dir} < 200°N$) and winds ($60°N < u_{dir} < 180°N$) are removed. Next, conditions are filtered based on wave height ($H_s < 1m$: 49%) and wind speed ($u_{10} < 5.5m/s$: 49%). The filtering criteria for wave height are based on Luijendijk et al. (2017). The wind speed is based on threshold velocity for the smallest sediment fraction (250 μm) to initiate aeolian transport, according to the applied transport formulation by Bagnold (1937). Conditions were only filtered out of the timeseries when all requirements were met simultaneously, resulting in a reduction of 39% of the total duration to be simulated, allowing for an increased computational speed of these comprehensive 2D simulations.

To further accelerate the simulation, a morphological acceleration factor of 3 is applied in DELFT3D-FM simulation, hereafter referred to as *morfac* (Ranasinghe et al., 2011). AEOLIS's smaller computational costs remove the need for applying acceleration techniques on the AEOLIS model component within this setup. To align the morphological timeframes of both model components, which operate with different *morfacs*, the coupling interval is adjusted for each component.

3.2.5. Evaluation of coupling approach

With the coupled model being set up and run for the 5-year period, we evaluate some key performance aspects of the coupled model compared to the model components.

Preservation of detail

To retain relevant aeolian landform information, such as foredune profile characteristics, the level of detail required by AeoLiS (12.5 m) surpasses that implemented in Delft3D-FM (finest grid resolution of 35 m). Therefore, it's important to ensure that during the transfer of information from the coarser Delft3D-FM grid to the finer AeoLiS grid, no details regarding the shapes of aeolian landforms are averaged out. As the central grid shares a similar cross-shore resolution with the AeoLiS grid, no information is lost when transferring the bed level data from the central to the AeoLiS grid. Likewise, as we only add bed level *changes* from Delft3D-FM to the bed level stored in the central grid, we retain the detail of the bed topography from the previous timesteps.

Mass-conservation

The coupling framework's ability to conserve mass is assessed by computing the net volumetric change based on the bed level changes introduced by individual model components and comparing it to the combined volumetric change. Over the 5-year simulation period, the bed level changes induced by Delft3D-FM resulted in a total net loss of 542,970 m^3 and AeoLiS induced a loss of 4,864 m^3. The total volumetric loss resulting from the individual model components is thus 547,834 m^3. These net volume changes result from sediment fluxes leaving the landward, offshore, or onshore boundaries of the computational domains. The total volumetric loss based on the coupled simulation result is 543,230 m^3, which is 4,605 m^3 less than the sum of the individual model components. This surplus of sediment in the coupled simulation is likely to be the result of the linear interpolation method. Although the chosen method appears to be not fully mass-conservative, the volumetric deviation is small enough (<1% of the net total losses) to assume that the impact on our main objective is negligible.

Computational costs

Continuous or frequent data exchange in the coupling framework could lead to significant computational costs due to the overhead associated with model input/output and re-initialization. To mitigate model slowdowns and enable efficient multi-year simulations, we employed pre-computed weight matrices that map the results from the model components to the central grid and vice versa. These weight matrices are generated based on the earlier described linear interpolation method. The total computation time for the 5-year hindcast can be separated into time for AeoLiS (17.5%), Delft3D-FM (70.4%), and SWAN (11.1%). The remainder, only 1.0% of the total computational time, is attributed to the coupling framework itself.

3.2.6. Data-model comparisons

We evaluate the coupled model's ability to reproduce the observed aeolian and marine landform evolution. The model components have previously been calibrated on the Sand Engine study site, and their predictive proficiency for their respective subdomains has been demonstrated (Hoonhout & de Vries, 2019; Luijendijk et al., 2017). In this study, our focus is on the added value created by enabling interactions between these domains. Comparing the model and measurement results, we find that the model accurately reproduces the observed erosion and deposition patterns in the nearshore domain (Figure 3.4d vs. Figure 3.4j).

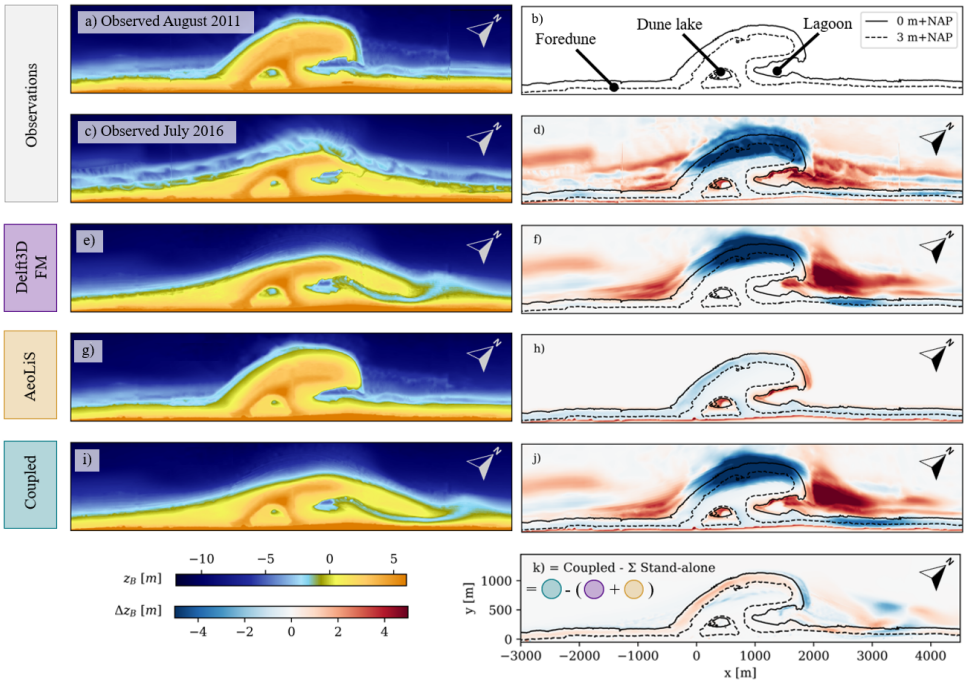

Figure 3.4.: Comparison between the modelled and observed morphological development. (a) The initial bed level just after construction and (b) contour lines after construction and key features. (c,d) The observed bed level and bed level change after 5 years. Modelled bed level and bed level change for DELFT3D-FM-only (e,f), AEOLIS-only (g,h) and coupled (i,j) simulations. Panel (k) shows the difference between the coupled simulation results and the sum of both stand-alone simulations

The shoreline retreat along the Sand Engine's main body, adjacent accretion, and overall development into a Gaussian-shaped platform correspond well with the observations (Figure 3.4c vs. Figure 3.4i). At the Sand Engine's tip (x=900 m in Figure 3.5), the shoreline (z_B = 0 m+NAP) retreated with 350 m after 5 years, which is slightly underestimated by the coupled model with 325 m.

Just south of the Sand Engine (x=-750 m in Figure 3.5), the shoreline has moved 120 m seaward, which is overestimated by the model with 180 m. The model's inability to simulate the cross-shore profile shape accurately is likely to affect these outcomes. The construction of the Sand Engine has resulted in the formation of sandbars at a depth of approximately -4 m+NAP (Huisman et al., 2021; Rutten et al., 2018). The model does not include these features, as the cross-shore profile is smoothed out (Figure 3.5c). We expect this to result from typical 2DH process-based (DELFT3D-FM) model shortcomings.

The largest discrepancies are found north of the Sand Engine. Although the existence of the northern spit-like feature and the closure of the lagoon, along with the formation of a tidal channel, are included in the model results, some precision is lacking (Figure 3.4c vs. Figure 3.4i). In the model results, the shoreline along the spit extends 305 m further seaward compared to observations (x=2000 m in Figure 3.5). This discrepancy is likely to be linked to the overestimation of the width en depth of the simulated tidal channel. The lowest observed bed level elevation within the tidal channel remains above 0 m+NAP, while the modelled tidal channel reaches a bed level lower than -1.5 m+NAP. We expect that the lack of run-up and overwash-related processes, in combination with a coarse cross-shore resolution, causes these deviations.

Along the entire domain, the observed upper beach remains relatively stable. Along the accretive southern flank (transect B, Figure 3.5), the observed average bed level elevation of the upper beach ($1 < z_B < 4$ m+NAP) is 2.2 m+NAP. Meanwhile, the model predicts erosion within the same area, resulting in an average bed level of 1.7 m+NAP. Aeolian sediment deposition along the edges of the dune lake, lagoon, and foredune ridge, locally accumulates up to over 5 m vertically and is visually similar between the model and measurements (see §3.2.6 for quantitative comparison).

In summary, visually, the simulation results of the coupled model align well with observations in both the aeolian and marine domains. This was already the case for the existing stand-alone simulations (Figure 3.4d-e vs. Figure 3.4f-g). However, the continuous exchange of information between the two subdomains has allowed the incorporation of the non-linear interactions between aeolian- and marine-driven morphodynamics. The sum of the two stand-alone simulations deviates from the coupled model results, as shown in Figure 3.4k. The largest differences can be observed within the intertidal area and along the northern spit, where the interaction between the aeolian and marine domains naturally is most prominent. The consequences of enabling these aeolian-marine interactions will be elaborated upon in Section 3.3.

Marine domain

To assess the model's ability to simulate marine developments, we examined the total eroded volume from the original Sand Engine domain and the corresponding accretion to the adjacent domains (Figure 3.6a).The model forecasts a total erosion volume of 4.1 Mm^3 from the main peninsula (blue in Figure 3.6a) over 5 years, slightly overestimating the observed volume of 3.9 Mm^3 by 4.6% (Figure 3.6b). Notably, the erosion from the marine domain diminishes over time, with the initial year showing particularly pronounced erosion (Roest et al., 2021). This trend is largely attributable to a stormy year and high initial shoreline gradients. On the other hand, the model underestimates accretion south of the Sand Engine, shown in green in Figure 3.6b (observed: 1.6 Mm^3, modelled: 1.4 Mm^3, -11.9%). Similar to the earlier visual comparison, the most significant deviations occur north of the Sand Engine, where the model overestimates the northward spit development, shown in pink in Figure 3.6b (observed: 1.9 Mm^3, modelled: 2.6 M^3, +38%).

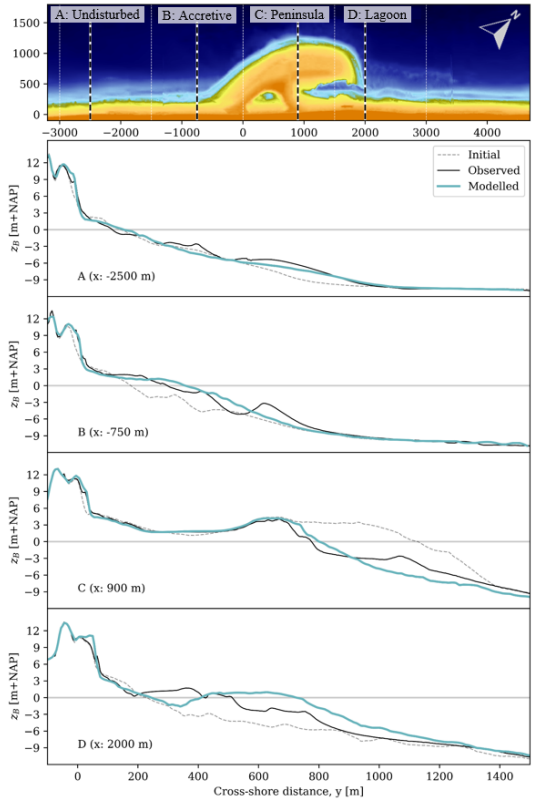

Figure 3.5.: Comparison between the modelled and measured cross-shore development for four transects within Sections A to D. The dotted, continuous black and continuous blue lines show the initial, observed and modelled bed levels, respectively.

Aeolian domain

To evaluate the model's ability to replicate aeolian sediment fluxes, we compared the modeled volume change within the dune lake domain to observations. The dune lake acts as a large catchment area for sediment transport driven exclusively by aeolian processes, regulated by both transport- and supply-limiting conditions.

We examined the volume changes within the dune lake region of influence, being the lake and the surrounding moist bed. We used the area enclosed by the 3 m+NAP isobath after construction as the region of influence (Figure 3.6c, blue patch) as it matches the extend of the moist zone seen in satellite imagery. The coupled model accurately reproduces the spatial pattern of deposition around the edge of the dune lake, with most deposition in the south-western part of the lake, corresponding with the most prevalent wind directions (Figure 3.6d vs. 3.6e). The simulated volume change within the dune lake domain slightly underestimates the observed infilling (-15%, Figure 3.6d). This discrepancy primarily arises during the first year. In subsequent years, the model better follows the observed trend.

3.3. Marine and aeolian process interactions

Building upon the demonstration of the coupled models' capability, we now use the model to analyse how the aeolian and marine domains influence each other. During analysis, we divided the evaluation domain into four distinct sections, A through D, each spanning 1500 meters and possessing unique characteristics (Figure 3.7). Section A is considered to be beyond the Sand Engine's influence zone. Section B is subject to progradation of the shoreline originating from the main peninsula. Section C includes the main peninsula and is marked by significant beach erosion. Section D encompasses the area where the spit and tidal channel are developing.

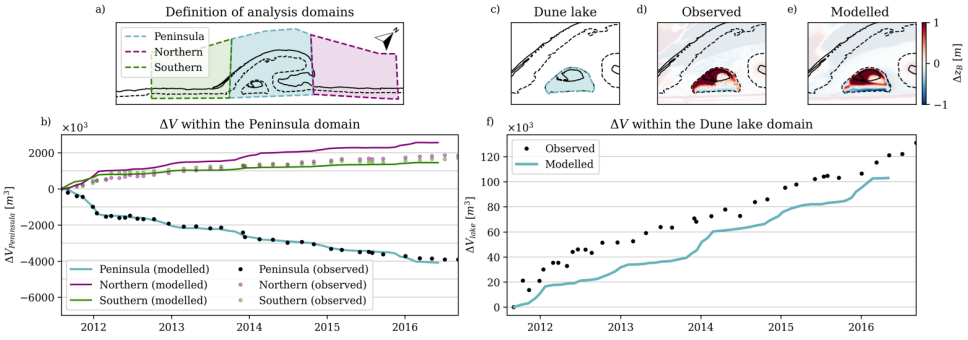

Figure 3.6.: Assessing the model's ability to simulate the marine (a,b) and aeolian (c,d) domains. (a) The Peninsula (purple), northern (pink) and southern (green) analysis domains and (b) the volumetric change over time within them. (c) The dune lake domain is indicated in blue. The observed (d) and modelled (e) bed level changes around the dune lake for comparison. (f) The volumetric change over time within the dune lake domain.

3.3.1. Aeolian and marine contributions

Both aeolian and marine processes influence the morphodynamic evolution of the Sand Engine. However, the magnitude of these processes differs in longshore and cross-shore directions. The longshore and cross-shore average bed level changes Δz_B [m] as computed by the coupled model are separated and individually examined in Figure 3.7. Aeolian-driven bed level changes are typically an order of magnitude smaller than those driven by marine processes. Averaged over the cross-shore profile (-50 m < y < 1450 m) the aeolian-driven bed level changes vary in the longshore direction from -0.22 to +0.18 m (Figure 3.7, bottom panel). These are substantially smaller than those driven by marine processes ranging from -1.51 to +0.98 m.

By averaging over the alongshore direction (Figure 3.7, left panel) the data shows that, near the foredune, the averaged bed level change is comparable in magnitude to marine-driven variations (both of order 1 m).

For a deeper exploration of aeolian and marine interactions in the intertidal domain, we examined the accretive region just south of the Sand Engine, section B (Figure 3.8). The marine-driven supply from the Sand Engine peninsula towards the intertidal zone characterises this section (purple in Figure 3.7 and Figure 3.8c). This deposited sediment is pickup up by aeolian processes and transported to the foredune (the orange patch in Figure 3.8c), illustrating the mutual exchange of sediment through the intertidal domain. The new dunes landward of the nourishment have been planted with marram grass (Figure 3.1b,c). Sedimentation has been observed at the base of this artificial dune, where grasses are capable of trapping sediment and using sand burial for enhanced growth (Nolet et al., 2018). Although minor deviations exist between the model and measurement results (Figure 3.8a, black vs. blue lines), the main accretive pattern is similar. However, zooming in on the supratidal area (Figure 3.8b) reveals that the model predicts erosion from this higher elevated beach, which is not evident from the measurements. In total, the bed level elevation of the aeolian zone, being the primary source for aeolian transport along Section B (20 m < y < 220, Figure 3.8b) m, is underpredicted with 0.36 m.

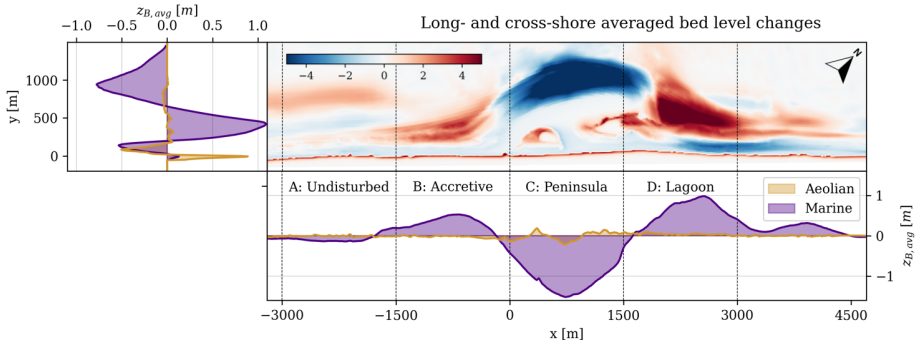

Figure 3.7.: The average bed level changes in long- and cross-shore direction due to marine (purple) and aeolian (green) processes.

3.3.2. Aeolian impact on longshore dispersion

The results above indicate that, although the magnitudes might differ, marine and aeolian processes shape the Sand Engine. In the upcoming sections, we aim to estimate the impact of the interactions between marine- and aeolian-driven morphodynamics on the system's integrated morphological development.

First, we evaluate the impact of aeolian processes on the primarily marine-driven longshore dispersion. We use the volumetric erosion from the peninsula (similar to §3.2.6 and Figure 3.6b) to quantify the impact of aeolian-driven processes on marine-driven sediment transport.

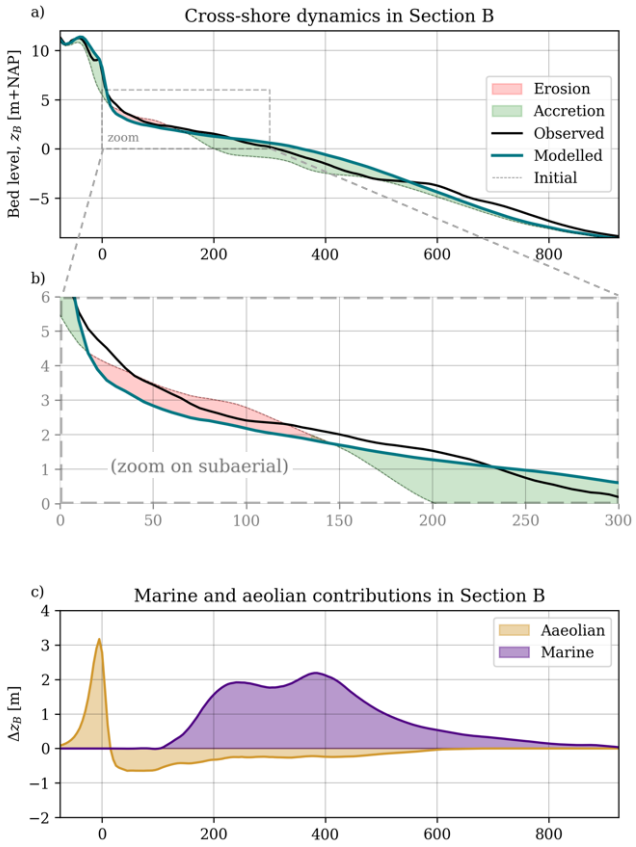

Figure 3.8.: The cross-shore varying dynamics within Section B (Accretive) over the 5-year period. (a) The observed and modelled cross-shore bed level changes (black and blue, resp.) are shown for the entire profile and (b) zoomed in on the aeolian part. (c) The purple and orange patches indicate the marine and aeolian contributions respectively.

During our 5-year evaluation period, the aeolian flux into the foredune along the Peninsula-polygon is 214,038 m^3. We expect this sediment to originate primarily from the intertidal domain, reducing sediment availability for marine-driven alongshore dispersion. We consider the marine-driven dispersion from the coupled simulation and compute the difference with the DELFT3D-FM-only simulation (§3.2.4) to estimate the aeolian contribution to marine-driven dispersion. In the DELFT3D-FM-only simulation, a total of 4.17 Mm^3 left the domain as a result of marine-driven transport. In the coupled simulation, the marine-driven transport was 4.10 Mm^3. This shows that the inclusion of aeolian transport reduces marine-driven dispersion by 69,661 m^3, which is 1.7% of the total 4.17 Mm^3. This reduction is relatively small compared to the total amount of sediment transported into the foredune (33% of 214,000 m^3).

3.3.3. Marine impact on foredune deposition

Alongshore variations in foredune deposition are examined to map the influence of marine-driven processes on the aeolian domain. To further discern the influence of marine-induced morphodynamics on aeolian dune growth, we analyzed the additional AEOLIS-only simulation (§3.2.4). For this foredune deposition analysis, we excluded the region north of the Sand Engine (x > 3000 m, see Figure 3.9b) since the beach entrances and restaurants heavily affect growth rates.

Within the central part of the modelled region (-3000 m > x > 3000 m) the average dune growth amounts to 83.7 m^3/m over a 5-year period, which is equivalent to 16.7 $m^3/m/year$ (Figure 3.9b). The model slightly overestimates this net dune growth with a predicted alongshore average of 95.2 m^3 over the 5-year period (19.0 $m^3/m/year$). These measured and predicted growth rates fall within the typical range of Dutch dune growth, which varies from 0-40 $m^3/m/year$ (de Vries et al., 2012). We explore the alongshore variations in the observed and modelled foredune deposition using four distinct coastal sections broken up into 1,500 m alongshore increments (see sections A-D in Figure 3.9b):

The "undisturbed" section (A: -3000 < x < -1500 m) lies just south of the Sand Engine and is assumed to be located beyond the Sand Engine's range of influence. The measured foredune growth here aligns with the domain average (88.9 $m^3/m/m$), which the model closely reproduces at 92.6 $m^3/m/m$.

The "accretive" section (B: -1500 < x < 0 m) is characterized by an accretive intertidal domain as a result of the longshore dispersion along the main peninsula. Observations show a noticeably higher dune growth rate in this region, averaging 110.2 m^3/m (A→B: +24%) over 5 years. Though the model reflects this increase, it does so conservatively at 106.4 m^3/m (A→B: +15%).

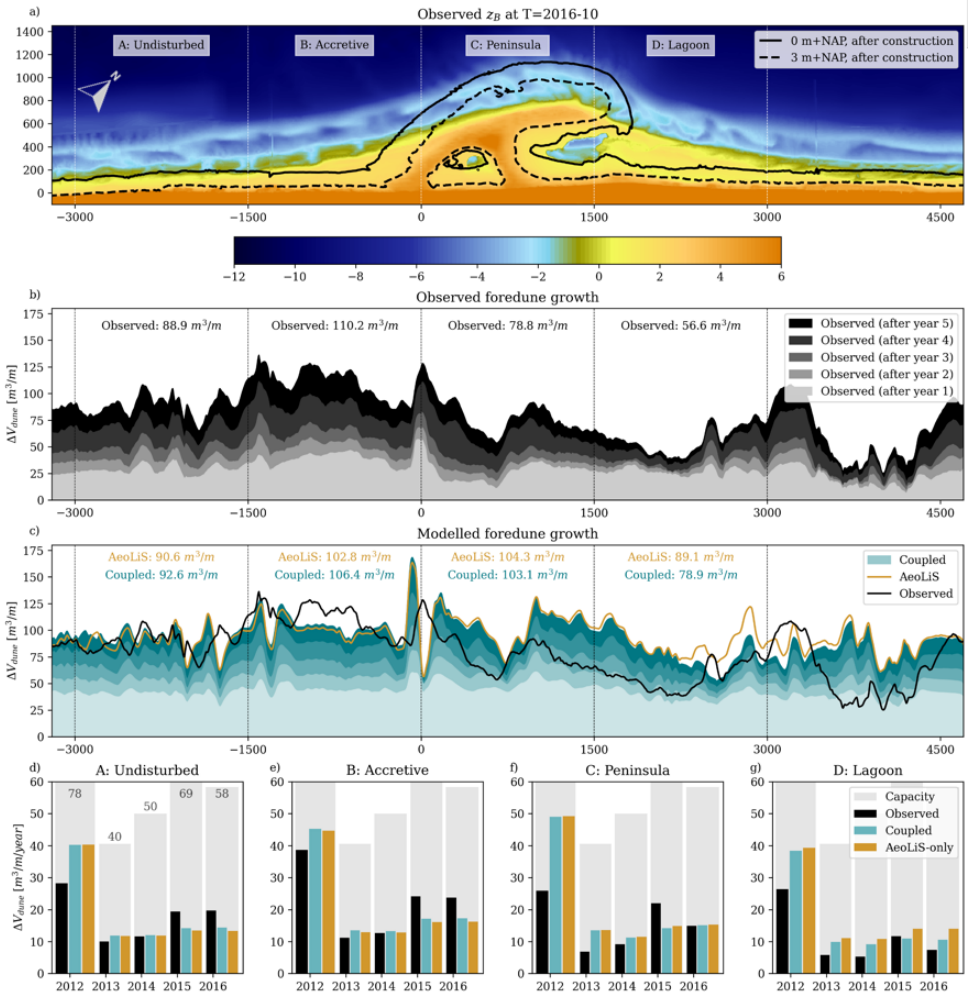

Figure 3.9.: (a) The bed level after the 10-year evaluation period and initial position of the Sand Engine indicated with contours. (b) The measured and (c) simulated longshore foredune deposition using the coupled model (blue), with yearly growth indicated by varying colour saturation. The foredune depositions after 5 years, as observed (black) and computed by AeoLiS-only (orange), are added for comparison. (d-g) Yearly growth rates for sections A-D computed for wind-driven capacity (grey), observations (black), coupled model results (blue) and AeoLiS-only results (orange).

The peninsula-section (C: 0 m < x < 1500 m), located behind the Sand Engine's initial position, measured a foredune growth of 78.8 m^3/m. This growth reduction of -11% with respect to the undisturbed section A contradicts initial predictions made during the Sand Engine's design phase (Mulder & Tonnon, 2011), in which the used empirical relation anticipated a doubling of foredune growth. The observed depression in foredune deposition aligns with the longshore position of the dune lake (Figure 3.9a-b). The centre of the foredune deposition depression (x = 800 m) is situated further north than the actual location of the dune lake (x = 400 m). We determined this centre by locating the point that stayed inundated the longest before accumulating the entire lake. The northward shift aligns with the prevailing wind direction, generally from south to southwest. The model overestimates dune growth slightly at 103.1 m^3/m across the zone. However, the model successfully predicted the local depression landward of the dune lake and the more northward-located centre and accurately predicted dune growth at this depression centre (observed: 53.6 m^3/m, model: 56.9 m^3/m).

The lagoon-section (D: 1500m < x < 3000 m) shows a continuing decline in observed foredune growth towards the Sand Engine's lagoon and the adjacent tidal channel. Both measurements (56.6 m^3/m) and model results (78.9 m^3/m) record the lowest dune growth along the examined coastal stretch. The model successfully replicates the spatial patterns in dune growth, including the decline in volumetric gains towards the tidal channel, but generally underrepresents its magnitude (observed: 38.4 m^3/m, modelled: 52.2 m^3/m, +36%), and locates this decline it roughly 500 meters more to the north than field data capture. The model overpredicts dune growth in this zone by 39%.

The observed foredune deposition shows significant annual variability throughout the evaluation period (black bars in Figure 3.9d-g). Especially the first year after construction shows a higher deposition rate. This is exemplified within the accretive region (section B), where dune growth reduces from 28.2 to 10.0 m^3/m/year between years 1 and 2. Similarly, landward of the lagoon (section D), dune growth decays from 26.4 m^3/m/year in year 1 to an average of 7.5 m^3/m/year over the subsequent four years. The observed annual variability can be partly attributed to the temporal fluctuations in potential wind-driven transport, as indicated by the grey bars in Figure 3.9d-g. Yet, the pronounced decrease in foredune growth from year 1 to 2, compared to the smaller decline in potential wind-driven capacity, underscores the influence of sediment availability on dune growth.

The model significantly overestimates dune growth in the first year (blue vs. black bars in Figure 3.9d-g), which is particularly apparent in Section C, the Sand Engine peninsula, where the initially modelled dune growth is 49.0 m^3/m compared to the observed 25.9 m^3/m. Although these deviations are most prominent in the first year, significant deviations are also present in subsequent years. While the model captures the second and third years (2013 and 2014) reasonably well, it underestimates the annual growth in the last two years. In the accretive domain (section B), the observed dune growth in the final year is 23.7 m^3/m compared to the model's prediction of 17.3 m^3/m.

Comparing the coupled simulation and AEOLIS-only results enables us to estimate the impact of the marine- driven morphodynamic development on the longshore variations in foredune deposition (see orange line in Figure 3.9c). Along Sections A and B, the coupled model predicts slightly higher foredune deposition than the AEOLIS-only results (2.3% and 3.5%, respectively). The local increase in foredune deposition indicates a positive impact that marine-driven morphodynamics have on the sediment availability for aeolian transport. On the contrary, in Section D, the coupled simulation predicts a significantly lower (-11.5%) foredune deposition compared to the AEOLIS-only simulation.

Although the deviations between the results for the different sections appear to be relatively small, they do increase over time, illustrated by the blue and orange bars in Figure 3.9d-g and Table 3.1. These evolving differences between the coupled and AEOLIS-only simulations indicate a cumulative effect of marine-aeolian interactions on foredune development. In Section B, the increase in foredune deposition due to the inclusion marine-driven morphodynamics increased from 1.3% in year 1 to 6.7% in year 5. Similarly, the reduction in foredune deposition in Section D increased from -2.4% in year 1 to -24.4% in year 5.

One of the largest deviations between the coupled and AEOLIS-only simulations is found at the location with the smallest dune growth along the entire domain (section D, x ≈ 2500 m). While the difference between the AEOLIS-only and coupled simulation at this location was relatively small after the first year (-4.2%), after year five, the coupled simulation predicted 48.5% lower dune growth (5.9 m^3/m/year) compared to the AEOLIS-only simulation (11.4 m^3/m/year). This finding not only shows the importance of the progressive nature of aeolian-marine interactions but also underscores that the importance of incorporating marine-aeolian interactions in numerical models can be very site-specific.

Section	Year					**Total**
	1	**2**	**3**	**4**	**5**	
A	−0.1	+1.0	+1.8	+5.7	+7.5	+2.3%
B	+1.3	+4.5	+3.2	+5.9	+6.7	+3.5%
C	−0.4	−0.3	−2.1	−4.4	−0.9	−1.2%
D	−2.4	−10.7	−15.1	−22.0	−24.4	−11.5%

Table 3.1.: Relative contribution (%) of including marine-driven morphodynamics in the coupled modelling for the predicted foredune deposition volumes in Sectors A-D during years 1 to 5.

In summary, although the model shows to be able to reproduce some longshore patterns, it underestimated the magnitude of the longshore variability in both accretive and erosive conditions. This is finally illustrated by comparing the dune growth along the accretive section B and sheltered section D. At section B, characterised by a growing beach and a surplus of sediment supply, foredune growth is observed to be 95% higher than at section D, where the beach has become narrower and is prone to sheltering from the developing spit. While the AEOLIS-only model does predict higher dune growth at section B compared to section D (+19%), the coupled model showed a more pronounced difference at 30%. As the Sand Engine continues to evolve, this discrepancy in dune growth becomes larger. After the fifth year, a difference of 219% between sections B and D is observed, compared to simulated differences of 16% and 64% by the AEOLIS-only and coupled simulation, respectively. The modelled impact of both aeolian and marine interactions on the integrated morphodynamics of the Sand Engine, and how developments in one domain affect the other, is summarized in Figure 3.10.

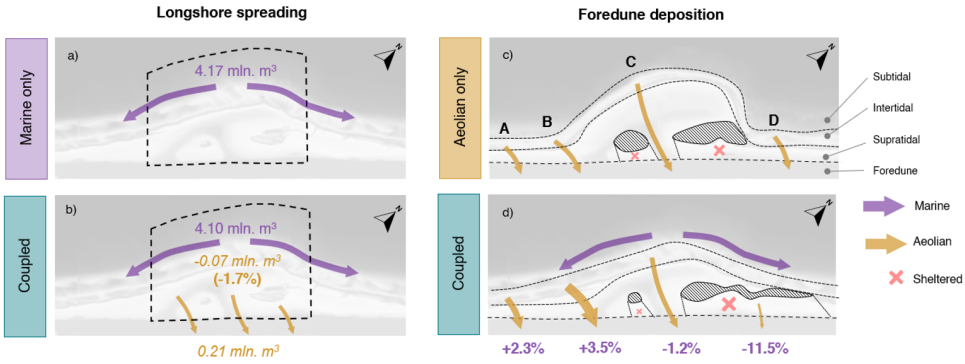

Figure 3.10.: Visual representation of the impact of interactions between aeolian and marine morphodynamics on longshore dispersion (left) and foredune deposition (right) in uncoupled (upper) and coupled (lower) situations. Comparing the marine-driven longshore dispersion without (a) and with (b) aeolian-driven development shows aeolian transport from beach to dune to cause a reduction in marine-driven longshore dispersion (-1.7%). The impact of marine-driven morphodynamics on aeolian-driven foredune deposition is shown by comparing the AEOLIS-only (c) and coupled (d) situations. Marine-driven morphodynamics result in accretion south of the Sand Engine (section B), coinciding with a local increase in foredune deposition (+3.5%), while northern spit development (section C) causes a local decrease in dune growth due to sheltering against waves (-11.5%).

3.4. Discussion

3.4.1. Advancements in numerical model coupling capabilities

Both wind and wave processes drive sediment transport in many coastal environments and can collectively be critical to their development at a broad range of time scales (storms to centuries) (Bauer & Davidson-Arnott, 2003; Garzon et al., 2022; Pellón et al., 2020; Ruessink et al., 2022). The interaction of marine and aeolian processes in part contributes to complex, alongshore varying evolution of coastal dunes (Cohn et al., 2018; Psuty, 2008). This connectivity between the marine domain and the growth rates or geomorphic characteristics of aeolian landforms has long been recognized through conceptual models (Houser, 2009; Pellón et al., 2020; Psuty, 2008; Sherman & Bauer, 1993; Short & Hesp, 1982), however our reliance on (often limited) long-term morphologic observations limits the transferability of trends yielded from conceptual models into predictive capabilities. Accurately forecasting coastal evolution, including the height of coastal foredunes, is critically important for quantifying present and future coastal risk.

To this point, numerical applications of coastal change in response have typically either focused exclusively on marine (Lesser et al., 2004) or aeolian (Durán & Moore, 2013; Hoonhout & de Vries, 2016) processes independently to forecast erosional or accretional dynamics across the coastal profile. Recent developments have also resulted in the coupling of models for simulating comprehensive 1D profile changes that incorporate both marine and aeolian effects on a range of timescales (Ciarletta et al., 2019; Cohn et al., 2019; Roelvink & Costas, 2019). While these 1D approaches provide an important step forward in both predictive technology of coastal profile change across the land-water interface and improved understanding of aeolian-marine feedback mechanisms, one-dimensional approaches require an assumption that alongshore variability in both forcing and response is negligible. This assumption is likely suitable for locations with wide flat beaches and long, continuous foredune ridges. Assumptions of longshore uniformity may have more limitations in sites with more spatially complex beach or dune morphology.

Only limited applications have expanded beyond the 1D characterization of coupled aeolian-marine systems. For example, Durán Vinent and Moore (2015) added capabilities into the aeolian Coastal Dune Model to additionally empirically assess wave-driven morphology change. However, the cross-shore only implementation of the wind solver in the model setup primarily focused on exploring the general behaviour of coastal systems moreso than the ability to hindcast specific wind and wave events. The cellular automata model of DUBEVEG uses a rule-based and probabilistic approach to modelling the general behaviour of beach, dune, and vegetation dynamics in 2D as well (Keijsers et al., 2016). However, this tool does not simulate underwater sediment transport and, therefore, perhaps neglects exchanges of sediment across the land-water interface and the resultant implications for sediment availability for wind-blown mobilization.

These various 1D and 2D tools all provide a valuable framework for advancing knowledge on nearshore-beach-dune interactions and potentially improving predictive skills for simulating coastal change hazards. However, only a fully 2D or 3D modelling framework can be used to assess (1) direct linkages of beach nourishment and its diffusion with time on long-term dune growth rates, (2) the role of spatially complex water bodies on sediment dynamics, and (3) the design of two-dimensional NBS.

The coupled model presented in this study shows the potential to describe the integrated spatiotemporal development of the nearshore-beach-dune system quantitatively on complex coastal landforms. This is achieved by facilitating the concurrent simulation of aeolian and marine development and integrating supply limitations based on dynamically changing conditions. Within a single framework, the ability to simulate marine redistribution of a mega nourishment through alongshore and cross-shore processes, tidal dynamics within a lagoonal setting and corresponding constraints on sediment availability, and armouring-related effects on wind-driven sediment transport are all demonstrated given confidence in the framework's ability to resolve the relevant morphodynamics of the system. As demonstrated, the presence of open coast and enclosed water bodies within the model domain imposes important implications on spatial patterns for both sediment mobilization and deposition, with the model successfully able to reproduce shadowing and supply effects of these water bodies on landward sediment fluxes into the dune (Figure 3.9a-b). One-dimensional tools could not effectively resolve such spatially complex trends. The relevance of integrating morphodynamics is proven by the increasing impact of marine transport on aeolian development (Figure 3.10) and aeolian transport on marine development (Table 3.1) over time. As the system evolves, so do the geomorphological characteristics that regulate aeolian and marine transport including beach widths and slopes. Both the impact of the accretive intertidal area on aeolian sediment availability and the sheltering effect of the evolving tidal channel (Figure 3.10d) could not have been depicted by static fetch-based approaches (Houser, 2009; Pellón et al., 2020). As such, as Sand Engine concept designs (Boskalis, 2022; Johnson et al., 2020) and other NBS (Arens et al., 2013a; Gerhardt-Smith et al., 2015; Kroon et al., 2022; Osswald et al., 2019; Steetzel et al., 2017) are being considered globally for cost-effectively protecting large coastal stretches through leveraging natural processes, the need to utilize appropriate 2D numerical frameworks to support cost justifications and to quantify benefits is encouraged.

However, these advancements are not without their drawbacks. Our attempt to provide a comprehensive, process-based depiction of the nearshore-beach-dune evolution exposed limitations in our understanding and modelling capabilities of the inter- and supratidal zones, as shown by the underpredicted bed level elevation of the beach in Figure 3.5. Simpler approaches allow for assumptions that reduce complexity and subsequent computational costs.

Suppose one is primarily interested in aeolian development. Would the slight increase in realism justify the five-fold increase in computational time necessitated by including marine-driven morphodynamics (§3.2.5)? These additional computational costs also result in more difficulties for efficient model calibration. Moreover, a complex coupled modelling approach introduces new technical challenges. Including increasingly more sophisticated models can lead to an increase in instabilities and errors, exponentially complicating error resolution as potential error sources multiply.

Lastly, we acknowledge that our results do not necessarily indicate a general improvement in predictive skill when using comprehensive coupling methods. The successful prediction of both aeolian and marine domains (Figure 3.6) can largely be attributed to the advantages of having two well-calibrated standalone models (Hoonhout & de Vries, 2019; Luijendijk et al., 2017), backed by an extensive dataset from the Sand Engine (Roest et al., 2021). Despite that, there are still missing physical processes in all of these tools, including direct simulation of groundwater effects, lack of infragravity processes on swash zone sediment transport and hydrodynamics, and simplification of eco-morphodynamic effects, which limit the ability to synthesize all of the dominant physical factors driving coastal change. Additionally, it is well recognized that even with an adequately calibrated model, model physics does not represent all complex eco-morphodynamic effects in coastal systems. Increasing complexity also doesn't necessarily translate into more accurate predictions (Salt, 2008). Thus, while coupled modelling frameworks serve as a tool for understanding system behaviour, model assumptions, lacking physics, and inherent limitations of models must be recognized in interpreting the results. The tradeoffs between model fidelity and computational grid sizes were chosen here specifically to simulate multi-year periods in a reasonable duration (e.g., weeks) with the ability to successfully simulate the primary drivers and controls on sediment transport across the land-water interface and into the dune. With the tool, we did show that the evolving interactions between aeolian and marine processes affect the complicated integrated development of NBS. The ability to simulate these complex 2D dynamics represents a step forward in capability that did not previously exist.

Deviations between field observations and model results in this study may underexpose the impact of the studied domain interactions on the integrated development. Still, they should not detract from the potential necessity of including domain interactions in future studies. We anticipate that including processes related to groundwater, meteorology, and swash could improve accurately simulating the supratidal domain. Additionally, these processes could also be necessary for the simulation of more complex aeolian landforms, such as blowouts (Hesp, 2002; van Kuik et al., 2022; Ruessink et al., 2018), embryonal dunes (van Puijenbroek et al., 2017b), or foredune dynamics (Moore et al., 2016), although it would require a more realistic description of vegetation dynamics (Durán & Moore, 2013); e.g. the relation of vegetation growth to sediment burial (Nolet et al., 2018). Future research should focus more on identifying coastal scenarios where these sophisticated coupled methods could add value and determining which processes should be included.

3.4.2. Interactions between marine and aeolian processes

Many studies have demonstrated that the concurrent evolution of nearshore-beach-dune systems is sculpted by both marine and aeolian processes (Aagaard et al., 2004; Bauer & Davidson-Arnott, 2003; Costas et al., 2020; González-Villanueva et al., 2023; Hallin et al., 2019a; Houser, 2009; Pellón et al., 2020; Sherman & Bauer, 1993; Short & Hesp, 1982; Silva et al., 2019). Many of these studies, while informed by field data, are largely conceptual, given the complexity of linking above and below-water processes. As such, more commonly, studies and models have traditionally focused on discrete compartments of the coastal tract, such as the nearshore, beach, or dune. However, the advancement of comprehensive numerical tools, such as the presented DELFT3D-SWAN-AEOLIS coupling framework, provides a tool to further understand and explore these interactions across the land-water divide.

In this study, we focus on assessing the impact of subaerial developments on the subaqueous domain, and vice versa. The former is assessed by quantifying the impact of aeolian processes on marine-driven longshore dispersion, and the latter by estimating the influence of marine-driven morphodynamics on longshore variability in dune growth.

During the Sand Engine's initial design phase, aeolian processes were not taken into account, completely ignoring the subaerial domain (Mulder & Tonnon, 2011). Throughout the 5-year evaluation period, significant subaerial landform development was observed and in total 214,000 m^3 of sediment was transported into the dunes along the peninsula-domain, as depicted in Figure 3.10. Over the Sand Engine's projected lifespan of more than 20 years, this volume can amount to least 1.5 Mm^3, considering the observed dune growth along the domain ($\approx$ 15 m^3/m/year) and its expanding longshore dimension (> 5 km) (Huisman et al., 2021). Considering that this volume is equivalent to a substantial Dutch shoreface nourishment (Brand et al., 2022), it is reasonable to anticipate that subtracting such volume from the sediment budget would have a significant impact on the Sand Engine's, marine-driven, longshore dispersion.

Comparing the DELFT3D-FM-only and coupled simulations enabled us to estimate the actual magnitude of aeolian processes on longshore spreading, which showed only a modest 1.7% reduction in volumetric erosion. Note that this result should be seen in the light of the (very) large longshore transport gradients as a result of the Sand Engine's construction. In such an extreme scenario, the relative impact of aeolian processes may appear minor, but in less dynamic interventions, aeolian transport to the dunes may play a more substantial role. For timescales beyond the 5 years assessed in this study, consistent aeolian sediment transport to the dunes (de Vries et al., 2012) will continue re-allocation of sediment from the intertidal and beach regions to regions further landward. This large sediment redistribution in turn has a feedback on the marine dynamics that could reduce the long term effectiveness of the Sand Motor for its downdrift sediment delivery and associated flood protection services that longshore sediment transport driven beach growth is expected to provide.

Finally, the computed decrease in longshore dispersion accounted for only 33% of the volume deposited in the dunes, partly because large amounts of sand were initially eroded from the supratidal beachface, not directly affecting the marine sediment balance. However, while the Sand Engine's shoreline will keep migrating onshore, erosion from the subaerial domain will eventually start to affect the volume of the onshore shifting subaqueous domain.

Similarly, we evaluated the impact of nearshore morphodynamics on the longshore variability in foredune growth. Past research has emphasized the critical role of marine supply in maintaining sediment availability for aeolian transport (Cohn et al., 2018; Houser, 2009; Pellón et al., 2020). Informed by the previously documented evolution of the Sand Engine via alongshore redistribution of sediment (Roest et al., 2021; de Schipper et al., 2016), we expected a substantial positive influence on foredune deposition along the southern flank of the Sand Engine (Figure 3.10). The available field observations partially affirmed this prediction, as volume changes increased in the main portion of the Sand Engine relative to the undisturbed region (A → B: +24%, Figure 3.9b).

Additionally, given a proposed relationship between foredune size and incoming wave energy (Moulton et al., 2021), in addition to the critical role of the intertidal domain as a source for aeolian pickup (Bauer et al., 2009; Hoonhout & de Vries, 2017), we anticipated the tidal channel north of the lagoon to contribute to reduced local foredune deposition. The formation of this tidal channel effectively disconnected the intertidal domain from the foredune, providing the landward beach increased shelter from oncoming waves. This sheltering effect minimizes the mixing frequency in the bed's top layer, leading to an increased impact of sediment sorting and armouring on sediment availability for aeolian transport. These expectations were again confirmed by the available field measurements, in which a decrease in foredune deposition was observed behind the tidal channel (A → D: -36%, Figure 3.9b).

By comparing the AeoLiS-only and coupled model results, we aimed to estimate the influence of marine-driven morphodynamics on foredune deposition quantitatively. Comparative analysis revealed a slight increase (+3.5%) in foredune deposition along the accretive region (Section B in Figure 3.9d). And behind the tidal channel, the model indeed predicted a reduction in foredune deposition as a result of marine-driven morphodynamics (-11.5%).

Although the coupled simulation only partially reproduces the observed longshore variability in dune growth (e.g., the difference between sections B and D), it has demonstrated its ability to replicate certain effects of nearshore morphological developments on dune growth. We expect that the model's inability to fully explain the observed longshore variability can be largely attributed to the model not being tailored to describe the integrated development of the nearshore-dune system, but rather to accurately depict both individual domains.

We do suspect that a better representation of the intertidal development in our model (i.e. the deviations illustrated in Figure 3.5) will result in a higher predictive accuracy of the alongshore and annual variability in foredune deposition, probably affecting the modelled aeolian-marine interactions. Despite the seeming importance of the intertidal zone in connecting the nearshore to the dunes, numerous processes that shape these zones are not included in this study. The intertidal, or swash, zone has a significant role in connecting the aeolian and marine domain (Chen et al., 2023; Roelvink & Otero, 2017), e.g. by transporting sediment from the nearshore to the upper beach during accretive conditions or beach recovery (Hine, 1979; Phillips et al., 2019). As swash morphodynamics are not included in our model description (van Rijn et al., 2011), the maximum elevation of marine-driven accretion is only 2.2 m+NAP (Figure 3.5c), much lower than the maximum total water level elevation at the site (van Bemmelen et al., 2020). This underscores the model's limited capacity to deposit sediment higher up into the beach profile, which is supported by the underpredicted bed level elevations in the upper swash zone (y < 200 m in Figure 3.5b). Swash-driven growth of the beachface could be vital in connecting nearshore sedimentation and aeolian-driven dune growth (Chen et al., 2023; Roelvink & Otero, 2017). The lack of swash-related processes could therefore be a reasonable explanation for the model's inability to fully reproduce the enhanced dune growth along accretive beaches, in this case mainly Section B.

Furthermore, in both simulations, a considerable amount of sediment was available for aeolian transport in the first year, as desert pavements need time to develop. This contrasts with Sand Engine's construction period, which spanned several months, potentially allowing for some degree of armouring before our simulation's starting point. Additionally, a uniform wind field is assumed, while shear perturbations (Durán et al., 2010; Kroy et al., 2002), or boundary layer formation, are found to shape the upper beach profile by reducing velocities towards dunes (Bauer et al., 2009). Observations show a relatively stable upper beach, while the model predicts erosion from the supratidal area (20 m < y < 100 m in Figure 3.5b). Consequently, during the first year, the supratidal zone temporarily served as a sediment source for aeolian transport, stimulating foredune growth in actual sediment-scarce sections (Figure 3.9f,g). These limitations are expected to strongly contribute to the overprediction of dune growth during the first year, distorting the comparative analysis between the coupled and AEOLIS-only simulations. Solving these model limitations could see a more accurate estimate of the impact of including aeolian-marine interactions in coupled modelling.

While the magnitude of the simulated feedback is relatively small (<15%) for the Sand Engine case study (Figure 3.9c), and probably underpredicted due to the described missing processes shaping the beach profile, the Sand Engine and other feeder nourishments are designed to provide benefits over the scale of decades. Aggregating flux modifications over these long timescales can drastically alter the total volume change and form of dune development. The 5-year evaluation period is short relative to the cumulative nature of the evaluated process interactions and dune-building timescales. Given the aggregating nature of the impacts evaluated, it might be

beneficial to extend the evaluation period to improve the quantification of their impact. These improvements also necessitate enhancing the framework's scalability, efficiency, and robustness. The spatio-temporal scale, two-dimensionality and high resolution of the presented nearshore-dune simulation are unprecedented. Despite this, the 5-year period is still relatively short compared to long-term morphological developments shaping the Sand Engine over its lifetime, potentially underexposing the importance of the impact that aeolian processes have on marine developments, and vice versa.

The Sand Engine case also represents a wide coastal beach setting with a large source area for aeolian transport and fewer sediment supply limitations than a narrow beach system with similar grain size attributes. It may be expected that there are other morphodynamic systems where simultaneous simulation of marine and aeolian is more critical to simulate long-term coastal behaviour effectively.

In light of the aforementioned study limitations, evaluating the predictive skill of our approach is further complicated by the fact that the original stand-alone setups were specifically calibrated to align with observed morphodynamics. If the DELFT3D-FM model component initially underpredicted longshore spreading, introducing aeolian-driven erosion from the intertidal area as an added factor limits sediment availability for longshore transport even further. This change reduces predictive accuracy, yet we believe it enhances the representation of the physical system. Conversely, if the AEOLIS model overpredicted foredune growth, adding marine-driven sediment supply would increase dune growth, potentially lowering the predictive score. Even though, in this study, including nearshore morphodynamics improved foredune predictions across all sections (e.g., for section B, AEOLIS-only: -6.7%, coupled: -3.5%; for section D, AEOLIS-only: +57.6%, coupled: +39.5%), these results are contingent on the original accuracy of the stand-alone models.

As stated by Barbour and Krahn (2004), the added value of numerical models is not limited to making predictions. Even though, in the context of the current study, both the impact of including aeolian-marine interactions and the improvement in predictive skill are minor, the fact that the coupled model has shown how aeolian processes can impact marine-driven longshore spreading and how nearshore morphodynamics can affect dune growth, the study has provided new insight into the integrated development of nearshore-dune systems. As initial predictions during the Sand Engine's design anticipated a significant increase in dune growth as a result of a large amount of nourished sediment, this study shows that the intricate interactions between marine and aeolian processes cause a much more complicated morphodynamic response of the nearshore-dune system.

3.5. Conclusions

In this study, we have quantified the impact of interactions between aeolian and marine morphodynamics on the nearshore-dune system. An intercomparison of numerical model simulations has shown the reduction of marine-driven longshore spreading as a result of aeolian fluxes towards the dunes, enhanced dune growth corresponding with nearshore sedimentation, and reduced dune growth along an eroding, sheltered beach. These findings align well with the available bathymetric and topographic measurements and our general system understanding based on existing literature on nearshore-dune dynamics. These findings can help increase the comprehensive understanding of the development of sandy Nature-based Solutions (NBS).

For this purpose, a novel coupling framework was presented that enables a continuous exchange (i.e. frequently during the simulation) of wave heights, bed-, and water levels between three model components: DELFT3D Flexible Mesh (DELFT3D-FM), SWAN and AEOLIS. This coupled model is then applied to simulate the first 5-year development of the Sand Engine: A large mega-nourishment constructed in the Netherlands.

The coupled model results show a concurrent development of the marine zone and the aeolian zone. The former is dominated by lateral dispersion of sand by marine processes with large quantities of sediment being eroded from the peninsula and deposition at the two adjacent beaches. The aeolian evolution is characterized by a growth of the foredune of O 15 m^3 per meter alongshore per year. This foredune growth varies in the alongshore as beach properties vary and artificial waterbodies acted as a sediment trap. The coupled model is able to reproduce the main volumetric changes well; i.e. less than 5% deviation of the erosion on the main peninsula (observed: 3.9 Mm^3, modelled: 4.1 Mm^3). The infilling of the artificial dune lake shows that the model can reproduce the aeolian sediment fluxes with an error in the volumetric change of 15%.

To enable the quantification the impact of aeolian and marine process interactions on the Sand Engine's integrated morphological development, the coupled and uncoupled (i.e. stand-alone) model results were compared. Our model results show that a persistent extraction of material by aeolian transport ($\approx$ 15 $m^3/m/year$) affects marine sediment transports. The relative impact of the aeolian component is small ($<$ 5 %) in the Sand Engine case. The last years in the simulations show a growing relative impact by the aeolian processes suggesting that the landward transport by aeolian transports cannot be ignored when assessing long-term alongshore sediment transport in the marine domain.

The variability in dune growth along the coast is likely influenced significantly by nearshore morphodynamics. At the southern end of the peninsula, which is characterized by marine-driven sedimentation, observed dune growth was 95% higher compared to the section that contains lagoon, spit and channel dynamics where the subaerial beach is small. The incorporation of marine-driven processes in the simulation indeed showed that the developing nearshore morphology impacts the foredune growth over time, leading to a decrease in average dune growth of -24.4% in the fifth year onshore of the lagoon, with maximum up to -48.5% at the most sheltered location. The large observed difference between the accretive part of the beach and lagoon/spit area was partially reproduced by the coupled model at a 30% difference, compared to a 19% difference in the stand-alone simulation, in which nearshore morphodynamics was not included.

This research represents a step towards an integrated approach in the numerical modelling of highly complex nearshore-beach-dune systems. Our first case study demonstrates the impact of including aeolian-marine interactions in the initial response phase of a large-scale Nature-based Solution, highlighting both the value of coupled numerical modelling and yielding new insights on marine-aeolian interactions on inter-annual coastal landform evolution. This newly demonstrated capability and approach opens the door to integrated landform modelling for a broad range of potential spatial (meters to 10s of kilometers) and temporal scales (hours to decades) in coastal systems where both winds and waves play an active role in sediment transport and net landscape change.

SEDIMENT PATHWAYS ACROSS DOMAINS

Traditional Eulerian analysis of sediment transport fields and morphological change reflects a mere shadow of coastal evolution - actual sediment movement remains hidden within simulation results. A novel Lagrangian tracking tool is introduced and applied to the model results from Chapter 3, revealing the origin, destination, and journey of particles across the coastal system.


4

Photo: Eric van der Eijk – https://duinlandschap.nl/

4

Sediment Pathways Across Domains

LAGRANGIAN MODELLING REVEALS SEDIMENT PATHWAYS AT EVOLVING COASTS

Abstract Coastal regions face increasing pressure from climate change, sea-level rise, and growing coastal populations. This "coastal squeeze" threatens both the systems' sustainability and their ecosystem services. Coastline perturbations—deviations from straight coastlines ranging from beach cusps to headlands, deltas, and artificial nourishments—exemplify this challenge. Although their diffusive morphological evolution is well understood, we have limited knowledge of the underlying sediment movement patterns driving this change. This study reveals how coastline perturbations alter sediment transport by tracing particles from origin to destination using Lagrangian tracking at the Sand Engine mega-nourishment. Our results demonstrate that perturbations alter both sediment dispersal and accumulation. During initial stages, the longshore dispersal of sediment is strongly restricted by rapid deposition and burial on both sides of the perturbation. A backward-tracing approach reveals that sediment deposition not only originates directly from the protruding part of the coastline, but also from updrift sources. As coastline perturbations diffuse over time, sediment movement patterns gradually converge toward those of an undisturbed coast. Increased understanding of sediment pathways enhances our ability to predict and communicate coastal response to interventions, supporting more effective management strategies.

This chapter is based on: van Westen, B., de Schipper, M.A., Pearson, S.G., & Luijendijk, A. P. (2025). Lagrangian modelling reveals sediment pathways at evolving coasts. *Scientific Reports 15*, 8793.

4.1. Introduction

Coastal regions face increasing pressure from climate change, sea-level rise, and growing coastal populations (Ranasinghe, 2016). This "coastal squeeze" threatens both the systems' sustainability and their ecosystem services (Pontee, 2013). Coastal systems provide numerous services to communities worldwide: recreational opportunities, unique habitats and biodiversity, protection against flooding, and drinking water provision (Arkema et al., 2013; Barbier et al., 2011; Sutton-Grier et al., 2015). The provision of coastal services depends on the availability of sediment within the coastal system. The spatial distribution of sediment (e.g., sand) evolves over time through complex transport patterns, making sediment transport understanding crucial for effective coastal management (Hanley et al., 2014; Mulder et al., 2011; Vitousek et al., 2017). Similar sediment redistribution along a coastline, or morphological change in general, can result from vastly different sediment pathways, a property known as equifinality (Beven, 1996; Ebel & Loague, 2006; Phillips, 1997). Understanding net morphodynamic change alone, i.e., the description of morphological evolution through erosion and deposition, is therefore insufficient for comprehensively understanding coastal evolution — it requires the ability to trace sediment movement across the system (Pearson et al., 2020; Ruggiero et al., 2016). This means not only quantifying how much sediment is redistributed but also tracking which sediment goes where, enabling better understanding and communication of causal relationships in coastal evolution.

The ability to map such sediment pathways has important practical applications, from finding sources of harbor sedimentation (Bastin et al., 1983; Ferreira et al., 2002) to tracking the dispersal of contaminated sediments from dam removals (Warrick et al., 2019) or dredged material from navigation channels and harbors (Smith et al., 2007), and evaluating the effectiveness of nutrient-enhanced dune nourishment (Pit et al., 2020). For example, coastal managers choosing an offshore disposal site for contaminated sediment need to evaluate how particles spread. While traditional Eulerian models can capture changes in bed levels or overall sediment budgets, they provide limited insight into whether sediments from a specific source migrate towards an area of interest. By building on widely used coastal models as a post-processing step, a Lagrangian approach uncovers these source-to-sink connections with minimal extra computational effort, offering a more direct way to inform management decisions.

Coastline perturbations, where the shoreline locally extends further seaward compared to its surroundings, provide a clear example where morphodynamic change alone cannot provide the complete explanation of coastal system evolution. These perturbations manifest across various spatial and temporal scales, occurring both naturally and anthropogenically, such as beaches on open coasts (Ashton et al., 2001), near tidal inlet systems (Elias et al., 2019; Stive et al., 2002), river mouths (Warrick et al., 2019), coastal structures (Black & Andrews, 2001; Stevens et al., 2024), deltas (Falqués & Calvete, 2005; Nienhuis et al., 2013; Pelnard-Considère, 1957), and artificial nourishments (Brand et al., 2022; van Duin et al., 2004; de Schipper et al., 2021; Stive et al., 2013).

While the diffusive evolution of coastline perturbations is well-documented (Dean & Yoo, 1992), existing descriptions predominantly focus on the net morphological response. Numerous studies have quantitatively described the erosion of the coastal sections protruding from the surrounding and deposition on their flanks(Dean & Yoo, 1992), yet the underlying sediment pathways remain largely unexplored. Due to morphological equifinality, this morphodynamic behavior can result from a range of sediment pathways. Therefore, to develop a more comprehensive understanding of the coastal response to coastline perturbations, we need to know how sediment movement is affected by their presence, rather than merely describing the resulting morphology. How far does the sediment from a perturbation spread alongshore, or is it primarily restricted to the observable diffusive region? And is the observed sediment depositions in the vicinity of the perturbation all originating from the perturbation, or does it include contributions from more distance shores sources?

The ambiguity between sediment transport and morphological development is not limited to coastline perturbations. Similar challenges arise in understanding breaker bar or sand wave evolution (Hoefel & Elgar, 2003), and subaerial landform development (van Westen et al., 2024b). Conventional Eulerian modeling approaches tabulate sediment fluxes on a grid of fixed points, and are insufficient to reveal the actual sediment pathways underlying the cumulative net response. By adopting a Lagrangian perspective, we can complement existing methods by simulating individual particle movements, thereby unraveling the sediment movement driving observed morphological changes.

Tracing sediment pathways requires complementing conventional Eulerian descriptions with Lagrangian analysis. However, mapping Lagrangian pathways poses significant challenges. Physical tracers (Bastin et al., 1983; Bertin et al., 2007; Black et al., 2007; Bosnic et al., 2017; Cheong et al., 1993; Ciavola et al., 1997; Drapeau & Long, 1985; Ferreira et al., 2023; Kato et al., 2014; Klein et al., 2007; Li et al., 2019; Miller & Warrick, 2012; Miller & Komar, 1979; Oliveira et al., 2017; Smith et al., 2007; Suzuki et al., 2019; White, 1998) can track sediment movement but have limitations: restricted spatiotemporal scales and labor-intensive procedures (Black et al., 2007; Pearson et al., 2021b; White, 1998). While numerical Lagrangian sediment methods exist (MacDonald et al., 2006; Pearson et al., 2021a; Romão et al., 2024; Soulsby et al., 2011; Stevens et al., 2020), their timescale of application is typically an order of magnitude smaller (~ months) than required for analyzing large-scale morphodynamic systems. They also generally neglect the trapping of sediment in regions with large deposition caused by morphodynamic evolution.

This study aims to understand the influence of coastline perturbations on longshore sediment movement by tracking particles across the coastal system. Through forward and backward tracing approaches, we address the following research question: How do coastline perturbations influence sediment pathways? Specifically, we focus on: (i) the dispersal of eroded sediment from perturbations along the coastline, and (ii) the source of deposited sediment on perturbation flanks, which is indicative of the mechanisms driving sediment accumulation.

We present a novel SedTRAILS-based approach (Pearson et al., 2021a) for tracing sediment movement with a Lagrangian framework. We apply our Lagrangian approach to simulate sediment pathways at the Sand Engine mega-nourishment (Stive et al., 2013) over multiple years of morphodynamic evolution. The Sand Engine presents an ideal case study for understanding coastal diffusion processes. Implemented in 2011 as a large artificial sediment pulse to nourish the Delfland coast over multiple decades (Stive et al., 2013), it represents a "pure" coastline perturbation, with evolution less convoluted than natural examples. The Results section presents two complementary analyses: a forward-tracing study revealing how sediment from the man-made perturbation disperses over time (i), and a backward-tracing investigation identifying the origins of sediment that was observed to accumulate at nearby coastal sections (ii). In the Discussion, we examine the broader implications of our findings for understanding coastline perturbations on sediment movement and evaluate the potential of Lagrangian approaches in large-scale morphodynamic systems. After summarizing key insights in the Conclusions, we detail our Lagrangian framework in the Methods section.

4.2. Results

Our novel Lagrangian tool builds on a validated morphological coastal area model by van Westen et al. (2024a), which integrates both marine and aeolian processes by coupling DELFT3D Flexible Mesh (Luijendijk et al., 2017) and AEOLIS (Hoonhout & de Vries, 2019; van Westen et al., 2024b) components. A 5-year brute-force hindcast, i.e., a simulation that captures the full period without schematizing or filtering conditions, is conducted, combining tides, wind, and waves (Luijendijk et al., 2019b). The numerical model effectively reproduces areas of erosion at the most protruding parts of the coastline as well as sedimentation at adjacent beaches, resulting in a diffusive development of the Sand Engine nourishment (Figure 4.1a,b). This Eulerian (grid-based, time-stepped) model is complemented by a Lagrangian post-processing method (Pearson et al., 2021a), assuming a uniform sand grain size diameter. This combination can now reveal sediment pathways that were previously undetectable.

The resulting individual pathways (Figure 4.1c) show significant variability in particle displacements, even when initial positions (e.g., particles with solid □, ◇ symbols) are close. These particles may be mobilized early in the simulation (greenish trajectories) or later (blue to purple trajectories) when the topography has evolved. Rapid displacements typically occur when particles are transported within the surf zone by wave-driven currents (e.g., △) or by aeolian transport on the subaerial beach (e.g., ◇), while slower, gradual movement is observed further offshore (e.g., ✠). Although net particle displacements can be similar, with starting and ending points close to each other, substantial differences in gross movement patterns can be present(e.g., ⛒- ☆).

Of the 400,000 initial particles seeded in the coastal cell, nearly 40,000 were mobilized during the 5-year simulation. We distinguish between two types of particles in our simulation: native particles representing particles already present before construction and nourished particles placed during the Sand Engine's construction. The large number of pathways enables volumetric analysis of the simulated Lagrangian particle movement. The combined sediment pathways, crossing the dry-wet interface, are analyzed to describe sediment movement along the coast.

4.2.1. Alongshore dispersal of nourished sediment

Over the five years since construction, nourished sediment is computed to disperse in both directions along the shoreline (Figure 4.2). Distinct asymmetry is visible in the sediment dispersal pattern and pathways, despite the more symmetrical transformation of the coastline, matching observations (Roest et al., 2021). Driven by predominantly southwestern waves and asymmetrical tidal forcing, northward movement dominates: 3.0 Mm^3 of the nourished sediment moves north compared to 0.4 Mm^3 south, while 81% of nourished sediment remains within the Sand Engine placement area during these first five years.

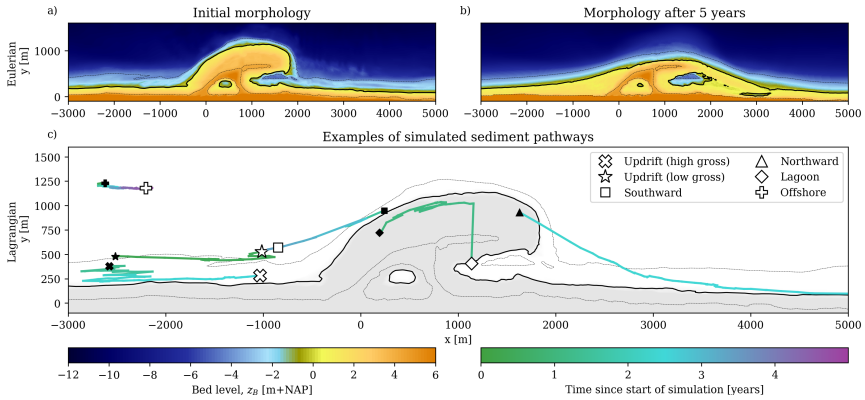

Figure 4.1.: Sediment redistribution in the Eulerian (a,b) and Lagrangian simulation results (c). Panel a) shows the initial Sand Engine morphology and panel b) the morphology after 5 years of simulated development using a validated coastal area model (van Westen et al., 2024a). Colors represent the bed level elevation relative to NAP (the Dutch reference for Mean Sea Level). Panel (c) shows the simulated trajectories of six selected sediment particles, each represented by a different symbol. The origin and destination of each pathway are shown as filled and open (white) markers, respectively. The pathway color indicates years elapsed since the simulations' start.

The spatial extent of dispersal also reflects this asymmetry. The computed southward dispersal reaches only approximately 2 km from the Sand Engine (Figure 4.2, beach section called "Monster"). In contrast, northward transport extends further, and most transported sediment (15.4% of total nourished volume) is deposited between 2 km and 4 km at the northern side ("Spit" section). Smaller fractions reach 4 to 6 km (0.91% at "Westduinpark") and 6 to 8 km (0.46% at "Duindorp") from the nourishment. Based on the simulations, no sediment travels beyond Scheveningen harbor (~ 8 km north).

The characteristics of the longshore dispersal of sediment evolves as the Sand Engine's morphology develops. To quantify this evolution, we analyze the one-year displacement of nourished particles from their initial mobilization, or release time. Figure 4.3c,d shows both net and gross longshore displacement, with particles grouped by their release year. For this particular analysis (i.e., Figure 4.3), we exclude particles released in the final year, as they experienced less than a full year of movement before being truncated by the simulation's end date. The figure also indicates the locations of representative particles from Figure 4.1c using matching symbols (including both native and nourished particles).

Both net and gross longshore particle displacement increase as the Sand Engine evolves. The average net displacement more than doubles from 646 m for first-year particles to 1496 m for fourth-year particles, as shown by the green and purple markers in Figure 4.3. Particles with the largest displacements also show this increase in displacement distance over time: the upper 5% of particles extend their northward reach from 1938 m in year 1 to 4335 m in year 4. Gross displacement distances follows a similar trend while on average being 2.9 times larger than the net displacement. Average gross movement increases from 1630 m in year 1 to 3124 m in year 4.

The directional distribution of particle movement evolves over time, transitioning from near-symmetrical movement in year 1 (i.e., skewness of Gaussian distribution $\gamma_1 = 0.11$), indicating dispersal to both sides, to strongly northward-skewed in year 4 ($\gamma_1 = 0.89$). As the Sand Engine evolves toward a straight coastline, both transport magnitude and directionality become stronger, indicating a stronger influence of the coastal perturbation during the initial phases of development.

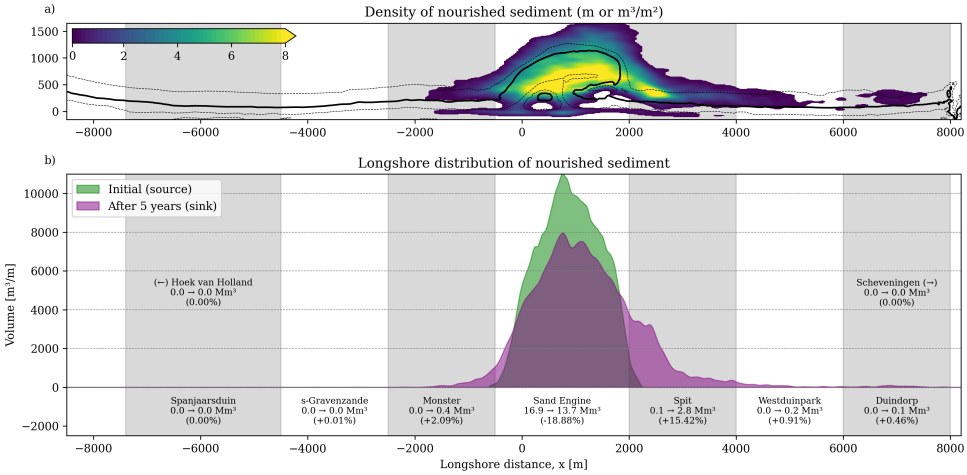

Figure 4.2.: Longshore distribution of nourished sediment particles five years after construction. Panel a) shows a density map of the spatial particle distribution, with color indicating sand volume of the nourished sediment per surface area (m³/m²). Low density patches (blue) reach from the Monster beach section (x ~ -2000 m) to Duindorp beach (x ~ 7500 m), showing the longshore region over which the nourished sediment is spread. Panel b) shows the initial distribution of sediment particles associated with the nourishment (referred to as 'source') in green and the sediment distribution after 5 years in purple ('sink'), highlighting the perturbations' asymmetric diffusion with dominant northward transport. Longshore regions are labelled, and volumetric and percentage changes over time are provided.

4.2.2. Morphodynamic-driven burial reduces longshore sediment dispersal

The shorter distances traveled by sediment during early stages result from rapid burial of nourished sediment at the Sand Engine's accumulating flanks. This burial effect is particularly strong during the first year (narrow green KDE in Figure 4.3a,b), when particles have less time to move before becoming trapped. As the Sand Engine evolves, the magnitude of bed level change decreases, enabling particles to remain mobile for longer periods. This evolution is reflected in burial statistics: the proportion of particles buried within their release year drops from 85% in year 1 to 55% in year 4.

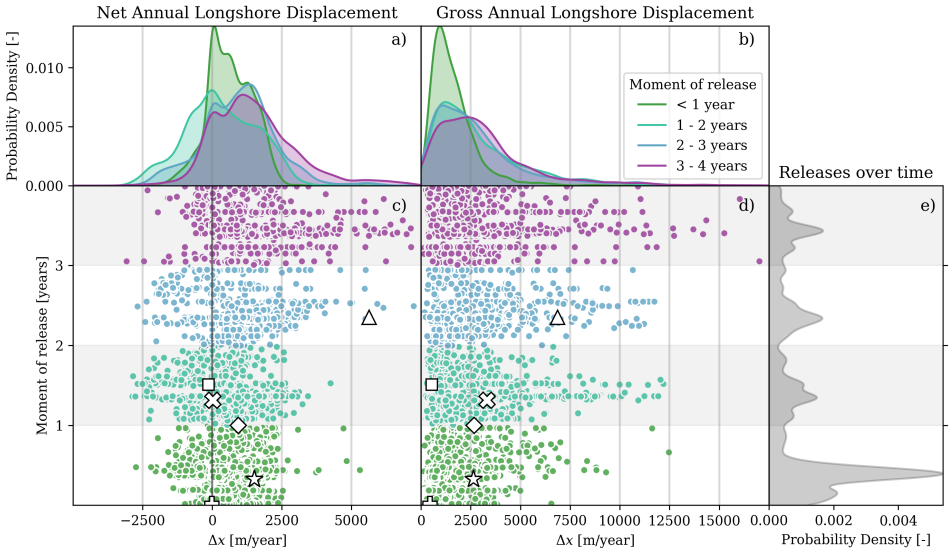

Figure 4.3.: Evolution of longshore particle displacement in time and space. The scatter plots show one-year net (c) (i.e., the Euclidean distance between release and burial locations) and gross (d) displacements (i.e., the distance travelled along the particle trajectory) of individual particles. The x-axis shows the displacement distance, and the y-axis the date of release, i.e., the moment of first mobilization. All particles are colored by release year. The northward shift in net movement shows the increase in asymmetric development over time, accompanied by generally larger net and gross longshore particle displacement. Selected particles from Figure 4.1c are highlighted using the same symbols. Panel a) and b) present kernel density estimations (KDE) of displacement distributions for each year, using matching colors. Panel e) shows temporal distribution of particle releases (number of initial mobilizations), with higher KDE values indicating more frequent mobilization events, particularly during the first storm season in the first year.

Existing Lagrangian descriptions of sediment movement do not account for the influence of burial on particle dispersal. To quantify the importance of burial on pathway distance, we compare our modeled longshore dispersal with expected movement along an unperturbed coastline (equation (4.11) in Methods). In the surfzone, where wave-driven currents dominate, the transport rates (Q_x) are typically in the order of 300-700 m³/m/year (Figure 4.8a) and mixing layer thickness (δ_{mix}) of 0.07-0.12 m (equation (4.5)), resulting in particle displacement estimates (Δx_p) from 2.5 to 10 km/year along an undisturbed coastline ranges. Simulated displacement around the perturbation shows much shorter distances, averaging only 200 m/year (~1000 m over five years), an order of magnitude below these theoretical estimates.

As time progresses and morphodynamic activity decreases, particle movement gradually approaches these estimated transport rates. This convergence is evidenced by the increasing proportion of particles achieving significant northward movement: while less than 1% of particles traveled at least 2.5 km in year 1, this fraction grew to 21% by year 4.

Near perturbations, morphodynamic activity (O(1 m)) can significantly exceed mixing depth (O(10^{-1} m)), substantially constraining sediment movement (Figure 4.4a,b). However, along straight, unperturbed coastlines where longshore transport gradients are minimal, morphodynamic activity and particle burial remain small. In these conditions, sediment dispersal is governed primarily by transport capacity and mixing layer thickness (equation (4.11), Figure 4.4c).

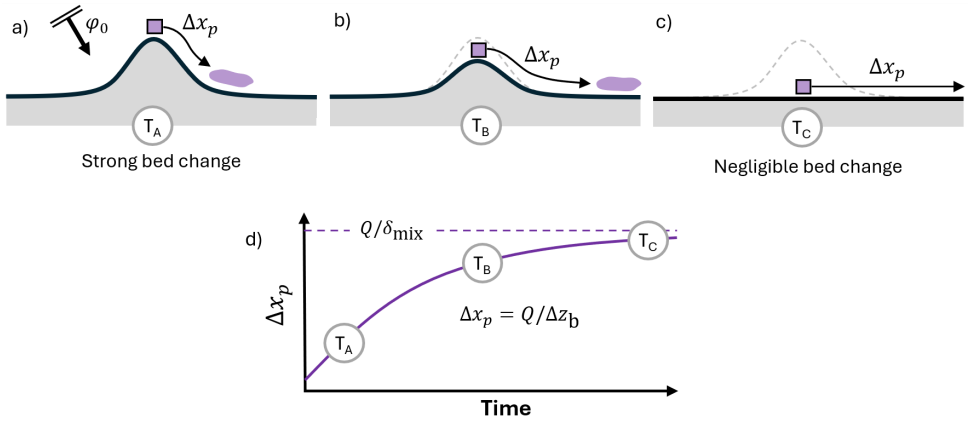

Figure 4.4.: Morphodynamic-driven burial restricts longshore particle movement in accretive areas. Top panels show planform schematics of the transition from a burial-limited (panel a, b) to transport-limited (panel c) state. Panel (d) shows the corresponding temporal change of particle displacement.

Conceptually, this can be captured in an adjusted displacement estimate for accretive coastal sections:

$$\overline{\Delta x_p} = \frac{Q_x}{\delta_{\text{mix}}} \min\left(\Delta t, \Delta t_{\text{burial}}\right) = \frac{Q_x}{\max\left(\delta_{\text{mix}}, \Delta z_{\text{b}}\right)} \Delta t \tag{4.1}$$

Where the Δz_{b} indicates the magnitude of the accretion, and Δt_{burial} the duration before a particle gets buried beyond the mixing layer depth. Using this adjusted formulation with typical values of Δz_{b} ($\sim$ 5 m) we see indeed a nearly tenfold reduction in pathway distance. As perturbations diffuse over time and deposition rates decrease, the system gradually transitions from this burial-limited state toward transport-limited conditions characteristic of natural coastlines (Figure 4.4d). Note that this only applies for accretive zones. In contrast, erosion of the bed could free particles that would otherwise have been trapped permanently, thus increasing the particle displacement.

4.2.3. Direct and indirect effects drive accumulation around perturbations

Tracing sediment origin at accumulating flanks reveals mechanisms underlying the diffusive evolution of coastline perturbations that are not apparent from morphological observations alone. While conventional understanding might suggest that flanking accretion results simply from sediment dispersing in both directions, our particle tracking analysis reveals a more complex reality (Figure 4.5).

Sediment accumulation may occur from two distinct sources: the "direct" effect of sediment accumulation with sediment from the perturbation that is relocated and the "indirect" effect of sediment from the adjacent coastlines that is deposited due to the presence of the perturbation and the altered transport gradients.

South of the Sand Engine, transport patterns show both of these contributions as the perturbation creates strong coastline gradients, enabling bidirectional transport. Figure 4.5a,b illustrates how the southern flank accumulates sediment through two mechanisms: directly from nourished sediment moving downdrift from the perturbation, and indirectly from native sediment arriving from updrift sources. This bidirectional transport emerges from the perturbation's effect on coastline orientation in combination with the dominant sediment transport direction. The initial deviation of the shoreline orientation (α) of up to 45° with respect to the surrounding coast creates conditions for opposing transport patterns, as conceptually illustrated in Figure 4.6a. In this region southward of the perturbation, on the updrift side relative to the dominant sediment transport direction on the perturbed coast, more than half of the accumulation does not originate from the perturbation itself. Especially during the first year, this results in a mixed accumulation pattern (Figure 4.5c): 59% from updrift sources (native particles; green bars) and 41% from downdrift transport (nourished particles; purple bars).

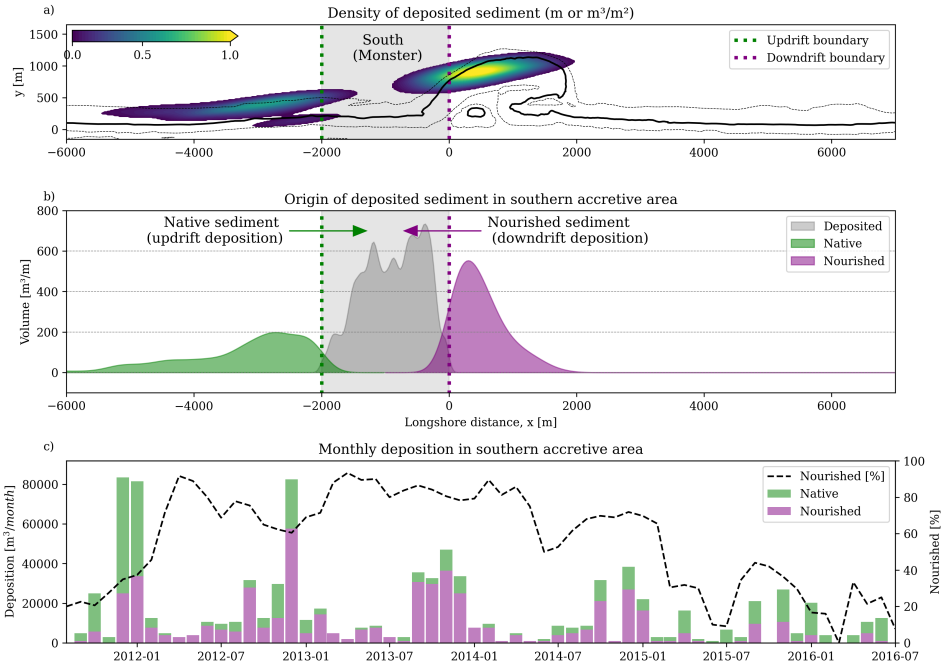

Figure 4.5.: Sediment pathway analysis leading to deposition on the southern side of the Sand Engine coastline perturbation. Panel a) shows the origin of sediment deposited in an area south of the Sand Engine (hatched control area called "South"), with colors indicating sediment quantity (m^3/m^2). Panel b) shows the longshore distribution of this sediment. Bi-directional accumulation is indicated by sediment originating from updrift (green) and downdrift (purple) sources. Panel c) quantifies the temporal contribution of these updrift and downdrift sources to sediment accumulation, with the dotted black line showing the percentage of downdrift deposition (nourished particles) relative to total accretion. Sediment accumulation is bi-directional, although the majority of sediment in the first three years originates from the nourishment. As the shoreline straightens over time, the majority of accumulation then comes from updrift, lowering the contribution of nourished particles (<40%).

Accumulation on the opposite northern side of the perturbation has a different source and ratio between nourished and native sediment. Being on the downdrift side of the dominant sediment transport direction, accretion follows a simple unidirectional pattern: nearly all deposited sediment (97%, Supplementary Figure S1) originates from the perturbation itself, and creating a spit-like feature. The contrasting ratio between direct and indirect accumulation effects for the different sides demonstrates how accretion mechanisms may vary with position relative to

both the perturbation and the predominant transport direction.

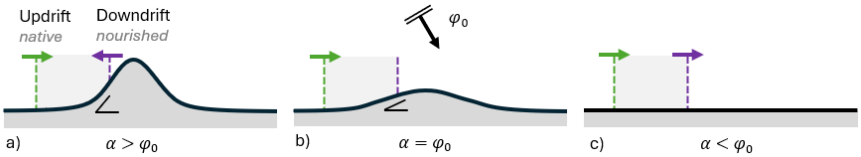

Figure 4.6.: Evolving coastline gradients change the source of deposited sediment. Evolution of deposited sediment origin from bidirectional (a) to unidirectional accretion (b), to no net morphodynamic change (c), illustrating the relationship between coastline orientation α, incident wave angle ϕ_0, and resulting changes in transport patterns (illustrated with the colored arrows).

Over time, coastline perturbations can become less pronounced and the local coastline orientation with respect to the surrounding coast decreases. Conceptually, at some point, the system passes through a transition point where sediment transport becomes predominantly unidirectional $\alpha = \phi_0$ (Figure 4.6b). This evolution manifests in the observed changing deposition patterns, as shown by the ratio of nourished particles contributing the accretion south of the Sand Engine (Figure 4.5 c, black dotted line in). Downdrift deposition diminishes (from 70% in year two to 30% in year five) as the system returns to predominantly updrift deposition characteristic of an undisturbed coastline. As the coastline diffuses further, not all sediment is deposited at the flanks anymore. Due to reduced burial influence and smaller longshore gradients, particles start to bypass the perturbation. Ultimately, the coast becomes straight again and the amount of sediment entering the domain equals leaving it (Figure 4.6c). This conceptual description is valid for coasts impinged by low-angle waves, and maybe differ in cases of high-angle waves (Ashton et al., 2001).

4.3. Discussion

Understanding sand movement along the coast is vital for effective coastal management (Hanley et al., 2014; Mulder et al., 2011; Ruggiero et al., 2016; Vitousek et al., 2017). While Eulerian approaches (Lesser et al., 2004; van Westen et al., 2024b) are able to effectively capture net morphological change in coastal systems, they cannot reveal the sediment pathways driving this development. And, due to morphological equifinality, these sediment pathways can not be inferred from the coastline change alone. This makes net morphological change alone an incomplete descriptor of coastal evolution. Understanding coastal evolution therefore requires looking beyond these net changes, and the ability to map sediment pathways can provide this insight.

Most existing particle tracking approaches are constrained by morphostatic assumptions with no morphodynamic-driven burial (Bertin et al., 2007; Black et al., 2007; Bosnic et al., 2017; Ciavola et al., 1997; Ferreira et al., 2023; Kato et al., 2014; Klein et al., 2007; Li et al., 2019; Miller & Warrick, 2012; Miller & Komar, 1979; Oliveira et al., 2017; Smith et al., 2007; Suzuki et al., 2019; White, 1998). These assumptions become particularly problematic when studying coastal perturbations that undergo significant morphological changes over multiple years, as demonstrated at our Sand Engine study site (Roest et al., 2021; de Schipper et al., 2016). Physical tracer studies (e.g., with colored particles) would be ideal; however this technique faces similar challenges: the practical difficulty of tracking particles through evolving morphology challenges long-term pathway analysis (Black et al., 2007; White, 1998). Although geochemical approaches can indicate provenance of sediment at larger scales (O(10-100 km)(Barnard et al., 2013)), these techniques may not have sufficient resolution to explain the evolution of coastal perturbations like the Sand Engine.

Our Lagrangian approach addresses these limitations through several key novelties. Using pre-computed Eulerian output reduces computational demands compared to calculating sediment velocities on a per-particle basis. By building upon frequently provided morphology and sediment transport fields from a validated Eulerian model (van Westen et al., 2024a), we achieve multiple advances:

- The incorporation of morphodynamic-driven burial through simulated bed level changes extends Lagrangian modeling beyond traditional short-term analyses to multi-year studies of evolving coasts.
- The direct coupling between spatial patterns in mobilization probability and validated transport rates ensures Lagrangian movement aligns with Eulerian predictions. This produces realistic free-to-trapped ratios that naturally capture spatiotemporal variations in transport capacity and burial—induced particle trapping, eliminating the need for empirical parameters required in other approaches (Soulsby et al., 2011).
- Our probabilistic approach to particle mobilization better represents the intermittent nature of sediment transport, particularly crucial for supply-limited aeolian processes (de Vries et al., 2014a). While alternative approaches

using reduced effective velocities (Romão et al., 2024; Stevens et al., 2020) offer computational advantages, they cannot capture the characteristic pattern of long burial periods punctuated by rapid, unidirectional movement.

The current method's primary limitations stem from the accuracy of underlying Eulerian transport estimates. Any limitations in the Eulerian input are inherited by the simulated pathways. The Lagrangian method does not provide validated pathways (doing so would require a physical tracer study, which can be challenging and cost-prohibitive (Black et al., 2007; White, 1998)), and thus should be considered as an alternative representation of Eulerian model results. This restricts the application range of the Lagrangian approach and the conclusions drawn within our study. In particular, cross-shore wave-driven and aeolian processes are only partly understood and underrepresented in the Eulerian results. Insufficient resolution of subgrid and intrawave processes in process-based morphodynamic models is known to result in unrealistic cross-shore morphodynamics, including cross-shore smoothing of surfzone bars (Grunnet et al., 2004). To mitigate these effects in the Eulerian model, cross-shore transport was deliberately reduced (van Westen et al., 2024a). Additionally, the Eulerian model underrepresents sediment exchange across the intertidal area (van Westen et al., 2024a) likely due to missing swash-driven processes (Chen et al., 2023; Roelvink & Costas, 2019). These limitations restricted us to drawing conclusions primarily on longshore development, and prevent application in complex situations where morphological changes rely on cross-shore or intertidal processes. Since we have confidence in the bulk longshore transport rates, as the resulting morphological change compared well with observations, it is reasonable to assume that the simulated longshore particle movement is a representative depiction of real-world pathways.

On the contrary, these inherent limitations also provide valuable insights. By revealing specific shortcomings in Eulerian models through particle tracking, our approach identifies areas where conventional morphodynamic models need improvement. The utility of Lagrangian approaches ultimately depends on the quality of underlying Eulerian transport predictions. As morphodynamic modeling capabilities advance, the application range of particle tracking will expand accordingly.

This study employs a single-fraction in the Lagrangian analysis, aiming to capture the bulk of sediment transport. This single-fraction setup is consistent with the validated, observed morphological evolution over this five-year period. Finer fractions of natural sediment are likely to be mobilized faster and transported over longer distances than coarser fractions. Moreover, sediment hiding and exposure by coarser grains may influence the behaviour for forcing conditions close to the threshold of motion. A multi-fraction framework could provide further insight into sediment dynamics in these more complex settings. However, this requires modifying both Eulerian models to account for multiple sediment fractions, falling outside the scope of our study. Note that subaerial armouring processes are accounted for in the Eulerian fluxes from the AEOLIS model, by increasing the threshold for sand mobilization as the proportion of non-erodible grains rises and thus affect bulk sediment transport.

Our results have implications for coastal management, as the Lagrangian analysis reveals that even seemingly simple morphological evolution can mask complex sediment transport dynamics. While the Sand Engine exhibits relatively straightforward diffusive behavior at the coastline scale, individual particle trajectories show convoluted and diverse pathways (Figure 4.1). Sediment starting from identical positions can reach vastly different destinations, and sediment with similar net displacements often follow different trajectories, as evidenced by varying gross-to-net displacement ratios. Sediment burial further complicates these patterns by intermittently restricting movement and influencing the timing of particle mobilization and deposition.

These detailed transport patterns, inaccessible through conventional Eulerian modeling, provide unique insights into sediment sources, pathways, and sinks.Although the observed accretion on both sides of the man made perturbation might initially suggest near-symmetric transport of nourished sand, our results clearly show that such conclusions cannot be drawn solely from bed level changes. A pathway analysis like the one presented here is highly valuable for coastal management and environmental impact assessments, as it can reveal the source material for harbour basin infilling(Ferreira et al., 2002) or define the influence zones of (contaminated) sediment deposits(Smith et al., 2007). This capability can also extend beyond traditional morphological response analysis by revealing the fate of specific sediment fractions, making it valuable for coastal management applications such as evaluating sediment release from dam removals (Warrick et al., 2019), and optimizing the placement of nutrient-enhanced sediment for dune development (Pit et al., 2020). Backward tracking (sink-to-source) revealed sediment origins (Figure 4.5) that may challenge basic intuition based solely on morphological evolution. This capability enhances our understanding of coastal interventions by revealing complex transport patterns, such as distinguishing between feeder- and leeside-effects in shoreface nourishments (van Duin et al., 2004; Huisman et al., 2019) and unraveling sediment exchange pathways near ebb-tidal deltas (Elias et al., 2019).

Regarding computational efficiency, the main cost is associated with the Eulerian model, while Lagrangian analysis adds relatively little overhead. Moreover, because each particle's trajectory is independent, the additional Lagrangian analysis is straightforward to parallelize, making it scalable for larger coastal systems.

Overall, Lagrangian simulation provide a more intuitive visualization of complex sediment transport processes compared to aggregated vector fields, for both scientists and stakeholders alike. The approach opens possibilities for advanced analytical techniques previously unexplored at these spatiotemporal scales. Examples of sophisticated analysis techniques to reveal information hiding in Eulerian model results are the identification of Lagrangian Coherent Structures (Gough et al., 2016; Pearson et al., 2023; Reniers et al., 2010; van Sebille et al., 2018), analysis of stratigraphic development (Pearson et al., 2022), quantification of sediment residence times (Hoffmann, 2015; Voepel et al., 2013), and connectivity analysis (Pearson et al., 2021a).

4.4. Conclusion

This study advances our understanding of how coastal perturbations affect sediment pathways by revealing the mechanisms controlling both dispersal and accumulation patterns. Through novel Lagrangian analysis based on Eulerian model predictions applied to the Sand Engine, chosen for its relatively simple diffusive evolution, we traced individual sediment pathways to uncover how perturbations impact sediment movement along the coast and thus coastal evolution.

As coastline perturbations diffuse, their sediment disperses along the coast. Our analysis of the Sand Engine reveals that nourished sediment initially moves in both directions, while movement is being constrained during these early stages. Strong morphological change leads to rapid deposition on the perturbation flanks. Under these conditions, burial reduces particle displacement distance by an order of magnitude compared to undisturbed coastlines. As the perturbation size decreases, the system gradually transitions to transport conditions similar to the unperturbed coast, which is evidenced by increasing sediment displacement distances.

Coastline perturbations introduce strong gradients in coastline orientation, creating complex patterns of sediment accumulation driven by two distinct mechanisms. First, sediment can accumulate through direct supply, where material from the perturbation itself moves downdrift. Second, the perturbation's presence modifies regional transport patterns, leading to indirect accumulation through updrift deposition. Model simulations revealed this dual mechanism during the Sand Engine's initial phase, where accretion south of the perturbation showed near equal contributions from nourished sediment moving downdrift (direct supply) and native sediment arriving from updrift sources (indirect response). As the perturbation diffuses and coastline gradients decrease, the system transitions back to unidirectional transport characteristic of unperturbed coastlines.

These insights were enabled by our Lagrangian approach that builds upon validated Eulerian model results. By incorporating morphodynamic-driven burial and directly relating particle mobility to sediment transport rates, the method reveals sediment pathways impossible to detect through conventional Eulerian approaches. The method extends Lagrangian analysis beyond traditional timescales to multi-year periods, enabling the study of morphodynamic systems. Through volumetric comparison with Eulerian results, we verified that the approach accurately represents sediment transport and redistribution patterns provided by the coastal area model.

Our findings have broad implications for coastal management and research. While conventional approaches reveal net sediment volumes (i.e., how much sand is moved), our Lagrangian approach enables tracking of individual sediment pathways (i.e., which sand goes where). Since similar morphological changes can result from vastly different sediment movement patterns (equifinality), describing only the morphodynamic response provides an incomplete image of coastal evolution. The ability to map sediment pathways enhances our understanding of, and capacity to communicate, coastal responses to both natural and anthropogenic perturbations. Although this study focuses on longshore transport, the framework shows promise for analyzing more complex coastal features such as tidal inlets, ebb-tidal deltas, and shoreface nourishments. Applying this approach to such features could improve our understanding of sediment movement throughout the coastal system and enhance the effectiveness and communication of management strategies.

4.5. Methods

We present a Lagrangian framework to analyze sediment pathways derived from Eulerian transport fields. While we refer to "particles" when describing sediment movement, our method differs from particle models that directly simulate particle advection based on hydrodynamic forcing. Instead, we employ a post-processing approach that conducts Lagrangian analysis on Eulerian model outputs while preserving the physical meaning of sediment parcel velocities. We adopt this particle terminology to facilitate clear description and visualization of transport patterns.

4.5.1. Eulerian model

Our Lagrangian analysis builds on results from a validated coupled morphodynamic model (van Westen et al., 2024a) that combines nearshore (DELFT3D-FM (Lesser et al., 2004)) and aeolian (AEOLIS (Hoonhout & de Vries, 2016; van Westen et al., 2024b)) processes at the Sand Engine mega-nourishment (Stive et al., 2013). This model successfully reproduces observed morphological evolution in both subaqueous and subaerial domains (van Westen et al., 2024a). While some cross-shore processes, particularly at the dry-wet interface, are not fully captured, the model provides realistic sediment transport rates for our focus on longshore sediment redistribution.

The Eulerian framework comprises an unstructured grid of 17,412 cells for the DELFT3D-FM domain and a structured grid of 513,300 cells (1740 × 295) for the AEOLIS domain. The AEOLIS domain covers the subaerial zone within the larger DELFT3D-FM domain. Model outputs are stored hourly over the five-year simulation period, yielding 43,800 timesteps with updated forcing conditions (van Westen et al. (2024a) for detailed model description).

4.5.2. Lagrangian transport model

The Eulerian model outputs are used to compute hourly spatial fields of i) sediment velocity, and ii) probability of transport. At a later stage, these Eulerian vector and scalar fields are used for the Lagrangian particle computation.

Sediment transport rates from both DELFT3D-FM and AEOLIS are provided as fluxes ($m^3/m/s$) rather than velocities. Since particle velocities differ from ambient current or wind velocities (U_c), we compute particle velocities based on bed shear stress relationships. Our approach distinguishes between three transport modes: nearshore bedload and suspended transport, and aeolian transport. A particle may experience any (combination) of these three modes during a model timestep, with its total particle displacement calculated as the sum the contribution for each mode. For nearshore transport, we follow the approach by Soulsby et al. (2011), taking the bedload particle velocity from (Fredsoe, 1992):

$$U_{\text{bed}} = 10 \cdot u_{\star_{\text{m}}} \left(1 - 0.7\sqrt{\frac{\theta_{\text{cr}}}{\theta_{\text{max}}}}\right) \tag{4.2}$$

where $u_{\star_{\text{m}}}$ [m/s] is the mean friction velocity over a wave cycle, and θ_{max} and θ_{cr} [-] represent the maximum and critical Shields parameters, respectively.

The ratio between bedload and current velocity is defined as $R_b = U_{\text{bed}}/U_c$. For suspended load, the velocity is computed as:

$$U_{\text{sus}} = \frac{U_{\text{bed}}(1-B)}{\left(\frac{8}{7}\right) - B} \cdot \frac{\left(\left(\frac{8}{7}R_b\right)^{8-7B} - 1\right)}{\left(\left(\frac{8}{7}R_b\right)^{7-7B} - 1\right)} \tag{4.3}$$

4

where the Rouse parameter $B = w_s/(0.4u_{\star\,\text{max}})$ describes the vertical distribution of suspended sediment. All parameters above are obtained from the DELFT3D-FM component of the coupled Eulerian model. For aeolian transport, particle velocity U_{aeolian} follows Sauermann et al. (2001):

$$\frac{(\vec{v_{\text{eff}}} - \vec{U_{\text{aeolian}}})|\vec{v_{\text{eff}}} - \vec{U_{\text{aeolian}}}|}{u_f^2} - \frac{\vec{U_{\text{aeolian}}}}{2\alpha|\vec{U_{\text{aeolian}}}|} - \nabla\vec{z_B} = 0 \tag{4.4}$$

where v_{eff} [m/s] is the effective wind velocity driving the grains, accounting for saltation layer feedback and depending on shear velocity u_* [m/s] and its threshold $u_{*,th}$ [m/s]. The grain settling velocity u_f [m/s] and bed slope ∇z_B [-] represent fall and gravity effects, respectively. The parameter $\alpha = 0.42$ [-] acts as an effective restitution coefficient for grain-bed interaction. These parameters are obtained from the AEOLIS model component.

Particles alternate between "free" and "trapped" states, as particles can be buried within the bed. To capture this behavior, we compute transport probability (P) for each transport mode (suspended load, bedload, and aeolian transport). When particles are free ($P = 1$), transport occurs at computed velocity; when trapped ($P = 0$), velocity reduces to zero. For a particle to potentially become mobilized, first of all, it should be located within the mixing layer. The mixing layer thickness δ_{mix} represents the vertical extent over which particles are actively mixed during transport. In physical tracer studies, this mixing depth typically corresponds to the level containing approximately 80% of recovered tracers (Ciavola et al., 1997; Ferreira et al., 2023; Kraus, 1985; White, 1998). Following Bertin et al. (2008), we relate mixing layer thickness to bed shear stress:

$$\delta_{\text{mix}} = 0.41\sqrt{\tau_{\text{max}} - \tau_{\text{cr}}} \tag{4.5}$$

where τ_{max} and τ_{cr} [N/m²] are the maximum and critical bed shear stresses obtained from DELFT3D-FM. We consider aeolian mixing negligible.

For particles within the mixing layer, transport probability is determined by the ratio between sediment in transport (δ_{bed}, δ_{sus}, or δ_{aeolian}) and sediment in the mixing layer (δ_{mix}).

$$P_{\text{i}} = \begin{cases} \delta_{\text{i}}/\delta_{\text{mix}} & \text{if } \delta_{\text{burial}} \leq \delta_{\text{mix}} \\ 0 & \text{if } \delta_{\text{burial}} > \delta_{\text{mix}} \end{cases} \tag{4.6}$$

where subscript 'i' represents either bedload, suspended load, or aeolian transport mode. These quantities are expressed as volumes per unit area [m³/m²] or equivalent thicknesses [m]. We compute the amount of sediment in transport by dividing the Eulerian transport fluxes [m³/m/s] by their respective particle velocities [m/s]:

$$\delta_{\text{i}} = \frac{Q_{\text{i}}}{U_{\text{i}}} \tag{4.7}$$

An important consequence of this approach is that particle velocity (U) has limited impact on collective movement patterns: higher velocities lead to more rapid movement of individual particles but at a lower transport probability, as these effects cancel each other. The total particle movement is ultimately governed by the transport rate (Q).

This probability-based approach differs from alternative methods that apply the ratio as a velocity reduction factor—where instead of moving at full speed 1% of the time, particles move continuously at 1% speed (Romão et al., 2024). While this alternative works adequately in the nearshore domain, it proves problematic for aeolian transport. With typical aeolian pickup rates being significantly lower compared to nearshore pickup, particles are infrequently, but more directly, moved from the intertidal zone to the dunes when mobilized. A velocity reduction approach would instead produce unrealistically slow, continuous movement.

Having computed all Eulerian fields of particle velocities and transport probabilities at hourly intervals over five years, we simulate particle movement using a timestep (Δt) of 60 seconds. The total displacement of each particle is determined by:

$$X_p(t+\Delta t) = X_p(t) + \sum_{\text{i}} \int_t^{t+\Delta t} P_{\text{i}} \cdot U_{\text{i}}(x,y,t)\, dt \tag{4.8}$$

where 'i' represents the summation of the bedload, suspended load, and aeolian transport modes. The integration is performed using a fourth-order Runge-Kutta advection scheme. The particle burial changes over time with bed level changes:

$$\delta_{\text{burial}}(t+\Delta t) = \delta_{\text{burial}}(t) + \int_t^{t+\Delta t} \Delta z_B(x,y,t)\, dt \tag{4.9}$$

where $\Delta z_B(x,y,t)$ represents the bed level change at the particle's location $(x_p(t), y_p(t))$ at time t.

4.5.3. Initial particle distribution

We initialize particles with uniform spatial distribution across both horizontal dimensions and depth. Particles are placed on an equidistant horizontal grid covering the entire Delfland coast (16.4 km × 1.8 km), with resolutions of 8.2 m and 9.0 m in the longshore and cross-shore directions, respectively. This grid comprises 2000 particles in the longshore direction and 200 in the cross-shore direction. Each particle is assigned a random depth of between 0 and 13 meters below the bed surface—corresponding to the maximum construction depth of the Sand Engine—ensuring coverage of the complete nourished volume. The particle grainsize is 250 μm, consistent with the settings of the DELFT3D-FM simulation (van Westen et al., 2024a).

4.5.4. Comparing Eulerian and Lagrangian transport

Eulerian and Lagrangian transport frameworks use different metrics: volumetric transport rates (m³/m/s) and particle velocities (m/s), respectively. These approaches can be related through a well-established relationship (Bosnic et al., 2017; Cheong et al., 1993; Drapeau & Long, 1985; Ferreira et al., 2023; Kraus et al., 1982; Romão et al., 2024; Sunamura & Kraus, 1984; White, 1998) between Eulerian longshore transport (Q_x [m³/m/s]) and Lagrangian tracer movement ($\overline{V_{x,p}}$ [m/s]):

$$Q_x = \overline{V_{x,p}} \times \delta_{\text{mix}} \tag{4.10}$$

Here, δ_{mix} [m] represents the mixing layer thickness—the active surface layer where sediment particles are mobilized during transport (equation (4.5)). The longshore particle velocity $\overline{V_{x,p}}$ [m/s] describes the average particle movement, calculated from collective displacement over time ($\overline{V_{x,p}} = \overline{\Delta x_p}/\Delta t$). Rearranging these terms yields the average longshore displacement of tracers, $\overline{\Delta x_p}$ [m]:

$$\overline{\Delta x_p} = \frac{Q_x}{\delta_{\text{mix}}} \Delta t \tag{4.11}$$

While this (cross-shore integrated longshore transport) formulation provides useful first-order estimates for simplified cases, our approach extends beyond these constraints by assigning volumetric dimensions to particles. By distributing 400,000 particles across 383,760,000 m³, each particle represents 959.4 m³ of sediment, enabling direct comparisons between Lagrangian movement and Eulerian redistribution patterns.

4.5.5. Verification of simulated pathways

To validate our Lagrangian approach, we compare the simulated particle pathways with Eulerian transport patterns. While direct comparison with physical tracer measurements is not possible at our study site, the underlying Eulerian model shows good agreement with observed morphological evolution (van Westen et al., 2024a). We focus our verification on two key metrics: volumetric sediment redistribution patterns and annual longshore transport rates.

The five-year morphological evolution of the Sand Engine provides our first verification case. Eulerian results show erosion at the most seaward parts of the perturbation (red area in Figure 4.7a) and accretion both north and south (blue areas). Quantitative analysis reveals maximum erosion of 3219 m³ per m alongshore at the tip, accretion of 2943 m³/m at the northern flank and 1000 m³/m along the southern flank (black line, Figure 4.7b). These patterns align well with field observations (Roest et al., 2021; van Westen et al., 2024a). Our Lagrangian approach, in combination with the particle seeding over a three-dimensional domain, enables volumetric comparison through particle tracking. Lagrangian particle movement from position A to B translates directly to volumetric Eulerian erosion at A and deposition at B. This particle-based redistribution (purple patch in Figure 4.7b) shows good agreement with Eulerian predictions, although slightly underestimating erosion (2902 m³/m) at the Sand Engine tip and accretion to its south (953 m³/m).

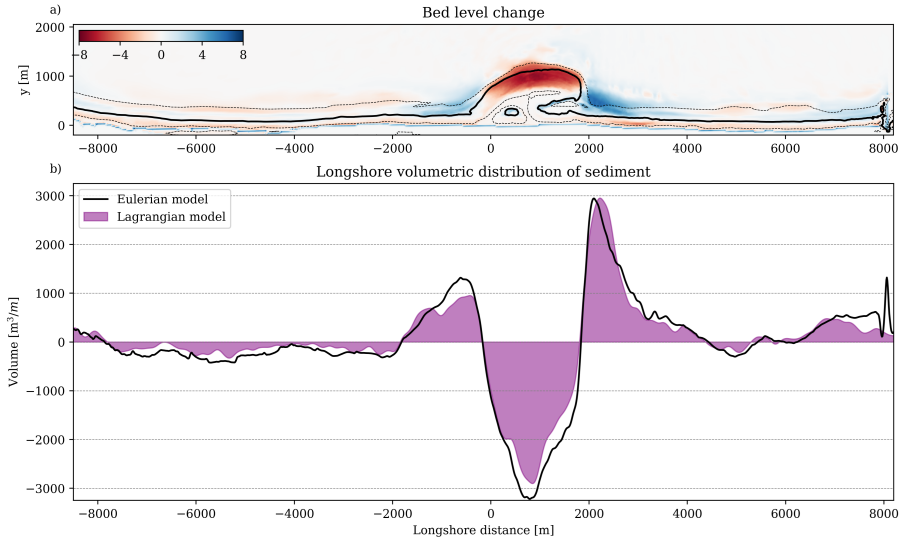

Figure 4.7.: Verification of Lagrangian approach through sediment redistribution patterns. (a) Cumulative bed level change in meters after five years showing erosion (red) and accretion (blue) zones from Eulerian model. (b) Comparison between Eulerian-computed redistribution (black line) and Lagrangian-derived volumetric changes (purple patch) along the coastline, demonstrating agreement between approaches.

We extend this verification to annual longshore transport rates, Q_x [m³/m/year]. Figure 4.8a presents longshore Eulerian transport in northward (purple) and southward (green) directions. For Lagrangian comparison (Figure 4.8b), we divide the domain into a structured grid. We count the number of particles crossing the cell edges and multiply this number of particle crossings by the particle representative volume (959.4 m³).

This comparison (purple patches vs. black lines in Figure 4.8c) demonstrates good agreement in transport patterns, with a notable exception at the Sand Engine tip where Lagrangian transport rates (0.63 Mm³/year) exceed Eulerian estimates (0.49 Mm³/year). The discrepancy emerges at a location that is prone to the confluence of complex flow patterns, steep transport gradients, and rapid bed level changes, making it difficult to isolate the precise cause of the mismatch. Nevertheless, the final particle distribution (Figure 4.7) still closely matches the Eulerian volumetric redistribution patterns. As our analysis focuses primarily on understanding sediment pathways and final distribution rather than longshore transport rates, these localized differences are considered to not significantly affect our main conclusions.

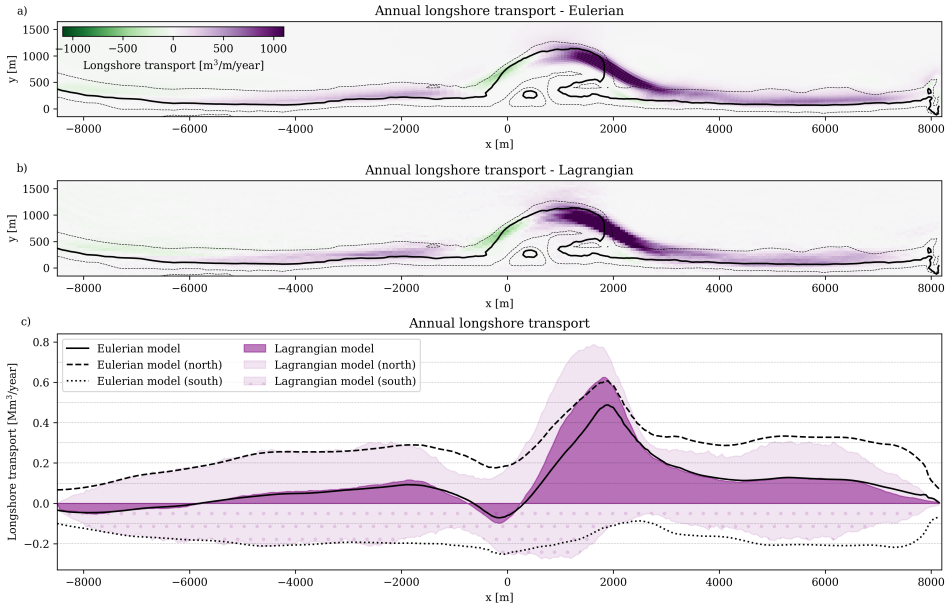

Figure 4.8.: Comparison of the Eulerian (a) and Lagrangian (b) annual longshore transport rates. The longshore transport integrated over the cross-shore is shown in panel c for the Eulerian (black lines) and Lagrangian (purple patches) simulations.

MODELLING IMPACT OF DESIGN

Process-based models across coastal domains might benefit the design of coastal interventions and sandy Nature-based Solutions that span the nearshore-dune system. This chapter explores how the tools developed throughout this thesis could inform practical decision-making in coastal management. Through model applications, we examine how specific nourishment design choices influence morphodynamics and sediment movement from beach to dunes.


5

Photo: Eric van der Eijk – https://duinlandschap.nl/

5

Modelling Impact of Design

MODELLING THE IMPACT OF NOURISHMENT DESIGN ON NEARSHORE–DUNE SYSTEMS

Abstract

State-of-the-art modelling approaches fail to capture the complex behaviour of coastal Nature-based Solutions (NBS) across domain boundaries. This study investigates how innovations in process-based modelling can be used to examine the impact of nourishment design choices on dune development. We employ three innovative tools: a process-based aeolian transport model (AEOLIS), a marine–aeolian coupling framework, and a Lagrangian particle-tracking method (SEDTRAILS). For the Sand Engine mega-nourishment, simulations reveal that removing its artificial dunelake would increase dune growth by 42,000 m³ after 10 years, with effects extending 1,200 m alongshore. A finer sediment composition enhanced dune growth by 65%, while lowering the crest elevation modestly increased sediment availability through more frequent mixing. At smaller scales, we explore regulating sediment supply as an abiotic condition for vegetation growth. Incorporating a lagoon in beach nourishment design reduced sediment supply toward the foredune with 62%. Due to the assumed dependency of vegetation on sediment burial, this reduced supply slowed vegetation growth. The resulting wider blowout entrances increased backdune deposition by 23%. These applications illustrate how the inclusion of dune development and nearshore-dune sediment exchange in process-based modelling might enable the inclusion of dune-related objectives in nourishment design. This provides engineers with new opportunities to evaluate the impact of changes in the design as they optimize for different coastal services (e.g., flood protection, ecology, recreation).

5.1. Introduction

Coastal systems provide a wide range of services, from recreational opportunities and habitat support to flood protection (Arkema et al., 2013; Barbier et al., 2011; Sutton-Grier et al., 2015). Effective coastal management, aimed at safeguarding these benefits, relies on a thorough understanding and the ability to predict processes across the nearshore–dune system (Hanley et al., 2014; Mulder et al., 2011; Vitousek et al., 2017).

Although the development of nearshore and dunes are highly interconnected (Short & Hesp, 1982), these have often been managed as discrete morphologic domains. In the Netherlands, millions of cubic meters of sand are nourished yearly to preserve the coastline at its 1990 position (Brand et al., 2022; Ministerie van Verkeer en Waterstaat, 1990). As a result of this consistent sediment surplus, dune growth has been regarded as a certainty. This has restricted the need for process-based descriptions of dune development in past nourishment design.

The recent emergence of sandy Nature-based Solutions (NBS) have exposed the shortcomings of excluding dunes from design considerations. NBS harness natural processes to deliver ecosystem services (van der Meulen et al., 2023), relying on sediment movement across the nearshore–dune system. They often yield more extensive and long-lasting effects than traditional sandy interventions (Barciela Rial, 2019; van der Meulen et al., 2014; Stive et al., 2013; Sutton-Grier et al., 2015; de Vriend et al., 2015).

A well-known example of NBS is the Sand Engine (Stive et al., 2013), a 21 Mm^3 mega-nourishment designed to feed the Delfland coast for decades. Stimulating dune growth was one of the Sand Engine's original objectives. Despite this objective, its dune growth predictions were based on a simple empirical relation between beach width and dune growth. This relation was derived from observations in more natural coastal settings (Mulder & Tonnon, 2011). As a result, the predictions significantly overestimated dune growth and failed to reproduce the observed spatial variability (Hoonhout & de Vries, 2017; Huisman et al., 2021; van Westen et al., 2024a).

The structural surplus of sediment along the Dutch coast, has enabled dune management to shift from merely dune growth to the restoration of natural dune dynamics (Arens et al., 2013a; Riksen et al., 2016; Terlouw & Slings, 2005). Worldwide, many dunes have become over-stabilized by vegetation ("global greening"), which reduces sediment flux into the backdune and diminishes overall landscape dynamics (van Boxel et al., 1997; da Silva et al., 2013; Jackson et al., 2019; McKeehan & Arbogast, 2023; Osswald et al., 2019; Riksen et al., 2016; Schwarz et al., 2018). Foredune blowouts are a characteristic feature of dynamic dunes, moving sand inland and allowing the entire dune system to keep pace with sea-level rise (Hesp, 2002; Laporte-Fauret et al., 2022; Schwarz et al., 2018). The excavation of notches or the removal of vegetation can help to initiate blowout development (Arens et al., 2013a; Meerkerk et al., 2007; Ruessink et al., 2018). The success of these interventions has been variable (Arens et al., 2013a). Because marram grass is an efficient dune builder with high burial-tolerance (Maun, 2009; Schwarz et al., 2018), a steady supply

of sediment is ideal for rapid vegetation stabilization (Hesp, 2002; Schwarz et al., 2018). This makes dynamic dune management under the current surplus-sediment conditions, such as along the Dutch coast, challenging.

Dune development reflects sediment availability across the nearshore-dune system (Short & Hesp, 1982). The success of interventions that aim to enhance either dune growth or dynamics require a thorough understanding of sediment movement from the nearshore to the dunes. Current process-based modelling approaches treat these as discrete morphologic domains, if dunes are included at all. This limitation restricts engineers to take dune development into account during nourishment design.

In this chapter, we examine the impact of certain decisions in nourishment design on dune development. By utilizing the modelling approaches presented in this thesis, we demonstrate the benefits they have in this regard. First, we examine how alternative design considerations of the Sand Engine mega-nourishment might have influenced dune growth. Second, we explore if nourishment design can be used to enhance dune dynamics. Here we utilize the characteristic response of dune vegetation to sediment supply.

5.2. Method

Building on the methods introduced throughout this dissertation, we aim to explore the impact of specific nourishment design decisions on dune development. We couple the marine and aeolian domains to simulate sediment exchange across the nearshore-dune system (Chapter 3). More detailed blowout development is described with the landform-shaping process implementations from Chapter 2. Finally, sediment pathways are mapped to assess the nearshore-dune connection as a result of the nourishment alternatives (Chapter 4).

First, we explore alternative design features for the Sand Engine mega-nourishment, illustrating how specific choices may influence long-term dune growth (Figure 5.1, Section 5.2.1). Second, we investigate two smaller-scale beach nourishment configurations to assess whether incorporating a lagoon could be used to control temporal sediment supply and the subsequent vegetation response (Figure 5.2, Section 5.2.2).

5.2.1. Sand Engine design alternatives

The original Sand Engine design includes several features whose effects on dune development were not fully explored during its design phase. Here, we use the nearshore–dune model described in Chapter 3 to examine the potential impact of three considerations in nourishment design on dune growth (Figure 5.1). For each design consideration, we examine the influence on dune growth by comparing the simulated foredune accumulation after 10 years, including the longshore variability in dune growth.

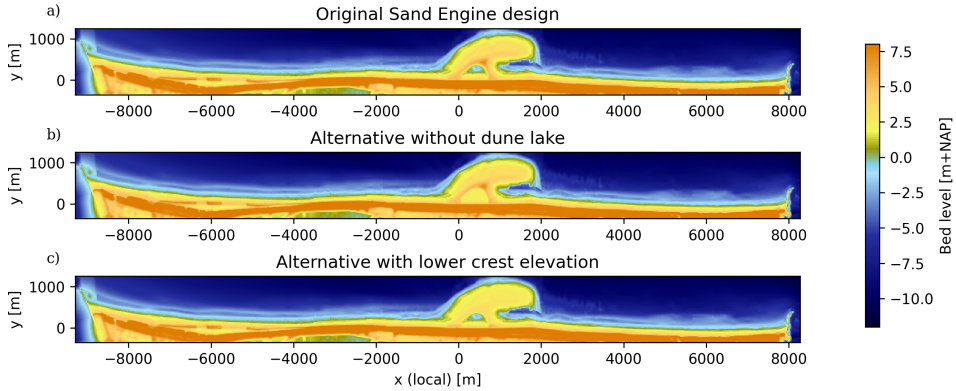

Figure 5.1.: Sand Engine design alternatives. The original design (a), an alternative without the artificial dune lake (b), and a lowered crest elevation (c). The spatial domain represents the AEOLIS bed level elevation.

Presence of artificial waterbodies: The original Sand Engine design includes an artificial waterbody that traps aeolian transport from the intertidal zone towards the dunes (at x = 0 m in Figure 5.1a). By removing this "dunelake", we examine its impact on dune growth in the Sand Engine's vicinity (Figure 5.1b).

Sediment composition: Sediment sorting and armouring have restricted sediment availability for aeolian pickup from the Sand Engine's higher elevated beaches. By reducing the share of coarse grains (diameter > 1 mm) from the nourished material (from 5% to 1%), we examine how a different grain size distribution could affect dune growth. The goal is to slow desert pavement formation and thereby increase aeolian transport. The topography is unchanged from the original design (Figure 5.1a). In practice, such situation could be achieved using different dredged material or regularly ploughing the beach ("tilling").

Crest elevation: The crest elevation in the original Sand Engine design exceeds maximum run-up limits. As a result, some areas are never mixed during storm events. By lowering the elevation of nourishment crest, we aim to increase the area prone to frequent inundation and mixing during storm events. We lowered the crest from 7 m+NAP to 3.5 m+NAP by removing approximately 0.8 million m^3 of sand. This reduces the area above 3 m+NAP from 72 ha to 24 ha, (Figure 5.1c).

5.2.2. Beach nourishment design alternatives

Conventional beach and shoreface nourishments provide a steady supply of sediment towards the dunes. We compare two beach nourishment concepts to explore if nourishment design can be used to steer supply and enhance the development of artificial notches in a vegetated foredune (Figure 5.2).

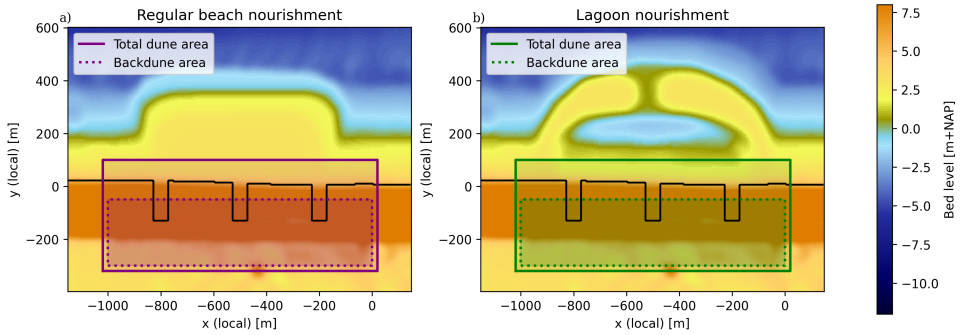

Figure 5.2.: The beach nourishment design alternatives. (a) A traditional beach nourishment and (b) a beach nourishment including an artificial lagoon. The black contour lines show the vegetation limit at the start of the simulation. The green and purple boxes indicate the control volumes of total dune (continuous) and backdune (dotted) growth.

The *regular nourishment* design (Figure 5.2a) represents a traditional beach nourishment. The nourishment extends 800 m in alongshore and 200 m in cross-shore direction, with a maximum elevation of 3 m+NAP. The nourishment design comprises a total volume of 750,000 m^3.

The *lagoon nourishment* design (Figure 5.2b) includes an artificial waterbody aiming to control temporal sand supply into the foredune. The nourished sediment volume is equal to the regular nourishment design. The beach immediately seaward of the foredune is narrowed to further limit initial sediment availability. Because of the included lagoon, the nourishment extends approximately 100 m farther offshore than the baseline coastline. A small channel (approximately 100 m wide, 1 m+NAP maximum elevation) connects the lagoon to the sea during high tides or storms.

For both design alternatives, three vegetation patches (50 m wide) are removed along the foredune (black contours in Figure 5.2). These patches extent from dunefoot to crest, allowing natural aeolian processes to initiate blowout formation. This approach does not include any topographic modification (i.e., notch excavation), but solely the removal of foredune vegetation.

Total dune growth is quantified over a 1 km longshore segment, with a seaward boundary located just seaward of the dune foot (purple and green boxes, continuous lines, in Figures 5.2). Because no dune erosion occurs in this scenario, dune growth serves as a direct indicator of sediment influx.

Similarly, backdune deposition is quantified along the same longshore segment, but with the seaward boundary at the dune crest (purple and green boxes, dotted lines, in Figures 5.2). We use the amount of backdune deposition as an indicator for dune dynamics. The response of vegetation growth to the varying sediment supply is assessed by comparing the change in vegetated area. Area is considered vegetated once vegetation density (ρ_{veg}) exceeds 0.1.

5.2.3. Modelling approach

We simulate the impact of nourishment design considerations on dune development by coupling DELFT3D-FM (Lesser et al., 2004) and AEOLIS (van Westen et al., 2024b), as shown in Figure 5.3. This framework expands upon the Sand Engine modelling setup presented in Chapter 3 (van Westen et al., 2024a). The marine and aeolian domains exchange bed level changes and water levels via the Basic Model Interface (BMI) (Hutton et al., 2020). The simulation period is extended to 10 years (instead of 5) and a morphological acceleration factor (*morfac*) of 3 is applied. Apart from tidal forcing, wave and wind inputs are similarly compressed in time.

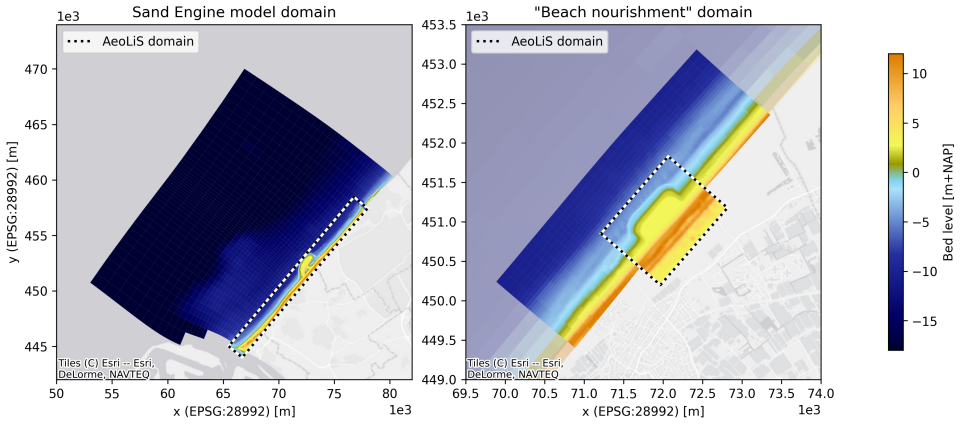

Figure 5.3.: Overview of the coupled DELFT3D-FM–AEOLIS model used to simulate the influence of mega- and beach-nourishment alternatives on dune development. (a) The larger DELFT3D-FM domain for the Sand Engine simulations, with the AEOLIS grid outline. This domain also provides boundary conditions for the smaller DELFT3D-FM domain for the beach nourishment alternatives in panel (b).

Delft3D Flexible Mesh (DELFT3D-FM)

DELFT3D-FM resolves marine hydrodynamics, sediment transport, and subaqueous morphological evolution. For the **Sand Engine** design alternatives, the computational setup is identical to Chapter 3 (van Westen et al., 2024a), with the exception of the longer simulation period.

The model setup for the smaller-scale **beach nourishments** has been modified with respect to the Sand Engine simulation. The horizontal grid resolution is refined from 35 m to 15 m to represent the nourishment designs in more detail and reduce deviations in resolution between the aeolian and marine domains. The higher resolution and extended simulation period increase computational costs. Therefore, we employ a nested modelling approach: a larger domain (i.e., the original Sand Engine model, Figure 6.4a) provides boundary conditions (water levels and wave conditions) to a nested, higher-resolution domain comprising the beach nourishments (Figure 6.4b). This setup reduces the number of cells that must be actively coupled with the aeolian domain from 17,715 to 4,158. An observed drawback of this nesting strategy is that alongshore development cannot be resolved accurately. As a result, approximately 2.5,Mm^3 of sediment is lost across the lateral boundaries over the 10-year simulation. Because both beach nourishment designs share the same losses, their relative outcomes can still be compared consistently.

AEOLIS

AEOLIS describes the aeolian sediment transport and dune development in the subaerial domain. The model setup of the **Sand Engine** simulations is largely similar to the original Sand Engine model from Chapter 3 (van Westen et al., 2024a). The domain is extended from 8 km to over 16 km. This larger longshore extend helps prevent boundary instabilities at the edge of the AEOLIS domain, while capturing a greater part of the "undisturbed" coastline. We also incorporate a one-dimensional approach to spatial shear variations, similar to Roelvink and Costas (2019), for more accurate representation of upper beachface development.

Wave run-up levels are computed to determine the upper inundation limit for sediment mixing and soil moisture content following Stockdon et al. (2006). In the original Sand Engine model (van Westen et al., 2024a), the run-up calculation was based on local (onshore) wave heights. Since the Stockdon et al. (2006) formulation is based on offshore wave heights, the original approach caused an underestimation in simulated run-up levels. Therefore, we use offshore wave heights in the new simulations. As a result, wave transformation is not included in the run-up calculation. The influence of offshore wave sheltering features, such as breaker bars, is neglected. To address this issue, we use a simplified approach to limit wave run-up based on the shallowest depth encountered by waves during landward propagation.

For the **beach nourishment** alternatives, more modifications to the AEOLIS setup are needed to accommodate smaller-scale landform development. To represent more detailed dune dynamics, the grid resolution is refined to 4 m.

Vegetation growth is modelled more realistically compared to the original AEOLIS setup. Growth peaks at 1 m/year with an optimal burial rate of 0.98 m/year (Durán & Moore, 2013). These values are chosen to mimic the burial-dependent nature of marram grass. A decaying inland gradient in vegetation growth is applied to account for species that tolerate less sand deposition. These vegetation-related assumptions have strong implications for the interpretation of the simulation results. These are discussed more elaborately in the Discussion section.

In contrast to the blowout simulations in Chapter 2 (van Westen et al., 2024b), we here rely on armouring of the bed to limit blowout-floor incision, rather than imposing a hard erosion cap. Specifically, a 5% fraction of non-erodible grains (2.5 mm) limits maximum erosion with the deflation basins. Future work will be needed to refine how the blowout floor develops and interacts with groundwater.

5.2.4. Particle tracking

We apply the Lagrangian particle-tracking method from Chapter 4 (van Westen et al., 2025) to the two **beach nourishment** scenarios, tracing sediment pathways across the marine and aeolian domains. We seed 187,500 particles in a 2,600 m × 900 m × 12 m volume, each representing 149.76 m^3 of sediment. Because the domain lacks no-flux boundaries (i.e., harbour breakwaters at the Delfland coast) some particles inevitably leave the modelled domain. We account for these losses during later analysis.

The longshore extent of the AEOLIS domain is smaller compared to that of DELFT3D-FM. To ensure consistent wind-driven transport across the modelled Eulerian (DELFT3D-FM) domain, we extrapolate the aeolian transport field from the lateral edges of the AEOLIS in longshore direction.

The beach nourishment simulations have a finer resolution compared to the Sand Engine simulation in Chapter 4 (van Westen et al., 2025). As a result, the CFL-condition for time-stepping in the Lagrangian analysis becomes more restrictive. Instead of using realistic transport velocities with a low probability of transportation, we now apply the transport probability as a reduction factor to the particle velocity. This results in slow, continuous particle movement rather than rapid probabilistic transport bursts. This relaxes the constraints by CFL conditions, making the Lagrangian analysis feasible at more reasonable computational costs.

5.3. Results

5.3.1. Sand Engine design

Presence of artificial waterbodies

An artificial waterbody was included in the original Sand Engine design. This "dunelake" (at $x = 0$ m in Figure 5.4a) was found to trap aeolian sand transport from the intertidal zone towards the dunes (Hoonhout & de Vries, 2017). By simulating an alternative Sand Engine design without the dunelake, we can examine its impact on dune development (cyan vs. black line in Figure 5.4b).

The simulation results show that the dunelake restricts a significant amount of sediment to reach the foredune. Over the first decade, the dunelake traps more than 42,000 m^3 of sand, locally equivalent to approximately 75 m^3/m of reduced dune growth. Notably, its effect extends approximately 1,200 m alongshore, well beyond the lake's own 300 m length.

Sediment composition

The Sand Engine was constructed using dredged sediment containing substantial coarse fractions and shells. The sediment composition of dredged material typically has a wider grain size distribution than the well-sorted sand found on natural beaches. According to the grain size distribution used by Hoonhout and de Vries (2019), approximately 5% of the nourished sand is non-erodible by aeolian processes. Wind-driven transport preferentially removes finer particles, leading to the development of a desert pavement that shields underlying finer fractions and progressively limits aeolian sediment pickup.

To examine how the coarse fractions in dredged sediment might influence dune development, we simulated an alternative scenario with reduced "non-erodible" content (1% instead of 5%) (Figure 5.4c). The simulation results indicate that the finer sediment composition results in approximately 65% more dune growth across the entire system, equivalent to almost 90 m^3/m over the 10 year simulation period. An important limitation to these findings is the spatially uniform grain size distribution applied in our model. The initial distribution is equal throughout the domain, including along non-nourished beaches. In reality, selecting well-sorted nourishment material would not influence adjacent beaches to the extent shown in our simulations. Nevertheless, these results highlight how even a modest proportion of coarse material can significantly reduce aeolian sediment supply to the dunes.

Sand Engine design with lower crest elevation

In the original Sand Engine design, large areas of the nourishment are located above typical storm surge levels, resulting in very infrequent mixing of the upper sediment layer. Consequently, aeolian sediment availability becomes limited due to uninterrupted desert pavement formation. By designing the Sand Engine with a lower crest elevation, we increase the area susceptible to periodic inundation and sediment mixing.

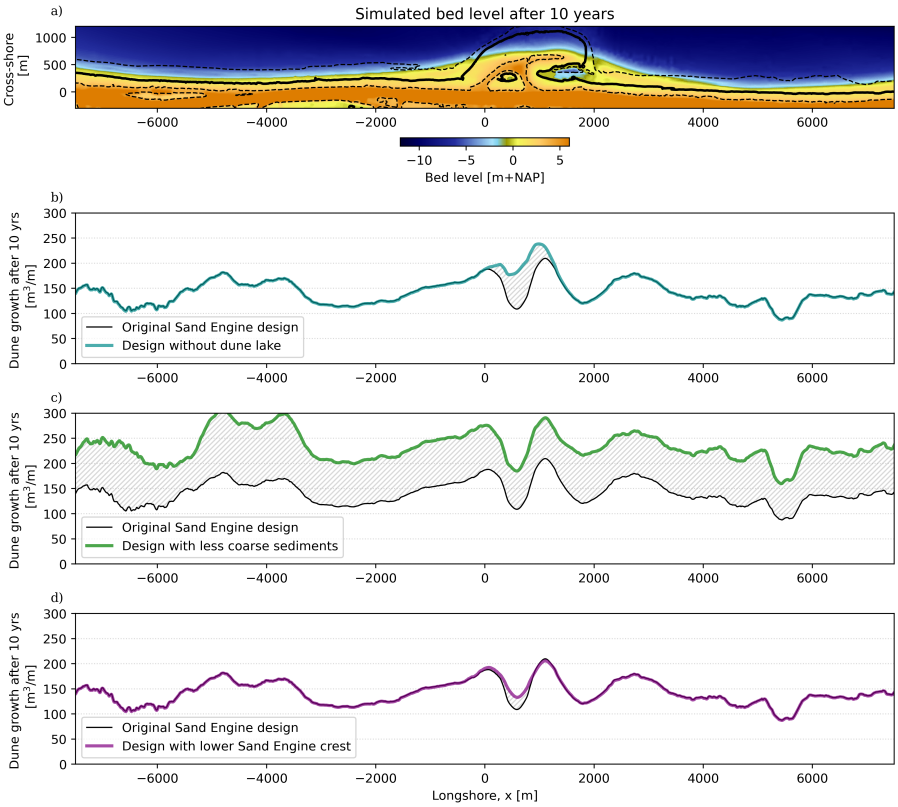

Figure 5.4.: Longshore dune growth for several Sand Engine design alternatives. Panel (a) shows the bed level at the end of the simulation, with black contour lines indicating the original Sand Engine design. Panels (b)–(d) illustrate the alongshore distribution of cumulative dune growth (m^3/m) relative to the original design (black lines). Panel (b) shows the influence of the artificial waterbody, i.e., dunelake, (c) the impact of coarse materials in the grain size distribution, and (d) of the designed crest elevation of the nourishment crest.

The spatial impact of this modification reveal a complex pattern of influence. In the immediate vicinity of the high-elevation crest in the original design (x = 500 m), lowering the crest locally enhanced dune growth by almost 15 m^3/m (Figure5.4d). This generates an additional 15,000 m^3 of dune growth in that region. Conversely, near the lagoon (x = 1000 m), dune growth decreased slightly (approximately 5 m^3/m), though this reduction is not immediately apparent in Figure6.4d. The remaining coastline exhibited a minor reduction in dune growth (< 1 m^3/m), amounting to a total loss of 11,500 ^{3}. The net effect of lowering the crest elevation is a modest overall increase of nearly 4,000 ^{3} in total dune volume.

5.3.2. Lagoon in beach nourishment design

The simulation outcomes of two beach nourishment alternatives are compared to examine if including an artificial waterbody in nourishment design could help to steer sediment supply towards the dune and enhance dune dynamics (Figure 5.5).

Nearshore-to-dune sediment supply

Both beach nourishment design alternatives are diffusing in longshore direction. The nourished area erodes (blue patches in Figure 5.5c,d), while the adjacent beaches accumulate (red patches). Aeolian processes subsequently transport sand from the beach into the dunes. At locations where vegetation is removed, wind mobilizes sediment and causes local erosion. Blowouts develop at the intended location and the eroded sediment deposits just landward of the deflation basin. Comparison shows that the total simulated dune growth after 10 years is approximately 62% higher without the lagoon (Figure 5.6a). The trapping effect of the lagoon weakens slightly over time as it fills: in the first four years, the relative difference is 66%, decreasing to 57% in the final four years.

Vegetation response to sediment supply

Based on the assumption of a burial-depend vegetation species, the reduced sediment supply into the dunes acts as an abiotic condition for vegetation growth. Comparing the simulated vegetated area (Figure 5.5e,f) shows that the lagoon presence reduces vegetation growth. After the 10-year simulation period, the increased vegetated area is roughly 50% more if the lagoon is not included (Figure 5.6b). This difference increases over time, growing from 24% in the first four years to 73% in the final four years. Due to faster vegetation expansion, the blowout entrances close more quickly, as shown by the white gaps in Figure 5.5e,f.

Backdune deposition

The widening of blowout entrances due to the presence of the lagoon enables greater sediment flux from the beach into the backdune. Over the 10-year simulation, the lagoon nourishment delivers a total of 57 m^3/m to the backdune, surpassing 46 m^3/m for the design without the lagoon (Figure 5.6c). This 23% increase in backdune influx occurs despite the lower overall dune growth due to trapping by the lagoon (Section 5.3.2). For the beach nourishment design, backdune deposition accounts for 31% of total dune growth, compared to 62% for the lagoon nourishment. In the first four years, the lagoon nourishment's backdune influx exceeds that of the beach nourishment by 11%, increasing to 32% in the final four years (black dotted line in Figure 5.6d).

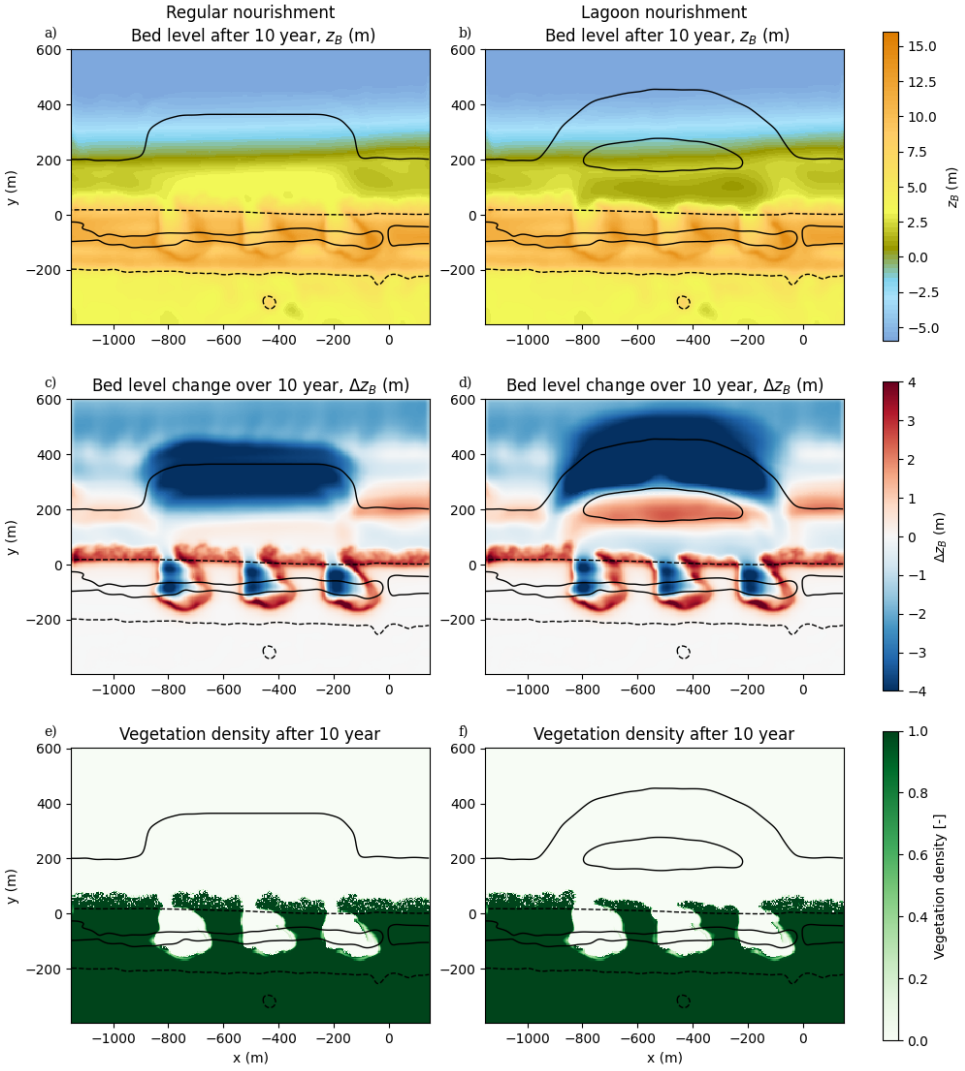

Figure 5.5.: Spatial comparison of the two nourishment designs after 10 years of development. Panels (a-b) show the final bed level for beach and lagoon nourishment, respectively. Panels (c-d) show bed level changes, with red indicating deposition and blue showing erosion. Panels (e-f) show the spatial distribution of vegetation density, where darker green indicates higher vegetation density. Black contours represent initial bed levels at 0 m, 6 m (dashed), and 11 m.

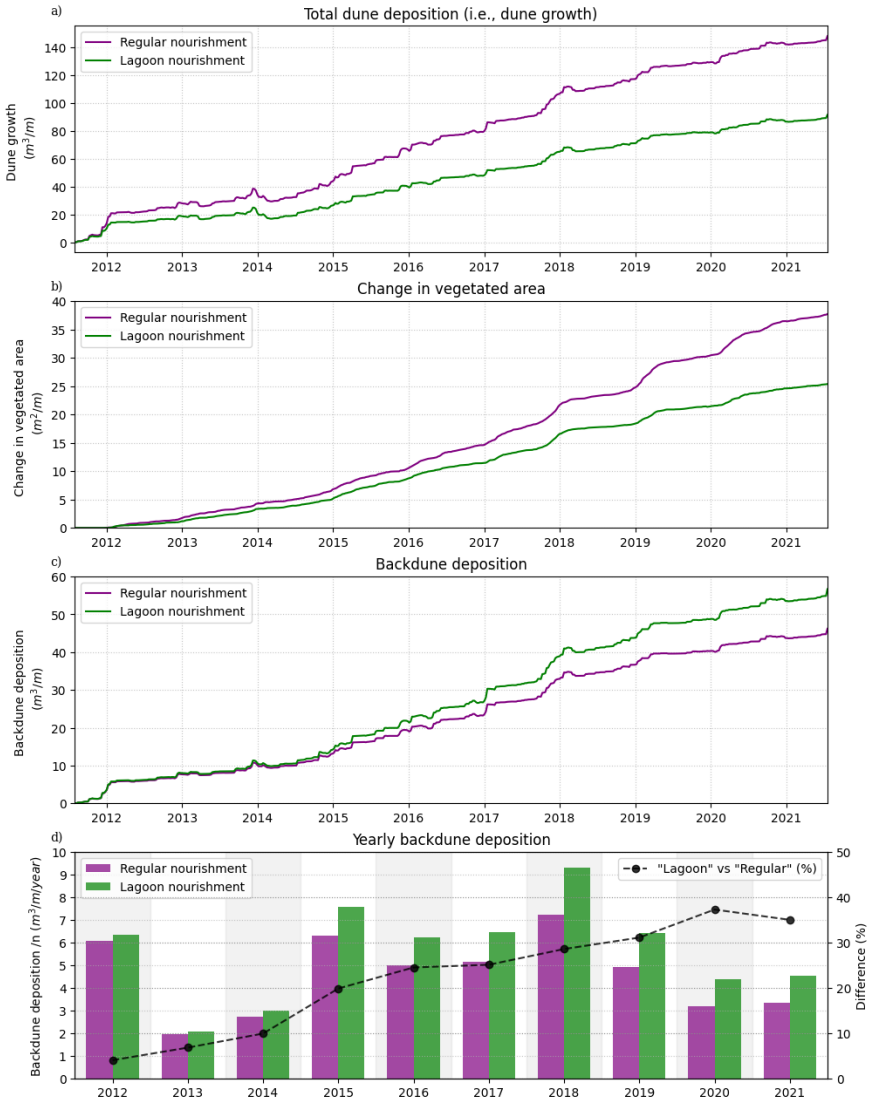

Figure 5.6.: Temporal dune development for both nourishment designs. Panel (a) presents cumulative dune growth (m^3/m) over time. Panel (b) shows the cumulative change in vegetated area (m^2/m). Panel (c) presents the cumulative backdune growth (m^3/m) over time. Panel (d) provides a year-by-year comparison of backdune deposition; bars represent the annual backdune growth, and the black dotted line denotes the relative difference between the lagoon and beach nourishment (positive values indicate greater backdune growth under the lagoon design).

Sediment pathways to the backdune

The simulations indicate a net positive influence on backdune deposition by including a lagoon in the design. However, the Eulerian results do not indicate where this deposited sand originates from. To examine the source of backdune deposition, we employ a Lagrangian approach that traces individual sediment particles ending up in the backdune. Particles are selected that begin seaward of the dune crest ($y_{p,0} > -50$ m, shown by circular markers in Figures 5.7a,b) and end landward of it ($y_{p,T} < -50$ m, marked by gray crosses). Of the 187,500 particles seeded, 222 are flagged as backdune deposition under the beach nourishment and 247 under the lagoon nourishment. These represent 33 m^3/m and 41 m^3/m, respectively, once multiplied by the representative particle volume of 149.76 m^3/particle. All traced particles are grouped by their initial source region (Figure 5.7): Foredune (green), nourished (purple), and the remaining particles or "shore" (cyan).

The sum of Lagrangian backdune deposits is approximately 28% lower than the Eulerian estimates for backdune deposition. Since the initial seeding domain does not extend upstream, no particles are imported from beyond the lateral boundary, while some do leave the domain downstream. This deficit implies that either 28% of the backdune material must be supplied from beyond the model boundaries or a deviation caused by differences in methodology (gray hatched regions in Figures 5.7c,d).

Particles originating from the foredune (green markers) effectively represent erosion of the blowout deflation basin and landward dune migration. For the beach nourishment, this source totals 19 m^3/m (41% of backdune deposition), whereas the lagoon nourishment yields 21 m^3/m (36%). Contrary to the overall trend, the beach nourishment transports more nourished material (purple) into the backdune (9 m^3/m, 20% of total) than the lagoon nourishment (8 m^3/m, 15%). These small differences indicate the limited effect of the presence of the lagoon on erosion of the blowout deflation basin and flux of nourished sediment into the backdunes.

The inclusion of the lagoon has a larger influence on pathways from further offshore. For the lagoon nourishment, the "shore" particles (cyan markers in Figure 5.7) contribute 12 m^3/m to the backdune - 2.4 times more than the 5 m^3/m observed with the beach nourishment. These simulation results indicate that the lagoon design facilitates pathways between the backdunes and more distant sources.

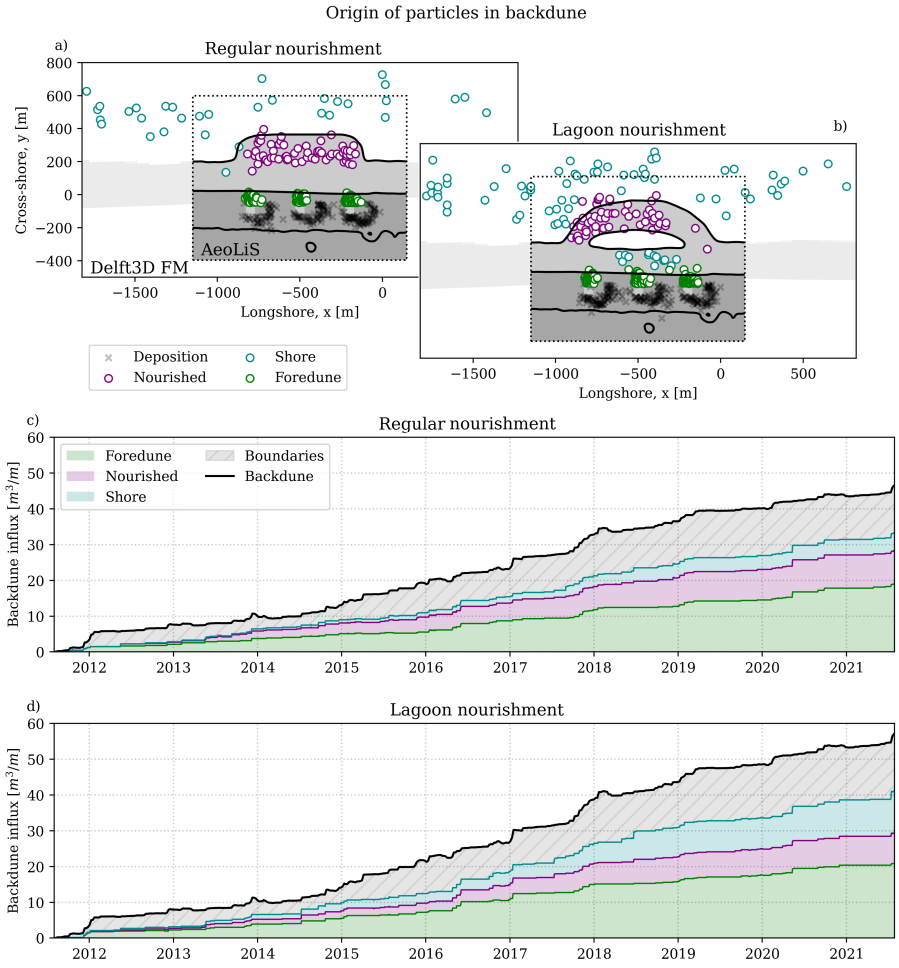

Figure 5.7.: Origin of sediment particles deposited in the backdune. Panels (a) and (b) depict the initial locations of the particles that were predicted to deposit in the backdune during the simulation. Particles are colour-coded by source region: green (foredune), purple (nourished area), and cyan (shore). The gray crosses mark each particle's final position in the backdune. Panels (c) and (d) show the cumulative contribution from each source region over time, using the same colours as the particle markers. The black line indicates the total Eulerian deposition. The gray hatched region corresponds to marks the difference between the Eulerian and Lagrangian results, which could be contributed to sediment originating from beyond the model boundaries or a difference due to methodology.

5.4. Discussion

The benefit of modeling the aeolian domain in nourishment design

Historically, modelling aeolian transport and dune growth in practical coastal applications have relied on simplistic empirical or analytical descriptions. The shortcomings of these simplified approaches became evident during the Sand Engine's design phase. Initial dune growth predictions (Mulder & Tonnon, 2011) relied on an empirical relationship between beach width and dune foot migration (de Vriend et al., 1989) (Figure 5.8). Based on this relationship and Delft3D modeling of subaqueous morphological change, the change in dune area was anticipated to nearly double compared to the reference case without nourishment. In reality, dune development was actually reduced in the Sand Engine's vicinity (van Westen et al., 2024a).

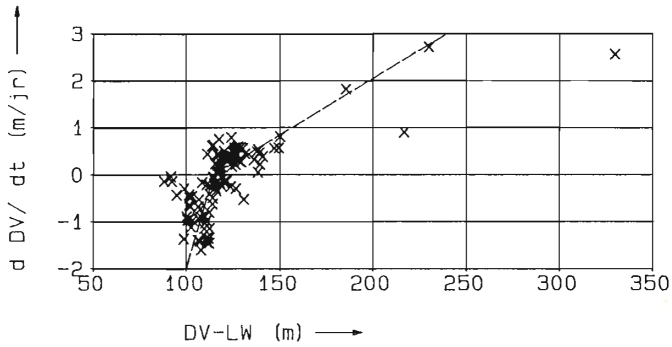

Figure 5.8.: Dune foot migration (dDV/dt) in relation to beach width (DV – LW],where DV = Dune Foot and LW = mean Low Water (from de Vriend et al. (1989)).

The applied empirical relation assumed aeolian sediment availability is controlled solely by beach width, but observed subaerial development revealed a more complex reality. Water bodies trapped moving sediment to the dunes, while the Sand Engine's elevated topography enhanced the effects of sediment sorting and mixing compared to natural beaches (Hoonhout & de Vries, 2017).

The complex dynamics at play at the Sand Engine require two-dimensional descriptions of sediment sorting and wave-driven sediment mixing and inundation. The influence of these supply-limiting processes is typically parametrized or addressed through fetch-based descriptions (Bauer et al., 2009; Ruessink et al., 2022; Strypsteen et al., 2024b; Van Rijn & Strypsteen, 2020). Therefore, these would not be suitable for the complex development at the Sand Engine. In this study we have shown that by having two-dimensional process-based descriptions, these processes can be taken into account in evaluating NBS design (Figure 5.4).

The benefit of coupled modelling in nourishment design

Dune development is not solely shaped by aeolian processes. Marine-driven morphodynamics and supply-limitations control sediment availability for dune growth. The influence of including these interactions through model coupling was already discussed in Chapter 3 (van Westen et al., 2024a). In the present study, we used an updated version of that model setup with a longer simulation period.

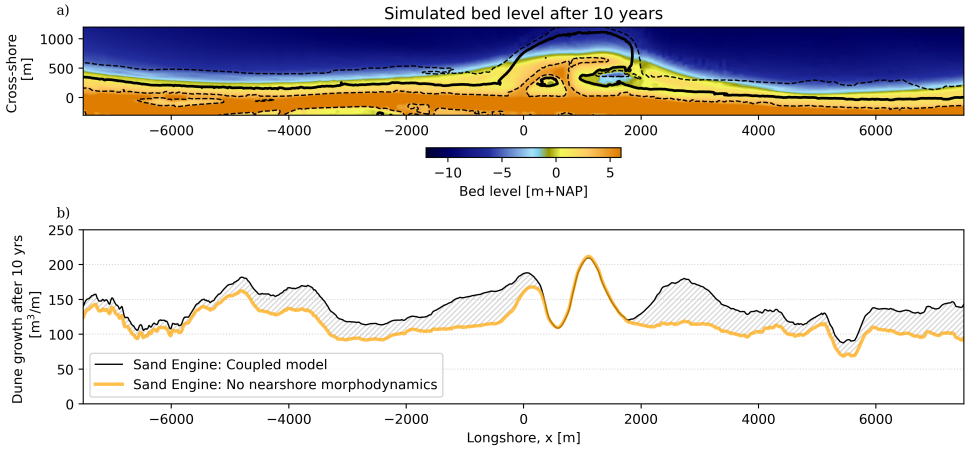

Figure 5.9.: Comparing the coupled (black) and stand-alone AEOLIS (yellow) simulated dune growth along the Sand Engine domain.

We repeat the same analysis, comparing the simulation results with and without the influence marine-driven morphodynamics on dune development (yellow vs. black lines in Figure 5.4). Along accretive beaches, the coupled model predicts substantially higher dune growth compared to simulations without nearshore morphodynamics. This effect is particularly evident at the southern and northern flanks (x = 1000 m, x = 3000 m) and northward toward Scheveningen (x > 6000 m). These results indicate the importance of hydrodynamic processes in providing sediment for aeolian transport. Compared to the original Sand Engine simulation in Chapter 3, hydrodynamic processes now appear to have a more pronounced effect on dune growth. Whether this increased impact stems from improved wave run-up computation, inclusion of spatial shear stress variations, or the longer simulation period requires further investigation.

For the beach nourishment simulations, sediment exchange across the nearshore-dune interface was leveraged to achieve desired dune development. Coupling marine and aeolian domains allowed us to examine how specific nourishment design decisions could influence sediment flux and subsequent vegetation response (van Westen et al., 2024a, Chapter 3).

Sediment supply as an abiotic condition in NBS design

The success of NBS relies on harnessing biophysical interactions. By controlling abiotic conditions, management can guide ecosystem development. Marram grass, being burial-dependent, requires consistent influx of fresh sediment to thrive (Arens et al., 2013a; Maun, 2009; Nolet et al., 2018; Schwarz et al., 2018). This characteristic has been utilized in dune management for centuries—planting marram grass to trap sand and promote dune growth and stabilization. In our study, we leverage these burial thresholds to enhance dynamics rather than stabilization.

Process-based descriptions of cross-domain sediment exchange enable us to connect nearshore development to abiotic conditions in the subaerial domain. Earlier applications of the AeoLiS model (Oude Vrielink et al., 2021; Strypsteen et al., 2024c) and the coupled model with Delft3D FM (van Westen et al., 2024a; 2023) have demonstrated the ability to simulate realistic aeolian fluxes to dunes. While the model successfully reproduces key phenomena in coastal dunes, the parametrisation of vegetation response remains simplified and confined to a single species. Maun (2009) conceptually described vegetation growth response to sediment deposition, as shown in Figure 5.10a. Various dune models implement this behavior differently: CDM (Durán & Herrmann, 2006; Durán et al., 2010) uses a linear description for vegetation response to erosion and sedimentation (Figure 5.10b). In this study, we extended that relation with the parameter $\Delta z_{B,opt}$ to shift optimal growth from a steady to an an accretive bed (dotted line Figure 5.10b). This allows to capture the burial-dependent nature of dune vegetation. The DUBEVEG model (Keijsers et al., 2016) accounts for multiple vegetation species with varying responses to sediment burial (Figure 5.10c). In reality, vegetation response depends on numerous abiotic conditions that our simplified approach cannot fully capture, as shown by the spread in the LIDAR observations by Nolet et al. (2018) in Figure 5.10d.

Burial is one of the primary physical stressors affecting vegetation growth in coastal dunes (Maun, 2009). This makes accurate representation of this relationship crucial for successfully predicting intervention outcomes. The simulations presented here explore the concept of such an intervention but do not prove their success. More realistic vegetation response modelling and thorough validation would be necessary before implementing such approaches in real-world scenarios.

Mapping sediment pathways in coastal design

Lagrangian transport analysis provides information beyond what Eulerian approaches can offer. Eulerian simulation results are limited to comparing net bed level changes and aggregate transport fields. We used Lagrangian analysis to reveal the origin and pathways of moving sediment. The resulting sediment pathways shows how different designs influence sediment movement from the nearshore into the dunes (van Westen et al., 2025, Chapter 4). Such results could be particularly valuable for proposals to feed back dunes with nutrient-rich sediment through nourishments (Pit et al., 2020). Here understanding sediment origins is crucial. Additionally, particle tracking visualization makes complex transport patterns and system connectivity more intuitive and easier to communicate.

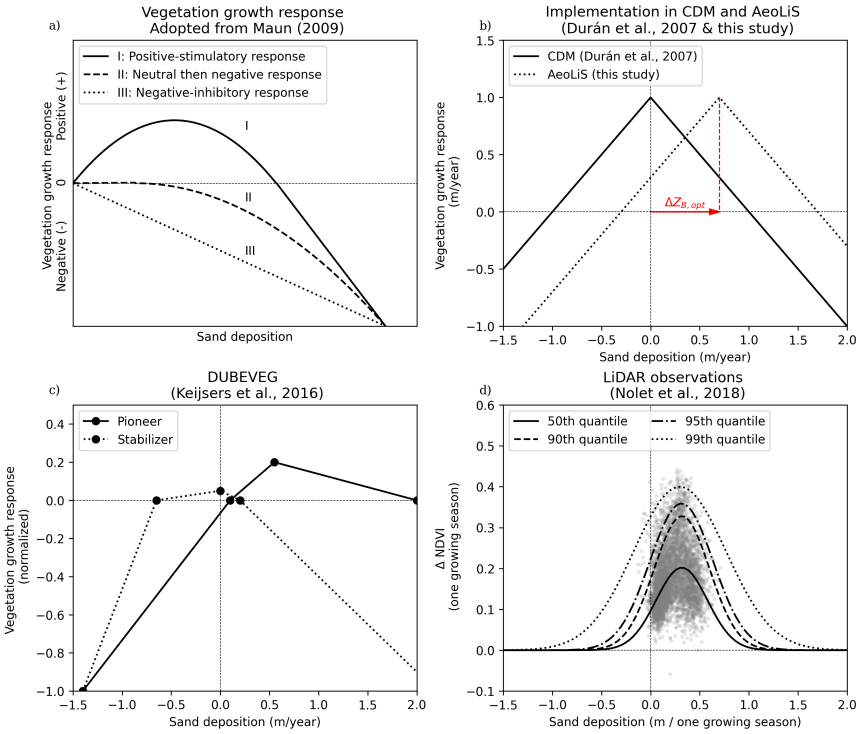

Figure 5.10.: Vegetation growth response (y-axes) to sediment deposition (x-axes). (a) Conceptual responses of vegetation growth to sediment deposition, as described by Maun (2009). (b) Implementation of vegetation growth response within models, comparing CDM (Durán & Herrmann, 2006) with a modified version for this study. (c) Vegetation growth response derived for the DUBEVEG model (Keijsers et al., 2016), showing distinct responses for pioneer and stabilizer species under varying sediment conditions. (d) Observed vegetation growth response using LiDAR measurements (Nolet et al., 2018), with fitted Gaussian distributions for NDVI responses to sand deposition.

5.5. Conclusion

This study has explored the utility of process-based modelling of the nearshore-dune system in informing nourishment design. Comparing alternatives for both mega- and beach nourishment design showed that certain design decisions can significantly influence dune development.

Obtaining these insights was enabled by three key advances in modelling techniques. A model coupling between marine and aeolian domains allowed for continuous sediment exchange across the nearshore-dune interface. This enabled exploration of how nourishment design decisions affect temporal availability of sediment for aeolian transport. Process-based descriptions of aeolian transport and dune development (AeoLiS) captured the landform-shaping processes required to describe spatiotemporal variability in dune growth. The Lagrangian particle-tracking approach (SedTRAILS) revealed the sources and pathways of sediment deposition, providing information beyond traditional Eulerian modeling approaches.

For the Sand Engine mega-nourishment, our results quantify how certain design consideration might have affected dune growth. Removing the artificial dune lake increased dune volume by approximately 42,000 m^3, with effects extending 1,200 m alongshore. Using a finer sediment composition increased dune growth by 65% across the entire domain. Lowering the nourishment crest elevation increased frequent inundation and mixing, resulting in modestly enhanced dune growth.

At smaller scale, our simulations demonstrate how deliberately incorporating a lagoon in beach nourishment design can regulate sediment supply to influence vegetation development. Despite a 62% reduction in total foredune sediment supply, the nourishment with lagoon enhanced backdune deposition by 23%. This regulatory effect on sediment availability slowed vegetation growth, maintained wider blowout entrances, and doubled the contribution from offshore sediment sources to backdune accumulation. The success of these interventions strongly depends on vegetation response to burial—a complex relationship difficult to capture in numerical models. The presented results do not predict accurate vegetation response and subsequent dune dynamics, but demonstrate the concept of using nourishment design to steer temporal sediment supply as an abiotic condition for vegetation growth.

The tools presented here enable exploring the impact of specific design choices on coastal morphodynamics across domain boundaries. The application range spans from large-scale longshore spreading to small-scale landscape development, highlighting the method's versatility. These innovations help coastal managers align nourishment designs with broader objectives beyond flood protection, including ecological and recreational value. This model coupling not only connects numerical domains but could also serve as a tool for connecting different communities, stakeholders and managers—for instance, aligning nourishment programming with dune management objectives.

6

Synthesis and Outlook

This dissertation advances our ability to model coastal processes across domain boundaries, connecting the marine and aeolian environments that have traditionally been studied separately. In this Synthesis chapter, we reflect on the utility of multi-domain modelling in coastal applications. Afterwards, we discuss the contributions of this dissertation towards the integrated description of the nearshore-dune system in coastal applications (Figure 6.4). We then summarize the primary challenges we faced that restrict our application range and impact possible future applications. Finally, we outline a vision for making multi-model, multi-scale approaches more accessible and feasible in engineering practice.

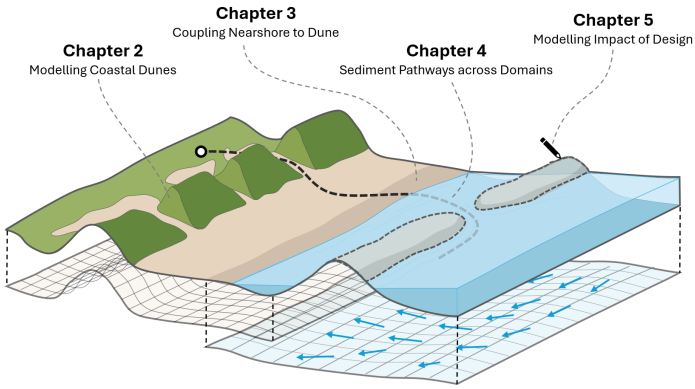

Figure 6.1.: The chapters' contributions to connecting coastal domains in morphodynamic modelling.

6.1. Modelling across Domains in Coastal Applications

Coastal systems are shaped by numerous physical and ecological processes and the intricate interplay between them. These biophysical process interactions make coastal environments complex to understand, let alone simulate. For various aspects of coastal evolution, predictive skill remains limited without prior system knowledge and calibration on observations (Amoudry & Souza, 2011). It is overly optimistic to believe that numerical models could ever fully predict coastal evolution with comprehensive detail and accuracy.

Modelling the comprehensive evolution of the nearshore-dune system requires simulating a variety of processes across multiple domains and their interactions. On the contrary, as Salt (2008) observes, two common pitfalls of modelling are the beliefs that "the more detailed the model, the better" and that "if one model is good, then connecting multiple models is necessarily better." On one hand, the complex reality of biophysical interactions are fundamental in shaping the nearshore-dune system (Houser, 2009; Short & Hesp, 1982), yet on the other hand simplification is the essence of modelling (Salt, 2008).

This duality is important when considering the utility of multi-domain modelling, and by extension the purpose of this dissertation. It raises a logical question: If multi-domain modelling requires significant investment and can result in decreased rather than improved predictive skill, why couple coastal models at all?

To answer this, it could be important to recognise that the potential value of numerical modelling for coastal applications might extend beyond mere predictions. This thesis never aimed to build "a single grand unified model of everything" (Salt, 2008), as such an attempt would be unrealistic given the inherent complexities of coastal systems. The primary benefit of coupled modelling in this thesis lies in leveraging models to investigate specific domain interactions (*understanding*) and to assess how certain decisions in coastal design might affect evolution across domains (*design*) (Barbour & Krahn, 2004).

Given that the benefits of multi-domain modelling primarily lies in studying specific interactions, coupling models might not be needed for every coastal management scenario. Based on experiences from this research, we identify three specific contexts in which multi-domain modelling may offer meaningful advantages for coastal design:

i) The intervention creates significant and persistent effects across multiple coastal domains (e.g., nearshore and dunes), spanning extensive spatial (kilometers or more) and temporal (years or longer) scales.

ii) The evolution and ultimate success of an intervention depends on processes and feedbacks that cross domain boundaries.

iii) The intervention aims to achieve multiple objectives across multiple coastal domains (e.g., recreation, biodiversity, and safety against flooding).

Historically, Dutch coastal management has employed various small-scale interventions (e.g., planting marram grass or placing dune fences) and later hard-engineering structures (e.g., groynes, breakwaters, and seawalls). These typically operate within a single domain (i), exhibit minimal evolution or rely on processes contained within that domain (ii), and pursue singular objectives like flood protection (iii).

The emergence of "soft" sandy solutions in the late twentieth century—culminating in the Dutch national nourishment strategy of the 1990s (Brand et al., 2022)—represented a shift toward more natural solutions. These nourishments do affect the sediment balance across domains and harness natural processes to achieve broader objectives. Despite, established simplistic and single-domain approaches have proven adequate for practical design purposes. The strategic and operational objectives of these nourishments are primary focussed on safety against flooding on longer timescales (Lodder & Slinger, 2022). Relatively simple descriptions of longshore sediment redistribution (Dean & Yoo, 1992; Pelnard-Considère, 1957; Roelvink et al., 2020; Tonnon et al., 2018) are typically sufficient to assess the long-term impact of beach and shoreface nourishments. Specific design decisions, for instance on crest elevation, typically don't have significant lasting effects on broader coastal evolution, as these nourishments gradually diffuse into the coastal system. Process-based, multi-domain modelling likely offers limited additional value relative to the increased uncertainties and resource requirements.

More recently, the rise of large-scale Nature-based Solutions (NBS) increases the need for process-based multi-domain modelling. NBS often satisfy all three criteria: they operate across multiple domains over large spatial (kilometers) and temporal (decades) scales (i), their evolution and functionality depend on processes from various domains (ii), and they typically pursue multiple simultaneous objectives (iii). The following examples demonstrate how model coupling could assist decision-making in future design and management of NBS.

Sand Engine

The Sand Engine (Stive et al., 2013) mega-nourishment was designed to enhance coastal safety and ecological value by naturally distributing sand along the coast through waves, tides, and wind (Figure 1.2). While marine-driven alongshore sediment transport was relatively well-predicted during its design, wind-driven dune growth was significantly overestimated, largely due to simplistic empirical assumptions (Mulder & Tonnon, 2011). In reality, processes such as desert pavement formation and the presence of water bodies limited sediment transport into the dunes. Process-based descriptions of supply-limited aeolian transport and nearshore-dune sediment exchange could have provided better insights into these processes during the design phase, potentially improving performance against desired state indicators such as sand accumulation in the dunes and dune habitat development.

The Marker Wadden & Hondbossche dunes

The Marker Wadden artificial islands (Figure 6.2) were constructed as a nature development project in the Dutch Markermeer. Here we focus on the protective sandy barrier surrounding these islands (Ton et al., 2021). The Hondbossche Dunes (Kroon et al., 2022) serve a similar purpose, being constructed as a sandy buffer in front of an existing dike. In both cases, wave- and wind-driven sediment distribution is important for the protective goals they serve. However, in neither case aeolian transport processes were explicitly considered during design. For the Marker Wadden's sandy barrier, instead of developing into "natural" vegetated dunes, the dry part of the profile became dominated by erosion, characterized by a lack of vegetation and strong desert pavement formation (van Westen et al., 2023). During the initial design of the Hondbossche Dunes, dune growth estimates were based on equilibrium coastal profile assumptions. Not explicitly considering aeolian transport processes resulted in large under-prediction of sediment accumulation in the dunes (Huisman et al., 2025), which partly contributed to higher required nourishment maintenance.

Figure 6.2.: Comparison of the original design (left) and the desert pavement formation at the southern sandy edge (right, Photo credits: Bert van der Valk).

Dynamic dune management

Reintroducing dune dynamics faces challenges when approached exclusively from a subaerial perspective, especially in nourished areas (Figure 1.3). Since dune development reflects sediment availability across the entire nearshore-dune system (Hesp, 2002; Short & Hesp, 1982), the ability to model supply from nearshore to dune could better inform the coordination between nourishment programming and dune management measures. Beyond technical applications, such models can also aid in communicating coastal processes to stakeholders and local communities, particularly important given recent public debates in the Netherlands regarding foredune notch excavations (AFP Netherlands, 2024; Nederlandse Omroep Stichting, 2025).

Spanjaards Duin

Spanjaards Duin (van der Meulen et al., 2014; Vrielink et al., 2021) is an artificial dune area constructed to compensate for habitat losses associated with the Maasvlakte II project by establishing a 6 ha moist dune slack (Figure 6.3). After construction, the groundwater table was observed to be lower than anticipated, restricting development of the intended habitat. To eventually achieve the required bed elevation, managers relied on aeolian erosion to lower the bed. However, desert pavement formation prevented further erosion. Additional mechanical excavation was required, causing further habitat disturbances and project delays. Process-based descriptions of the interactions between aeolian transport, groundwater dynamics and sediment sorting might have anticipated this development, prompting an earlier intervention. Alternatively, a design with a lower initial bed level that would allow wind-driven deposition, rather than erosion, to achieve the desired elevation.

Figure 6.3.: The constructed dune slack at Spanjaardsduin. Photo credits: Kees Vertegaal (https://duinbehoud.nl/spanjaards-duin-tien-jaar-jong/)

6.2. Contributions of this Dissertation

The advancements presented in this dissertation collectively address the need for tools to quantitatively describe the integrated development of the nearshore-dune system. Traditional coastal models typically focus on discrete morphologic domains—either the nearshore (Lesser et al., 2004; Roelvink et al., 2009) or dunes (Durán et al., 2010; Keijsers et al., 2016)—with limited consideration of cross-domain interactions. While conceptual models have long recognized the interconnected nature of coastal systems (Bauer et al., 2009; Moulton et al., 2021; Short & Hesp, 1982), quantitative tools for simulating these interactions have remained underdeveloped. This work bridges that gap through four complementary advancements, each addressing a specific aspect of modelling sediment movement and morphodynamics across the nearshore-dune system.

Demonstrating Feasibility and Benefits of Coupled Modeling

One of the fundamental goals of this project was to explore and demonstrate both the technical feasibility and the added value of coupling numerical models. Previous efforts have already examined model coupling in nearshore–dune settings (Cohn et al., 2019; Hovenga et al., 2023; Roelvink & Costas, 2019; Teixeira et al., 2024; van Westen et al., 2023; Zhang et al., 2015). These studies provide insight into how data exchange among model domains can enhance our understanding of coastal evolution. Some focused on one-dimensional domains (Cohn et al., 2019; Roelvink & Costas, 2019), which are insightful for mapping sediment exchange along more longshore-uniform coastlines. Others, based on cellular automata (Teixeira et al., 2024; Zhang et al., 2015), are computationally efficient and capable of simulating coastal evolution over decades. While these studies underscore the relevance of model coupling, their approaches have limitations for applicability on engineering scales in coastal environments. They either lack the spatial scale or dimensions required to simulate complex coastal designs, or miss the process-based descriptions required to examine the impact of specific design decisions on coastal evolution. Chapter 3 addresses these limitations by developing a coupled modelling framework that represents a significant advancement beyond these existing approaches. This framework extends process-based descriptions to a two-dimensional domain, spanning multiple kilometers, over a five-year simulation period—scales directly relevant to coastal management decisions. The approach overcomes technical challenges, including the exchange of parameters between different model grids with disparate resolutions.

Beyond the Nearshore: Introducing Dunes in Coastal Applications

Chapter 2 addresses coastal dunes; a domain typically simplified through analytical or empirical methods when considered at all in coastal projects. In most natural systems, dune development is governed by a dynamic equilibrium between wind-driven growth and storm-induced erosion, meaning that stand-alone aeolian models only tell part of the picture. As a result, the real-world benefits of stand-alone aeolian transport and dune models may be limited for most practical applications.

With the ability to couple dune processes with hydromorphological models (as explored in Chapter 3), dune modelling could become more directly relevant to practical engineering. The combined development of coupling techniques (Chapter 3) and advanced, process-based dune modelling (Chapter 2) thus paves the way for integrating dunes into coastal design. Rather than treating dunes merely as static flood barriers, such an approach can be used to describe their response to both marine and aeolian forcing. This perspective aligns with literature emphasizing the need for more holistic approaches to coastal management (Arens et al., 2013a; Bridges et al., 2021b; van der Meulen et al., 2023). This approach also creates opportunities for incorporating other often under-represented domains in coastal applications, such as groundwater (Huizer et al., 2018) and ecology (Gielen, 2023; Willemsen et al., 2022).

Revealing Sediment Movement: Lagrangian Pathways Across Domains

Where Chapters 2 and 3 concentrate on the introduction of new model domains and their integration, Chapter 4 enhances the ability to interpret the resulting outputs and deepen system understanding. By introducing Lagrangian pathway analysis, it becomes possible to visually trace sediment movement between domains and to connect sediment sources to sinks. In Chapter 3, nearshore influences on dune development were assessed by comparing morphodynamic changes from coupled versus stand-alone simulations. However, interpreting these comparative results, such as spatial patterns in bed-level changes and sediment budgets can be unintuitive for those less familiar with morphological models. Instead of indirectly inferring connectivity from morphological comparisons, this Lagrangian approach allows one to explicitly follow sediment particles. These sediment pathways simplify interpretation and facilitate clearer communication of otherwise complex sediment movement.

The Lagrangian approach developed in Chapter 4 overcomes key limitations of traditional morphological analysis. While existing Lagrangian approaches have typically been constrained to short timescales (Pearson et al., 2021a; Soulsby et al., 2011) or neglect burial processes (MacDonald et al., 2006), our approach enables multi-year tracking that accounts for morphodynamic evolution. This new capability reveals insights impossible to detect through conventional Eulerian methods. Highlighted examples are the bidirectional accumulation patterns around coastal perturbations and the burial-limited nature of sediment dispersal. The presented findings challenge simplistic assumptions about how coastal perturbations evolve and demonstrate the added value of pathway analysis to capture coastal sediment dynamics. By visualizing sediment movement patterns, this approach not only enhances scientific understanding but also improves communication with stakeholders and decision-makers.

From Theory to Practice: Informing Design and Decision-Making

Finally, Chapter 5 demonstrates the practical value of the presented tools through two hypothetical design scenarios. The beach nourishment case study illustrates how each tool developed in this dissertation contributes unique, complementary insights to inform coastal design. The coupled model from Chapter 3 quantified how different nourishment configurations affect nearshore-to-dune sediment supply. This enables explicit consideration of dune growth in nourishment design. The dune model from Chapter 2 allowed to examine how sediment supply could steer vegetation development and subsequent dune dynamics, utilizing supply as an abiotic condition for vegetation development. Despite the simplistic description of vegetation response, this ability can potentially inform decisions about when and where to introduce notches in foredunes. Finally, the Lagrangian pathway analysis from Chapter 4 uncovered source-to-sink relationships that would remain hidden in conventional approaches. By tracing sediment back to its origin, we discovered that the increase in backdune deposition originated primarily from the nearshore domain, demonstrating an enhanced connection between the nearshore and backdune. As sediment pathways reveal the source of sediment deposited in the backdunes, managers could use these findings to design nourishments that optimize the flux of nutrient-rich sediment into the backdunes (Pit et al., 2020).

By quantifying how design choices influence dune development, this work provides coastal managers with tools to examine cross-domain impacts of their decisions on both morphological and ecological development. The evolution of the Sand Engine has demonstrated that a simplistic description of sediment availability—expressed merely as beach width—is not a sufficient indicator of dune growth potential. Since mega-nourishments like the Sand Engine differ from natural coasts, more complex process-interactions affect dune development, resulting in spatiotemporal variations in dune growth that cannot be explained by simple assumptions. Recent developments have advanced our understanding of these complex interactions and how specific design parameters influence bio-geomorphological development. For example, Teixeira et al. (2024) highlighted the impact of different characteristics, such as armouring and longshore diffusion, on dune development at the Sand Engine over decadal timescales. The approach presented in this thesis complements this capability by describing the underlying processes that cause this spreading and armouring to occur, enabling designers to quantify how their design decisions influence these processes. The Sand Engine alternatives explored in Chapter 5 demonstrate how lowering the initial bed level affects sediment sorting and mixing, subsequently influencing armouring development and ultimately dune growth patterns. Similarly, for beach nourishments, the tools can predict how morphodynamic development of design elements (such as lagoons) affects temporal variations in sediment supply, thereby influencing vegetation growth and dune dynamics. While each component in this process chain introduces uncertainties, the integrated approach provides engineers with insight into how specific design choices cascade through the coastal system to influence both ecological and morphological development.

6.3. Recommendations for Future Development

Throughout the development and application of the tools presented in this dissertation, various challenges emerged that potentially restrict broader application. Below, we discuss key recommendations to increase the application range of multi-domain modelling for coastal applications.

Knowledge gaps and missing processes

Coupling models frequently exposes knowledge gaps that remain inconsequential in stand-alone simulations. Swash-driven morphodynamics provide an example of this. When considered in isolation, the swash zone may be treated differently from each domain's perspective. From an aeolian modelling standpoint, the swash zone is dominated by hydrodynamics and therefore often merely serves as a static sediment source. Meanwhile, from a nearshore modelling perspective, its detailed dynamics may seem negligible relative to larger-scale nearshore processes. This might explain why swash processes have been historically under-represented in both domains independently.

As swash processes are the primary conduit for sediment exchange between marine and aeolian domains (Chen et al., 2023; Roelvink & Otero, 2017), this interface becomes crucial when coupling them. In our larger-scale coupled simulations (Chapters 3 and 5), the lack of detailed swash-related processes prevented us from examining detailed sediment exchange across the intertidal zone. Incorporating these processes in future modelling efforts would enable the numerical investigation of key processes connecting the marine and aeolian domains, such as intertidal sandbar welding (Cohn et al., 2017) or beach berm formation.

Beyond swash dynamics, several other cross-domain processes remain unexplored in this thesis. For instance, multi-fraction sediment exchange between model domains was not implemented, despite evidence that grain-size sorting significantly influences morphological development in both subaqueous (Huisman et al., 2016; 2018) and subaerial (Hoonhout & de Vries, 2017) environments. The interaction between these sorting processes likely creates feedbacks that affect sediment availability and transport gradients throughout the coastal profile, potentially altering the evolution of both domains.

The exclusion of storm-driven processes such as dune erosion, overwash, and breaching limited our applications primarily to accretive environments. Including a model like XBeach (Roelvink et al., 2009) would enable simulation of these high-energy events and their impact on dune evolution. The ability to include dune-erosion in our simulations might support simulating more natural long-term dune evolution, by including the equilibrium between episodic storm erosion and wind-driven recovery. Such capability would be valuable for assessing coastal resilience under climate change scenarios, where both increased storm intensity and rising sea levels may alter the natural balance between erosive and accretive processes in dune systems (Heminway et al., 2023).

Several entire disciplines were excluded or underrepresented in this work, specifically ecological and hydrological processes. Groundwater dynamics play an important role in dune ecosystems and morphological development: they influence aeolian transport through moisture-induced supply limitations (Hallin et al., 2023a), regulate vegetation establishment and growth (Maun, 2009), define the lower erosion threshold in blowout deflation basins (Hesp, 2002), and govern freshwater lens formation and the provision of drinking water. Yet, groundwater processes were greatly simplified in this work, represented only as a static non-erodible layer in some AEOLIS simulations. This simplification restricts the model's ability to capture feedback mechanisms between eco-morphological evolution and groundwater dynamics.

Vegetation dynamics were similarly constrained in the modelling framework. While basic vegetation growth and sediment trapping were included (van Westen et al., 2024b), more complex ecological processes—species competition, anthropogenic disturbance through trampling, climatic and seasonal factors, and groundwater dependencies—were lacking. This shortcoming particularly affects the simulation of dune dynamics, where complex ecological feedback and succession shape dune development (Maun, 2009). Consequently, the simulated vegetation response to management interventions should be interpreted cautiously, recognizing that actual ecological dynamics likely exhibit greater complexity than represented in the model.

Beyond these cross-domain limitations, both the aeolian and marine modelling domains retain inherent limitations that originate within their respective disciplines. In aeolian transport modelling, challenges persist in capturing the full range of supply-limiting conditions. Factors such as moisture thresholds and crust and shell pavement formation remain difficult to quantify and parametrize effectively (Hallin et al., 2023b; Strypsteen & Rauwoens, 2023). Similarly, the current implementation of topographic steering of wind flow represents a significant simplification of complex three-dimensional boundary layer dynamics, particularly in rough terrain with steep slopes and vegetation (Cecil et al., 2024).

In the marine domain, challenges in simulating cross-shore profile evolution persist, particularly regarding breaker-bar dynamics. Current process-based models struggle to accurately predict bar generation, migration, and welding processes that are essential for understanding shoreface evolution (van Duin et al., 2004). Reliable descriptions of cross-shore profile evolution would enable a wider application of coupled models and mapping sediment pathways, such as simulating post-storm recovery or studying the impact of shoreface nourishments.

Technical Challenges to Practical Feasibility

Model coupling is time-consuming and introduces uncertainty. We experienced that coupling two models can require roughly triple the setup time: doubling effort for an extra model component plus additional time to establish inter-model communication. Many tasks related to the setup and coupling of models, such as gridding, boundary condition processing, interpolation, and post-processing of model outcomes, are similar tasks across models and projects. Reducing the required time investment is an important step for the feasibility of multi-domain modelling in coastal applications, which asks for systematic, automated workflows.

We experienced the most time-consuming aspect of model coupling to be regridding of data between computational domains with different spatial resolutions, and often on dissimilar grid types. Ensuring mass conservation while maintaining sufficient detail on both grids is non-trivial, and different variable types (e.g., cumulative bed-level changes vs. instantaneous water levels) require different exchange strategies. Unforeseen instabilities can occur when coupling "black-box" models, complicating diagnosis. By providing pre-built tools that address these challenges, much of the extra time and uncertainty can be reduced.

Although individual models may support parallel runs across multiple nodes and cores (Luijendijk et al., 2019b), their coupled counterparts do not. Parallelizing inter-model communication for large-scale applications is substantially more complex. Without a scalable setup, coupled models could become prohibitively slow, reducing their practical feasibility compared to stand-alone alternatives. Solving this will likely require more extensive exchange frameworks that handle partitioned simulations across distributed computing environments.

This work has demonstrated the feasibility of coupled modelling at engineering scales and identified key challenges that must be addressed for broader application. These challenges should not be viewed as constraints but as guidance for future research and development. The next section outlines a vision for how these challenges might be overcome, moving from proof-of-concept toward practical implementation in coastal engineering practice.

6.4. A Vision for a Future Modelling Ecosystem

This section presents a personal vision of a modelling ecosystem designed to couple numerical models with other models in coastal settings, potentially supported by other innovative data- and AI-powered applications.

Several existing coastal models leverage the Basic Model Interface (BMI) for inter-model and model-data communication; a standardized set of functions designed to enable model coupling (Hutton et al., 2020). Current BMI-compatible models in coastal contexts address diverse processes, such as hydromorphodynamics (Lesser et al., 2004; Roelvink et al., 2009), aeolian transport (van Westen et al., 2024b), vegetation dynamics (Willemsen et al., 2022), compound flooding (Leijnse et al., 2021), and groundwater processes (Hughes et al., 2022). However, coupling efforts using BMI remain scattered across the research landscape. This fragmentation creates inefficiencies: developers repeatedly solve similar technical challenges, while users lack a central resource of compatible models. Inspired by the LANDLAB toolkit (Hobley et al., 2017), we propose developing a modelling ecosystem (Figure 6.4) that should mbody three core characteristics: —*Feasibility*, *Accessibility*, and *Modularity*:

> *A modelling ecosystem composed of multiple model- and data-components, each dedicated to processes within their respective physical domain. These are supported by components, potentially AI- or data-driven, that manage initialization, execution, interconnections, and (advanced) result interpretation.*

Feasibility For coupled modelling to be *feasible* in engineering contexts, its labour-intensive nature, added uncertainty, and computational costs must be reduced. Time-consuming technical hurdles, typically recurring across projects, can deter modellers. A well-maintained toolkit of plug-and-play components could streamline the workflow. Besides, computational parallelization and efficiency must match that of the sum of individual models. Addressing these challenges frees modellers to focus on the physical domain rather than technical details.

Accessibility The ecosystem must be *accessible* to a wide community for sustainable development. Open-source, well-documented code allows more scientists and engineers to contribute, refine, and experiment with innovative modules. Such a community-based model is crucial given that model coupling demands diverse expertise. Co-creation mitigates the reliance on a small group of specialist modellers and stimulates the incorporation of novel insights from the coastal community.

Modularity Achieving feasibility and accessibility requires a *modular* approach. Coastal systems involve a range of processes, domains, and scales. By organizing models as discrete components, users can select only those components needed for their application, while developers can seamlessly add new ones.

The rise of AI- and data-driven techniques offers further opportunities for integration with the ecosystem. Automated AI agents might convert remote sensing data into coupled model setups, or data assimilation could refine cross-shore profile behaviour continuously during simulation. Advanced visualization methods (e.g., Virtual or Augmented Reality) could also leverage this interface, making model outcomes accessible to a broader range of users. Furnishing a shared interface between model components and tools from the wider community can reduce barriers and open new pathways for innovation in coastal modelling and beyond.

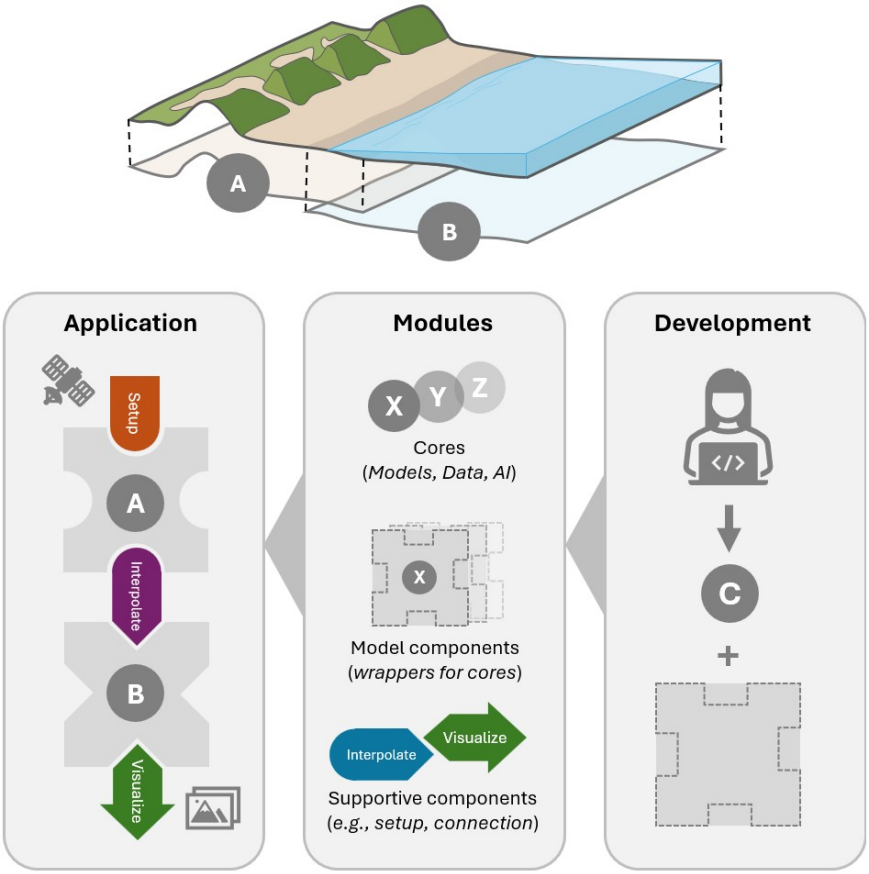

Figure 6.4.: Conceptual diagram of the proposed modelling ecosystem for standardizing model coupling with other models and data in coastal applications. The ecosystem provides a structured framework where various model and support components can be integrated through standardized interfaces.

7

Conclusions

The coast provides numerous services to communities worldwide by reducing flood risks for densely inhabited areas, offering recreational spaces, and sustaining diverse habitats. Coastal management strategies aim to preserve and enhance these services. Due to the rising popularity of "soft" and Nature-based Solutions (NBS), coastal interventions have grown increasingly complex.

NBS are typically designed to fulfil multiple objectives, while having lasting impact crossing multiple domains (e.g., nearshore, beach and dunes). The success of NBS relies on natural processes driving their evolution. To assess the effectiveness and impacts of NBS across the coast, modelling tools crossing domain boundaries are required to simulate the process interactions shaping the nearshore-dune system.

This dissertation advances process-based modelling across the nearshore–dune system by addressing four interconnected objectives: developing process-based descriptions of dune development (**Objective A**), enabling the interaction between the nearshore and dune domains (**Objective B**), unravelling sediment movement across the coastal system (**Objective C**), and demonstrating the practical utility of these interdisciplinary tools for coastal design (**Objective D**). Collectively, these objectives contribute to enabling the connection of coastal domains in morphodynamic and sediment transport modelling.

Objective A

Enable process-based simulations of coastal dune development on engineering scales, by implementing landform-shaping processes in an aeolian transport model.

Coastal dunes are typically under-represented in practical coastal applications, such as the design of sandy interventions. Existing aeolian transport and dune development models typically lack sufficient quantitative predictive capability or engineering scale for feasible application in coastal engineering projects. To address this gap, Chapter 2 presents the implementation of coastal dune evolution in the aeolian transport model AeoLiS . Landform-shaping processes, such as vegetation growth, avalanching, and shear stress perturbations, were added to the model's supply-limited sediment transport descriptions.

This implementation of processes enabled the simulation of multiple characteristic landforms observed in desert and coastal environments under real-world conditions. Barchan dunes were simulated by computing sediment transport influenced by topographic steering and avalanching. The model accurately reproduced the characteristic crescent barchan dune shape and key dimensional relationships (height-to-volume and width-to-height ratios) for observed Moroccan barchan dunes. Simulated migration velocities aligned with established theoretical relationships.

The simulation of parabolic dunes was enabled by including vegetation dynamics. Vegetation stabilize the parabolic dune flanks, prompting the evolution toward a characteristic parabolic shape. Simulated migration rates were consistent with observed parabolic dune migration in Brazil. The formation and development of embryo dunes was effectively simulated by incorporating a probabilistic approach to vegetation establishment. The model reproduced observed seasonal variability in embryo dune development and sheltering effects on embryo dune growth rates on a wide beach in the Netherlands.

The model's practical engineering applicability was validated through the simulation of five foredune notches constructed along the Dutch coast. The model reproduced the spatial pattern of erosion in the blowout deflation basins, slightly overestimating the notch erosion 25% compared to observations. The simulated magnitude and spatial patterns of subsequent backdune deposition were less accurate.

The advancements made to the AeoLiS model improve our ability to simulate dune development in coastal applications, paving the way for the incorporation of dunes into engineering-scale coastal modelling.

Objective B

Explore and demonstrate the technical feasibility and added value of coupling numerical models in morphodynamic modelling of the nearshore-dune system.

The nearshore and dune domains function as an integrated system, with dune development intrinsically reflecting sediment availability throughout the entire coastal profile. Building upon the ability to describe dune development from Chapter 2, Chapter 3 establishes a coupling between the nearshore and dune domains.

A coupling framework was developed that facilitates continuous exchange of wave heights, bed levels, and water levels between three process-based model components: DELFT3D Flexible Mesh, SWAN, and AEOLIS. This model coupling enables an integrated description of the nearshore-dune system.

The coupled model was applied to simulate the initial 5-year morphological evolution of the Sand Engine; a mega-nourishment constructed along the Dutch coast in 2011. The coupled model accurately reproduced key morphological developments, with only 4.6% deviation in predicting the erosion volume from the main peninsula (modelled: 4.1 Mm^3, observed: 3.9 Mm^3) and a 15% underestimation of the aeolian sediment trapping deposition at the dune lake.

Coupling the nearshore and dune domains, allowed to examine the impact of aeolian-marine process interactions on coastal evolution. Coupled and uncoupled (stand-alone) model results were compared to quantify this influence. Analysis revealed that persistent aeolian sediment extraction from the shared sediment budget into the dunes ($\approx$ 15 m^3/m/year) reduced marine-driven longshore spreading by 1.7%. While this percentage appears small, it is expected to accumulate into a significant volume over the Sand Engine's projected lifespan of more than 20 years, potentially surpassing 1.5 Mm^3.

Vice versa, the coupled model also captured the hydrodynamic influence on the spatial variability in foredune growth. As a result of marine-driven erosion and accretion, the simulations show enhanced deposition along accretive beaches accretion (+3.5%) and diminished growth along sheltered beach due to spit development (-11.5%). The simulated impact of hydrodynamic influences on dune growth increased over time, with reduction in foredune deposition in sheltered areas growing from -2.4% in year 1 to -24.4% by year 5, and reaching up to -48.5% at the most sheltered location.

The research demonstrates the feasibility of coupling models at scales relevant to coastal management—spanning multiple kilometres over several years. This approach opens new possibilities for the assessment and design of NBS with a variety of objectives crossing domains.

Objective C

Map sediment pathways across a dynamically evolving coast by tracing particles from source to sink using Lagrangian analysis.

Understanding sediment movement through the coast is important for effective coastal management, yet traditional coastal (Eulerian) modelling does not capture the complete picture of coastal evolution. Chapter 4 advances our understanding of coastal sediment movement through the development of a novel Lagrangian particle tracking methodology that builds upon validated Eulerian model predictions of the Sand Engine from Chapter 3.

We extented the Lagrangian SEDTRAILS framework by implementing morphodynamic-driven particle burial and relating particle mobility to Eulerian sediment transport rates. These additions increased the application range of sediment pathway analysis to decadal simulation periods. We applied SEDTRAILS to the Sand Engine mega-nourishment. The validation against Eulerian results showed good agreement in both volumetric redistribution and annual longshore transport rates.

By analysing simulated sediment pathways, we first traced the dispersal of nourished Sand Engine sediment. The Sand Engine's dispersal showed asymmetry over the five-year period, with 3.0 Mm^3 of nourished sediment moving north compared to only 0.4 Mm^3 south. While particles along undisturbed coastlines are expected to travel 2.5-10 km/year under similar conditions, the average simulated particle displacement of nourished sand was only 200 m/year. This movement is an order of magnitude smaller due to rapid burial at its accretive flanks. As the perturbation diffused, net particle displacement more than doubled from 646 m for first-year particles to 1496 m for fourth-year particles. In the first year, less than 1% of nourished particles travelled at least 2.5 km, which grew to 21% by the fourth year.

The backward-tracing capabilities of the Lagrangian approach revealed the origins of sediment accumulation at the Sand Engine's flanks. South of the Sand Engine, accretion resulted from both nourishment dispersion (41% from nourished sediment) and trapping due to transport gradients (59% from updrift native sediment). As the coastline straightened, this bidirectional pattern evolved, with the contribution from nourished material decreasing from 70% in year two to 30% in year five. In contrast, nearly all sediment (97%) deposited on the northern flank originated directly from the Sand Engine itself.

The presented Lagrangian approach provides a tool for understanding and communicating sediment movement. Rather than indirectly inferring connectivity from Eulerian morphological comparisons, sediment pathways explicitly visualize sediment movement between domains. This enables improved understanding of the connection between sources to sinks and the causal relationships that drive coastal evolution.

Objective D

Demonstrate the utility of the presented multi-domain tools for better informed decision-making in NBS design.

Chapter 5 demonstrates how the presented tools might inform practical decision-making for NBS design. We explored how specific aspects of nourishment design might influence dune development. By incorporating dune development and nearshore-dune interactions in nourishment design considerations, we showcase the added value of multi-domain modelling in practical coastal applications.

First, we examined the influence of several Sand Engine design alternatives on dune growth. Removing the artificial dunelake increased dune growth by approximately 42,000 m^3 after 10 years. Its effect extents approximately 1,200 m alongshore, roughly four times the lake's 300 m length. Selecting a different sediment composition, i.e., reducing the proportion of non-erodible sediment from 5% to 1%, significantly slowed desert pavement formation. This yielded about 65% more dune growth system-wide. An alternative method to limit the impact of desert pavement formation is lowering the crest elevation in the Sand Engine's design. Lowering the higher elevated beaches from 7 m+NAP to 3.5 m+NAP increased the area frequently inundated and subsequent sediment mixing. This measure resulted in an increased dune growth up to 15 m^3 /m near the crest location.

Secondly, we examined the influence of smaller-scale beach nourishment design on dune dynamics. We explored how nourishment design could leverage sediment supply as an abiotic condition to influence vegetation growth and subsequent dune dynamics. Incorporating an artificial lagoon into beach nourishment design limited sediment supply toward the foredune by 62% compared to a conventional beach nourishment. Based on the assumed vegetation dependency on sediment burial, the lagoon-based design resulted in approximately 50% less vegetated area after the 10-year simulation. This reduction in vegetation growth helped maintain wider blowout entrances (70 m versus 40 m) and thus a more active connection between the beach and backdunes. Despite lower sediment supply into the dunes, the inclusion of a lagoon in the nourishment design resulted in 23% more sediment transport into the backdune. We used Lagrangian analysis to trace back the origin of particles deposited in the backdune. Particles from the nearshore contributing 2.4 times more to backdune deposition in case of the lagoon-based nourishment, indicating enhanced connection between distant nearshore sources and the backdune.

The simulation results demonstrate the ability to include dunes into certain consideration of NBS design. Its application suits a range of spatio-temporal scales, from longshore sediment distribution along an entire coastal cell to local dune dynamics. The presented toolkit not only enables the connection of numerical domains but also that of different coastal communities responsible for various parts of the coast. The ability to examine the influence of nourishment design on dune development has the potential of addressing questions relevant for both programming nourishments and dune management.

References

Aagaard, T., Davidson-Arnott, R., Greenwood, B., & Nielsen, J. (2004). Sediment supply from shoreface to dunes: Linking sediment transport measurements and long-term morphological evolution. *Geomorphology*, *60*, 205–224. https://doi.org/10.1016/j.geomorph.2003.08.002 (cit. on pp. 4, 48, 73).

AFP Netherlands. (2024, November 8). *'Gaten' in duinen beschermen tegen de zeespiegelstijging, ze vormen geen overstromingsrisico* (Last updated 2024-11-19). Factcheck Nederland. Retrieved April 3, 2025, from https://factchecknederland.afp.com/doc.afp.com.36LU9WT (cit. on p. 132).

Amoudry, L. O., & Souza, A. J. (2011). Deterministic coastal morphological and sediment transport modeling: A review and discussion. *Reviews of Geophysics*, *49*(2) (cit. on p. 130).

Anthonsen, K. L., Clemmensen, L. B., & Jensen, J. H. (1996). Evolution of a dune from crescentic to parabolic form in response to short-term climatic changes: Råbjerg mile, skagen odde, denmark [Response of Aeolian Processes to Global Change]. *Geomorphology*, *17*(1), 63–77 (cit. on pp. 18, 38).

Arens, S. M., Mulder, J. P., Slings, Q. L., Geelen, L. H., & Damsma, P. (2013a). Dynamic dune management, integrating objectives of nature development and coastal safety: Examples from the netherlands. *Geomorphology*, *199*, 205–213 (cit. on pp. 3, 14, 19, 38, 71, 110, 126, 135).

Arens, S. M., Slings, Q. L., Geelen, L. H., & van der Hagen, H. G. (2013b). Restoration of dune mobility in the netherlands. *Restoration of coastal dunes*, 107–124 (cit. on p. 48).

Arens, S. M., de Vries, S., Geelen, L. H., Ruessink, G., van der Hagen, H. G., & Groenendijk, D. (2020). Comment on 'is 're-mobilisation'nature restoration or nature destruction? a commentary'by i. delgado-fernandez, rgd davidson-arnott & pa hesp. *Journal of Coastal Conservation*, *24*, 1–4 (cit. on p. 14).

Arens, S. (1996). Patterns of sand transport on vegetated foredunes. *Geomorphology*, *17*(4), 339–350 (cit. on p. 17).

Arkema, K. K., Guannel, G., Verutes, G., Wood, S. A., Guerry, A., Ruckelshaus, M., Kareiva, P., Lacayo, M., & Silver, J. M. (2013). Coastal habitats shield people and property from sea-level rise and storms. *Nature Climate Change*, *3*, 913–918. https://doi.org/10.1038/nclimate1944 (cit. on pp. 1, 84, 110).

Ashton, A., Murray, A. B., & Arnoult, O. (2001). Formation of coastline features by large-scale instabilities induced by high-angle waves. *Nature*, *414*(6861), 296–300 (cit. on pp. 84, 94).

Baas, A. C. W., & Nield, J. M. (2007). Modelling vegetated dune landscapes. *Geophysical Research Letters*, *34*(6) (cit. on pp. 5, 17, 18, 39).

Bagnold, R. A. (1937). The transport of sand by wind. *The Geographical Journal*, *89*(5), 409–438 (cit. on pp. 17, 46, 57, 183).

Bakker, M. A., van Heteren, S., Vonhögen, L. M., van der Spek, A. J., & van der Valk, B. (2012). Recent coastal dune development: Effects of sand nourishments. *Journal of Coastal Research*, *28*(3), 587–601 (cit. on p. 14).

Bakker, T. W., & Stuyfzand, P. J. (1993). Nature conservation and extraction of drinking water in coastal dunes: The meijendel area. In *Landscape ecology of a stressed environment* (pp. 244–262). Springer. (Cit. on p. 14).

Barbier, E. B., Hacker, S. D., Kennedy, C., Koch, E. W., Stier, A. C., & Silliman, B. R. (2011). The value of estuarine and coastal ecosystem services. *Ecological monographs*, *81*(2), 169–193 (cit. on pp. 1, 5, 14, 84, 110).

Barbour, S. L., & Krahn, J. (2004). Numerical modelling–prediction or process. *Geotechnical News*, *22*(4), 44–52 (cit. on pp. 5, 50, 76, 130).

Barchyn, T. E., & Hugenholtz, C. H. (2012). A process-based hypothesis for the barchan–parabolic transformation and implications for dune activity modelling. *Earth Surface Processes and Landforms*, *37*(13), 1456–1462 (cit. on pp. 18, 38).

Barciela Rial, M. (2019). *Consolidation and drying of slurries: A building with nature study for the marker wadden* [Doctoral dissertation, Delft University of Technology]. (Cit. on pp. 2, 46, 110).

Barnard, P. L., Foxgrover, A. C., Elias, E. P., Erikson, L. H., Hein, J. R., McGann, M., Mizell, K., Rosenbauer, R. J., Swarzenski, P. W., Takesue, R. K., et al. (2013). Integration of bed characteristics, geochemical tracers, current measurements, and numerical modeling for assessing the provenance of beach sand in the san francisco bay coastal system. *Marine Geology*, *345*, 181–206 (cit. on p. 95).

Bastin, A., Malherbe, B., & Caillot, A. (1983). Zeebrugge port extension sediment transport: Measurement on and off the belgian coast by means of tracers. *8th International Harbour Congress* (cit. on pp. 84, 85).

Bauer, B. O. (1991). Aeolian decoupling of beach sediments. *Annals of the Association of American Geographers*, *81*(2), 290–303 (cit. on p. 17).

Bauer, B. O., & Davidson-Arnott, R. G. (2003). A general framework for modeling sediment supply to coastal dunes including wind angle, beach geometry, and fetch effects. *Geomorphology*, *49*(1-2), 89–108 (cit. on pp. 48, 70, 73).

Bauer, B. O., Davidson-Arnott, R. G., Walker, I. J., Hesp, P. A., & Ollerhead, J. (2012). Wind direction and complex sediment transport response across a beach–dune system. *Earth Surface Processes and Landforms*, *37*(15), 1661–1677 (cit. on p. 17).

Bauer, B. O., & Wakes, S. J. (2022). Cfd simulations of wind flow across scarped foredunes: Implications for sediment pathways and beach–dune recovery after storms. *Earth Surface Processes and Landforms*, *47*(12), 2989–3015 (cit. on p. 23).

Bauer, B., Davidson-Arnott, R., Hesp, P., Namikas, S., Ollerhead, J., & Walker, I. (2009). Aeolian sediment transport on a beach: Surface moisture, wind fetch, and mean transport. *Geomorphology*, *105*(1-2), 106–116 (cit. on pp. 4, 17, 18, 47, 48, 74, 75, 124, 134).

van Bemmelen, C. W. T., de Schipper, M. A., Darnall, J., & Aarninkhof, S. G. J. (2020). Beach scarp dynamics at nourished beaches. *Coastal Engineering*, *160*, 103725 (cit. on p. 75).

Bertin, X., Castelle, B., Anfuso, G., & Ferreira, Ó. (2008). Improvement of sand activation depth prediction under conditions of oblique wave breaking. *Geo-Marine Letters*, *28*(2), 65–75 (cit. on p. 100).

Bertin, X., Deshouilieres, A., Allard, J., & Chaumillon, E. (2007). A new fluorescent tracers experiment improves understanding of sediment dynamics along the arcay sandspit (france). *Geo-Marine Letters*, *27*, 63–69 (cit. on pp. 85, 95).

Beven, K. (1996). 12 equifinality and uncertainty in geomorphological modelling. *The Scientific Nature of Geomorphology: Proceedings of the 27th Binghamton Symposium in Geomorphology, Held 27–29 September 1996*, *27* (cit. on p. 84).

Biel, R. G., Hacker, S. D., Ruggiero, P., Cohn, N., & Seabloom, E. W. (2017). Coastal protection and conservation on sandy beaches and dunes: Context-dependent tradeoffs in ecosystem service supply. *Ecosphere*, *8*(4), e01791 (cit. on pp. 5, 14).

van der Biest, K., de Nocker, L., Provoost, S., Boerema, A., Staes, J., & Meire, P. (2017). Dune dynamics safeguard ecosystem services. *Ocean & coastal management*, *149*, 148–158 (cit. on p. 14).

Black, K. P., & Andrews, C. J. (2001). Sandy shoreline response to offshore obstacles part 1: Salient and tombolo geometry and shape. *Journal of coastal research*, 82–93 (cit. on p. 84).

Black, K. S., Athey, S., Wilson, P., & Evans, D. (2007). The use of particle tracking in sediment transport studies: A review. *Geological Society, London, Special Publications*, *274*(1), 73–91 (cit. on pp. 85, 95, 96).

Bochev-van der Burgh, L., Wijnberg, K. M., & Hulscher, S. J. (2011). Decadal-scale morphologic variability of managed coastal dunes. *Coastal engineering*, *58*(9), 927–936 (cit. on pp. 29, 30).

Bonte, D., Batsleer, F., Provoost, S., Reijers, V., Vandegehuchte, M. L., van de Walle, R., Dan, S., Matheve, H., Rauwoens, P., Strypsteen, G., et al. (2021). Biomorphogenic feedbacks and the spatial organization of a dominant grass steer dune development. *Frontiers in Ecology and Evolution*, 670 (cit. on pp. 17, 19).

Booij, N., Ris, R. C., & Holthuijsen, L. H. (1999). A third-generation wave model for coastal regions: 1. model description and validation. *Journal of geophysical research: Oceans*, *104*(C4), 7649–7666 (cit. on pp. 49, 53).

Borsje, B. W., van Wesenbeeck, B. K., Dekker, F., Paalvast, P., Bouma, T. J., van Katwijk, M. M., & de Vries, M. B. (2011). How ecological engineering can serve in coastal protection. *Ecological Engineering*, *37*(2), 113–122 (cit. on p. 14).

Boskalis. (2022, March). Boskalis to protect eroded togo and benin coastline and construct innovative sand engine concept for beach replenishment. https://boskalis.com/press/press-releases-and-company-news/boskalis-to-protect-eroded-togo-and-benin-coastline-and-construct-innovative-sand-engine-concept-for-beach-replenishment (cit. on p. 71).

Bosnic, I., Cascalho, J., Taborda, R., Drago, T., Hermínio, J., Rosa, M., Dias, J., & Garel, E. (2017). Nearshore sediment transport: Coupling sand tracer dynamics with oceanographic forcing. *Marine Geology*, *385*, 293–303 (cit. on pp. 85, 95, 102).

van Boxel, J., Jungerius, P., Kieffer, N., & Hampele, N. (1997). Ecological effects of reactivation of artificially stabilized blowouts in coastal dunes. *Journal of Coastal Conservation*, *3*, 57–62 (cit. on pp. 3, 14, 110).

Brand, E., Ramaekers, G., & Lodder, Q. (2022). Dutch experience with sand nourishments for dynamic coastline conservation–an operational overview. *Ocean & Coastal Management*, *217*, 106008 (cit. on pp. 2, 14, 73, 84, 110, 131).

Bridges, T. S., King, J. K., Moynihan, E. B., Allen, C. L., Vann, C. S., & Rhea, K. L. (2021a). *Engineering with nature*. US Army Engineer Research; Development Center (ERDC). (Cit. on p. 4).

Bridges, T. S., King, J. K., Simm, J. D., Beck, M. W., Collins, G., Lodder, Q., & Mohan, R. K. (2021b). *Overview: International guidelines on natural and nature-based features for flood risk management*. Engineer Research; Development Center (US). (Cit. on pp. 46, 135).

Brodie, K., Conery, I., Cohn, N., Spore, N., & Palmsten, M. (2019). Spatial variability of coastal foredune evolution, part a: Timescales of months to years. *Journal of Marine Science and Engineering*, *7*(5), 124 (cit. on p. 14).

Carter, R. (1976). Formation, maintenance and geomorphological significance of an aeolian shell pavement. *Journal of Sedimentary Research*, *46*(2), 418–429 (cit. on pp. 4, 17, 47).

Castelle, B., Laporte-Fauret, Q., Marieu, V., Michalet, R., Rosebery, D., Bujan, S., Lubac, B., Bernard, J.-B., Valance, A., Dupont, P., et al. (2019). Nature-based solution

along high-energy eroding sandy coasts: Preliminary tests on the reinstatement of natural dynamics in reprofiled coastal dunes. *Water*, *11*(12), 2518 (cit. on pp. 3, 14, 38).

Cecil, O., Cohn, N., Farthing, M., Dutta, S., & Trautz, A. (2024). Examination of analytical shear stress predictions for coastal dune evolution. *EGUsphere*, *2024*, 1–34 (cit. on pp. 24, 39, 138).

Chen, W., van der Werf, J. J., & Hulscher, S. J. M. H. (2023). A review of practical models of sand transport in the swash zone. *Earth-Science Reviews*, 104355 (cit. on pp. 75, 96, 137).

Cheong, H.-F., Shankar, N. J., Radhakrishnan, R. t., & Toh, A.-C. (1993). Estimation of sand transport by use of tracers along a reclaimed shoreline at singapore changi airport. *Coastal engineering*, *19*(3-4), 311–325 (cit. on pp. 85, 102).

Ciarletta, D. J., Shawler, J. L., Tenebruso, C., Hein, C. J., & Lorenzo-Trueba, J. (2019). Reconstructing coastal sediment budgets from beach- and foredune-ridge morphology: A coupled field and modeling approach. *Journal of Geophysical Research: Earth Surface*, *124*(6), 1398–1416. https://doi.org/https://doi.org/10.1029/2018JF004908 (cit. on p. 70).

Ciavola, P., Taborda, R., Ferreira, O., & Dias, J. A. (1997). Field measurements of longshore sand transport and control processes on a steep meso-tidal beach in portugal. *Journal of Coastal Research*, 1119–1129 (cit. on pp. 85, 95, 100).

Cohn, N., Hoonhout, B. M., Goldstein, E. B., de Vries, S., Moore, L. J., Vinent, O. D., & Ruggiero, P. (2019). Exploring marine and aeolian controls on coastal foredune growth using a coupled numerical model. *Journal of Marine Science and Engineering*, *7*. https://doi.org/10.3390/jmse7010013 (cit. on pp. 46, 49, 51, 70, 134).

Cohn, N., Ruggiero, P., de Vries, S., & García-Medina, G. (2017). Beach growth driven by intertidal sandbar welding. *Proceedings of coastal dynamics*, *1*(99), 12–16 (cit. on pp. 4, 48, 137).

Cohn, N., Ruggiero, P., de Vries, S., & Kaminsky, G. M. (2018). New insights on coastal foredune growth: The relative contributions of marine and aeolian processes. *Geophysical Research Letters*, *45*(10), 4965–4973 (cit. on pp. 14, 18, 70, 74).

Cooper, A., & Jackson, D. (2021). Dune gardening? a critical view of the contemporary coastal dune management paradigm. *Area*, *53*(2), 345–352 (cit. on p. 14).

Costas, S., de Sousa, L. B., Kombiadou, K., Ferreira, Ó., & Plomaritis, T. A. (2020). Exploring foredune growth capacity in a coarse sandy beach. *Geomorphology*, *371*, 107435 (cit. on pp. 4, 46, 48, 73).

Davidson, S. G., Hesp, P. A., DaSilva, M., & Da Silva, G. M. (2022). Flow dynamics over a high, steep, erosional coastal dune slope. *Geomorphology*, *402*, 108111 (cit. on p. 23).

Davidson-Arnott, R. G., & Law, M. N. (1996). Measurement and prediction of long-term sediment supply to coastal foredunes. *Journal of coastal research*, 654–663 (cit. on p. 17).

Davis, E. H., Hein, C. J., Cohn, N., White, A. E., & Zinnert, J. C. (2024). Differences in internal sedimentologic and biotic structure between natural, managed, and constructed coastal foredunes. *Geomorphology*, 109083 (cit. on p. 39).

Dean, R. G., & Yoo, C.-H. (1992). Beach-nourishment performance predictions. *Journal of waterway, port, coastal, and ocean engineering*, *118*(6), 567–586 (cit. on pp. 85, 131).

Delgado-Fernandez, I. (2010). A review of the application of the fetch effect to modelling sand supply to coastal foredunes. *Aeolian Research*, *2*(2-3), 61–70 (cit. on pp. 38, 48).

Delgado-Fernandez, I., Davidson-Arnott, R. G., & Hesp, P. A. (2019). Is 're-mobilisation'nature restoration or nature destruction? a commentary. *Journal of Coastal Conservation*, *23*, 1093–1103 (cit. on p. 14).

Deltares. (1982). Deltares integrated model runner. (Cit. on p. 56).

Derijckere, J., Strypsteen, G., & Rauwoens, P. (2022). Initial development of an artificial dune: Dune-in-front-of-a-dike site ostend oosteroever-belgium. *NCK Days 2022, Date: 2022/03/16-2022/03/18, Location: Enschede, The Netherlands*, 18–18 (cit. on p. 14).

Derijckere, J., Strypsteen, G., & Rauwoens, P. (2023). Early-stage development of an artificial dune with varying plant density and distribution. *Geomorphology*, *437*, 108806 (cit. on p. 14).

Dickey, J., Wengrove, M., Cohn, N., Ruggiero, P., & Hacker, S. D. (2023). Observations and modeling of shear stress reduction and sediment flux within sparse dune grass canopies on managed coastal dunes. *Earth Surface Processes and Landforms*, *48*(5), 907–922 (cit. on p. 39).

Drapeau, G., & Long, B. (1985). Measurements of bedload transport in the nearshore zone using radioisotopic sand tracers. *Coastal Engineering 1984*, 1252–1264 (cit. on pp. 85, 102).

van Duin, M., Wiersma, N., Walstra, D., van Rijn, L., & Stive, M. (2004). Nourishing the shoreface: Observations and hindcasting of the egmond case, the netherlands. *Coastal Engineering*, *51*(8-9), 813–837 (cit. on pp. 84, 97, 138).

Durán, O. (2007). *Vegetated dunes and barchan dune fields* [Doctoral dissertation, Universität Stuttgart]. (Cit. on p. 22).

Durán, O., & Herrmann, H. J. (2006). Vegetation against dune mobility. *Phys. Rev. Lett.*, *97*, 188001 (cit. on pp. 17, 18, 25, 28, 33, 34, 126, 127).

Durán, O., & Moore, L. J. (2013). Vegetation controls on the maximum size of coastal dunes. *Proceedings of the National Academy of Sciences*, *110*(43), 17217–17222 (cit. on pp. 17, 19, 23, 25, 26, 38, 55, 70, 72, 116).

Durán, O., Parteli, E. J., & Herrmann, H. J. (2010). A continuous model for sand dunes: Review, new developments and application to barchan dunes and barchan dune fields. *Earth Surface Processes and Landforms*, *35*(13), 1591–1600 (cit. on pp. 5, 18, 28, 32, 49, 75, 126, 134).

Durán, O., Silva, M., Bezerra, L., Herrmann, H. J., & Maia, L. (2008). Measurements and numerical simulations of the degree of activity and vegetation cover on parabolic dunes in north-eastern brazil. *Geomorphology*, *102*(3-4), 460–471 (cit. on pp. 18, 28, 38).

Durán Vinent, O., & Moore, L. J. (2015). Barrier island bistability induced by biophysical interactions. *Nature Climate Change*, *5*(2), 158–162 (cit. on p. 70).

Ebel, B. A., & Loague, K. (2006). Physics-based hydrologic-response simulation: Seeing through the fog of equifinality. *Hydrological Processes: An International Journal*, *20*(13), 2887–2900 (cit. on p. 84).

Elias, E. P., van der Spek, A. J., Pearson, S. G., & Cleveringa, J. (2019). Understanding sediment bypassing processes through analysis of high-frequency observations of ameland inlet, the netherlands. *Marine Geology*, *415*, 105956 (cit. on pp. 84, 97).

Everard, M., Jones, L., & Watts, B. (2010). Have we neglected the societal importance of sand dunes? an ecosystem services perspective. *Aquatic Conservation: Marine and Freshwater Ecosystems*, *20*(4), 476–487 (cit. on p. 14).

Falqués, A., & Calvete, D. (2005). Large-scale dynamics of sandy coastlines: Diffusivity and instability. *Journal of Geophysical Research: Oceans*, *110*(C3) (cit. on p. 84).

Ferreira, C. C., Silva, P. A., Bernabeu, A. M., & Abreu, T. (2023). Transport of heterometric sediments in wave-dominated flows–tracer experiments. *Marine Geology*, *459*, 107042 (cit. on pp. 85, 95, 100, 102).

Ferreira, Ó., Fachin, S., Coli, A. B., Taborda, R., Dias, J. A., & Lontra, G. (2002). Study of harbour infilling using sand tracer experiments. *Journal of Coastal Research*, (36), 283–289 (cit. on pp. 84, 97).

Finkel, H. J. (1959). The barchans of southern peru. *The journal of geology*, *67*(6), 614–647 (cit. on pp. 32, 38).

Fredsoe, J. (1992). *Mechanics of coastal sediment transport*. World Scientific. (Cit. on p. 99).

Garzon, J. L., Costas, S., & Ferreira, O. (2022). Biotic and abiotic factors governing dune response to storm events. *Earth Surface Processes and Landforms*, *47*(4), 1013–1031 (cit. on p. 70).

Geelen, L., Kamps, P., & Olsthoorn, T. (2017). From overexploitation to sustainable use, an overview of 160 years of water extraction in the amsterdam dunes, the netherlands. *Journal of coastal conservation*, *21*(5), 657–668 (cit. on p. 14).

Gerhardt-Smith, J. M., McDonald, J. S., Rees, S. I., Lovelace, N. D., et al. (2015). *Deer island aquatic ecosystem restoration project* (tech. rep.) Environmental Laboratory (US). (Cit. on p. 71).

Gielen, C. T. (2023). *Evaluation of the morphological and ecological response to a conceptual artificial bypass system at ijmuiden port* [Master's thesis]. Delft University of Technology. http://resolver.tudelft.nl/uuid:298f972c-24fb-43b9-8790-4c0ff32e0f25 (cit. on p. 135).

Goldstein, E. B., Mullins, E. V., Moore, L. J., Biel, R. G., Brown, J. K., Hacker, S. D., Jay, K. R., Mostow, R. S., Ruggiero, P., & Zinnert, J. C. (2018). Literature-based latitudinal distribution and possible range shifts of two us east coast dune grass species (uniola paniculata and ammophila breviligulata). *PeerJ*, *6*, e4932 (cit. on p. 39).

González-Villanueva, R., Pastoriza, M., Hernández, A., Carballeira, R., Sáez, A., & Bao, R. (2023). Primary drivers of dune cover and shoreline dynamics: A conceptual model based on the iberian atlantic coast. *Geomorphology*, *423*, 108556 (cit. on pp. 4, 48, 73).

Goudie, A. (2011). Parabolic dunes: Distribution, form, morphology and change. *Annals of arid zone*, *50*(3&4), 1–7 (cit. on pp. 28, 34).

Gough, M. K., Reniers, A., Olascoaga, M. J., Haus, B. K., MacMahan, J., Paduan, J., & Halle, C. (2016). Lagrangian coherent structures in a coastal upwelling environment. *Continental Shelf Research*, *128*, 36–50 (cit. on p. 97).

Grunnet, N. M., Walstra, D.-J. R., & Ruessink, B. (2004). Process-based modelling of a shoreface nourishment. *Coastal Engineering*, *51*(7), 581–607 (cit. on p. 96).

Hallin, C., Huisman, B. J., Larson, M., Walstra, D.-J. R., & Hanson, H. (2019a). Impact of sediment supply on decadal-scale dune evolution—analysis and modelling of the kennemer dunes in the netherlands. *Geomorphology*, *337*, 94–110 (cit. on pp. 48, 73).

Hallin, C., van IJzendoorn, C., Homberger, J.-M., & de Vries, S. (2023a). Simulating surface soil moisture on sandy beaches. *Coastal Engineering*, *185*, 104376 (cit. on pp. 17, 18, 20, 21, 138).

Hallin, C., van IJzendoorn, C., Skaden, J., & de Vries, S. (2023b). Evaluation of threshold-based models to account for surface moisture in meso-scale aeolian sediment transport simulations. *The Proceedings of the Coastal Sediments Conference*, 670–683 (cit. on pp. 4, 26, 47, 138).

Hallin, C., Larson, M., & Hanson, H. (2019b). Simulating beach and dune evolution at decadal to centennial scale under rising sea levels. *PLoS One*, *14*(4), e0215651 (cit. on p. 49).

Hamdan, M., Refaat, A., & Wahed, M. A. (2016). Morphologic characteristics and migration rate assessment of barchan dunes in the southeastern western desert of egypt. *Geomorphology*, *257*, 57–74 (cit. on p. 18).

Hanley, M., Hoggart, S., Simmonds, D., Bichot, A., Colangelo, M. A., Bozzeda, F., Heurtefeux, H., Ondiviela, B., Ostrowski, R., Recio, M., et al. (2014). Shifting sands? coastal protection by sand banks, beaches and dunes. *Coastal Engineering*, *87*, 136–146 (cit. on pp. 84, 95, 110).

Hastenrath, S. L. (1967). The barchans of the arequipa region, southern peru. *Zeitschrift für Geomorphologie*, *11*(3), 300–331 (cit. on pp. 32, 38).

Heminway, S. S., Davis, E. H., Cohn, N., Skaden, J., Anderson, D., & Hein, C. J. (2023). Modeled changes in foredune morphology influenced by variable storm intensity and sea-level rise. In *Coastal sediments 2023: The proceedings of the coastal sediments 2023* (pp. 684–697). World Scientific. (Cit. on p. 137).

Hersbach, H., Bell, B., Berrisford, P., Hirahara, S., Horányi, A., Muñoz-Sabater, J., Nicolas, J., Peubey, C., Radu, R., Schepers, D., et al. (2020). The era5 global reanalysis. *Quarterly Journal of the Royal Meteorological Society*, *146*(730), 1999–2049 (cit. on p. 27).

Hersen, P. (2004). On the crescentic shape of barchan dunes. *The European Physical Journal B-Condensed Matter and Complex Systems*, *37*, 507–514 (cit. on pp. 18, 38).

Hersen, P., Douady, S., & Andreotti, B. (2002). Relevant length scale of barchan dunes. *Physical Review Letters*, *89*(26), 264301 (cit. on p. 18).

Hervouet, J.-M., & Bates, P. (2000). The telemac modelling system special issue. *Hydrological Processes*, *14*(13), 2207–2208 (cit. on p. 49).

Hesp, P. A. (1989). A review of biological and geomorphological processes involved in the initiation and development of incipient foredunes. *Proceedings of the Royal Society of Edinburgh, Section B: Biological Sciences*, *96*, 181–201 (cit. on p. 19).

Hesp, P. A. (2002). Foredunes and blowouts: Initiation, geomorphology and dynamics [29th Binghamton Geomorphology Symposium: Coastal Geomorphology]. *Geomorphology*, *48*(1), 245–268 (cit. on pp. 14, 17, 19, 72, 110, 111, 132, 138).

Hesp, P. A., & Hastings, K. (1998). Width, height and slope relationships and aerodynamic maintenance of barchans. *Geomorphology*, *22*(2), 193–204 (cit. on pp. 18, 28, 38).

Hesp, P. A., & Smyth, T. A. (2016). Surfzone-beach-dune interactions: Flow and sediment transport across the intertidal beach and backshore. *Journal of Coastal Research*, (75), 8–12 (cit. on p. 14).

Hesp, P. A., & Smyth, T. A. (2017). Nebkha flow dynamics and shadow dune formation. *Geomorphology*, *282*, 27–38 (cit. on p. 19).

Hesp, P. A., & Smyth, T. A. (2021). Cfd flow dynamics over model scarps and slopes. *Physical Geography*, *42*(1), 1–24 (cit. on p. 38).

Hesp, P. A., Smyth, T. A., Nielsen, P., Walker, I. J., Bauer, B. O., & Davidson-Arnott, R. (2015). Flow deflection over a foredune. *Geomorphology*, *230*, 64–74 (cit. on pp. 17, 23).

Hine, A. C. (1979). Mechanisms of berm development and resulting beach growth along a barrier spit complex. *Sedimentology*, *26*(3), 333–351 (cit. on p. 75).

Hobley, D. E., Adams, J. M., Nudurupati, S. S., Hutton, E. W., Gasparini, N. M., Istanbulluoglu, E., & Tucker, G. E. (2017). Creative computing with landlab: An open-source toolkit for building, coupling, and exploring two-dimensional numerical models of earth-surface dynamics. *Earth Surface Dynamics*, *5*(1), 21–46 (cit. on p. 140).

Hoefel, F., & Elgar, S. (2003). Wave-induced sediment transport and sandbar migration. *Science*, *299*(5614), 1885–1887 (cit. on p. 85).

Hoffmann, T. (2015). Sediment residence time and connectivity in non-equilibrium and transient geomorphic systems. *Earth-Science Reviews*, *150*, 609–627 (cit. on p. 97).

Homberger, J.-M., Lynch, A., Riksen, M., & Limpens, J. (2024). Growth response of dune-building grasses to precipitation. *Ecohydrology*, e2634 (cit. on pp. 17, 39).

Hoonhout, B. (2016). Windsurf. (Cit. on pp. 51, 52).

Hoonhout, B., & de Vries, S. (2017). Aeolian sediment supply at a mega nourishment. *Coastal Engineering*, *123*, 11–20 (cit. on pp. 4, 5, 14, 17, 46, 47, 49, 51, 74, 110, 117, 124, 137).

Hoonhout, B. M., & de Vries, S. (2019). Simulating spatiotemporal aeolian sediment supply at a mega nourishment. *Coastal Engineering*, *145*, 21–35 (cit. on pp. 20, 22, 40, 49, 53, 55, 59, 72, 87, 117, 183).

Hoonhout, B. M., & de Vries, S. (2016). A process-based model for aeolian sediment transport and spatiotemporal varying sediment availability. *Journal of Geophysical Research: Earth Surface*, *121*(8), 1555–1575 (cit. on pp. 5, 15, 20–22, 38, 49, 51–53, 70, 99).

Houser, C. (2009). Synchronization of transport and supply in beach-dune interaction. *Progress in Physical Geography*, *33*, 733–746. https://doi.org/10.1177/0309133309350120 (cit. on pp. 4, 18, 47, 48, 70, 71, 73, 74, 130).

Hovenga, P. A., Ruggiero, P., Itzkin, M., Jay, K. R., Moore, L., & Hacker, S. D. (2023). Quantifying the relative influence of coastal foredune growth factors on the us

mid-atlantic coast using field observations and the process-based numerical model windsurf. *Coastal Engineering*, *181*, 104272 (cit. on pp. 49, 134).

Hughes, J. D., Russcher, M. J., Langevin, C. D., Morway, E. D., & McDonald, R. R. (2022). The modflow application programming interface for simulation control and software interoperability. *Environmental Modelling & Software*, *148*, 105257 (cit. on p. 140).

Huisman, B., Vermeer, N., van Kuik, N., & Brand, E. (2025, April 11). *Evaluatie suppletiebehoefte Hondsbossche Duinen* (tech. rep. No. 11210366-001-ZKS-0005). Rijkswaterstaat Water, Verkeer en Leefomgeving (RWS) and Deltares. (Cit. on p. 132).

Huisman, B. J., Walstra, D.-J. R., Radermacher, M., de Schipper, M. A., & Ruessink, B. G. (2019). Observations and modelling of shoreface nourishment behaviour. *Journal of Marine Science and Engineering*, *7*(3), 59 (cit. on p. 97).

Huisman, B., de Schipper, M., & Ruessink, B. (2016). Sediment sorting at the sand motor at storm and annual time scales. *Marine Geology*, *381*, 209–226 (cit. on p. 137).

Huisman, B., Ruessink, B., de Schipper, M., Luijendijk, A., & Stive, M. (2018). Modelling of bed sediment composition changes at the lower shoreface of the sand motor. *Coastal Engineering*, *132*, 33–49 (cit. on pp. 5, 137).

Huisman, B., Wijsman, J., Arens, S., Vertegaal, C., van der Valk, L., van Donk, S., Vreugdenhil, H., & Taal, M. (2021). *Evaluatie van 10 jaar zandmotor: Bevindingen uit het monitoring-en evaluatie programma (mep) voor de periode 2011 tot 2021* (tech. rep.) Deltares. (Cit. on pp. 5, 46, 51, 60, 73, 110).

Huizer, S., Radermacher, M., de Vries, S., Oude Essink, G. H., & Bierkens, M. F. (2018). Impact of coastal forcing and groundwater recharge on the growth of a fresh groundwater lens in a mega-scale beach nourishment. *Hydrology and Earth System Sciences*, *22*(2), 1065–1080 (cit. on p. 135).

Hutton, E. W., Piper, M. D., & Tucker, G. E. (2020). The basic model interface 2.0: A standard interface for coupling numerical models in the geosciences. *Journal of Open Source Software*, *5*(51), 2317 (cit. on pp. 51, 114, 140).

van IJzendoorn, C. O., Hallin, C., Reniers, A. J. H. M., & de Vries, S. (2023a). Modeling multi-fraction coastal aeolian sediment transport with horizontal and vertical grain-size variability. *Journal of Geophysical Research: Earth Surface*, *128*(7), e2023JF007155 (cit. on pp. 4, 17, 20, 21, 47).

van IJzendoorn, C. O., Hallin, C., Cohn, N., Reniers, A. J., & de Vries, S. (2023b). Novel sediment sampling method provides new insights into vertical grain size variability due to marine and aeolian beach processes. *Earth Surface Processes and Landforms*, *48*(4), 782–800 (cit. on p. 47).

Jackson, D. W., Costas, S., González-Villanueva, R., & Cooper, A. (2019). A global 'greening'of coastal dunes: An integrated consequence of climate change? *Global and Planetary Change*, *182*, 103026 (cit. on p. 110).

Jackson, D., Beyers, J., Lynch, K., Cooper, J., Baas, A., & Delgado-Fernandez, I. (2011). Investigation of three-dimensional wind flow behaviour over coastal dune morphology under offshore winds using computational fluid dynamics (cfd) and ultrasonic anemometry. *Earth Surface Processes and Landforms*, *36*(8), 1113–1124 (cit. on p. 23).

Jackson, N. L., & Nordstrom, K. F. (2011). Aeolian sediment transport and landforms in managed coastal systems: A review. *Aeolian research*, *3*(2), 181–196 (cit. on p. 14).

Johnson, M., Goodliffe, R., Doygun, G., & Flikweert, J. (2020). The uk's first sandscaping project (bacton, norfolk) from idea to reality. In *Coastal management 2019: Joining forces to shape our future coasts* (pp. 333–345). ICE Publishing. (Cit. on p. 71).

Kato, S., Okabe, T., Aoki, Y., & Kamohara, S. (2014). Field measurement of sand movement on river-mouth tidal flat using color sand tracing. *Coast. Eng. Proc*, *1*(61), 10–9753 (cit. on pp. 85, 95).

Keijsers, J., de Groot, A., & Riksen, M. (2015). Vegetation and sedimentation on coastal foredunes. *Geomorphology*, *228*, 723–734 (cit. on p. 17).

Keijsers, J., de Groot, A., & Riksen, M. (2016). Modeling the biogeomorphic evolution of coastal dunes in response to climate change. *Journal of Geophysical Research: Earth Surface*, *121*(6), 1161–1181 (cit. on pp. 17, 19, 25, 26, 29, 49, 70, 126, 127, 134).

Kernkamp, H. W., van Dam, A., Stelling, G. S., & de Goede, E. D. (2011). Efficient scheme for the shallow water equations on unstructured grids with application to the continental shelf. *Ocean Dynamics*, *61*, 1175–1188 (cit. on pp. 52–54).

Klein, M., Zviely, D., Kit, E., & Shteinman, B. (2007). Sediment transport along the coast of israel: Examination of fluorescent sand tracers. *Journal of Coastal Research*, *23*(6), 1462–1470 (cit. on pp. 85, 95).

Kombiadou, K., Costas, S., & Roelvink, D. (2023). Exploring controls on coastal dune growth through a simplified model. *Journal of Geophysical Research: Earth Surface*, *128*(9), e2023JF007080 (cit. on pp. 24, 38).

van Koningsveld, M., & Mulder, J. P. M. (2004). Sustainable coastal policy developments in the netherlands. a systematic approach revealed. *Journal of Coastal Research*, *20*(2), 375–385 (cit. on p. 51).

Kraus, N. C. (1985). Field experiments on vertical mixing of sand in the surf zone. *Journal of Sedimentary Research*, *55*(1), 3–14 (cit. on p. 100).

Kraus, N. C., Isobe, M., Igarashi, H., Sasaki, T. O., & Horikawa, K. (1982). Field experiments on longshore sand transport in the surf zone. *Coastal Engineering 1982*, 969–988 (cit. on p. 102).

Kroon, A., de Schipper, M., de Vries, S., & Aarninkhof, S. (2022). Subaqueous and subaerial beach changes after implementation of a mega nourishment in front of a sea dike. *Journal of Marine Science and Engineering*, *10*(8), 1152 (cit. on pp. 3, 14, 71, 132).

Kroy, K., Sauermann, G., & Herrmann, H. J. (2002). Minimal model for aeolian sand dunes. *Physical Review E*, *66*(3), 031302 (cit. on pp. 23, 75, 176).

van Kuik, N., de Vries, J., Schwarz, C., & Ruessink, G. (2022). Surface-area development of foredune trough blowouts and associated parabolic dunes quantified from time series of satellite imagery. *Aeolian Research*, *57*, 100812 (cit. on pp. 17, 19, 72).

Laporte-Fauret, Q., Castelle, B., Marieu, V., Nicolae-Lerma, A., & Rosebery, D. (2022). Foredune blowout formation and subsequent evolution along a chronically eroding high-energy coast. *Geomorphology*, *414*, 108398 (cit. on pp. 19, 110).

Larson, M., Erikson, L., & Hanson, H. (2004). An analytical model to predict dune erosion due to wave impact. *Coastal Engineering*, *51*(8-9), 675–696 (cit. on p. 49).

Larson, M., Palalane, J., Fredriksson, C., & Hanson, H. (2016). Simulating cross-shore material exchange at decadal scale. theory and model component validation. *Coastal Engineering*, *116*, 57–66 (cit. on p. 49).

Leijnse, T., van Ormondt, M., Nederhoff, K., & van Dongeren, A. (2021). Modeling compound flooding in coastal systems using a computationally efficient reduced-physics solver: Including fluvial, pluvial, tidal, wind-and wave-driven processes. *Coastal Engineering*, *163*, 103796 (cit. on p. 140).

Lesser, G. R., Roelvink, J. A., van Kester, J. A., & Stelling, G. S. (2004). Development and validation of a three-dimensional morphological model. *Coastal engineering*, *51*(8-9), 883–915 (cit. on pp. 5, 49, 52–54, 70, 95, 99, 114, 134, 140).

Li, H., Beck, T. M., Moritz, H. R., Groth, K., Puckette, T., Marsh, J., & Sánchez, A. (2019). Sediment tracer tracking and numerical modeling at coos bay inlet, oregon. *Journal of Coastal Research*, *35*(1), 4–25 (cit. on pp. 85, 95).

Lodder, Q., & Slinger, J. (2022). The 'research for policy'cycle in dutch coastal flood risk management: The coastal genesis 2 research programme. *Ocean & Coastal Management*, *219*, 106066 (cit. on p. 131).

Luijendijk, A., & van Oudenhoven, A. (2019). *The sand motor: A nature-based response to climate change: Findings and reflections of the interdisciplinary research program naturecoast*. Delft University Publishers. (Cit. on p. 46).

Luijendijk, A., de Vries, S., van het Hooft, T., & de Schipper, M. (2019a). Predicting dune growth at the sand engine by coupling the delft3d flexible mesh and aeolis

models. *Coastal Sediments 2019: Proceedings of the 9th International Conference*, 1319–1326 (cit. on pp. 49, 51, 52, 57).

Luijendijk, A. P., de Schipper, M. A., & Ranasinghe, R. (2019b). Morphodynamic acceleration techniques for multi-timescale predictions of complex sandy interventions. *Journal of marine science and engineering*, *7*(3), 78 (cit. on pp. 87, 139).

Luijendijk, A. P., Ranasinghe, R., de Schipper, M. A., Huisman, B. A., Swinkels, C. M., Walstra, D. J., & Stive, M. J. (2017). The initial morphological response of the sand engine: A process-based modelling study. *Coastal engineering*, *119*, 1–14 (cit. on pp. 5, 46, 49, 53, 54, 57, 59, 72, 87).

Lynch, K., Jackson, D. W., & Cooper, J. A. G. (2009). Foredune accretion under offshore winds [Contemporary research in aeolian geomorphology]. *Geomorphology*, *105*(1), 139–146 (cit. on p. 39).

MacDonald, N. J., Davies, M. H., Zundel, A. K., Howlett, J. D., Demirbilek, Z., Gailani, J. Z., Lackey, T. C., & Smith, J. (2006). Ptm: Particle tracking model report 1: Model theory, implementation, and example applications. *ERDC/CHL TR-06-20. Vicksburg, MS: US Army Engineer Research and Development Center. http://acwc. sdp. sirsi. net/client/search/asset/1000777* (cit. on pp. 85, 135).

Martínez, M. L., Hesp, P. A., & Gallego-Fernández, J. B. (2013). Coastal dune restoration: Trends and perspectives. *Restoration of coastal dunes*, 323–339 (cit. on p. 14).

Martínez, M. L., & Psuty, N. P. (2004). *Coastal dunes*. Springer. (Cit. on p. 14).

Matias, A., Ferreira, O., Mendes, I., Dias, J. A., & Vila-Concejo, A. (2005). Artificial construction of dunes in the south of portugal. *Journal of Coastal Research*, *21*(3), 472–481 (cit. on p. 14).

Maun, M. A. (2009). *The biology of coastal sand dunes*. Oxford University Press. (Cit. on pp. 17, 110, 126, 138).

McKeehan, K. G., & Arbogast, A. F. (2023). The geography and progression of blowouts in the coastal dunes along the eastern shore of lake michigan since 1938. *Quaternary Research*, *115*, 25–45 (cit. on p. 110).

Meerkerk, A., Arens, S., van Lammeren, R., & Stuiver, H. (2007). Sand transport dynamics after a foredune breach: A case study from schoorl, the netherlands. *Geomorphology*, *86*(1-2), 52–60 (cit. on p. 110).

van der Meulen, F., van der Valk, B., Baars, L., Schoor, E., & van Woerden, H. (2014). Development of new dunes in the dutch delta: Nature compensation and 'building with nature'. *Source: Journal of Coastal Conservation*, *18*, 505–513. https://doi.org/10.1007/s (cit. on pp. 2, 3, 46, 110, 133).

van der Meulen, F., IJff, S., & van Zetten, R. (2023). Nature-based solutions for coastal adaptation management, concepts and scope, an overview. *Nordic Journal of Botany*, *2023*(1), e03290 (cit. on pp. 2, 46, 110, 135).

van der Meulen, F., & de Haes, H. U. (1996). Nature conservation and integrated coastal zone management in europe: Present and future. *Landscape and Urban Planning*, *34*(3-4), 401–410 (cit. on pp. 5, 14).

Miller, I. M., & Warrick, J. A. (2012). Measuring sediment transport and bed disturbance with tracers on a mixed beach. *Marine Geology*, *299*, 1–17 (cit. on pp. 85, 95).

Miller, M. C., & Komar, P. D. (1979). Measurements of sand spreading rates under near-bottom wave orbital motions. *The Journal of Geology*, *87*(6), 593–608 (cit. on pp. 85, 95).

Ministerie van Verkeer en Waterstaat. (1990). *Kustverdediging na 1990: Beleidskeuze voor de kustlijnzorg* (tech. rep.) Rijkswaterstaat, RIKZ. (Cit. on pp. 2, 110).

Montreuil, A.-L., Bullard, J. E., Chandler, J. H., & Millett, J. (2013). Decadal and seasonal development of embryo dunes on an accreting macrotidal beach: North lincolnshire, uk. *Earth Surface Processes and Landforms*, *38*(15), 1851–1868 (cit. on p. 19).

Moore, L. J., Vinent, O. D., & Ruggiero, P. (2016). Vegetation control allows autocyclic formation of multiple dunes on prograding coasts. *Geology*, *44*(7), 559–562 (cit. on p. 72).

Moulton, M. A., Hesp, P. A., da Silva, G. M., Keane, R., & Fernandez, G. B. (2021). Surfzone-beach-dune interactions along a variable low wave energy dissipative beach. *Marine Geology*, *435*, 106438 (cit. on pp. 48, 74, 134).

Mulder, J. P., Hommes, S., & Horstman, E. M. (2011). Implementation of coastal erosion management in the netherlands. *Ocean & coastal management*, *54*(12), 888–897 (cit. on pp. 84, 95, 110).

Mulder, J. P., & Tonnon, P. K. (2011). " sand engine": Background and design of a mega-nourishment pilot in the netherlands. *Coastal Engineering Proceedings*, (32), 35–35 (cit. on pp. 5, 46, 67, 73, 110, 124, 131).

Nederlandse Omroep Stichting. (2025, November 12). *Complotdenkers bedreigen bedrijf dat gaten in de duinen maakt* [Nieuwsbericht gepubliceerd via NOS] (Last updated 2025-11-11). Retrieved April 3, 2025, from https://nos.nl/regio/noord-holland/artikel/575961-complotdenkers-bedreigen-bedrijf-dat-gaten-in-de-duinen-maakt (cit. on p. 132).

Nield, J. M., & Baas, A. C. (2008). Investigating parabolic and nebkha dune formation using a cellular automaton modelling approach. *Earth Surface Processes and Landforms*, *33*(5), 724–740 (cit. on p. 19).

Nienhuis, J. H., Ashton, A. D., Roos, P. C., Hulscher, S. J., & Giosan, L. (2013). Wave reworking of abandoned deltas. *Geophysical research letters*, *40*(22), 5899–5903 (cit. on p. 84).

Nolet, C., van Puijenbroek, M., Suomalainen, J., Limpens, J., & Riksen, M. (2018). Uav-imaging to model growth response of marram grass to sand burial: Implications for coastal dune development. *Aeolian Research*, *31*, 50–61 (cit. on pp. 17, 39, 63, 72, 126, 127).

Nordstrom, K. F., Lampe, R., & Vandemark, L. M. (2000). Reestablishing naturally functioning dunes on developed coasts. *Environmental management*, *25*, 37–51 (cit. on p. 14).

Oliveira, S., Moura, D., Horta, J., Nascimento, A., Gomes, A., & Veiga-Pires, C. (2017). The morphosedimentary behaviour of a headland–beach system: Quantifying sediment transport using fluorescent tracers. *Marine Geology*, *388*, 62–73 (cit. on pp. 85, 95).

Osswald, F., Dolch, T., & Reise, K. (2019). Remobilizing stabilized island dunes for keeping up with sea level rise? *Journal of Coastal Conservation*, *23*(3), 675–687 (cit. on pp. 71, 110).

Oude Vrielink, J., Eleveld, M., van der Valk, B., van Westen, B., Hendriksen, G., IJff, S., van der Meulen, F., de Zeeuw, R., van Eerden, M., Borst, K., et al. (2021). The rise of spanjaards duin: Factors regulating sediment fluxes over an engineered foredune and adjacent dune slack. *NCK Days 2021* (cit. on p. 126).

Palalane, J., Fredriksson, C., Marinho, B., Larson, M., Hanson, H., & Coelho, C. (2016). Simulating cross-shore material exchange at decadal scale. model application. *Coastal Engineering*, *116*, 26–41 (cit. on p. 49).

Paola, C., & Voller, V. R. (2005). A generalized exner equation for sediment mass balance. *Journal of Geophysical Research: Earth Surface*, *110*(F4) (cit. on p. 22).

Parteli, E. J., Duran, O., & Herrmann, H. J. (2007). Minimal size of a barchan dune. *Physical Review E*, *75*(1), 011301 (cit. on p. 18).

Parteli, E. J., Durán, O., Bourke, M. C., Tsoar, H., Pöschel, T., & Herrmann, H. (2014). Origins of barchan dune asymmetry: Insights from numerical simulations. *Aeolian Research*, *12*, 121–133 (cit. on p. 18).

Pearson, S., Elias, E., van Ormondt, M., Roelvink, F., Lambregts, P., Wang, Z., & van Prooijen, B. (2021a). Lagrangian sediment transport modelling as a tool for investigating coastal connectivity. *Proc., Coastal Dynamics Conf* (cit. on pp. 85–87, 97, 135).

Pearson, S. G., Elias, E. P., van Prooijen, B. C., van der Vegt, H., van der Spek, A. J., & Wang, Z. B. (2022). A novel approach to mapping ebb-tidal delta morphodynamics and stratigraphy. *Geomorphology*, *405*, 108185 (cit. on p. 97).

Pearson, S. G., van Prooijen, B. C., Elias, E. P., Vitousek, S., & Wang, Z. B. (2020). Sediment connectivity: A framework for analyzing coastal sediment transport pathways. *Journal of Geophysical Research: Earth Surface*, *125*(10), e2020JF005595 (cit. on pp. 6, 84).

Pearson, S. G., van Prooijen, B. C., Poleykett, J., Wright, M., Black, K., & Wang, Z. B. (2021b). Tracking fluorescent and ferrimagnetic sediment tracers on an energetic ebb-tidal delta to monitor grain size-selective dispersal. *Ocean & Coastal Management*, *212*, 105835 (cit. on p. 85).

Pearson, S. G., Reniers, A., & van Prooijen, B. (2023). Revealing the hidden structure of coastal sediment transport pathways using lagrangian coherent structures. In *Coastal sediments 2023: The proceedings of the coastal sediments 2023* (pp. 1212–1221). World Scientific. (Cit. on p. 97).

Pellón, E., de Almeida, L., González, M., & Medina, R. (2020). Relationship between foredune profile morphology and aeolian and marine dynamics: A conceptual model. *Geomorphology*, *351*, 106984 (cit. on pp. 4, 48, 70, 71, 73, 74).

Pelnard-Considère, R. (1957). Essai de theorie de l'evolution des formes de rivage en plages de sable et de galets. *Journées de L'hydraulique*, *4*(1), 289–298 (cit. on pp. 84, 131).

Perk, L., van Rijn, L., Koudstaal, K., & Fordeyn, J. (2019). A rational method for the design of sand dike/dune systems at sheltered sites; wadden sea coast of texel, the netherlands. *Journal of Marine Science and Engineering*, *7*(9), 324 (cit. on p. 3).

Phillips, J. (1997). Simplexity and the reinvention of equifinality. *Geographical Analysis*, *29*(1), 1–15 (cit. on p. 84).

Phillips, M., Blenkinsopp, C., Splinter, K., Harley, M., & Turner, I. (2019). Modes of berm and beachface recovery following storm reset: Observations using a continuously scanning lidar. *Journal of Geophysical Research: Earth Surface*, *124*(3), 720–736 (cit. on p. 75).

Pit, I. R., Wassen, M. J., Kooijman, A. M., Dekker, S. C., Griffioen, J., Arens, S. M., & van Dijk, J. (2020). Can sand nourishment material affect dune vegetation through nutrient addition? *Science of the total environment*, *725*, 138233 (cit. on pp. 84, 97, 126, 136).

Pontee, N. (2013). Defining coastal squeeze: A discussion. *Ocean & coastal management*, *84*, 204–207 (cit. on pp. 1, 84).

Pourteimouri, P., Campmans, G., Wijnberg, K., & Hulscher, S. (2023). Modelling the influence of beach building pole heights on aeolian morphology and downwind sediment transport. *Geomorphology*, 108791 (cit. on p. 23).

Powell, E. J., Tyrrell, M. C., Milliken, A., Tirpak, J. M., & Staudinger, M. D. (2019). A review of coastal management approaches to support the integration of ecological

and human community planning for climate change. *Journal of coastal conservation*, *23*(1), 1–18 (cit. on p. 4).

Provoost, S., Jones, M. L. M., & Edmondson, S. E. (2011). Changes in landscape and vegetation of coastal dunes in northwest europe: A review. *Journal of Coastal Conservation*, *15*, 207–226 (cit. on p. 14).

Psuty, N. (2008). The coastal foredune: A morphological basis for regional coastal dune development. In *Coastal dunes* (pp. 11–27). Springer. (Cit. on p. 70).

van Puijenbroek, M. E., Teichmann, C., Meijdam, N., Oliveras, I., Berendse, F., & Limpens, J. (2017a). Does salt stress constrain spatial distribution of dune building grasses ammophila arenaria and elytrichia juncea on the beach? *Ecology and Evolution*, *7*(18), 7290–7303 (cit. on p. 17).

van Puijenbroek, M. E., Limpens, J., de Groot, A. V., Riksen, M. J., Gleichman, M., Slim, P. A., van Dobben, H. F., & Berendse, F. (2017b). Embryo dune development drivers: Beach morphology, growing season precipitation, and storms. *Earth Surface Processes and Landforms*, *42*(11), 1733–1744 (cit. on pp. 19, 39, 72).

van Puijenbroek, M. E. B., Nolet, C., de Groot, A. V., Suomalainen, J. M., Riksen, M. J. P. M., Berendse, F., & Limpens, J. (2017c). Exploring the contributions of vegetation and dune size to early dune development using unmanned aerial vehicle (uav) imaging. *Biogeosciences*, *14*(23), 5533–5549 (cit. on pp. 29, 36).

Pye, K. (1983). Coastal dunes. *Progress in Physical Geography*, *7*(4), 531–557 (cit. on p. 14).

Quartel, S., Kroon, A., & Ruessink, B. (2008). Seasonal accretion and erosion patterns of a microtidal sandy beach. *Marine Geology*, *250*(1-2), 19–33 (cit. on pp. 4, 48).

Rahn, P. H. (1969). The relationship between natural forested slopes and angles of repose for sand and gravel. *Geological Society of America Bulletin*, *80*(10), 2123–2128 (cit. on p. 39).

Ranasinghe, R. (2016). Assessing climate change impacts on open sandy coasts: A review. *Earth-science reviews*, *160*, 320–332 (cit. on pp. 1, 84).

Ranasinghe, R., Swinkels, C., Luijendijk, A., Roelvink, D., Bosboom, J., Stive, M., & Walstra, D. (2011). Morphodynamic upscaling with the morfac approach: Dependencies and sensitivities. *Coastal engineering*, *58*(8), 806–811 (cit. on p. 57).

Ranwell, D. S., & Rosalind, B. (1986). *Coastal dune management guide*. Institute of terrestrial Ecology. (Cit. on p. 14).

Raupach, M., Gillette, D., & Leys, J. (1993). The effect of roughness elements on wind erosion threshold. *Journal of Geophysical Research: Atmospheres*, *98*(D2), 3023–3029 (cit. on p. 17).

Reitz, M. D., Jerolmack, D. J., Ewing, R. C., & Martin, R. L. (2010). Barchan-parabolic dune pattern transition from vegetation stability threshold. *Geophysical Research Letters*, *37*(19) (cit. on pp. 18, 38).

Reniers, A. J., MacMahan, J., Beron-Vera, F., & Olascoaga, M. (2010). Rip-current pulses tied to lagrangian coherent structures. *Geophysical Research Letters*, *37*(5) (cit. on p. 97).

Rijkswaterstaat. (2024). Waterinfo [Accessed: 2024-02-12]. (Cit. on p. 29).

van Rijn, L., & Strypsteen, G. (2020). A fully predictive model for aeolian sand transport. *Coastal Engineering*, *156*(March 2020), 1–19 (cit. on p. 23).

van Rijn, L. C. (1997). Sediment transport and budget of the central coastal zone of holland. *Coastal Engineering*, *32*(1), 61–90 (cit. on p. 48).

van Rijn, L. (1995). Sand budget and coastline changes of the central coast of holland between den helder and hoek van holland, period 1964-2040. *H2129* (cit. on p. 51).

van Rijn, L. C., Tonnon, P. K., & Walstra, D. J. R. (2011). Numerical modelling of erosion and accretion of plane sloping beaches at different scales. *Coastal Engineering*, *58*(7), 637–655 (cit. on p. 75).

Riksen, M. J., Goossens, D., Huiskes, H. P., Krol, J., & Slim, P. A. (2016). Constructing notches in foredunes: Effect on sediment dynamics in the dune hinterland. *Geomorphology*, *253*, 340–352 (cit. on pp. 3, 38, 110).

Roelvink, D., & Otero, S. C. (2017). Beach berms as an essential link between subaqueous and subaerial beach/dune profiles. *Geotemas (Madrid)*, (17), 79–82 (cit. on pp. 75, 137).

Roelvink, D., & Costas, S. (2019). Coupling nearshore and aeolian processes: Xbeach and duna process-based models. *Environmental Modelling & Software*, *115*, 98–112 (cit. on pp. 5, 19, 20, 49, 70, 96, 115, 134).

Roelvink, D., Huisman, B., Elghandour, A., Ghonim, M., & Reyns, J. (2020). Efficient modeling of complex sandy coastal evolution at monthly to century time scales. *Frontiers in Marine Science*, *7*, 535 (cit. on p. 131).

Roelvink, D., Reniers, A., van Dongeren, A., de Vries, J. v. T., McCall, R., & Lescinski, J. (2009). Modelling storm impacts on beaches, dunes and barrier islands. *Coastal engineering*, *56*(11-12), 1133–1152 (cit. on pp. 5, 20, 49, 51, 134, 137, 140).

Roelvink, J., & Walstra, D.-J. (2004). Keeping it simple by using complex models. *Advances in Hydro-science and Engineering*, *6*, 1–11 (cit. on p. 54).

Roest, B., de Vries, S., de Schipper, M., & Aarninkhof, S. (2021). Observed changes of a mega feeder nourishment in a coastal cell: Five years of sand engine morphodynamics. *Journal of Marine Science and Engineering*, *9*(1), 37 (cit. on pp. 46, 61, 72, 74, 87, 95, 103, 179).

Romão, S., Silva, P. A., Taborda, R., Cascalho, J., Silva, A. N., & Baptista, P. (2024). Assessing shoreface sediment transport at costinha beach, aveiro, portuguese northwest coast. *Marine Geology*, *467*, 107200 (cit. on pp. 85, 96, 101, 102).

Ruessink, B., Arens, S., Kuipers, M., & Donker, J. (2018). Coastal dune dynamics in response to excavated foredune notches. *Aeolian Research*, *31*, 3–17 (cit. on pp. 3, 14, 17, 29, 36, 38, 72, 110).

Ruessink, G., Sterk, G., Smit, Y., de Winter, W., Hage, P., Donker, J. J., & Arens, S. M. (2022). Predicting monthly to multi-annual foredune growth at a narrow beach. *Earth Surface Processes and Landforms*, *47*(7), 1845–1859 (cit. on pp. 4, 5, 17, 20, 47, 48, 70, 124).

Ruggiero, P., Kaminsky, G. M., Gelfenbaum, G., & Cohn, N. (2016). Morphodynamics of prograding beaches: A synthesis of seasonal-to century-scale observations of the columbia river littoral cell. *Marine Geology*, *376*, 51–68 (cit. on pp. 6, 84, 95).

Rutten, J., Ruessink, B., & Price, T. (2018). Observations on sandbar behaviour along a man-made curved coast. *Earth Surface Processes and Landforms*, *43*(1), 134–149 (cit. on p. 60).

Salt, J. D. (2008). The seven habits of highly defective simulation projects. *Journal of Simulation*, *2*, 155–161 (cit. on pp. 72, 130).

Sauermann, G., Kroy, K., & Herrmann, H. J. (2001). Continuum saltation model for sand dunes. *Physical Review E*, *64*(3), 031305 (cit. on pp. 22, 23, 100).

Sauermann, G., Rognon, P., Poliakov, A., & Herrmann, H. J. (2000). The shape of the barchan dunes of southern morocco. *Geomorphology*, *36*(1-2), 47–62 (cit. on pp. 18, 27, 28, 32, 38).

de Schipper, M. A., Ludka, B. C., Raubenheimer, B., Luijendijk, A. P., & Schlacher, T. A. (2021). Beach nourishment has complex implications for the future of sandy shores. *Nature Reviews Earth & Environment*, *2*(1), 70–84 (cit. on pp. 14, 46, 84).

de Schipper, M. A., de Vries, S., Ruessink, G., de Zeeuw, R. C., Rutten, J., van Gelder-Maas, C., & Stive, M. J. (2016). Initial spreading of a mega feeder nourishment: Observations of the sand engine pilot project. *Coastal Engineering*, *111*, 23–38 (cit. on pp. 46, 51, 74, 95, 179).

Schwarz, C., Brinkkemper, J., & Ruessink, G. (2018). Feedbacks between biotic and abiotic processes governing the development of foredune blowouts: A review. *Journal of Marine Science and Engineering*, *7*(1), 2 (cit. on pp. 19, 110, 111, 126).

van Sebille, E., Griffies, S. M., Abernathey, R., Adams, T. P., Berloff, P., Biastoch, A., Blanke, B., Chassignet, E. P., Cheng, Y., Cotter, C. J., et al. (2018). Lagrangian ocean analysis: Fundamentals and practices. *Ocean modelling*, *121*, 49–75 (cit. on p. 97).

Sherman, D. J., & Bauer, B. O. (1993). Dynamics of beach-dune systems. *Progress in Physical Geography*, *17*(4), 413–447 (cit. on pp. 4, 48, 70, 73).

Sherman, D. J., & Li, B. (2012). Predicting aeolian sand transport rates: A reevaluation of models. *Aeolian Research*, *3*(4), 371–378 (cit. on p. 46).

Short, A. D., & Hesp, P. A. (1982). Wave, beach and dune interactions in southeastern australia. *Marine geology*, *48*(3-4), 259–284 (cit. on pp. 4, 14, 18, 19, 48, 70, 73, 110, 111, 130, 132, 134).

Sigren, J. M., Figlus, J., & Armitage, A. R. (2014). Coastal sand dunes and dune vegetation: Restoration, erosion, and storm protection. *Shore Beach*, *82*(4), 5–12 (cit. on p. 14).

da Silva, G. M., Martinho, C. T., Hesp, P., Keim, B. D., & Ferligoj, Y. (2013). Changes in dunefield geomorphology and vegetation cover as a response to local and regional climate variations. *Journal of Coastal Research*, (65), 1307–1312 (cit. on p. 110).

Silva, F. G., Wijnberg, K. M., de Groot, A. V., & Hulscher, S. J. (2019). The effects of beach width variability on coastal dune development at decadal scales. *Geomorphology*, *329*, 58–69 (cit. on pp. 48, 73).

Smith, S., Marsh, J., & Puckette, T. (2007). Analysis of fluorescent sediment tracer for evaluating nearshore placement of dredged material. *Proceedings XVIII World Dredging Congress 2007*, 1345–1358 (cit. on pp. 84, 85, 95, 97).

Smyth, T., Jackson, D., & Cooper, J. (2011). Computational fluid dynamic modelling of three-dimensional airflow over dune blowouts. *Journal of Coastal Research*, 314–318 (cit. on p. 23).

Sørensen, M. (2004). On the rate of aeolian sand transport. *Geomorphology*, *59*(1-4), 53–62 (cit. on p. 46).

Soulsby, R., Mead, C., Wild, B., & Wood, M. (2011). Lagrangian model for simulating the dispersal of sand-sized particles in coastal waters. *Journal of waterway, port, coastal, and ocean engineering*, *137*(3), 123–131 (cit. on pp. 85, 95, 99, 135).

Steetzel, H., van der Goot, F., Fiselier, J., de Lange, M., Penning, E., van Santen, R., & Vuik, V. (2017). Building with nature pilot sandy foreshore houtribdijk design and behaviour of a sandy dike defence in a lake system. *Coastal Dynamics: Port of Spain, Trinidad and Tobago* (cit. on p. 71).

Stevens, A. W., Elias, E., Pearson, S., Kaminsky, G. M., Ruggiero, P. R., Weiner, H. M., & Gelfenbaum, G. R. (2020). *Observations of coastal change and numerical modeling of sediment-transport pathways at the mouth of the columbia river and its adjacent littoral cell* (tech. rep.) US Geological Survey. (Cit. on pp. 85, 96).

Stevens, A. W., Ruggiero, P., Parker, K. A., Vitousek, S., Gelfenbaum, G., & Kaminsky, G. M. (2024). Climate controls on longshore sediment transport and coastal morphology adjacent to engineered inlets. *Coastal Engineering*, *194*, 104617 (cit. on p. 84).

Stive, M. J., Aarninkhof, S. G., Hamm, L., Hanson, H., Larson, M., Wijnberg, K. M., Nicholls, R. J., & Capobianco, M. (2002). Variability of shore and shoreline evolution. *Coastal engineering*, *47*(2), 211–235 (cit. on p. 84).

Stive, M. J., de Schipper, M. A., Luijendijk, A. P., Aarninkhof, S. G., van Gelder-Maas, C., van Thiel de Vries, J. S., de Vries, S., Henriquez, M., Marx, S., & Ranasinghe, R. (2013). A New Alternative to Saving Our Beaches from Sea-Level Rise: The Sand Engine. *Journal of Coastal Research*, *29*(5), 1001–1008 (cit. on pp. 2, 14, 40, 46, 51, 84, 86, 99, 110, 131).

Stockdon, H. F., Holman, R. A., Howd, P. A., & Sallenger Jr, A. H. (2006). Empirical parameterization of setup, swash, and runup. *Coastal engineering*, *53*(7), 573–588 (cit. on pp. 26, 55, 115).

Strypsteen, G. (2023). The importance of grain-related shear velocity in predicting multi-monthly dune growth. *Earth Surface Processes and Landforms*, *48*(15), 3287–3301 (cit. on p. 23).

Strypsteen, G., Bonte, D., Taelman, C., Derijckere, J., & Rauwoens, P. (2024a). Three years of morphological dune development after planting marram grass on a beach. *Earth Surface Processes and Landforms* (cit. on pp. 3, 14).

Strypsteen, G., Delgado-Fernandez, I., Derijckere, J., & Rauwoens, P. (2024b). Fetch-driven aeolian sediment transport on a sandy beach: A new study. *Earth Surface Processes and Landforms*, *February 2024* (cit. on p. 124).

Strypsteen, G., & Rauwoens, P. (2023). Aeolian sand transport on a natural beach with shells and moist sand patches. *Journal of Coastal Research*, *39*, 700–711 (cit. on pp. 17, 138).

Strypsteen, G., de Sloover, L., de Wulf, A., & Rauwoens, P. (2020). Downwind evolution of aeolian saltation across an artificially constructed coastal berm. *Aeolian Research*, *47*, 100627 (cit. on p. 17).

Strypsteen, G., de Vries, S., van Westen, B., Bonte, D., Homberger, J.-M., Hallin, C., & Rauwoens, P. (2024c). Vertical growth rate of planted vegetation controls dune growth on a sandy beach. *Coastal Engineering*, *194*, 104624 (cit. on p. 126).

Sunamura, T., & Kraus, N. C. (1984). Prediction of average mixing depth of sediment in the surf zone. *Marine Geology*, *62*(1-2), 1–12 (cit. on p. 102).

Sutton-Grier, A. E., Wowk, K., & Bamford, H. (2015). Future of our coasts: The potential for natural and hybrid infrastructure to enhance the resilience of our coastal communities, economies and ecosystems. *Environmental Science and Policy*, *51*, 137–148. https://doi.org/10.1016/j.envsci.2015.04.006 (cit. on pp. 1, 2, 46, 84, 110).

Suzuki, T., Inami, Y., Yanagishima, S., Sakihama, S., & Cox, D. T. (2019). Sediment particle movements observed using tracers under accretive wave conditions in the nearshore zone. *Coastal Engineering Journal*, *61*(4), 472–485 (cit. on pp. 85, 95).

Teixeira, M., Horstman, E. M., & Wijnberg, K. M. (2024). Exploring the bio-geomorphological evolution of mega nourishments with a cellular automata model. *Geomorphology*, *463*, 109371 (cit. on pp. 134, 136).

Terlouw, L., & Slings, R. (2005). Dynamic dune management in practice–remobilization of coastal dunes in the national park zuid-kennemerland in the netherlands. *Proceedings 'dunes and estuaries*, *19*, 211–217 (cit. on pp. 3, 110).

Ton, A. M., Vuik, V., & Aarninkhof, S. G. (2021). Sandy beaches in low-energy, non-tidal environments: Linking morphological development to hydrodynamic forcing. *Geomorphology*, *374*, 107522 (cit. on pp. 3, 132).

Tonnon, P. K., Huisman, B., Stam, G., & van Rijn, L. (2018). Numerical modelling of erosion rates, life span and maintenance volumes of mega nourishments. *Coastal Engineering*, *131*, 51–69 (cit. on pp. 5, 46, 131).

Uphues, C. F., van IJzendoorn, C. O., Hallin, C., Pearson, S. G., van Prooijen, B. C., Miot da Silva, G., & de Vries, S. (2022). Coastal aeolian sediment transport in an active bed surface layer: Tracer study and conceptual model. *Earth Surface Processes and Landforms*, *47*(13), 3147–3162 (cit. on p. 17).

Van Rijn, L., & Strypsteen, G. (2020). A fully predictive model for aeolian sand transport. *Coastal Engineering*, *156*, 103600 (cit. on p. 124).

Vitousek, S., Barnard, P. L., & Limber, P. (2017). Can beaches survive climate change? *Journal of Geophysical Research: Earth Surface*, *122*(4), 1060–1067 (cit. on pp. 84, 95, 110).

Voepel, H., Schumer, R., & Hassan, M. A. (2013). Sediment residence time distributions: Theory and application from bed elevation measurements. *Journal of Geophysical Research: Earth Surface*, *118*(4), 2557–2567 (cit. on p. 97).

Vousdoukas, M. I., Ranasinghe, R., Mentaschi, L., Plomaritis, T. A., Athanasiou, P., Luijendijk, A., & Feyen, L. (2020). Sandy coastlines under threat of erosion. *Nature climate change*, *10*(3), 260–263 (cit. on p. 1).

Vrielink, J. O., Eleveld, M., van Westen, B., Galiforni-Silva, F., & Wijnberg, K. M. (2021). Factors regulating sediment fluxes over an engineered foredune and adjacent dune slack. *Coastal Dynamics 2021: Zandmotor Monitoring* (cit. on pp. 3, 133).

de Vriend, H. J., van Koningsveld, M., Aarninkhof, S. G., B. de Vries, M., & Baptist, M. J. (2015). Sustainable hydraulic engineering through building with nature. *Journal of Hydro-Environment Research*, *9*, 159–171. https://doi.org/10.1016/j.jher.2014.06.004 (cit. on pp. 2, 46, 110).

de Vriend, H. J., Rijkswaterstaat, & Roelvink, J. A. (1989). *Innovatie van kustverdediging: Inspelen op het kustsysteem*. Ministerie van Verkeer en Waterstaat. (Cit. on pp. 46, 124).

de Vries, S., de Vries, J. v. T., van Rijn, L., & Arens, S. (2014a). Aeolian sediment transport in supply limited situations. *Aeolian Research*, *12*, 75–85 (cit. on pp. 4, 17–22, 46, 95).

de Vries, S., Arens, S., de Schipper, M., & Ranasinghe, R. (2014b). Aeolian sediment transport on a beach with a varying sediment supply. *Aeolian Research*, *15*, 235–244. https://doi.org/https://doi.org/10.1016/j.aeolia.2014.08.001 (cit. on p. 46).

de Vries, S., Southgate, H., Kanning, W., & Ranasinghe, R. (2012). Dune behavior and aeolian transport on decadal timescales. *Coastal Engineering*, *67*, 41–53 (cit. on pp. 65, 73).

Wakes, S. J., Maegli, T., Dickinson, K. J., & Hilton, M. J. (2010). Numerical modelling of wind flow over a complex topography. *Environmental Modelling & Software*, *25*(2), 237–247 (cit. on p. 23).

van der Wal, D. (2004). Beach-dune interactions in nourishment areas along the dutch coast. *Journal of Coastal Research*, *20*(1), 317–325 (cit. on pp. 14, 48).

Walker, I. J., Eamer, J. B., & Darke, I. B. (2013). Assessing significant geomorphic changes and effectiveness of dynamic restoration in a coastal dune ecosystem. *Geomorphology*, *199*, 192–204 (cit. on pp. 3, 14).

Walker, I. J., Hilgendorf, Z., Gillies, J. A., Turner, C. M., Furtak-Cole, E., & Nikolich, G. (2023). Assessing performance of a "nature-based" foredune restoration project, oceano dunes, california, usa. *Earth Surface Processes and Landforms*, *48*(1), 143–162 (cit. on p. 14).

Walker, I. J., & Nickling, W. G. (2002). Dynamics of secondary airflow and sediment transport over and in the lee of transverse dunes. *Progress in Physical Geography*, *26*(1), 47–75 (cit. on p. 17).

Walker, S. L., & Zinnert, J. (2022). Whole plant traits of coastal dune vegetation and implications for interactions with dune dynamics. *Ecosphere*, *13*(5), e4065 (cit. on p. 39).

Warren, I., & Bach, H. (1992). Mike 21: A modelling system for estuaries, coastal waters and seas. *Environmental Software*, *7*(4), 229–240 (cit. on p. 49).

Warrick, J. A., Stevens, A. W., Miller, I. M., Harrison, S. R., Ritchie, A. C., & Gelfenbaum, G. (2019). World's largest dam removal reverses coastal erosion. *Scientific Reports*, *9*(1), 13968 (cit. on pp. 84, 97).

Weng, W., Hunt, J., Carruthers, D., Warren, A., Wiggs, G., Livingstone, I., & Castro, I. (1991). Air flow and sand transport over sand-dunes. *Aeolian grain transport: The erosional environment*, 1–22 (cit. on pp. 23, 39, 176).

Wengrove, M. E., Henriquez, M., De Schipper, M. A., Holman, R., & Stive, M. (2013). Monitoring morphology of the sand engine leeside using argus' cbathy. *Coastal Dynamics*, *2013*, 7th (cit. on p. 2).

van Westen, B., Luijendijk, A. P., de Vries, S., Cohn, N., Leijnse, T. W., & de Schipper, M. A. (2024a). Predicting marine and aeolian contributions to the sand engine's evolution using coupled modelling. *Coastal Engineering*, *188*, 104444 (cit. on pp. 14, 18, 40, 87, 88, 95, 96, 99, 102, 103, 110, 114, 115, 124–126, 181).

van Westen, B., Leijnse, T., de Schipper, M., Cohn, N., & Luijendijk, A. (2023). Integrated modelling of coastal landforms. *Coastal Sediments 2023: The Proceedings of the Coastal Sediments 2023*, 760–771 (cit. on pp. 49, 126, 132, 134).

van Westen, B., de Vries, S., Cohn, N., van IJzendoorn, C., Strypsteen, G., & Hallin, C. (2024b). Aeolis: Numerical modelling of coastal dunes and aeolian landform development for real-world applications. *Environmental Modelling & Software*, *179*, 106093 (cit. on pp. 85, 87, 95, 99, 114, 116, 138, 140).

van Westen, B., de Schipper, M. A., Pearson, S. G., & Luijendijk, A. P. (2025). Lagrangian modelling reveals sediment pathways at evolving coasts. *Scientific reports*, *15*(1), 1–16 (cit. on pp. 116, 126).

White, T. E. (1998). Status of measurement techniques for coastal sediment transport. *Coastal Engineering*, *35*(1-2), 17–45 (cit. on pp. 85, 95, 96, 100, 102).

Wijnberg, K., Poppema, D., Mulder, J., van Bergen, J., Campmans, G., Galiforni-Silva, F., Hulscher, S., & Pourteimouri, P. (2021). Beach-dune modelling in support of building with nature for an integrated spatial design of urbanized sandy shores. *Research in Urbanism Series*, *7*, 241–260 (cit. on pp. 14, 19).

Willemsen, P., Smits, B., Borsje, B., Herman, P., Dijkstra, J., Bouma, T., & Hulscher, S. (2022). Modeling decadal salt marsh development: Variability of the salt marsh edge under influence of waves and sediment availability. *Water resources research*, *58*(1), e2020WR028962 (cit. on pp. 135, 140).

Wittebrood, M., de Vries, S., Goessen, P., & Aarninkhof, S. (2018). Aeolian sediment transport at a man-made dune system; building with nature at the hondsbossche dunes. *Coastal Engineering Proceedings*, (36), 83–83 (cit. on p. 14).

de Zeeuw, R., de Schipper, M. (, & de Vries, S. ((2017). Sand motor topographic survey, actual surveyed path. https://doi.org/10.4121/UUID:3836E5A5-4FDF-4122-84BD-A9BB679FB84C (cit. on p. 179).

Zhang, D., Narteau, C., & Rozier, O. (2010). Morphodynamics of barchan and transverse dunes using a cellular automaton model. *Journal of Geophysical Research: Earth Surface*, *115*(F3) (cit. on p. 18).

Zhang, J., & Larson, M. (2022). A numerical model to simulate beach and dune evolution. *Journal of Coastal Research*, *38*(4), 776–784 (cit. on p. 49).

Zhang, W., Schneider, R., Kolb, J., Teichmann, T., Dudzinska-Nowak, J., Harff, J., & Hanebuth, T. J. (2015). Land–sea interaction and morphogenesis of coastal foredunes—a modeling case study from the southern baltic sea coast. *Coastal Engineering*, *99*, 148–166 (cit. on p. 134).

A

Topographic steering

The shear stress perturbation in the x- and y-directions ($\delta\tau_x$ and $\delta\tau_y$) is computed in Fourier space according to the following equations:

$$\delta\tilde{\tau}_x(\vec{k}) = \frac{2\tilde{z}_b(\vec{k})}{U^2(l)}\frac{{k_x}^2}{|\vec{k}|}\left\{-1+\left(2\ln\frac{l}{z_0'}+\frac{|k|^2}{{k_x}^2}\right)\sigma\frac{K_1(2\sigma)}{K_0(2\sigma)}\right\} \tag{A.1}$$

$$\delta\tilde{\tau}_y(\vec{k}) = \frac{2\tilde{z}_b(\vec{k})}{U^2(l)}\frac{k_x k_y}{|\vec{k}|}2\sqrt{2}\sigma K_1(2\sqrt{2}\sigma) \tag{A.2}$$

$$\sigma = \sqrt{iLk_x z_0'/l} \tag{A.3}$$

where ˜ indicates the Fourier-transformed components of the parameters, k_x and k_y are the components of the wave vector $\vec{k}$ in Fourier space and K_0 and K_1 are modified Bessel functions. l [m] (see Figure A.1) is the depth of the inner layer of flow, L [m] is the typical length scale of the hill, and z_m [m] is the height of the middle layer of flow:

$$l = \frac{2\kappa^2 L}{\ln\frac{l}{z_0'}} \qquad U(l) \equiv \frac{\ln\frac{l}{z_0'}}{\ln\frac{z_m}{z_0'}} \qquad z_m = \sqrt{\frac{L^2}{\ln\frac{z_m}{z_0'}}} \tag{A.4}$$

where $U(l)$ [-] is the dimensionless vertical velocity profile at height l.

For one-dimensional situations, a simplified solution of the shear perturbation approach is implemented, ignoring some minor terms, leading to a less computationally expensive approach (Kroy et al., 2002):

$$\delta\tau = \alpha \int_{-\infty}^{\infty} d\xi \frac{\frac{\delta z_b}{\delta x}(x-\xi)}{\pi\xi} + \beta \frac{\delta z_b}{\delta x}(x) \tag{A.5}$$

where α [-] and β [-] both depend on L/z_0, but are not computed in the model but are user-defined fixed variables. ξ [-] is the normalized cross-shore distance x/L.

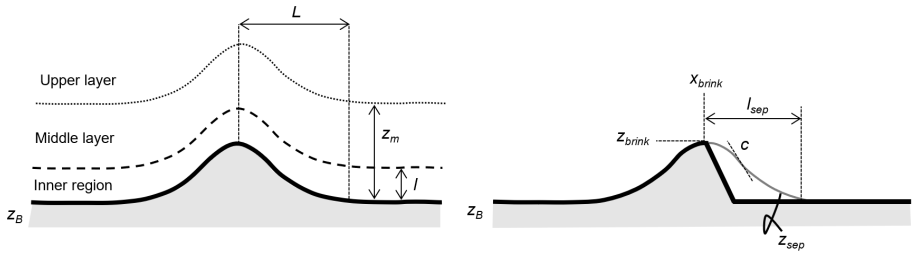

Figure A.1.: Schematic overview of shear perturbation and flow separation approach. Based on (Kroy et al., 2002; Weng et al., 1991).

The separation bubble surface z_{sep} [m] is modelled by a third-order polynomial. The dimensions of the separation bubble are shown in A.1. The height of the brinkline, or the location where the separation bubble starts to detach from the bed, is defined by $z_b(x_{\text{brink}}) \equiv z_{\text{brink}}$. Assuming a maximum slope c [deg] for the separation surface, determining the shape of the separation bubble, the reattachment length l is obtained by:

$$l \approx \frac{3z_{\text{brink}}}{2c}\left(1 + \frac{z_{\text{brink}}}{4c} + 2\left(\frac{z_{\text{brink}}}{4c}\right)^2\right) \tag{A.6}$$

A

The separation bubble z_{sep} is calculated as:

$$z_{sep}(x) = a_3(x - x_{brink})^3 + a_2(x - x_{brink})^2 + z'_{brink}(x - x_{brink}) + z_{brink} \tag{A.7}$$

where:

$$a_2 = -\frac{3z_{brink} + 2z'_{brink}l}{l^2} \tag{A.8}$$

$$a_3 = \frac{2z_{brink} + z'_{brink}l}{l^3} \tag{A.9}$$

B

Simulation overview

Table B.1.: Overview of all landform simulations performed within this study.

Landform Demonstrating the model's ability to describe ...	*Sim. name*	*Figure*
Barchan dunes (§2.5.1)		Video S4
... barchan dunes under varying wind directions.	1. *barchan_[a1..c3]*	Fig. 2.6
... barchan dunes under Moroccan conditions.	2. *barchan_[m1..m8]*	Fig. 2.7
Parabolic (§2.5.2)		Video S5
... stabilization for varying fixation levels.	3. *parabolic_[a1..a3]*	Fig. 2.8
... migration velocity under Brazilian conditions.	4. *parabolic_[b1,b2]*	Fig. 2.9
Embryo dunes (§2.5.3)		Video S6
... vegetation establishment and dune formation.	5. *embryo*	Fig. 2.10
Blowouts (§2.5.4)		Video S7
... real-world excavated foredune notches.	6. *blowouts*	Fig. 2.11

B

C

Data description and post-processing

For this study, we have reconstructed the 5-year morphodynamic development of the Sand Engine using four bathymetric and topographic datasets: *Sand Engine*, *Nemo*, *JarKuS*, and *LiDAR* surveys by Rijkswaterstaat. All datasets are obtained from de Zeeuw et al. (2017). The spatial coverage of each dataset is depicted in Figure C.1b and detailed in Table C.1a. In-depth information on these datasets and the Sand Engine's subaqueous development over five years is available in Roest et al. (2021).

We have chosen an analysis domain spanning 15 km alongshore and 2.5 km cross-shore, as outlined in black in Figure C.1b and c. A local coordinate system similar to that in de Schipper et al. (2016) was used, originating at the 'Schelpenpad' beach entrance (x_{RD}: 72421.9 m, y_{RD}: 451326.1 m), and rotated 48 degrees to create a shore-orthogonal grid. All datasets are interpolated onto a 5m x 5 m grid using linear interpolation.

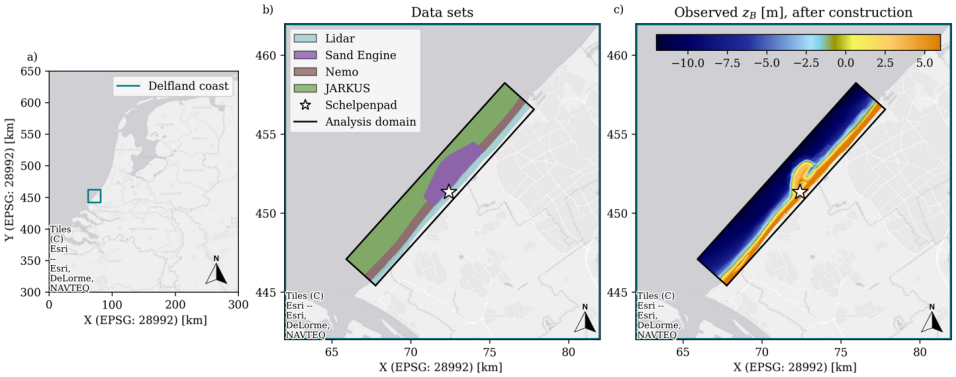

Figure C.1.: (a) Location of the Delfland coast (blue), (b) Overview of the Delfland coast displaying the various datasets utilized in this study. The schelpenpad beach entrance (star symbol) is used as the origin of the shore-orthogonal coordinate system used in the analyses, (c) bed level z_B [m] for the composite DEM directly after construction.

For the general model-data comparison (Figure 3.4 and Figure 3.8) and sediment budget analysis (Figure 3.6), we merged all datasets into a composite DEMs (Table C.1b). The *Sand Engine* data predominantly covers the assigned analysis domain (Figure 3.6). Where data are missing, they are supplemented with the most recent *Nemo* or *JarKus* data. The *LiDAR* dataset, used only landwards of the analysis domain, does not affect these results (Figure C.1b). We applied smoothing around the transitions between the *Nemo* and *Sand Engine* datasets to maintain realistic transition gradients. Additionally, a temporary sand stockpile present after construction, and subsequently removed by machinery (19,000 m^3, 220m in length, alongshore density of 86 m^3/m), is filtered out of the topography.

The coupled model provides weekly outputs, and the closest output moment to each comparison in time is chosen based on the survey date of the *Sand Engine* dataset, which is generally conducted during calm periods. As such, the influence of morphological differences between datasets with differing survey dates is likely to be minimal. The most significant deviation between reference and survey dates is in the *JarKus* data. However, as this data is used only to fill the stable offshore portion of the domain, its impact is deemed insignificant.

For the foredune deposition analysis specifically, we solely utilize the *LiDAR* dataset (Table C.1c), minimizing deviations between model and measurement dates.

Table C.1.: Overview of datasets used for the Sand Engine's morphodynamic reconstruction. (a) The dataset's coverage, resolution, and survey count. (b) Dates and corresponding survey numbers (*in brackets*), used for the visual comparison (Fig. 3.4 and Fig. 3.8), and sediment balance analysis (Fig. 3.6). (c) The dates related to the foredune deposition analysis (Fig. 3.9). Note: In this table version, only month and year are provided (days have been omitted for formatting purposes). For the complete details, please refer to the original article (van Westen et al., 2024a).

a) Spatiotemporal coverage

	Lidar	**Sand Engine**	**Nemo**	**JarKus**
Resolution	2m x 2m	40m x 5m	25m x 5m	250m x 5m
Nr. of surveys	19	52	21	12

b) Composite DEMs [Dates *(nr. of survey)*].

	Lidar	**Sand Engine**	**Nemo**	**JarKus**
Initial	07/2011 *(2)*	08/2011 *(2)*	*JarKus*	02/2011 *(1)*
After 5 years	02/2016 *(11)*	07/2016 *(37)*	05/2016 *(19)*	04/2015 *(5)*

c) Dates *(survey numbers)* : Foredune deposition *(Figure 3.9)*

	Lidar	**Sand Engine**	**Nemo**	**JarKus**
Initial	07/2011 *(2)*			
After 1 year	10/2012 *(4)*			
After 2 years	10/2013 *(6)*		Not used	
After 3 years	10/2014 *(8)*			
After 4 years	10/2015 *(10)*			
After 5 years	10/2016 *(12)*			

D

Theoretical potential dune growth

The potential aeolian-driven transport capacity, Q_{pot} [kg/s], is calculated using the same Bagnold transport equation (Bagnold, 1937) used by the AEOLIS model:

$$Q_{pot} = f(u_*, u_{th}) \tag{D.1}$$

In this equation, the input shear velocity, u_* [m/s], is based on the same wind speed, u_{10} [m/s], that drives the AEOLIS model, and the velocity threshold, u_{th} [m/s], is determined with the most prevalent grain size, D = 354 μm (Hoonhout & de Vries, 2019). The computed transport capacity is only an estimate that serves as a proxy to determine the relative importance of the prevailing environmental conditions. This transport rate is converted to potential dune volume change per running meter, to enable to compare with actual observations:

$$\Delta V_{pot} = \frac{Q_{pot} f_{\theta,os} \Delta T}{(1-p)\rho_{grain}} \tag{D.2}$$

Potential dune growth, ΔV_{pot} $[m^3/m]$, is computed by integrating over time (ΔT), converting from mass to volume based on porosity p (=0.4) and grain density ρ_g (=2650 kg/m^3), and considering only the onshore wind directions (θ_u), following Hoonhout's (2016) approach:

$$f_{\theta,os} = max(0; \cos 312° - \theta_u) \tag{D.3}$$

List of Publications

Journal Articles

First Author

3. **van Westen, B.**, de Schipper, M. A., Pearson, S. G., & Luijendijk, A. P. (2025). Lagrangian Modelling Reveals Sediment Pathways at Evolving Coasts. *Scientific Reports, 15*(1), 1–16

2. **van Westen, B.**, Luijendijk, A. P., de Vries, S., Cohn, N., Leijnse, T. W., & de Schipper, M. A. (2024). Predicting Marine and Aeolian Contributions to the Sand Engine's Evolution using Coupled Modelling. *Coastal Engineering, 188*, 104444

1. **van Westen, B.**, de Vries, S., Cohn, N., van IJzendoorn, C., Strypsteen, G., & Hallin, C. (2024). Aeolis: Numerical Modelling of Coastal Dunes and Aeolian Landform Development for Real-World Applications. *Environmental Modelling & Software, 179*, 106093

Co-Author

1. Strypsteen, G., de Vries, S., **van Westen, B.**, Bonte, D., Homberger, J.M., Hallin, C., & Rauwoens, P.(2024). Vertical Growth Rate of Planted Vegetation Controls Dune Growth on a Sandy Beach. *Coastal Engineering, 194*, 104624

Conference Proceedings and Talks

First Author

7. **van Westen, B.**, Luijendijk, A.P., de Vries, S., Pearson, S.G., de Schipper, M.A. (2025). Innovative Tools for Nature-based Solutions: Enhancing Dune Mobilization through Nourishment Design. *NCK Days 2025, Oosterscheldekering, Netherlands*

    - **Awarded Best Poster**

6. **van Westen, B.**, de Vries, S., Cohn, N., Strypsteen, G., Hallin, C., et al. (2024c). Aeolis: Modelling coastal dunes for real-world applications. *NCK Days 2024. Amersfoort, Netherlands*

    - **Awarded Best Oral Presentation**

5. **van Westen, B.**, Leijnse, T., Luijendijk, A.P., de Schipper, M. A., de Vries, S., & Cohn, N. (2024d). Predicting sediment pathways across the nearshore-dune system. *International Conference on Coastal Engineering 2024. Rome, Italy.*

4. **van Westen, B.**, Leijnse, T., de Schipper, M.A., Cohn, N., & Luijendijk, A.P. (2023). Integrated modelling of coastal landforms. *Coastal Sediments 2023: The Proceedings of the Coastal Sediments 2023,* 760–771

    - **Awarded Best Student Paper**

3. **van Westen, B.**, Leijnse, T., Luijendijk, A., de Schipper, M. A., de Vries, S., & Cohn, N. (2024e). Developing a generic framework for coupled modelling of foreshore, beach and dune interactions. *NCK Days 2022. Enschede, Netherlands*

2. **van Westen, B.**, Leijnse, T., Meijer, L., McCall, R., de Vries, S., & Cohn, N. (2021). Marine and aeolian processes in the coastal zone described in a coupled model. *Coastal Dynamics 2021: Zandmotor Monitoring*

1. **van Westen, B.**, de Vries, S., Reniers, A. J. H. M., den Bieman, J. P., Hoonhout, B. M., Rauwoens, P., & Van Puijenbroek, M. E. B. (2019). Aeolian modelling of coastal landform development. *Coastal Sediments 2019: Proceedings of the 9th International Conference*.

    - **Awarded Best Student Paper**

Co-Author

3. Oude Vrielink, J., Eleveld, M., van der Valk, B., **van Westen, B.**, Hendriksen, G., IJff, S., van der Meulen, F., de Zeeuw, R., van Eerden, M., Borst, K., et al. (2021). The rise of spanjaards duin: Factors regulating sediment fluxes over an engineered foredune and adjacent dune slack. *NCK Days 2021*

2. Vrielink, J. O., Eleveld, M., **van Westen, B.**, Galiforni-Silva, F., & Wijnberg, K. M. (2021). Factors regulating sediment fluxes over an engineered foredune and adjacent dune slack. *Coastal Dynamics 2021: Zandmotor Monitoring*

1. Cohn, N., Brodie, K., Ruggiero, P., **van Westen, B.**, & de Vries, S. (2019). Coastal inlet infilling from aeolian sediment transport. *Coastal Sediments 2019: Proceedings of the 9th International Conference*, 1212–1225

Software

2. de Vries, S., Hallin, C., van IJzendoorn, C., **van Westen, B.**, Cohn, N., Strypsteen, G., Skaden, J., Agrawal, N., & Garcia Alvarez, M. (2023, November). AeoLiS. https://doi.org/10.5281/zenodo.10071595

1. van Westen, B. (2025). *Data and scripts underlaying the PhD Dissertation of Bart van Westen* (Version 2). 4TU.ResearchData. https://doi.org/10.4121/4CF9E7E3-771A-4135-B1AF-8E1686A55449.V2

6. Deltares. (2023). *Duurzaam kustonderhoud in de nabije en verre toekomst; Synthesedocument onderzoek Dutch Coastline Challenge* (tech. rep. No. 11207047-005-HYE-0002). Deltares

5. Technische Universiteit Delft (2023a). *TKI Dutch Coastline Challenge: Inventarisatie kustonderhoudsconcepten.* Memo TU Delft.

4. Technische Universiteit Delft (2023b). *TKI Dutch Coastline Challenge: Description of the setup of the Delft3D Flexible Mesh model and validation of the hydrodynamics.* Memo TU Delft.

3. Technische Universiteit Delft (2023c). *TKI Dutch Coastline Challenge: Evaluation of the morphological predictive skills of the Delft3D FM model based on simulations of the Sand Engine.* Memo TU Delft.

2. Technische Universiteit Delft (2023d). *TKI Dutch Coastline Challenge: Morphological and ecological indicators.* Memo TU Delft.

1. Technische Universiteit Delft (2023e). *TKI Dutch Coastline Challenge: morphological and ecological evaluation of nourishment concepts.* Memo TU Delft.

Acknowledgements

Pursuing a PhD is often portrayed as a solitary journey. My experience couldn't have been more different. Over the past four years, I have been surrounded by wonderful people—both familiar faces and new ones-who generously shared their time, knowledge, and advice. Most importantly, they filled these years with amazing memories. Without their support, this work would not have been possible, and it certainly wouldn't have been as much fun.

Among the people who made this journey so enjoyable and rewarding, I want to start by thanking my supervisors and promotors. Matthieu, thank you for all your energy, patience, and constructive input. Our discussions and your questions pushed me to become more critical toward my own work, which was definitely needed at times. Despite an overall great journey, there were of course some hurdles along the way. During these moments, you spared no effort to clear your agenda and help me out. Without your critical views, countless reads, and writing assistance, this project would not have ended the way it eventually did. I hope we'll have many more opportunities to meet in the future—perhaps even out on the water, though that requires quite a bit more practice on my part.

Arjen, thank you for giving me the opportunity to embark on this incredible journey. I'm guessing "enabling" is already quite high on your buzzword-list, but I truly couldn't think of a better word to describe you. All your efforts, ranging from your own PhD work to the support you've provided over the years, ultimately enabled tackling all conceivable technical and logistical challenges. I hope that learning from your pragmatic mindset toward project management, technical issues, deadlines, framing of results, and rebuttals one day enables me to develop these skills myself. During this project, we have had the privilege to celebrate some successes—may those successes continue, whether at Deltares or in de Kuip.

Sierd, thank you for introducing me to so many great colleagues and places around the world—and, of course, on top of it all-to AeoLiS. Your ability to connect people not only helped me but shaped the basis of many meaningful collaborations. Your consistent honesty improved my ability to model, write, research, and perhaps, one day, even to properly introduce myself at conferences. While nothing quite compares to the triumph of a mass-conservative efficient blowout simulation, I'll admit it's probably better not to say that out loud. I hope your energy continues to spark momentum in the dune community—both real-world and numerical—and I hope to stay a part of that momentum (yes, including the sprints). Good busy!

I would like to thank two people who are currently enjoying retirement or a functie elders. Peter, thank you for your ever-critical view and for asking the right questions at the right moment. What initially felt like a setback ultimately helped steer the project in the right direction. Enjoy your well-deserved retirement. Stefan, thank you for your valuable contributions during the start of the project. Your flexibility and cooperation allowed this research to continue, for which I'm deeply grateful. Good luck with your new position—perhaps we'll meet again at Dean's drinks. I also want to thank the independent members of my doctoral committee for their review of this thesis: Prof. dr. ir. Roelvink, Prof. dr. Wijnberg, Prof. dr. Overeem, Prof. dr. Long, and Prof. dr. ir. Reniers.

Although it feels like ages ago, this project began amid the pandemic with the Dutch Coastline Challenge. The numerous workshops and meetings broadened my perspective on coastal management and offered the opportunity to familiarize myself with the various study sites, nourishment alternatives, and models that eventually formed the foundation of this PhD. I want to thank all colleagues involved in the DCC, with special appreciation to Wiebe for managing the entire project, Marcel and Stéphanie for synthesizing the project results, and Carlo, Coen, Helène, Leon, and Thomas for sharing their expertise during our weekly meetings.

To all my Deltares colleagues, thank you for the opportunity to pursue this PhD by providing all the support needed. Helena, thank you for making time for me and facilitating all my needs, despite all the-probably often cumbersome-requests. I'm really looking forward to the coming years! Similar gratitude to Marcel and Jan-Joost for their earlier support as former managers. Thanks also to Bas and Joost for supervising my MSc and later mentoring me during my first years at Deltares.

Thanks to the AeoLiS-team. I feel incredibly spoiled looking back at the people we've met, the adventures we've shared, and the places we've visited — and of course-subsequently modelled them. Coding and drinking—it's not only Nick's delight. Caroline, Christa, Glenn, Nick, and Sierd, thanks for bringing me into this amazing team, organizing the sprints and for co-authoring the AeoLiS publication. To the newer additions—Janelle, Maddy, Manuel, Niket, Olivier, Quintin, and Selwyn—thanks for sharing so many great times. Whether it was mountain biking, hiking, bowling, nerding on the beach, the CS23 workshop, Dune Drinks, Brew Threw, or the guilty pleasure quizzes; these were definite highlights of my PhD years, with hopefully many more to come.

Thanks to the SedTRAILS-team for welcoming me to this exciting new development. Aysun, Hassan, Johan, Manuel, Monica, and Natascia, thanks for the Wednesday sessions. It's been fascinating to witness the (re-)development of a novel tool from the ground up and its definitely heading down the right pathway to make SedTRAILS a great success. Stuart, many thanks for making so much time for me. For just letting me walk into your office and firing random questions at you. Thanks for always answering with a genuine unparalleled level of enthusiasm. Always in a hurry, but always time to help. Thanks for your assistance with the SedTRAILS publication and for spearheading this exciting new development.

Gracias Tim, Milan y Jesse. Aún necesito Google Translate para algo tan simple, así que mejor omitimos el español. Still not entirely sure what sparked my interest in coastal engineering during our time in Havana – it were the mojitos – but it turned out to be a key turning point in my studies and eventual career. Thanks for the unforgettable adventures we had, and here's to plenty more in the future. Tim, special thanks for dragging me into Deltares, let me discover my excitement for modelling and for keeping that alive during our Haamstede sprints.

A huge thank you to everyone at TU Delft for being such fantastic colleagues. Ad, Ana, Anna (2x), Anne, Bas, Bram, Bregje, Camilo, Christa, Daan, Dorette, Filipe, Floor, Hassan, Inge, Jill, Jos, José, Ligaya, Lisa, Marlein, Marlies, Marion, Matthijs, Menno, Mia, Natascia, Otti, French Paul, Paulina, Romy, Roy, Sander, Tess, Tom, and Valentina—you made my time there truly memorable. Thanks for the laughs at PSOR and the lunches of truly unique culinary quality. Special thanks to my roommates Floris, Gijs, Jakob, Mario, Kevin, Marthe, Paul, Su, Tosca, and Vincent. For the countless coffee breaks, music hour, and the occasional moaning about what not, all whilst somehow still being productive at times. And of course, for the adventures we shared far beyond the insanely nicely decorated walls of 3.62.

To Aaron, Andrea, Chris, Esther, Jeroen, Job, Lisa, Reinoud and Tom, thank you for allowing me to be a part of your MSc projects. Your hard work, dedication, and enthusiasm were inspiring and I hope that these projects were at least as valuable for you as they were for me.

Thanks to Peter and Meagan for hosting us at OSU and of course for introducing us to tubing and the Vegetable Olympics. I also want to thank the ESPin-team at CSDMS for the great experience in Boulder, and the organizers of the NCK Summerschool for a wonderful week on Texel.

Returning home, I want to thank all my friends and family. First, once and for all, let me save myself some time: 's-Gravendeel[1], korfball[2]. I hope that one day, you'll be able to fully enjoy the beach again, without an overload of information on embryo dunes and desert pavements ruining the coast's natural beauty. In the meantime, thank you for all the travels, dinners, festivals, drinks, matches, and the overall amazing company you've all been!

En tot slot-pa, ma, opa, Brittje, Lot, Michael en Denis. Dat ik de afgelopen jaren verwend ben mogen we gerust een understatement noemen. Enorm bedankt voor alles. Voor de hulp bij het verbouwen en bijhouden van alles in en rondom de Molendijk. Voor het toch nog maar een keertje meenemen van deze verstekeling op vakantie. Me achter m'n laptop vandaan te sleuren om een bakje koffie te doen. En altijd maar weer interesse tonen. Maar vooral voor het leren genieten van de dingen die er toe doen! Zonder jullie was dit allemaal nooit gelukt.

[1] https://nl.wikipedia.org/wiki/%27s-Gravendeel
[2] https://en.wikipedia.org/wiki/Korfball

About the Author

Bart van Westen was born on the 7th of September in 's-Gravendeel, the Netherlands. After graduating from the Johan de Witt Gymnasium in Dordrecht, he started his BSc. Civil Engineering at the Delft University of Technology in 2012.

In 2015, he started the MSc. specialized in Coastal Engineering. He completed his MSc thesis in 2018 on the implementation of dune development processes in the numerical model AeoLiS. After graduation, he worked at Deltares, during which he has contributed to the further development of AeoLiS, supported physical model testing in the Deltaflume combined with CFD modelling.

In spring 2021, he started his PhD journey at the Technical University of Delft and Deltares. The first two years as a PhD candidate were part of the Dutch Coastline Challenge, which sought to identify and evaluate innovative nourishment solutions for the Dutch coast that are scalable, sustainable, and emission-free. During his PhD study, Bart was part of the AeoLiS and SedTRAILS development teams.